DECLASSIFIED

CONFIDENTIAL

Copy 94
RM L57E17

NACA RM L57E17

JUL 25 1957

NACA

RESEARCH MEMORANDUM

TIME-HISTORY DATA OF MANEUVERS PERFORMED BY A REPUBLIC F-84F AIRPLANE DURING SQUADRON OPERATIONAL TRAINING

By Harold A. Hamer, John P. Mayer, and Donald B. Case

Langley Aeronautical Laboratory
Langley Field, Va.

CLASSIFICATION CHANGED TO
DECLASSIFIED AUTHORITY
CM 10-79 9-1-59

[redacted]

[redacted]

NATIONAL ADVISORY COMMITTEE
FOR AERONAUTICS
WASHINGTON
July 22, 1957

CONFIDENTIAL

T62-19223-F

NATIONAL ADVISORY COMMITTEE FOR AERONAUTICS

RESEARCH MEMORANDUM

TIME-HISTORY DATA OF MANEUVERS PERFORMED BY A REPUBLIC F-84F AIRPLANE DURING SQUADRON OPERATIONAL TRAINING

By Harold A. Hamer, John P. Mayer, and Donald B. Case

SUMMARY

Results of a control-motion study program with a jet fighter airplane are presented in time-history form. These time histories represent a cross section of tactical maneuvers performed by a Republic F-84F airplane during squadron operational training. Data were recorded at altitudes up to about 42,000 feet, indicated airspeeds up to 600 knots, and at Mach numbers up to about 1.1. In addition, normal-load-factor data covering the entire flight investigation are separated into several different types of missions and summarized as envelopes of load factor plotted against indicated airspeed and Mach number.

INTRODUCTION

With a view toward providing information for the appraisal of the design requirements of future airplanes, the National Advisory Committee for Aeronautics has been conducting a statistical study of the pilot input, the corresponding airplane motions, and the loads imposed on a number of fighter-type airplanes during military training operations. The data obtained thus far have been summarized in references 1 to 3.

This paper presents data in time-history form of typical maneuvers performed by a Republic F-84F airplane during regularly scheduled operational training missions, which include the LABS (low-altitude bombing system) technique. The time histories contain a cross section of the various tactical maneuvers and include the more severe maneuvers to show what maximum values of control and airplane motions can be expected during routine operational training. In addition, envelopes of normal load factor plotted against indicated airspeed and Mach number for several altitude ranges are presented for the complete flight program as well as for specific types of missions.

SYMBOLS

H_p	pressure altitude, ft
V_i	indicated airspeed, knots
M	Mach number
δ_a	aileron angle, deg
δ_{as}	aileron or spoiler stick angle, deg
δ_r	rudder angle, deg
δ_{ss}	stabilator stick angle, deg
δ_s	stabilator angle, deg
F_a	aileron stick force, lb
F_r	rudder pedal force, lb
F_s	stabilator stick force, lb
n_T	transverse load factor
n_V	normal load factor
n_L	longitudinal load factor
q	pitching velocity, radians/sec
$\dot{q}$	pitching acceleration, radians/sec/sec
p	rolling velocity, radians/sec
$\dot{p}$	rolling acceleration, radians/sec/sec
r	yawing velocity, radians/sec
$\dot{r}$	yawing acceleration, radians/sec/sec
β	sideslip angle, deg
α	angle of attack, deg
$\bar{c}$	mean aerodynamic chord, in.

AIRPLANE

A standard U. S. Air Force F-84F-55RE airplane was used in these tests. A photograph of the test airplane is shown in figure 1. The Republic F-84F is a single-place jet-propelled fighter-bomber airplane having a swept wing and empennage. The airplane is equipped to carry a wide assortment of weapons and external fuel tanks at inboard and outboard stations along the wing.

A one-piece stabilator is used for longitudinal control. A damper is incorporated in this system to decrease control sensitivity and prevent overcontrol. In addition, with the landing gear retracted, the control stick travel per degree of stabilator movement is increased to reduce control sensitivity. Included in the lateral-control system are spoilers which are located on the upper surface of both wings immediately forward of the flaps. The spoilers are actuated by the control-stick lateral deflection. The spoilers operate when the landing gear is in the retracted position and move in the up-direction only. As the aileron moves up from 0° to about 11°, the corresponding spoiler moves up proportionally from 0° to about 45° and remains at 45° for the remainder of aileron travel. All control surfaces are hydraulically actuated. A hydraulically operated speed brake is installed on each side of the rear fuselage.

Neither the external appearance (except for the installation of a nose boom) nor the weight and balance of the airplane was altered by the addition of the instrumentation. A three-view drawing of the F-84F test airplane is presented in figure 2, its dimensions and physical characteristics are given in table I, and its mass characteristics are given in table II. The moments of inertia given in table II for the various airplane configurations are values estimated in accordance with the best information available.

INSTRUMENTS

Standard NACA photographically recording instruments were used to measure (1) the quantities defining the flight conditions - that is, airspeed, altitude, Mach number, and speed-brake position (open or closed), (2) the imposed control-stick and control-surface motions along with the corresponding stick and pedal forces, and (3) the response of the airplane in terms of load factors, angular velocities, angular accelerations, angle of sideslip, and angle of attack. The recorders were synchronized at 1-second intervals by means of a common timing circuit. Microswitches incorporated in the airplane bombing system were used to indicate the times at which the bomb switch and bomb release mechanism were actuated.

In order to relieve the pilot of any recording-instrument switching procedure and thus to assist in obtaining normal operation, a pressure switch was employed to operate the recording instruments automatically at take-off.

A standard two-cell pressure recorder connected to the airplane service system was used to measure the pressure altitude, indicated airspeed, and Mach number. The service system was of the usual total-pressure-tube and flush static-pressure-orifice type. (See fig. 2.)

The control-stick and control-surface deflections were recorded with a multiple-channel oscillograph having remote-recording variable-resistance-type transmitters installed at or near the control stick and control surfaces. Spoiler deflection was not measured at the surface since it varies directly with aileron deflection. The stick and pedal forces were recorded with the oscillograph by the use of NACA strain-gage-type transmitters mounted on the control stick and rudder pedals. A microswitch installed at the speed brake was used to indicate whether the speed brake was in the open or closed position.

Recorders containing gyroscopic sensing elements were used to record angular velocities and angular accelerations about three mutually perpendicular axes in which the longitudinal reference axis is the one commonly used for leveling the airplane. (See fig. 2.) Load factors along these three axes were measured by an NACA magnetically damped, three-component recording accelerometer. The accelerometer was located in the vertical plane passing through the fuselage center line, 15 inches forward and 12 inches above the average "in flight" center of gravity (21.4 percent of the wing mean aerodynamic chord and 3 inches below the fuselage reference line).

The angle of attack and sideslip angle were measured by a flow-direction recorder in combination with vanes mounted on a boom extending from the upper right nose-gun port. (See figs. 1 and 2.)

ACCURACY

Table III is a summary of the quantities measured and the estimated accuracies of the measurements. The accuracies are based on maximum possible instrument error plus the error resulting from preparing and reproducing the time-history figures. In order to give the correct response to the maneuver, all recording instrument elements were damped to about 0.65 of critical damping and their natural frequencies were selected to give the best compromise value which would minimize the magnitude of extraneous airplane vibrations.

In addition to the instrument and reproduction errors, it should be noted that no corrections are made to the recorded load factors for the effect of angular velocities and angular accelerations due to the displacement of the accelerometer from the airplane center of gravity. Since the accelerometer was near the center of gravity, these effects are negligible except for the effect of very large values of rolling acceleration on the recorded transverse load factor. The sideslip-angle and angle-of-attack measurements are uncorrected for angular velocity, sidewash, and upwash effects. It is estimated that the effects of sidewash and upwash increase the measured sideslip angle and angle of attack by approximately 5 percent and 10 percent, respectively. The effect of boom bending on the sideslip-angle and angle-of-attack measurements has been determined to be small.

TESTS

All the flights made during these tests were performed by service pilots undergoing regular squadron operational training. Measurements were obtained of 53 operational training flights with approximately 45 hours of flight time being recorded. The maneuvers performed during these tests include most of the tactical maneuvers that are within the capabilities of the airplane. The operational flights included such missions as LABS (low-altitude bombing system), dive-bombing, simulated strafing, in-flight refueling, formation flying, "rat-racing" or dog fighting, and transition flying or familiarization (which usually consists of various acrobatic-type maneuvers). Data were recorded at altitudes from ground level to about 42,000 feet, at airspeeds varying from the stalling airspeed to about the maximum service limit airspeed (610 knots), and at Mach numbers up to about 1.1. Although not requested, most of the maneuvers were performed in smooth air except for those near the ground where turbulence was encountered.

Other than to request that the airplane be used in as many types of missions as were normally carried out by the squadron, no attempt was made to specify the type or severity of maneuvers. Since the pilots were aware of the instrumentation, it was stressed that this was not to restrict their normal handling of the airplane.

Sufficient film was available during each flight to obtain approximately 80 minutes of continuous records. This amount of time was generally enough to record the complete flight. The flights were made with the clean airplane configuration and also with various external-store loading arrangements. Table IV is a summary of the flights from which time histories are presented.

METHOD AND RESULTS

The sign convention used for the airplane motions and control positions is illustrated in figure 3. The basic results obtained are presented in figures 4 to 64 as time histories of the measured quantities. The data presented herein are a small percentage of the total amount recorded during the tests, but are a cross section of all the operational maneuvers that were performed. In general, the maximum values of the control inputs and airplane responses obtained during the tests are included in these time-history figures.

In addition, envelopes of normal load factor plotted against indicated airspeed and Mach number for several altitude ranges are presented in figures 65 to 80. These plots contain normal-load-factor data, read at 1/2-second intervals, for the complete flight program. The normal-load-factor data are separated into three types of missions, namely: (1) LABS (low-altitude bombing system), (2) dive-bombing, and (3) general flying, which includes all other types of missions.

The time histories shown in figures 4 to 64 were obtained by accurately tracing the flight-record traces (except for altitude, indicated airspeed, and Mach number, which were plotted) directly on master sheets. The vertical scales on the figures which conform to the instrument calibrations are linear and because of limited space are shown only in one direction for most quantities.

In some cases a time-history figure contains more than one maneuver. Care was taken to begin and end each time-history figure at a relatively normal steady-flight condition. The time-history figures are arranged according to the maneuver classification shown in table V. Where a figure included more than one maneuver, its classification was established by that portion which was of greatest interest. Included in the figure legends are a description of the type of maneuver or maneuvers and the estimated in-flight airplane weight and center-of-gravity location, which were determined by interpolation with respect to total amount of fuel used and the length of time for the flight including warm-up and taxiing. The flight from which each time-history figure was obtained is also included so that reference can be made to table IV.

In the time histories, the altitude is the NACA standard pressure altitude and the airspeed is given in terms of indicated airspeed which is defined as the reading of a differential-pressure airspeed indicator, calibrated in accordance with the accepted standard adiabatic formula to indicate true airspeed for standard sea-level conditions only (uncorrected for instrument error). No corrections have been made to the indicated airspeed and Mach number for position error associated with the location of the static orifices. Periods during which the speed brake was open are indicated on the figures by dashed lines and the words "brake open."

The control-surface and control-stick positions shown in the figures were measured with respect to their neutral position. Only the left aileron position was measured. Control forces were measured normal to the stick and pedals, and pedal force is given as the algebraic sum of the forces on both pedals.

The sideslip angle shown in the figures is the angle between the longitudinal axis and the projection of the relative wind in the horizontal plane of the airplane. The angle of attack is the angle between the longitudinal axis and the projection of the relative wind in the vertical plane of the airplane.

In the time-history figures, the angular velocities are shown as solid traces and the angular accelerations as dashed traces. The time histories of aileron stick force are generally identified by traces with short dashes and those of rudder force with long dashes. Also, when the trace of any quantity intersects another, one of the traces is dashed in the region where trace identification might be confusing.

DISCUSSION

Although this investigation was limited to a relatively small amount of flight time, the data obtained represent a cross section of the maneuvers performed during operational training and include most of the tactical maneuvers within the capabilities of the F-84F airplane.

Time-History Figures

In general, the maximum values of the control inputs and airplane responses obtained during the tests are included in the time-history figures. Each group of time-history figures, as classified in table V according to type of maneuver, will be briefly discussed:

Take-offs.- The time histories shown in figures 4 and 5 are representative values of control and airplane motions during take-off. In figure 4, the unsymmetrical load of a full 450-gallon fuel tank (3,175 pounds) on the inboard pylon required that aileron angles up to 10° be used to maintain level wings at take-off. Also the automatic shifting of the ratio of control-stick travel to stabilator angle to a higher value may be noted in figure 4 (approximately at times 12 to 20 seconds) after the landing gear is retracted.

It can be seen in figure 5 that the longitudinal load factor during a jet-assisted take-off (JATO) is increased from about 0.1 to 0.3. As a matter of comparison the longitudinal load factor obtained during take-off for a normal weight (fig. 4) is about 0.2.

Turns.- Some of the highest normal load factors recorded during the tests were obtained in turns such as in the left and right turns shown in figure 7. In these turns, normal-load-factor values up to about 6 were reached.

During the type of maneuvering used in rat racing or tail chases, it was not unusual to record long-duration turns made at relatively high normal load factors. Figure 8 is an example of such a maneuver.

Rolls.- In the full-aileron rolls (figs. 14 and 15), rolling velocities up to 3.8 radians per second were recorded; these values are about the maximum obtainable for the airplane for this flight condition. The maximum spoiler angle of 45° is reached during these rolls. The highest rolling accelerations recorded were 11 radians per second per second at indicated airspeeds of 350 knots to 400 knots as shown in figure 14 at time 38 seconds and in figure 15 at time 30 seconds. It is of interest to note that the highest rolling accelerations were for the most part obtained as the roll was being checked.

During rolling pullouts and barrel rolls (which are essentially rolling pullouts), large rolling velocities and rolling accelerations were obtained in combination with relatively high normal load factor at high speed. (For example, see fig. 18.) The magnitudes of yawing velocity, yawing acceleration, and sideslip angle, however, were small. According to calculations made for this type of maneuver being performed at this speed, this result might be expected. (For example, see ref. 2.) The calculations indicate that the values of these quantities would probably be considerably larger during rolling pullouts made at lower speeds at high lift coefficients. It can be seen in figure 16 that for about 1 minute a number of barrel rolls were made during which time the normal load factor was continuously about 4.

Boost and speed-brake operation.- The time-history data shown in figure 20 were obtained during the portion of a flight where the control-boost system was turned on after it had intentionally been turned off for a period of time. It is of interest to note the abrupt angular motions of the airplane together with relatively large angular accelerations as the controls are automatically trimmed when the boost is restored.

The large aileron deflections resulted from the aileron stick force of about 12 pounds which the pilot was using when boost was restored. During most of the time when the boost was off, the aileron stick force was off-scale (higher than 27 pounds). In another flight where the boost was off, aileron-stick-force measurements made with a measuring element with a higher range were found to be as high as 80 pounds. In this particular instance, the airplane carried an inboard 230-gallon external fuel tank which was almost full (1,370 pounds). The 80-pound force was required to make a gradual bank to 30° (in a direction away from the tank) at 350 knots and at an altitude of 9,000 feet.

Figure 22 is an example of the effect of speed-brake operation. For the particular flight condition shown, a longitudinal deceleration of about 0.5g was caused by use of the speed brake.

Dives.- Time histories of dives are presented in figures 24 to 29. Some of these dives pertain to what the pilots termed "Mach runs." These were merely steep dives from high altitude to speeds greater than a Mach number of 1. All high-speed dives shown in figures 24 to 29 were made with the clean airplane configuration, except for the one shown in figure 29. For this run the airplane carried a full 230-gallon external fuel tank.

Upon examination of the Mach run time histories (for example, fig. 24), some points of interest can be noted such as the "heavy" tendency of the left wing and the movement of the rudder to angles up to about 2° without any apparent intent of the pilot. (See the rudder force.) Also shown at or above Mach number 1 are the effects of shock waves on the sideslip-angle and angle-of-attack transmitter vanes. During these runs longitudinal decelerations up to about 1.2g (fig. 26) were measured in the pullout.

The highest dynamic pressure recorded during the tests was 1,200 pounds per square foot and was obtained in a shallow dive to low altitude. (See fig. 25 at time 75 seconds.) This pressure occurred at an altitude of about 3,000 feet and at a Mach number of about 0.95.

Dive-bombing runs.- In figures 30 to 35 are shown typical time histories of various types of dive-bombing maneuvers. The maneuver shown in figure 30 is that of an ordinary dive-bomb run which is usually made from an altitude of about 8,000 feet to an altitude of about 3,000 or 4,000 feet. A glide-bomb run (fig. 31) is made at a smaller dive angle. The skip-bomb run shown in figure 32 is a maneuver made as close to the ground as possible, the bomb being skipped into the target. The runs shown in figures 33 to 35 are dive-bomb runs made at higher altitudes. In these three runs practice bombs were dropped, the time at which the pilot released the bomb being indicated in each figure. In figures 34 and 35 it can be noted that sideslip angles up to 6° were obtained in lining up the dive-bomb runs.

LABS (low-altitude bombing system) runs.- The bombing runs shown in figures 39 to 46 are known as LABS maneuvers and are a technique developed to drop bombs from low altitude. It can be seen from the figures and by referring to table IV that some of these runs were simulated (no bombs dropped), some were made dropping small practice bombs, and some were made dropping a 1,700-pound practice bomb. A LABS run consists of a straight-and-level, high-speed (approximately 500 knots) pass at near-ground level followed by an abrupt pull-up to a prescribed normal load factor of 4, the bomb automatically releasing at a predetermined attitude angle. After the bomb is released the half-loop is carried to completion, a 180° roll being made on top. It is usually necessary to reduce the normal load factor as the speed decreases to keep the airplane at lift coefficients below the stall and pitch-up region.

There are essentially two types of LABS missions, as indicated in the figures. In an over-the-shoulder run the pull-up is made directly over the target, the pilot in most cases putting the bomb switch to the on-position at the beginning of the pull-up. The bomb is released at an airplane attitude angle greater than 90°, the angle depending upon such factors as altitude of target, wind velocity, and wind direction. In the cases where bombs were actually released, as indicated in the figures, the release settings were 119° for figures 39 and 40 and 96° for figures 42 and 43. (Those at 96° are known as vertical bomb drops.)

In the initial-point run, the pull-up is made over what is called an initial point which is selected ahead of the target. When the airplane passes over the initial point, the pilot puts the bomb switch to the on-position and then, after a predetermined elapsed time (depending on the distance from the initial point to the target), makes the pull-up. In comparison with the over-the-shoulder approach, the bomb releases at a smaller attitude angle while the airplane is still at a distance in front of the target. The angle setting for the initial-point LABS run shown in figure 46 was 38.8°.

The high-speed portions of the runs often resulted in an extremely rough ride (and occasionally caused the pilot's head to hit the canopy), especially when a 1,700-pound practice bomb was carried (figs. 41, 42, 43, 45, and 46). The turbulence encountered at this speed and altitude caused aileron and rudder control-surface oscillations (about 1 cycle per second) with amplitudes as large as ±3° and ±1°, respectively. It was learned that the pilots were unaware of causing these motions and that they were merely trying to hold the stick fixed and were resting their feet on the rudder pedals. During the longitudinal and directional oscillations of the airplane, pitching accelerations as large as ±2.5 radians per second per second, yawing accelerations as large as ±1.4 radians per second per second, transverse load factors as large as ±0.8, and normal-load-factor variations up to ±1.5 were measured at the high airspeeds. These values of pitching and yawing acceleration and transverse load factor are higher than those measured in all types of maneuvering during previous tests made on other fighter airplanes during squadron operations (ref. 1). Examination of the time histories also shows that noticeable stabilator control-surface deflections occur with little or no corresponding pilot-induced stick movement (under normal conditions the stabilator moves about 0.37° for 1° of stick travel). In fact, at times the stabilator and stick are moving in opposite directions. These inadvertent stabilator motions which are much more noticeable when the 1,700-pound practice bomb is on the airplane cause the large incremental changes in normal load factor. In addition, these inadvertent motions appear to be associated with the severe directional oscillations. It is possible, therefore, that bending or twisting of the fuselage-tail combination could be enough to operate the valve on the power control system and would force the stabilator to move. (Calculations of tail loads and hinge moments indicated that the hinge moments were not high enough to overpower the control system.)

In the bombing runs in which a 1,700-pound practice bomb was released, an increase in normal load factor of about 1.5 (from 4 to 5.5) was recorded in an initial-point release (fig. 46) and about 0.7 (from 2.7 to 3.4) in an over-the-shoulder release (fig. 43).

Rat racing.- The term "rat racing" was used by the pilots to define the type of maneuvering which may be employed in dog-fighting tactics. In figures 47 to 50 showing time histories of the data recorded during these rat-racing maneuvers, the test airplane was either being chased by or chasing another fighter airplane. Examination of the time histories shows that numerous lateral-control motions were used in this type of maneuvering and that the occurrence of stalls and pitch-ups was not unusual. In the pitch-up in figure 49 it is of special interest to note where the airplane went completely out of control (starting at about time 93 seconds) in a climb during a tail chase. It can be seen that a sideslip angle of 20° and angles of attack as large as 26° (nose up) were recorded as well as pitching and yawing velocities of about 0.5 radian per second.

Pitch-ups.- A number of pitch-ups of varying degrees of severity were recorded during the tests, a few of which are presented in figures 51 to 58. Sometimes the pitch-ups were unintentional. In many cases they were intentionally performed since the service pilots did not consider the pitch-up of this airplane to be dangerous at high altitude. Examples of intentional pitch-ups are given in figures 51, 55, 56, and 57. During the pitch-up shown in figure 51, angles of attack up to 27° (nose up), pitching velocities up to 0.65 (nose up) radian per second, and pitching accelerations up to 4.0 (nose down) radians per second per second were measured.

The pitch-up shown in figure 57 was made at considerably higher indicated airspeed as compared with that for the other pitch-ups. Upon examination at time 4.5 to 6.5 seconds, it can be seen that during this pitch-up the stabilator control-surface deflection does not correspond to the control-stick motion. (Note that, for clarity, the time scale has been expanded for this figure.) An analysis was made of the maneuver by calculating the horizontal-tail loads and hinge moments from wind-tunnel data given in reference 4. The results of this analysis are given in figure 58 as time histories of the incremental structural (aerodynamic plus inertia) tail load and structural hinge moment (taken about a hinge line $6\frac{1}{4}$ inches forward of the trailing edge at the root chord). Included in the figure are the control stick and measured stabilator control-surface positions plotted on an enlarged vertical scale. In addition, the stabilator surface is shown as it would move under normal conditions.

The tail loads given in figure 58 do not appear to be excessive; however, the wind-tunnel tests show that the hinge-moment-coefficient value increases rapidly with angle of attack at large angles of attack (above 12°) due to an outboard shift of the tail load. These large hinge-moment coefficients in combination with the relatively large dynamic pressures produce hinge moments up to about 14,000 foot-pounds, which is above the 9,000 foot-pound capacity of the power-control system. It can be seen in figure 58 that the movement of the stabilator surface is apparently being affected by the large hinge moments which overpower the power control system.

Formation flying, ground control approach, in-flight refueling, and so forth.- Figures 59 to 61 are presented to show the type of control motions normally used while a pilot is attempting to remain in a fixed line of flight. For the instrument let down (ILD) and ground control approach (GCA) shown in figure 59 the test airplane was flying the wing position with another airplane. For the formation flying shown in figure 60 the test airplane was part of a large formation of airplanes. The time histories shown in figure 61 are for an in-flight refueling operation in which the pilot reported little or no difficulty experienced in hooking-up or remaining with the tanker airplane.

Landings.- It can be seen that, in the "break" or turn in the landing pattern (fig. 62), large rolling velocities (about 3 radians per second) and large rolling accelerations (about 9 radians per second per second) were obtained. These magnitudes, which can be considered unnecessary, are near the maximum rolling capabilities of the airplane.

In figure 63 it is of interest to note the dynamically unstable characteristics of the airplane during the landing approach as shown by the large directional oscillations. Figure 64 is an example of a landing in which a large amount of sideslip was used.

V-n and M-n Envelopes

All normal-load-factor data collected during the test program are summarized as envelopes of load factor plotted against indicated airspeed and Mach number (herein denoted as V-n and M-n envelopes). These plots were made using automatic plotting equipment. These V-n and M-n envelopes are presented in figures 65 to 80 along with the design and service diagrams for comparison of the test results with the operational limits. Essentially, the envelopes are composed of approximately 45 hours of load-factor data tabulated for every 1/2 second. In some of the figures there are noticeable areas where the data are less dense (for instance, in fig. 65 between load factors of 1 and 3 and at the lower airspeeds up to 400 knots). Because of the large mass of data in this region only enough points were plotted to adequately define the envelope.

Figures 65 to 70 contain load-factor data, separated into three altitude ranges, for general flying which pertain to all types of flying other than that during flights scheduled solely for bombing missions. (The service limit load factor is shown for the clean airplane configuration since some of these data were obtained with this configuration.) Figures 71 to 74 represent load factors obtained in two altitude ranges during LABS missions and figures 75 to 78 include load factors recorded in two altitude ranges during dive-bombing missions. (The service limit load factor is shown for the external stores configuration since all these data were obtained with this configuration.)

The boundaries of the combined load-factor data for general flying, LABS, and dive-bombing runs at all altitudes are shown in figures 79 and 80 plotted against indicated airspeed and Mach number. It is indicated that, as in similar tests made with other fighter airplanes (ref. 1), the service pilots utilized the positive portion of the V-n or M-n diagram but did not approach the negative-load-factor limits.

Inspection of figures 65 and 66 shows that the data do not extend up to the stall boundary of the V-n diagram whereas they do when plotted on the M-n diagrams. This condition can also be noticed for some of the other sets of V-n and M-n plots. This condition occurs because the effect of altitude on the M-n stall boundary is large as compared with that on the V-n stall boundary. The data points in figure 66 which fall on or near the M-n 5,000-foot-altitude stall boundary were obtained near sea level. In the M-n diagram the sea-level stall boundary will be higher than the 5,000-foot stall boundary whereas the sea-level and 5,000-foot boundaries in the V-n diagram are about the same; therefore, the position of the data with respect to the sea-level boundary will be the same in the two figures.

In the envelopes for general flying for the altitude range from sea level to 15,000 feet (figs. 65 and 66), the highest load factors of 6.4 and 6.1 were measured during the pullout from the simulated dive-bomb run shown in figure 27. The other high load factors above 6 were recorded during the tight turns shown in figure 7. For the general-flying maneuvers at 15,000 feet to 30,000 feet (figs. 67 and 68), the load factors shown at 5.5 and above were recorded in the pitch-up shown in figure 57. The load factors above the stall boundary in the vicinity of 275 knots were, of course, also obtained during pitch-ups. The negative-load factors shown in figures 67 and 68 were recorded during portions of flights where load factors of less than 1 were intentionally applied in checking out new engines. In the envelopes for 30,000 feet to 42,000 feet, all load factors above 2.8, as well as those above the stall boundary (see fig. 69) at the lower airspeeds, resulted from pitch-ups.

CONCLUDING REMARKS

A flight investigation conducted on a Republic F-84F service airplane during routine squadron operations has indicated that the service pilots utilized the positive portion of the V-n or M-n diagram when performing various tactical maneuvers. In the flight time recorded in these tests, however, the negative normal-load-factor limits were not approached.

The maximum values of rolling velocity and rolling acceleration recorded were 3.8 radians per second and 11 radians per second per second, respectively. The maximum values of pitching velocity and pitching acceleration resulted from pitch-ups and were 3.8 radians per second and 4 radians per second per second, respectively. In addition, directional oscillations at the high speeds during LABS (low-altitude bombing system) missions produced yawing accelerations up to 1.4 radians per second per second and transverse load factors up to 0.8. All these values are considerably higher than any previously recorded during similar tests made with other fighter airplanes.

Langley Aeronautical Laboratory,
National Advisory Committee for Aeronautics,
Langley Field, Va., April 19, 1957.

REFERENCES

1. Mayer, John P., Hamer, Harold A., and Huss, Carl R.: A Study of the Use of Controls and the Resulting Airplane Response During Service Training Operations of Four Jet Fighter Airplanes. NACA RM L53L28, 1954.

2. Mayer, John P., and Hamer, Harold A.: A Study of Service-Imposed Maneuvers of Four Jet Fighter Airplanes in Relation to Their Handling Qualities and Calculated Dynamic Characteristics. NACA RM L55E19, 1955.

3. Mayer, John P., and Hamer, Harold A.: Applications of Power Spectral Analysis Methods to Maneuver Loads Obtained on Jet Fighter Airplanes During Service Operations. NACA RM L56J15, 1957.

4. Hallissy, Joseph M., Jr., and Kudlacik, Louis: A Transonic Wind-Tunnel Investigation of Store and Horizontal-Tail Loads and Some Effects of Fuselage-Afterbody Modifications on a Swept-Wing Fighter Airplane. NACA RM L56A26, 1956.

TABLE I.- DIMENSIONS AND PHYSICAL CHARACTERISTICS OF THE REPUBLIC F-84F TEST AIRPLANE

Wing (true dimensions and areas):	
Total wing area (including flaps, ailerons, and 50.6 sq ft covered by fuselage), sq ft	324.7
Span, ft	33.6
Aspect ratio	3.45
Taper ratio, (Tip chord/Root chord)	0.578
Theoretical root chord (measured parallel to fuselage center line), in.	148.6
Theoretical tip chord (measured parallel to fuselage center line), in.	86.0
Mean aerodynamic chord (at wing station 90.6 measured normal to fuselage center line), in.	120.5
Distance from nose to leading edge of wing mean aerodynamic chord (parallel to fuselage center line), in.	187.6
Vertical location of wing mean aerodynamic chord (25 percent) in reference to fuselage center line, in.	14.44
Sweepback (measured at 25-percent-chord line), deg	40
Theoretical root and tip airfoil section (measured normal to 25-percent-chord line)	NACA 64A010
Airfoil thickness ratio (measured parallel to fuselage center line), percent chord	8.1
Incidence, deg	1.5
Geometric twist, deg	0
Cathedral, deg	3.5
Aileron area (two), sq ft	27.9
Aileron static control limits, deg	±18
Spoiler area (two), sq ft	7.7
Spoiler static control limit (up only), deg	45
Stabilator:	
Total area, sq ft	55.8
Span, ft	14.17
Aspect ratio	3.59
Taper ratio	1.0
Chord (measured parallel to fuselage center line), in.	48.0
Mean aerodynamic chord, in.	48.0
Root and tip airfoil section (measured normal to leading edge)	NACA 64A009
Airfoil thickness ratio (measured parallel to fuselage center line), percent chord	6.9
Sweepback, deg	40
Dihedral, deg	0
Tail length (25 percent wing mean aerodynamic chord to 25 percent stabilator mean aerodynamic chord), ft	19.6

TABLE I.- DIMENSIONS AND PHYSICAL CHARACTERISTICS OF THE REPUBLIC F-84F TEST AIRPLANE - Concluded

Static control limits, deg from neutral position	
Trailing edge up (gear up)	11.25
Trailing edge up (gear down)	16.5
Trailing edge down (gear up)	4.25
Trailing edge down (gear down)	4.5
Vertical tail:	
Total area (does not include dorsal and ventral fin area), sq ft	42.9
Theoretical root chord (measured parallel to fuselage center line), in.	87.0
Location of theoretical root chord above fuselage center line, in.	15.25
Dorsal fin area, sq ft	2.02
Ventral fin area, sq ft	2.12
Span (from theoretical root chord), ft	8.5
Aspect ratio	1.68
Taper ratio	0.402
Mean aerodynamic chord (located 60 inches above fuselage center line), in.	64.6
Root and tip airfoil section (measured normal to 25-percent-chord line)	NACA 64A011
Sweepback (measured at 25-percent-chord line), deg	41.27
Tail length (25 percent wing mean aerodynamic chord to 25 percent vertical-tail mean aerodynamic chord), ft	18.0
Rudder area, sq ft	10.37
Rudder static control limits, deg	±23.5
Fuselage:	
Length (excluding nose boom), ft	38.42
Maximum width, ft	4.17
Frontal area (excluding canopy), sq ft	19.43
Speed brake area (two), sq ft	11.7
General:	
Power plant (one)	Wr.J-65-B3
Airplane serial number	AF 52-6984
Weight of empty 230-gallon tank, lb	
Inboard	173
Outboard	90
Weight of empty 450-gallon tank, lb	249
Weight of outboard pylon (one), lb	80
Weight of 1 gallon of fuel (assumed), lb	6.5
Spanwise location of inboard pylon, in.	44
Spanwise location of outboard pylon, in.	149.5

TABLE II.- MASS CHARACTERISTICS OF THE REPUBLIC F-84F TEST AIRPLANE

Configuration and loading (a)	Measured weight, lb (b)	Measured center-of-gravity location (gear up), percent $\bar{c}$ (b)	Approximate moments of inertia about airplane axes (gear up), slug-ft^2 (b)		
			I_X(roll)	I_Y(pitch)	I_Z(yaw)
Clean; no fuel	14,780	24.3	13,600	29,700	41,400
Clean; full fuel	18,540	20.0	17,700	32,700	48,100
Clean plus one empty 230-gallon tank (inboard); full internal fuel	18,710	20.2	17,900	32,700	48,100
Clean plus one full 230-gallon tank (inboard); full internal fuel	20,210	20.3	19,000	33,800	49,300
Clean plus two empty 230-gallon tanks (inboard); full internal fuel	18,890	20.4	18,000	32,900	48,400
Clean plus two full 230-gallon tanks (inboard); full internal fuel	21,880	20.6	20,200	34,600	50,400
Clean plus one empty 450-gallon tank (inboard); full internal fuel	18,790	20.0	17,900	33,000	48,400
Clean plus one full 450-gallon tank (inboard); full internal fuel	21,710	19.5	20,300	36,000	51,500
Clean plus one empty 450-gallon tank (inboard) and one 1,700-pound practice bomb (inboard); full internal fuel	20,490	18.1	19,300	34,600	50,000
Clean plus one full 450-gallon tank (inboard) and one 1,700-pound practice bomb (inboard); full internal fuel	23,410	17.9	21,600	37,400	53,100
Clean plus one empty 450-gallon tank (inboard), one 1,700-pound practice bomb (inboard), and two empty 230-gallon tanks (outboard); full internal fuel	20,670	18.4	20,300	34,800	51,100
Clean plus one full 450-gallon tank (inboard), one 1,700-pound practice bomb (inboard), and two full 230-gallon tanks (outboard); full internal fuel	26,580	22.8	38,200	40,500	70,200

[a] Clean includes two inboard and two outboard pylons.

[b] Weight of 200-pound pilot included. External fuel is normally used before internal fuel.

TABLE III.- SUMMARY OF MEASURED QUANTITIES

Quantity	Maximum instrument error plus reproduction error
Pressure altitude, H_p, ft	*±200
Indicated airspeed, V_i, knots	*±10
Mach number, M	*±0.02
Stabilator angle, δ_s, deg	±0.2
Rudder angle, δ_r, deg	±0.5
Aileron angle, δ_a, deg	±0.5
Spoiler angle, deg	±2.0
Stabilator stick angle, δ_{ss}, deg	±0.5
Aileron or spoiler stick angle, δ_{as}, deg	±0.5
Stabilator stick force, F_s, lb	±0.8
Aileron stick force, F_a, lb	
For flights 2 through 25	±0.8
For flights 26 through 53	±3.0
Rudder force, F_r, lb	±5.0
Normal load factor, n_V	±0.1
Transverse load factor, n_T	±0.05
Longitudinal load factor, n_L	±0.05
Pitching velocity, q, radians/sec	±0.02
Yawing velocity, r, radians/sec	±0.02
Rolling velocity, p, radians/sec	±0.15
Pitching acceleration, $\dot{q}$, radians/sec^2	±0.2
Yawing acceleration, $\dot{r}$, radians/sec^2	±0.08
Rolling acceleration, $\dot{p}$, radians/sec^2	±0.5
Sideslip angle, β, deg	*±0.4
Angle of attack, α, deg	*±0.4
Time, sec	±0.2

*Value does not include position error.

TABLE IV.- SUMMARY OF FLIGHTS

Flight	Pilot	Take-off weight, lb	Take-off center-of-gravity location, percent $\bar{c}$	Configuration (a)	Mission (b)
2	A	18,200	20.8	Clean	Transition
3	B	18,250	20.3	Clean (minus one outboard pylon)	Transition
5	C	18,200	20.0	Clean (minus two outboard pylons)	Transition
7	D	18,150	20.1	Clean (minus two outboard pylons)	Transition
9	E	18,200	20.0	Clean (minus two outboard pylons)	Transition
11	F	17,850	20.8	Clean (minus two outboard pylons)	Transition
13	G	18,150	20.1	Clean (minus two outboard pylons)	Transition
14	H	18,200	20.0	Clean (minus two outboard pylons)	Rat-racing and dive-bombing
15	G	18,250	19.9	Clean (minus two outboard pylons)	Transition
16	H	19,800	19.7	230-gallon tank on right inboard pylon (minus two outboard pylons)	Bombing, strafing, and rat-racing
17	C	19,800	19.7	230-gallon tank on right inboard pylon (minus two outboard pylons)	Formation flying
18	I	20,000	20.1	230-gallon tank on right inboard pylon	Transition and strafing
19	J	20,000	20.1	230-gallon tank on right inboard pylon	Transition
20	J	20,000	20.1	230-gallon tank on right inboard pylon	Transition
25	K	19,900	20.0	230-gallon tank on right inboard pylon	Formation flying
26	L	18,300	20.5	Clean	Transition
28	B	18,350	20.4	Clean	Transition
29	M	21,650	20.4	Two 230-gallon tanks on inboard pylons and 3-pound practice bombs	LABS
31	M	21,700	20.4	Two 230-gallon tanks on inboard pylons and 3-pound practice bombs	LABS
34	N	21,600	20.3	Two 230-gallon tanks on inboard pylons and 3-pound practice bombs	LABS
37	M	21,700	20.4	Two 230-gallon tanks on inboard pylons and 3-pound practice bombs	Dive-bombing
40	O	20,000	20.2	230-gallon tank on right inboard pylon and 3-pound practice bombs	Dive-bombing
47	P	21,450	19.0	450-gallon tank on right inboard pylon	Transition and rat-racing
48	K	23,100	17.3	450-gallon tank on right inboard pylon and 1,700-pound practice bomb on left inboard pylon	LABS
49	O	27,200	25.2	450-gallon tank on right inboard pylon, 1,700-pound practice bomb on left inboard pylon, two 230-gallon tanks on outboard pylons, and JATO unit	In-flight refueling
50	P	23,200	17.5	450-gallon tank on right inboard pylon and 1,700-pound practice bomb on left inboard pylon	LABS
51	Q	19,300	18.7	450-gallon tank on right inboard pylon	Transition
52	A	20,400	19.0	450-gallon tank on right inboard pylon, 1,700-pound practice bomb on left inboard pylon, and two 230-gallon tanks on outboard pylons	In-flight refueling
53	R	22,750	16.8	450-gallon tank on right inboard pylon, 1,700-pound practice bomb on left inboard pylon, and 3-pound practice bombs	LABS

[a] Airplane equipped with two outboard pylons (unless otherwise stated) and with two inboard pylons.

[b] Transition refers to familiarization flying which usually includes various acrobatic-type maneuvers.

TABLE V.- MANEUVER CLASSIFICATION

Type of maneuver:	Figures
Take-offs	4 to 5
Turns	6 to 9
Rolls	10 to 18
Immelman, loop, rudder kick, and so forth	19 to 23
Dives	24 to 29
Dive-bombing runs	30 to 35
Strafing runs	36 to 38
LABS (low-altitude bombing system) runs	39 to 46
Rat-racing	47 to 50
Pitch-ups	51 to 58
Formation flying, ground control approach, in-flight refueling, and so forth	59 to 61
Landings	62 to 64

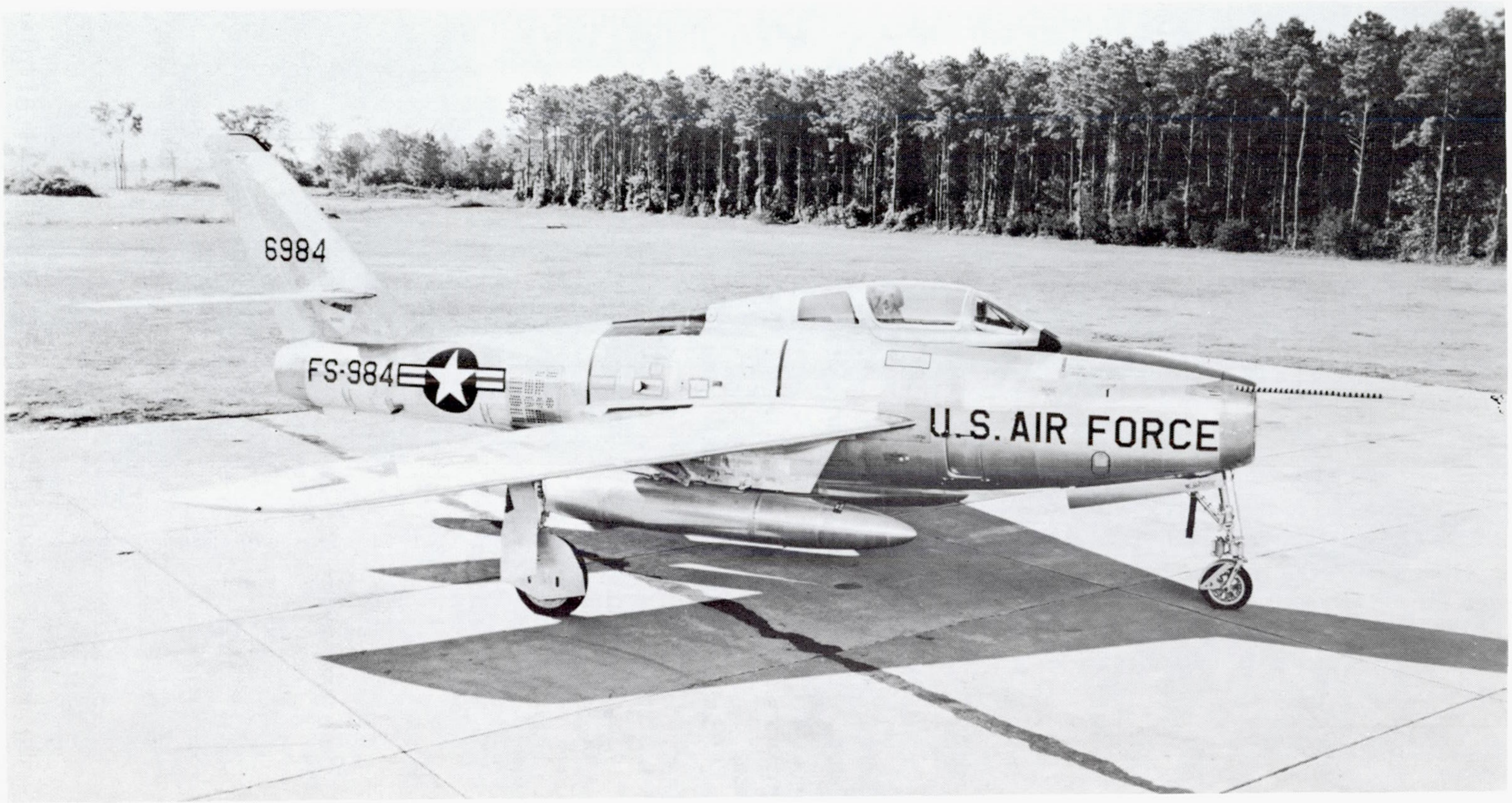

Figure 1.- Republic F-84F test airplane. L-91212

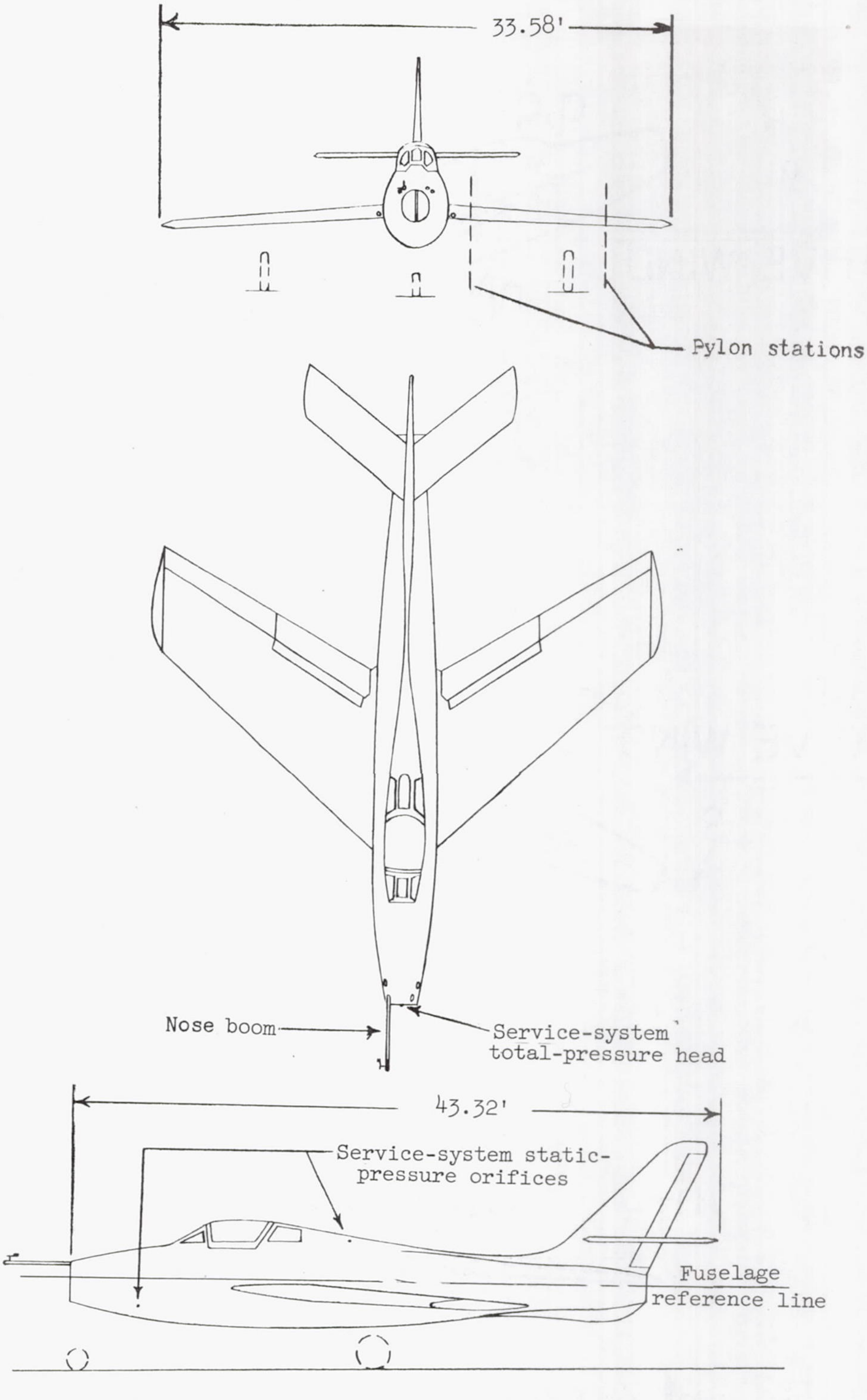
33.58'
Pylon stations
Nose boom
Service-system total-pressure head
43.32'
Service-system static-pressure orifices
Fuselage reference line

Figure 2.- Three-view drawing of Republic F-84F test airplane.

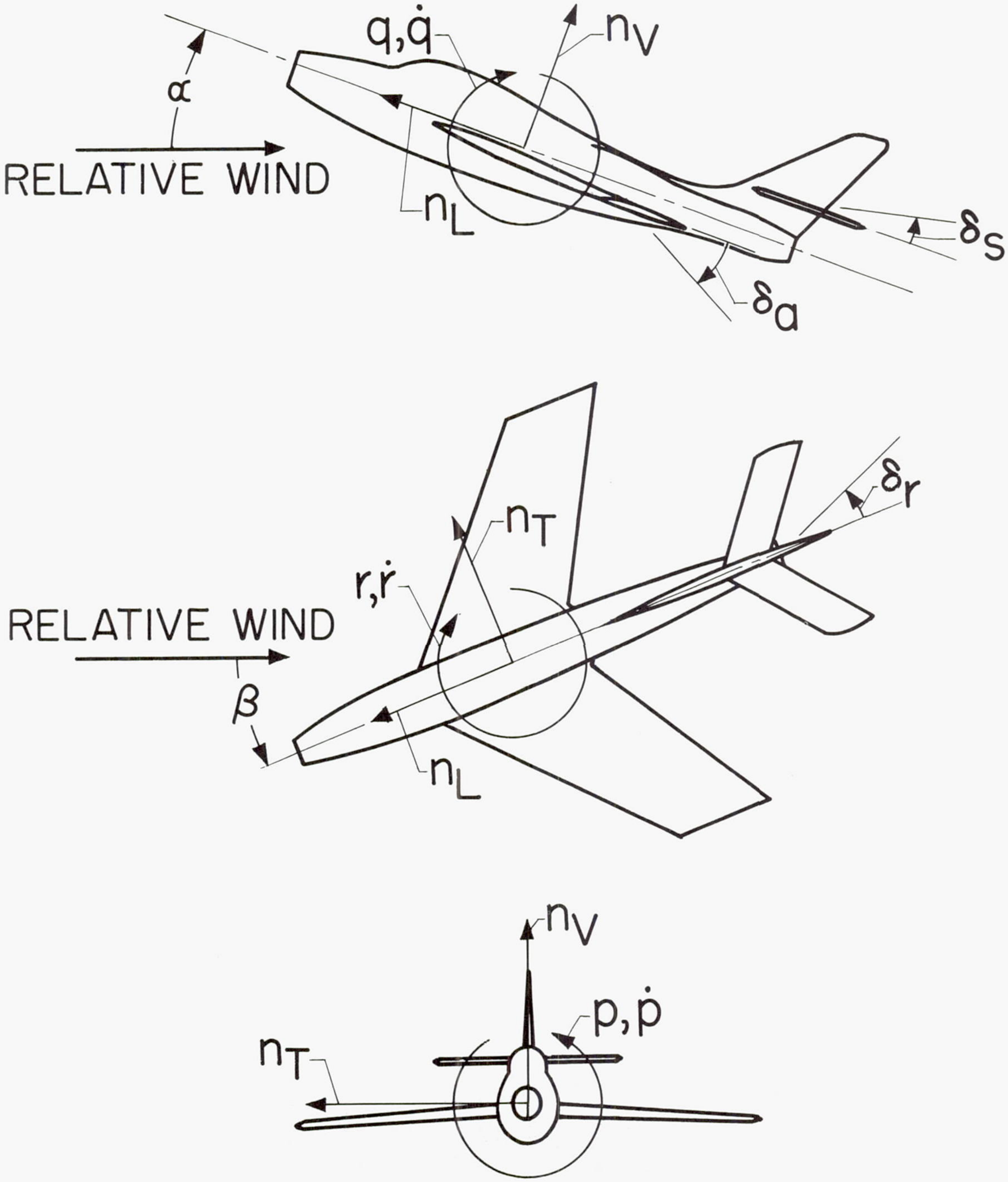

Figure 3.- Body-axis system showing positive directions.

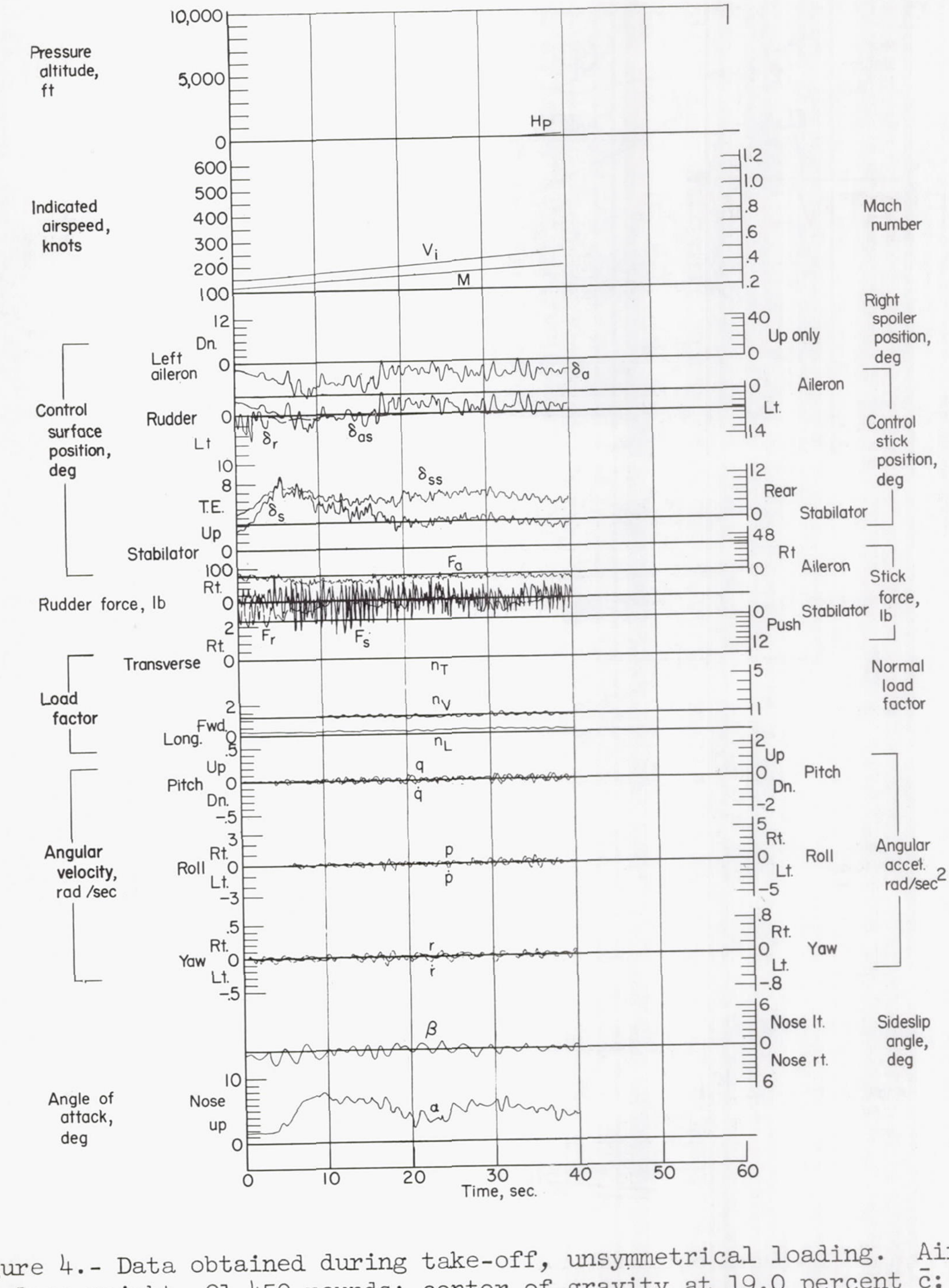

Figure 4.- Data obtained during take-off, unsymmetrical loading. Airplane weight, 21,450 pounds; center of gravity at 19.0 percent $\bar{c}$; flight 47.

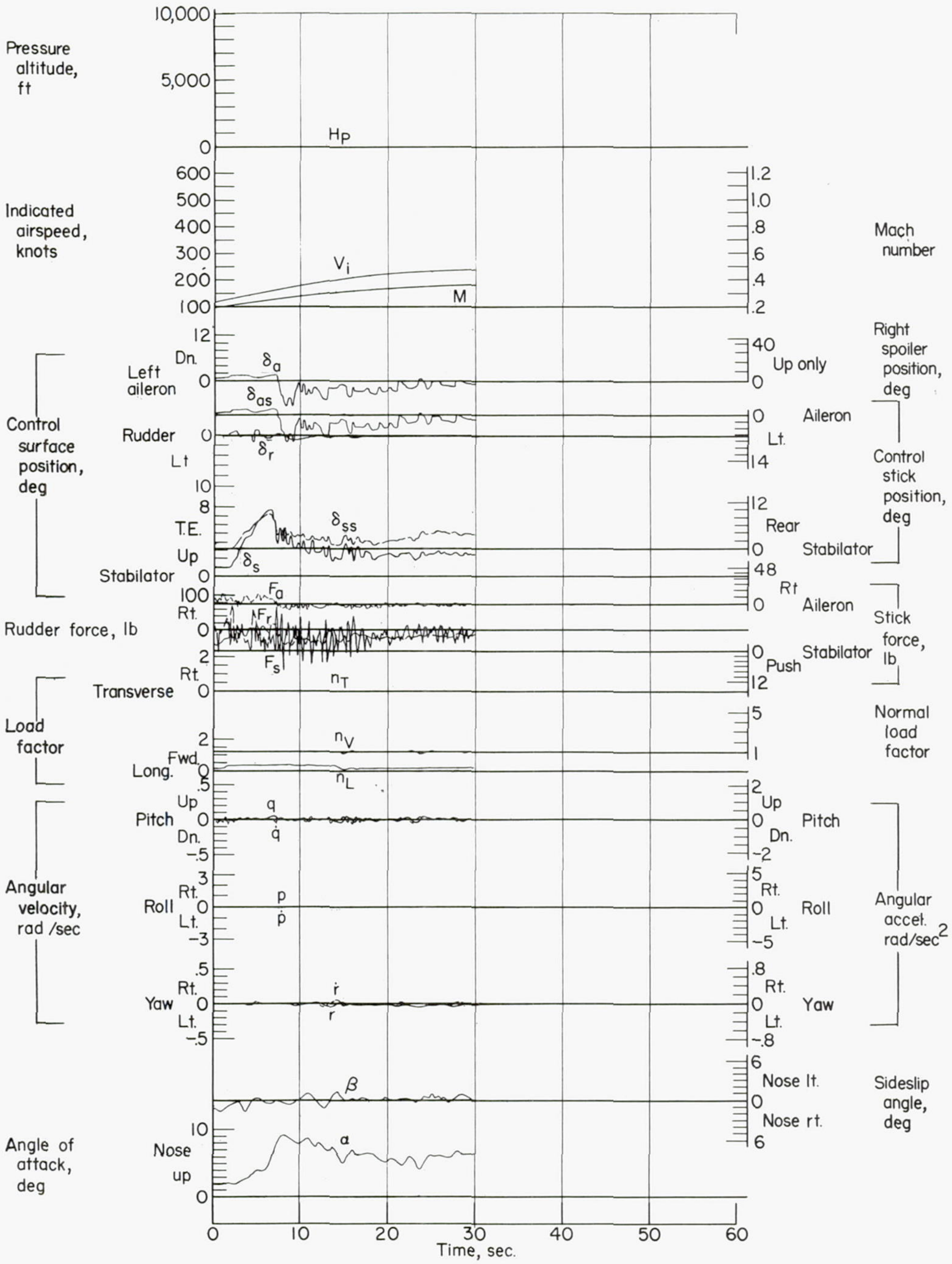

Figure 5.- Data obtained during take-off (JATO). Airplane weight, 27,050 pounds; center of gravity at 24.8 percent $\bar{c}$; flight 49.

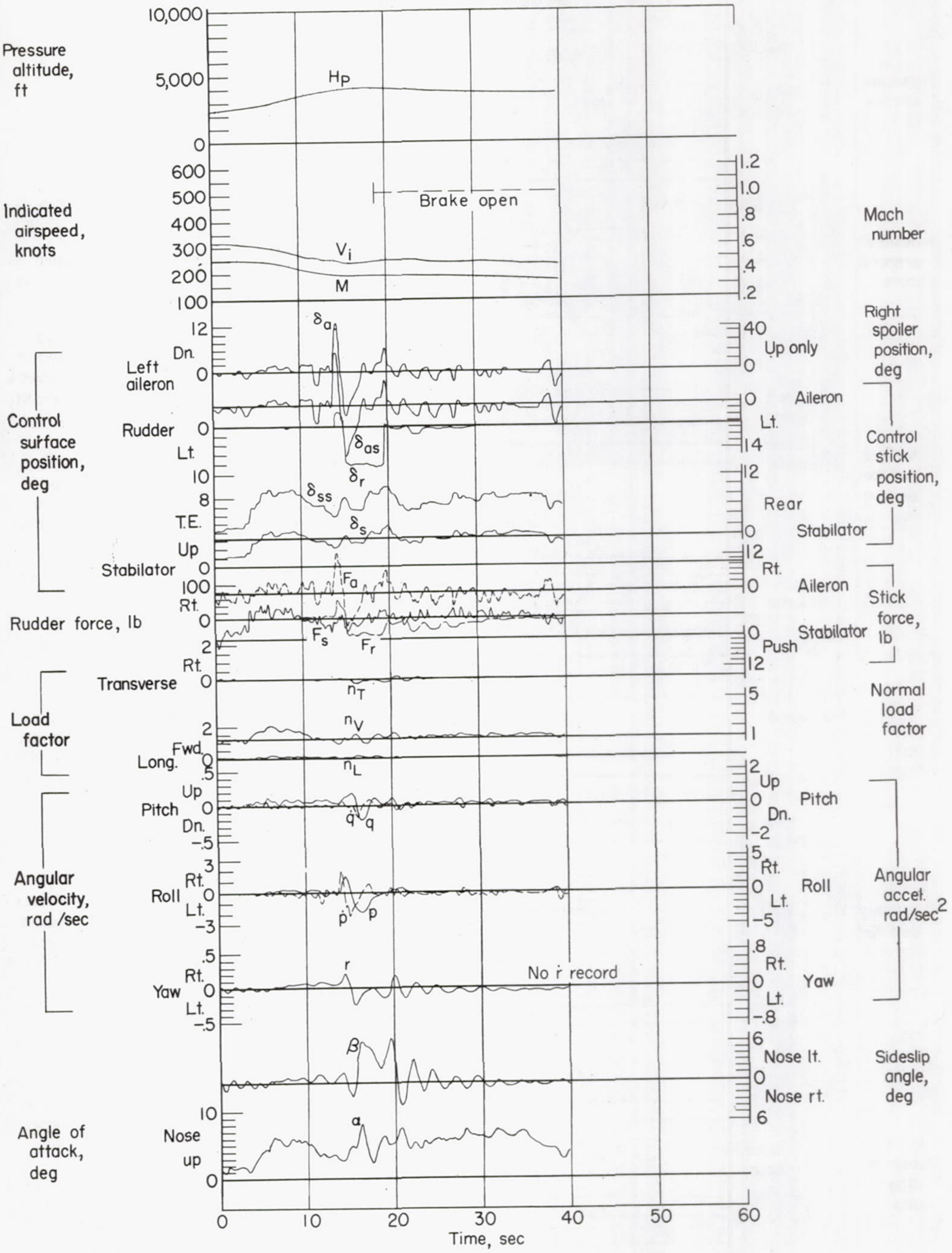

Figure 6.- Data obtained for a low-speed turn, flaps down. Airplane weight, 18,100 pounds; center of gravity at 21.0 percent $\bar{c}$; flight 2.

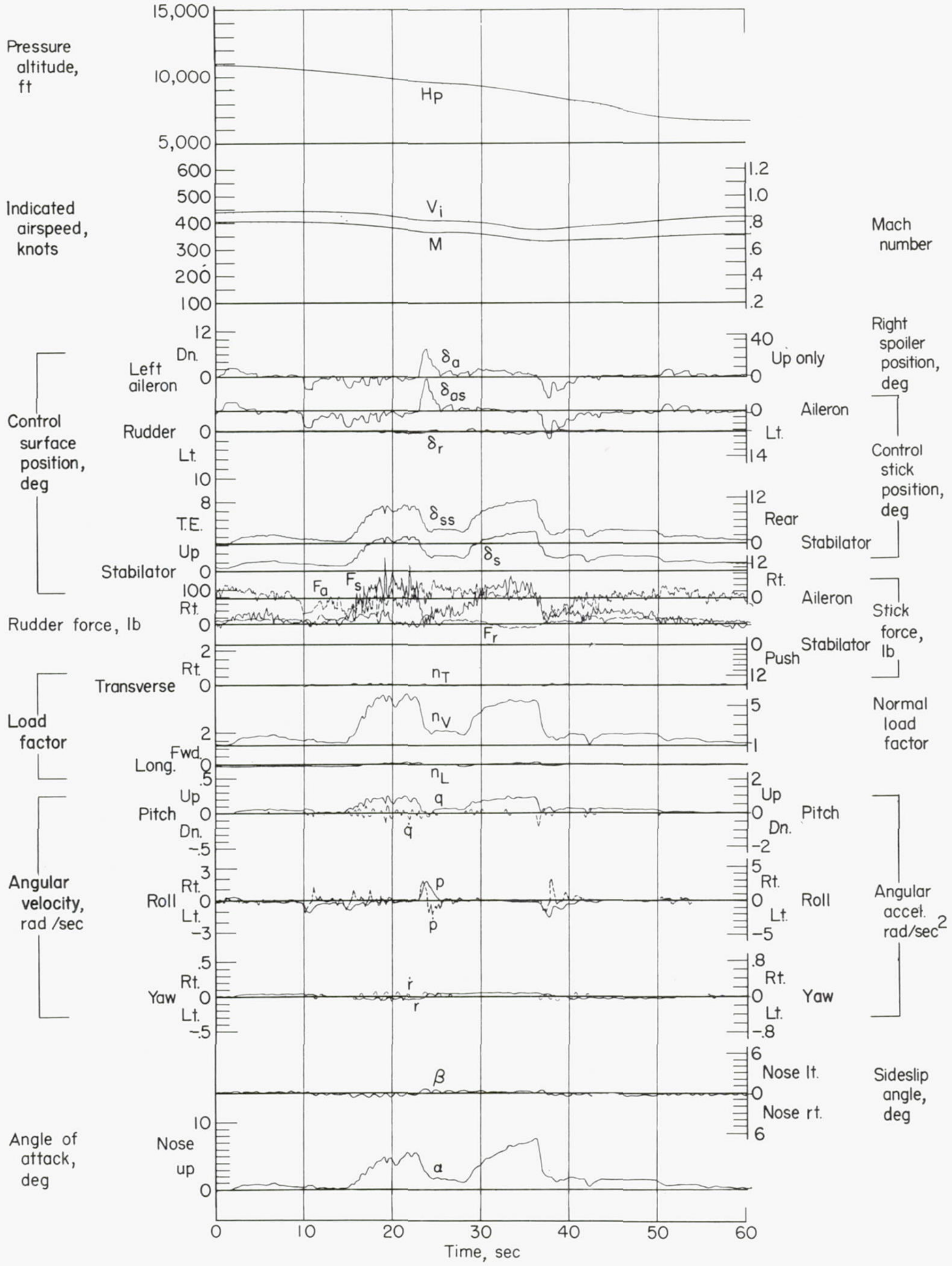

Figure 7.- Data obtained during tight turns. Airplane weight, 15,550 pounds; center of gravity at 22.3 percent $\bar{c}$; flight 14.

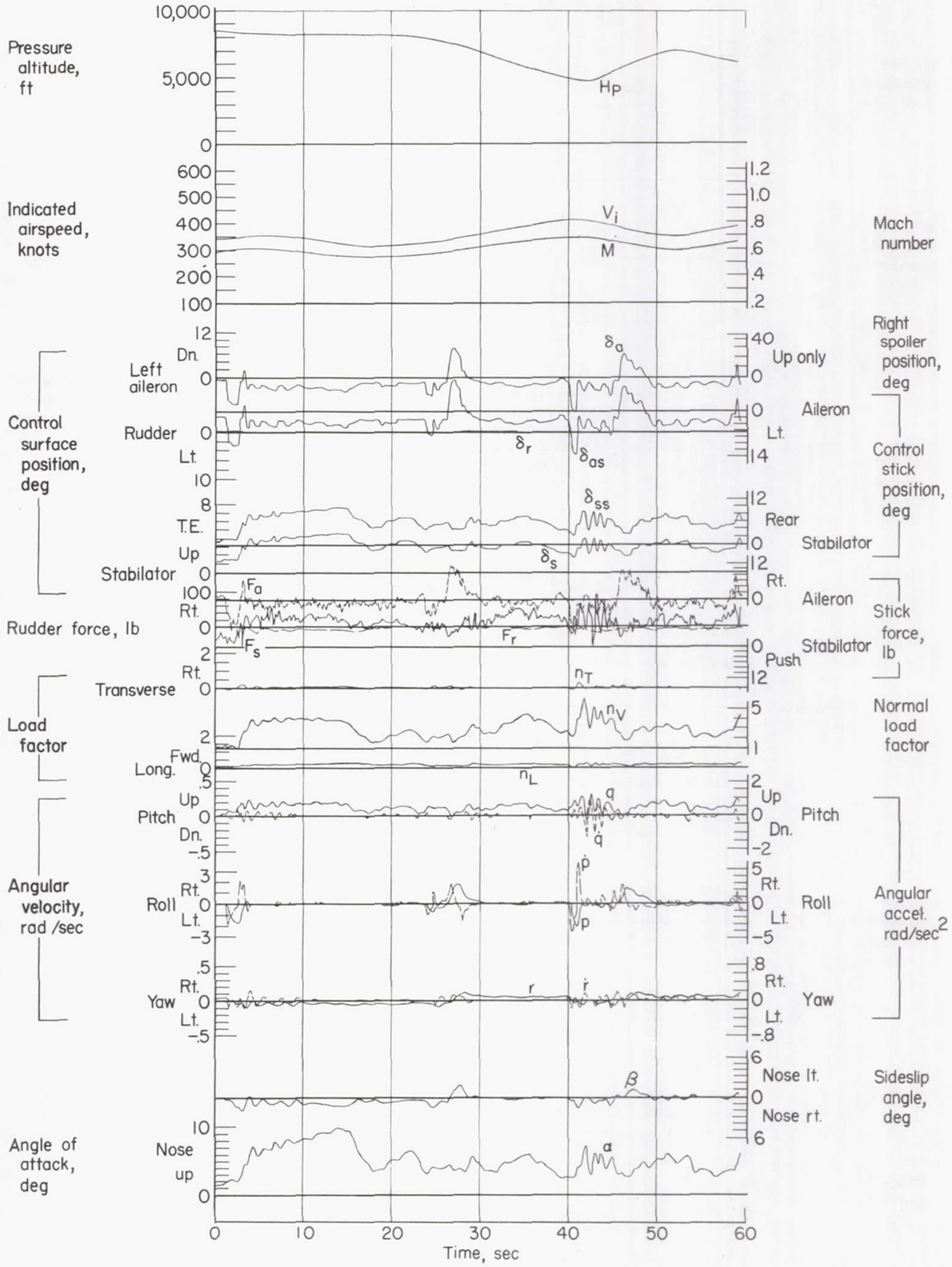

(a)

Figure 8.- Data obtained during series of turns. Airplane weight 17,400 pounds; center of gravity at 22.5 percent $\bar{c}$; flight 18.

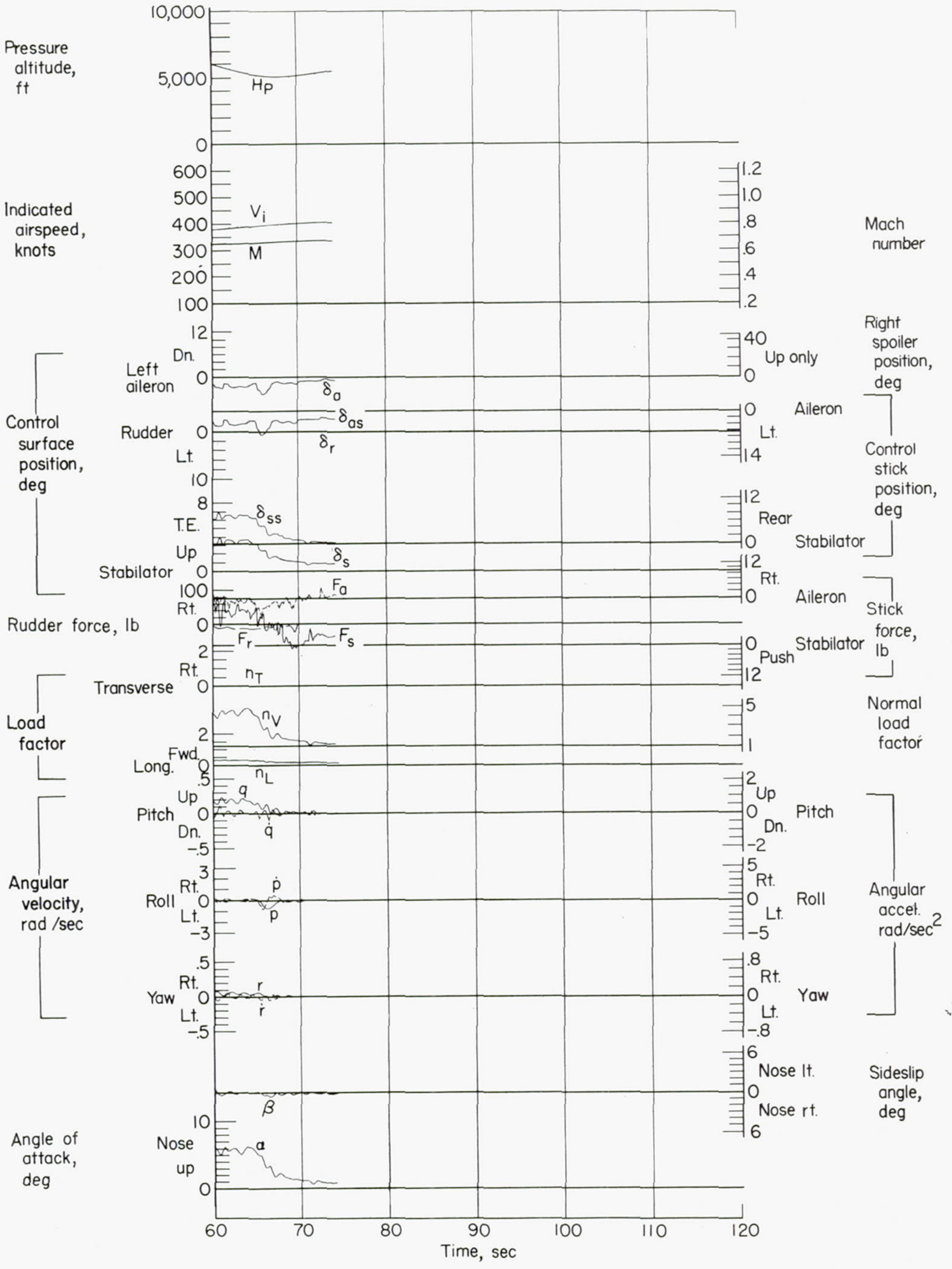

(b)

Figure 8.- Concluded.

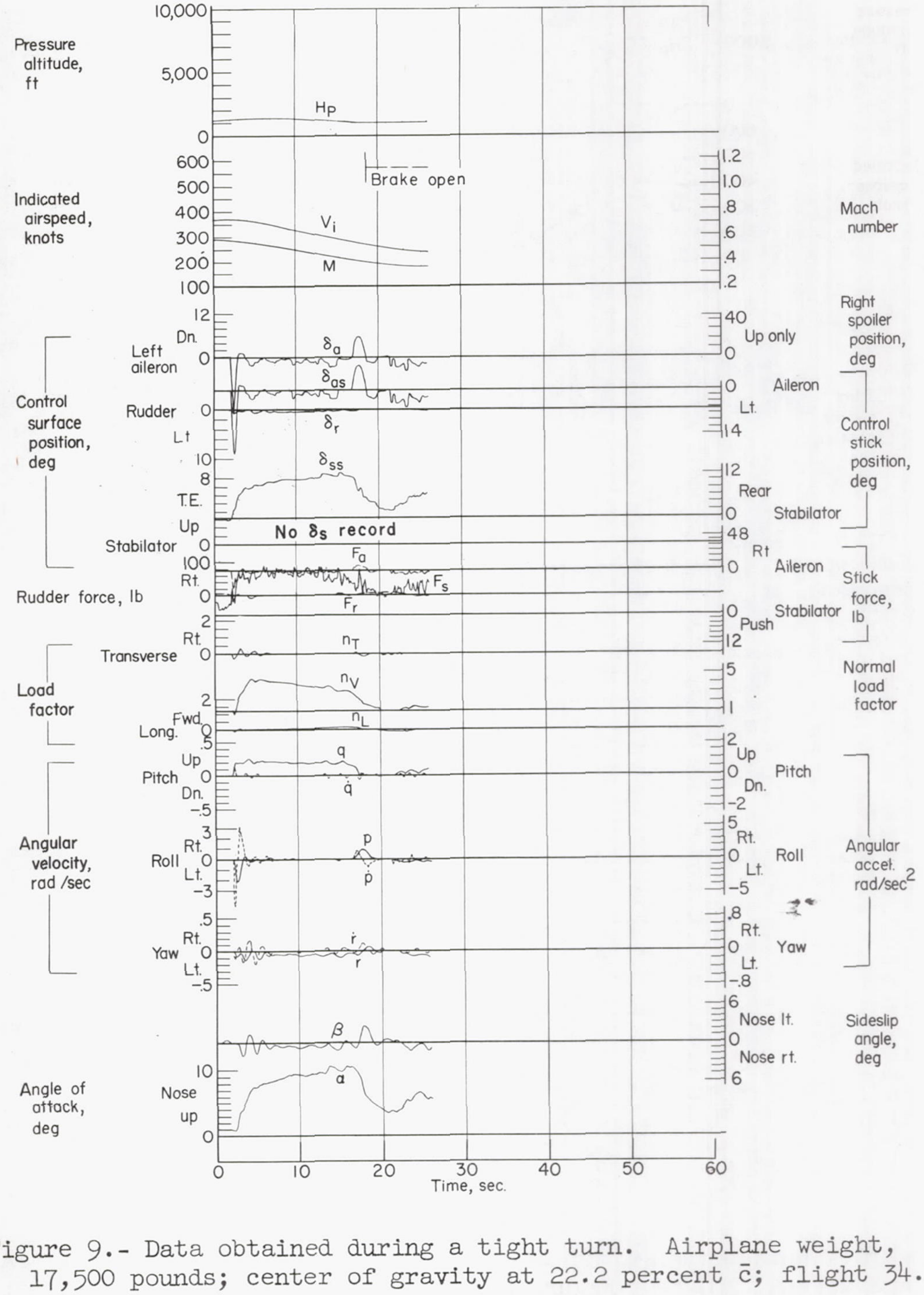

Figure 9.- Data obtained during a tight turn. Airplane weight, 17,500 pounds; center of gravity at 22.2 percent $\bar{c}$; flight 34.

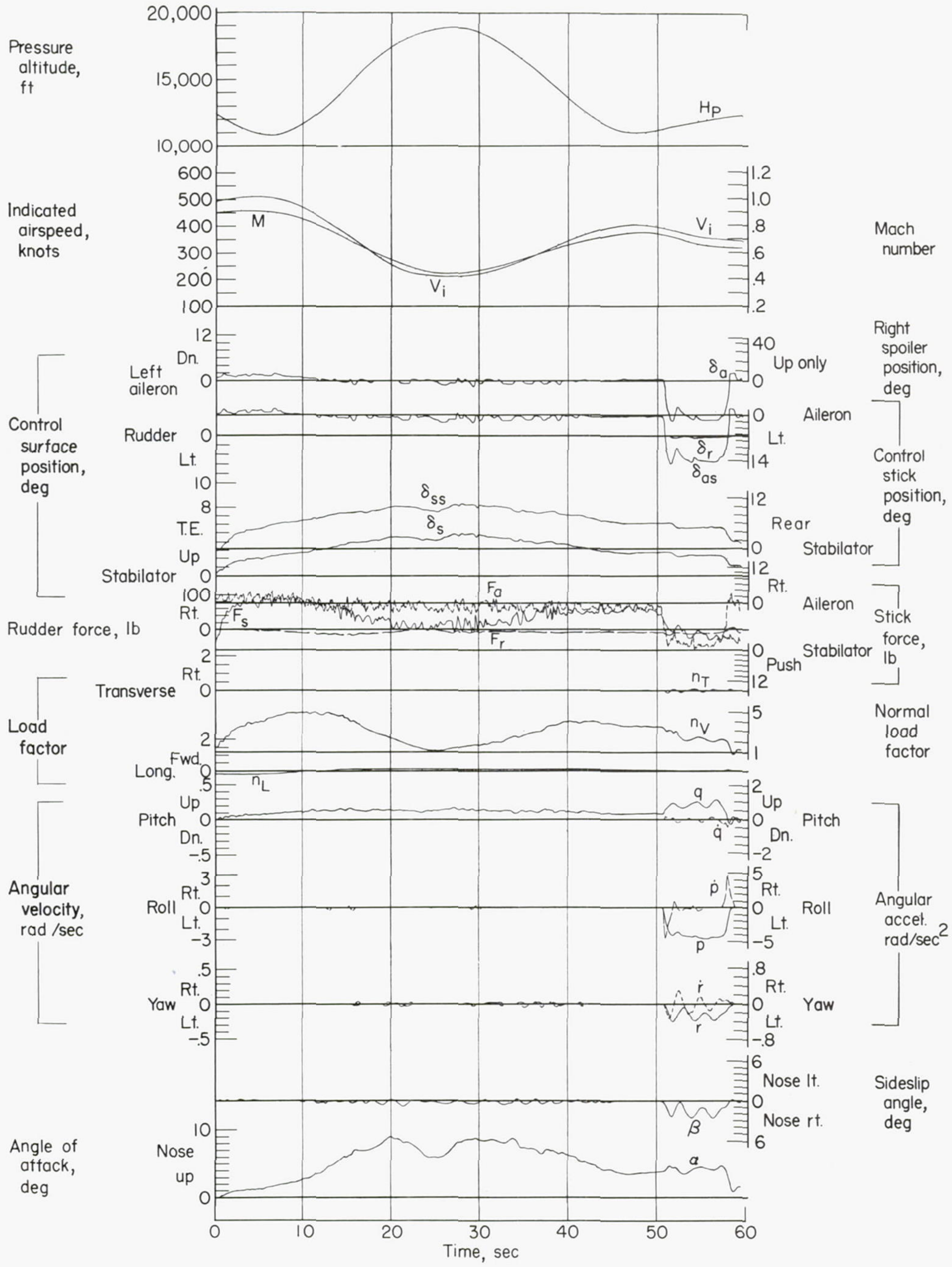

Figure 10.- Data obtained for a loop followed by rolling pullout. Airplane weight, 16,750 pounds; center of gravity at 22.1 percent $\bar{c}$; flight 3.

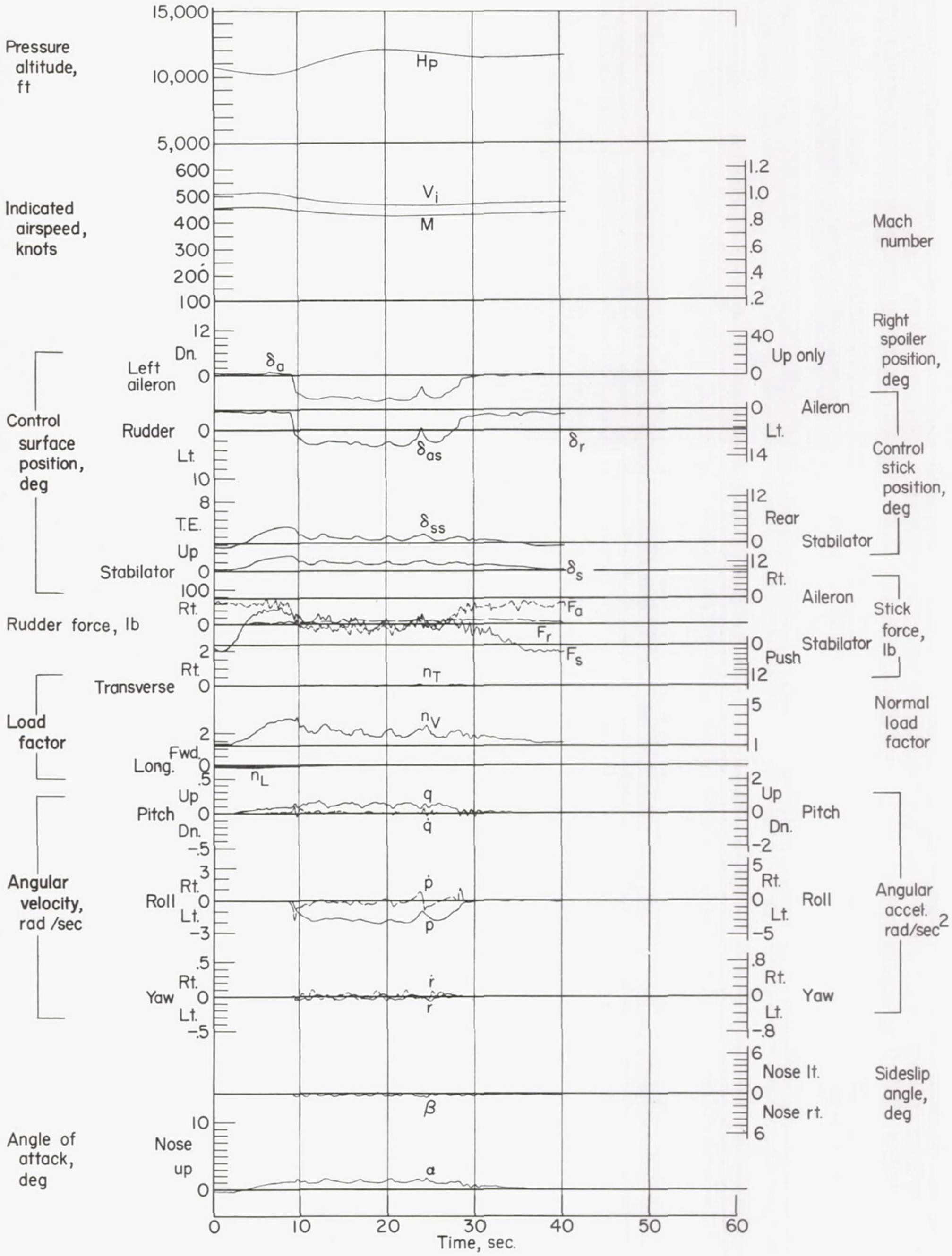

Figure 11.- Data obtained during eight consecutive barrel rolls. Airplane weight, 16,300 pounds; center of gravity at 22.0 percent $\bar{c}$; flight 7.

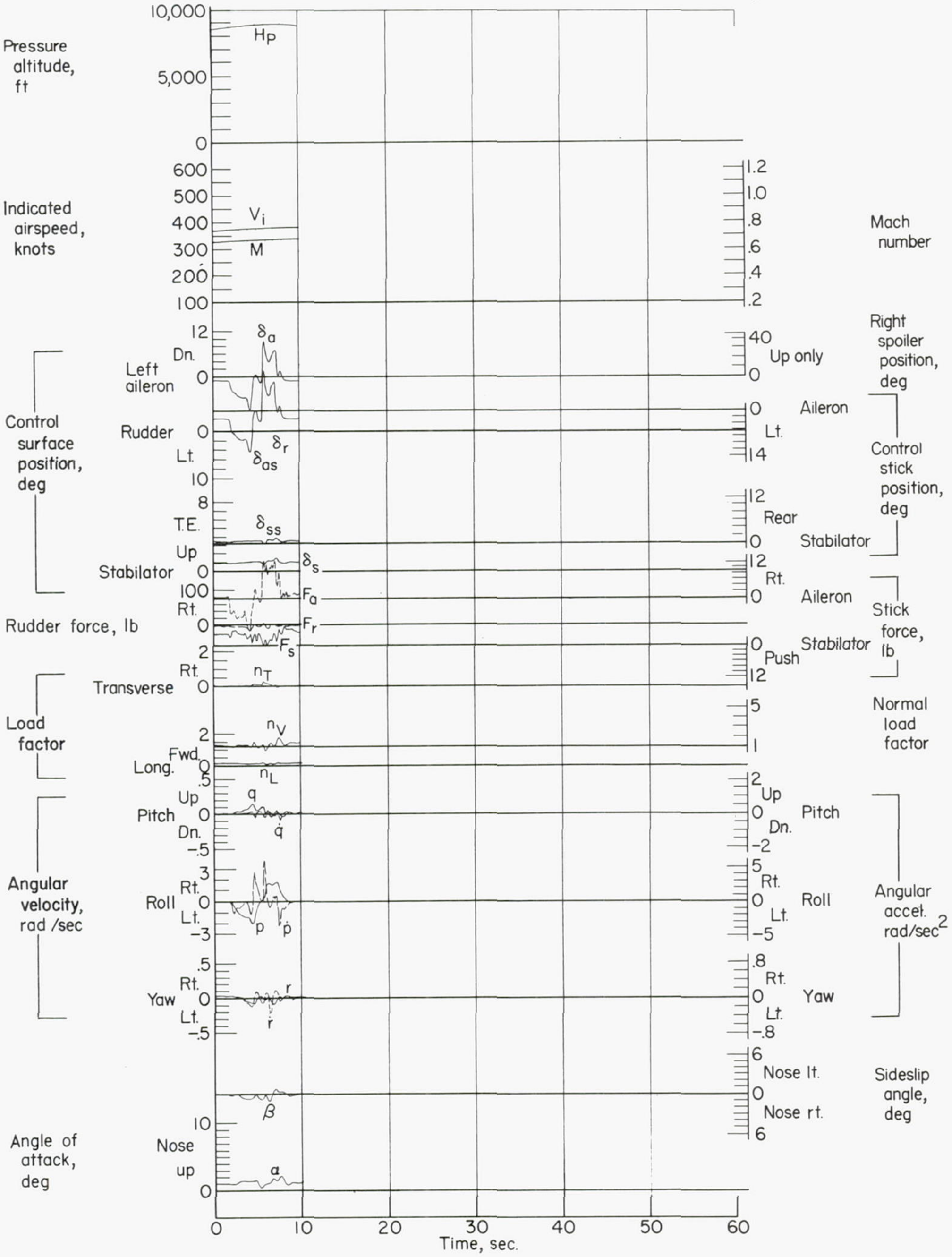

Figure 12.- Data obtained during rolls. Airplane weight, 16,900 pounds; center of gravity at 22.6 percent $\bar{c}$; flight 18.

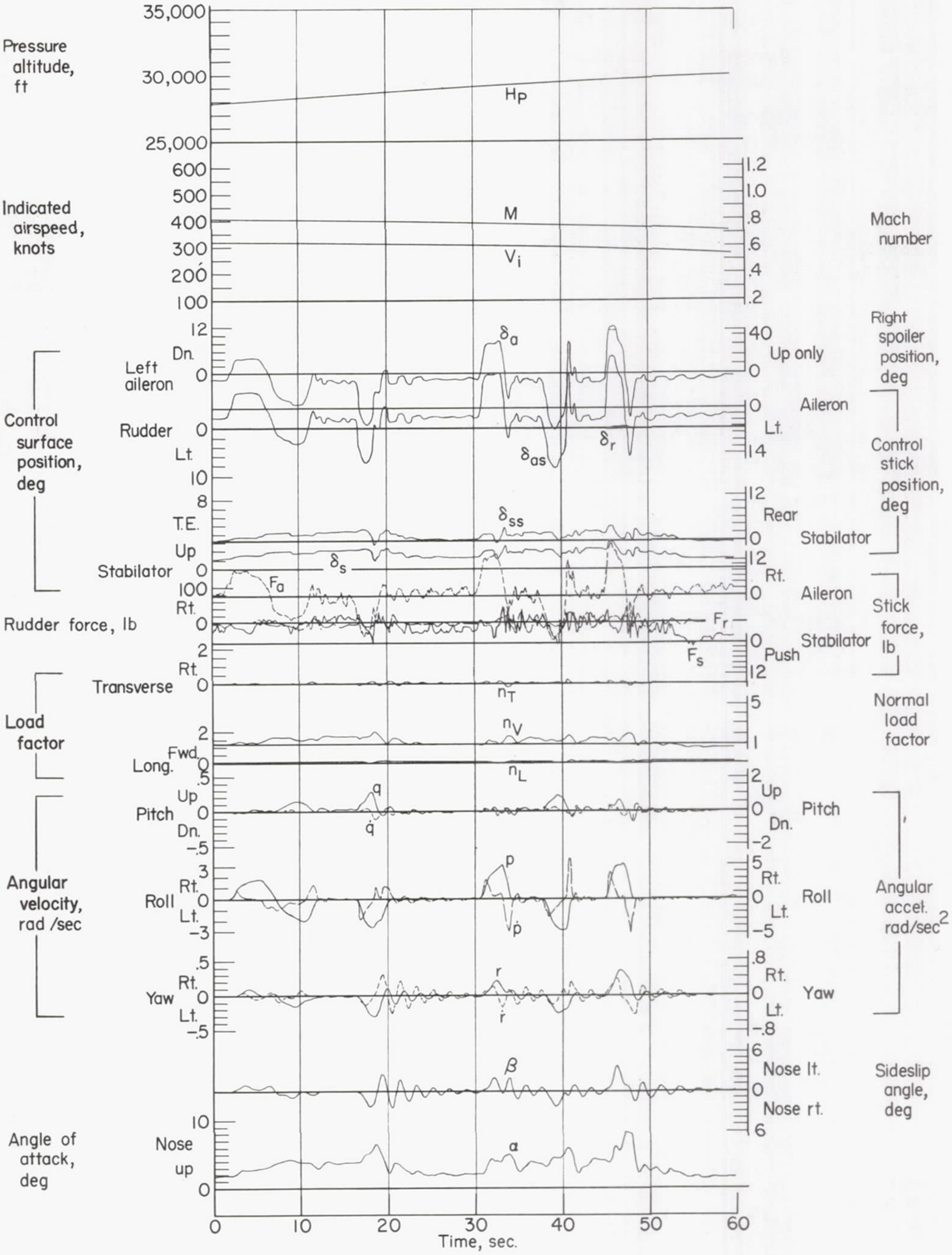

Figure 13.- Data obtained during abrupt rolls. Airplane weight, 18,550 pounds; center of gravity at 20.6 percent $\bar{c}$; flight 19.

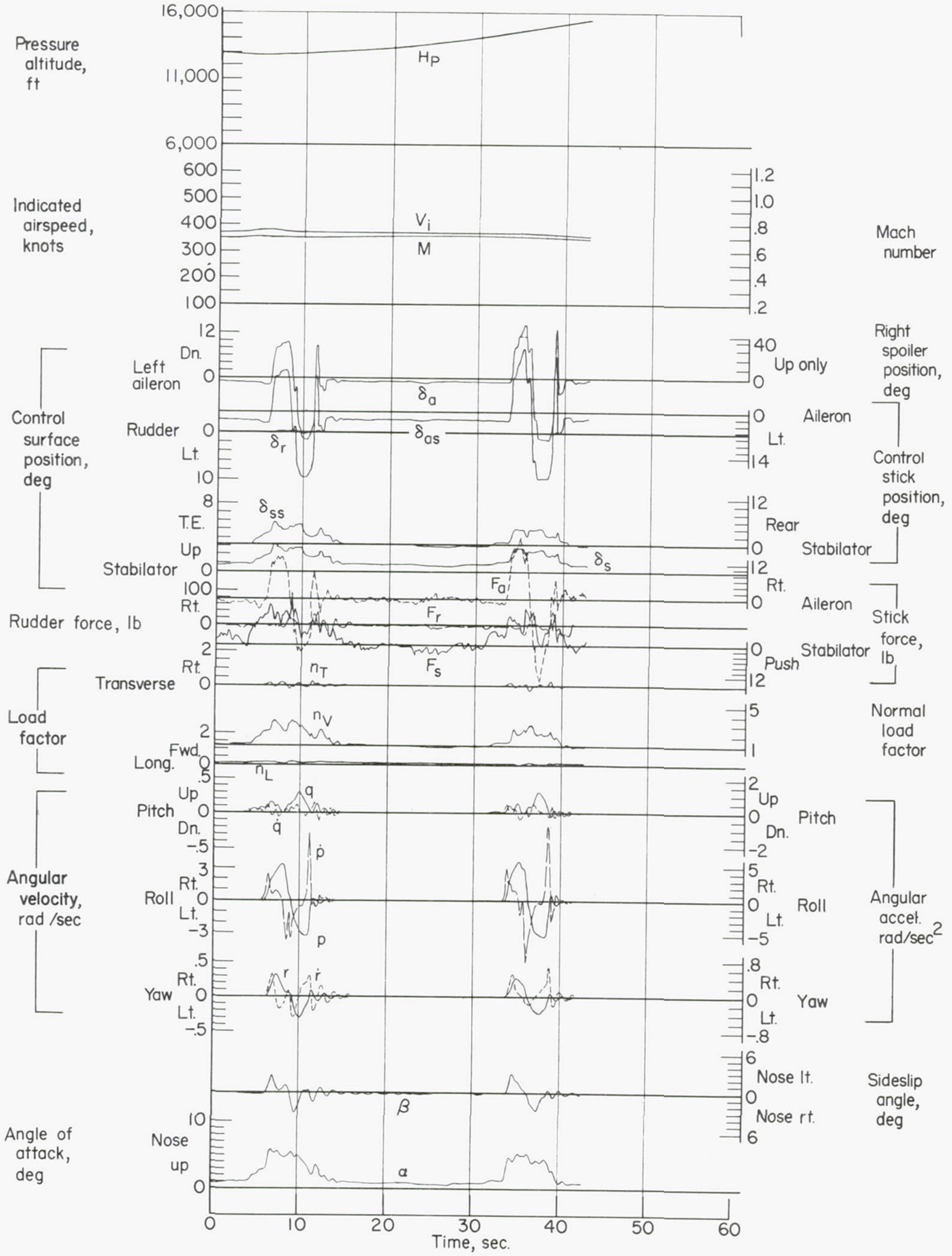

Figure 14.- Data obtained during full-aileron rolls. Airplane weight, 16,900 pounds; center of gravity at 22.6 percent $\bar{c}$; flight 19.

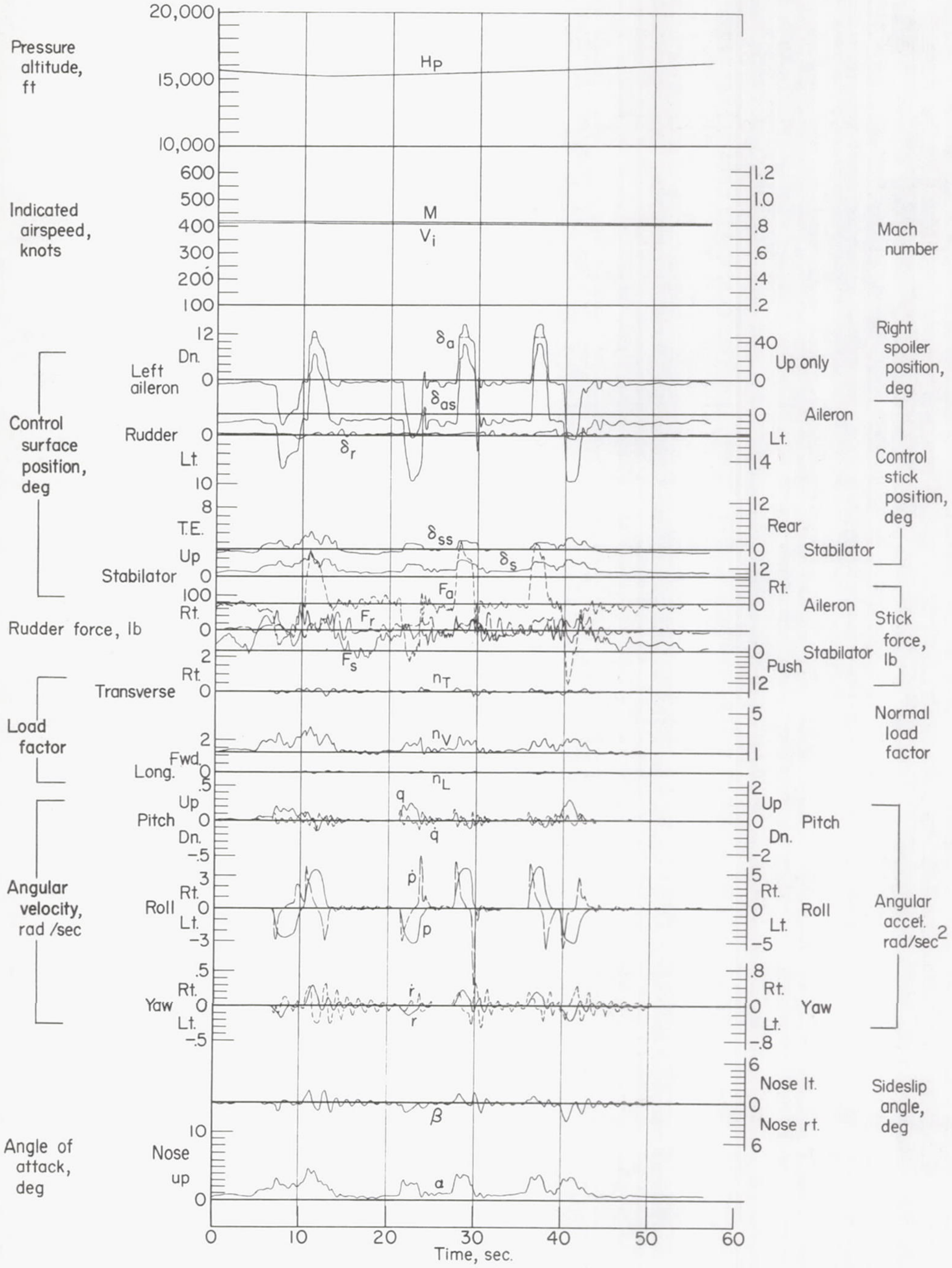

Figure 15.- Data obtained during full-aileron rolls. Airplane weight, 18,600 pounds; center of gravity at 20.5 percent $\bar{c}$; flight 20.

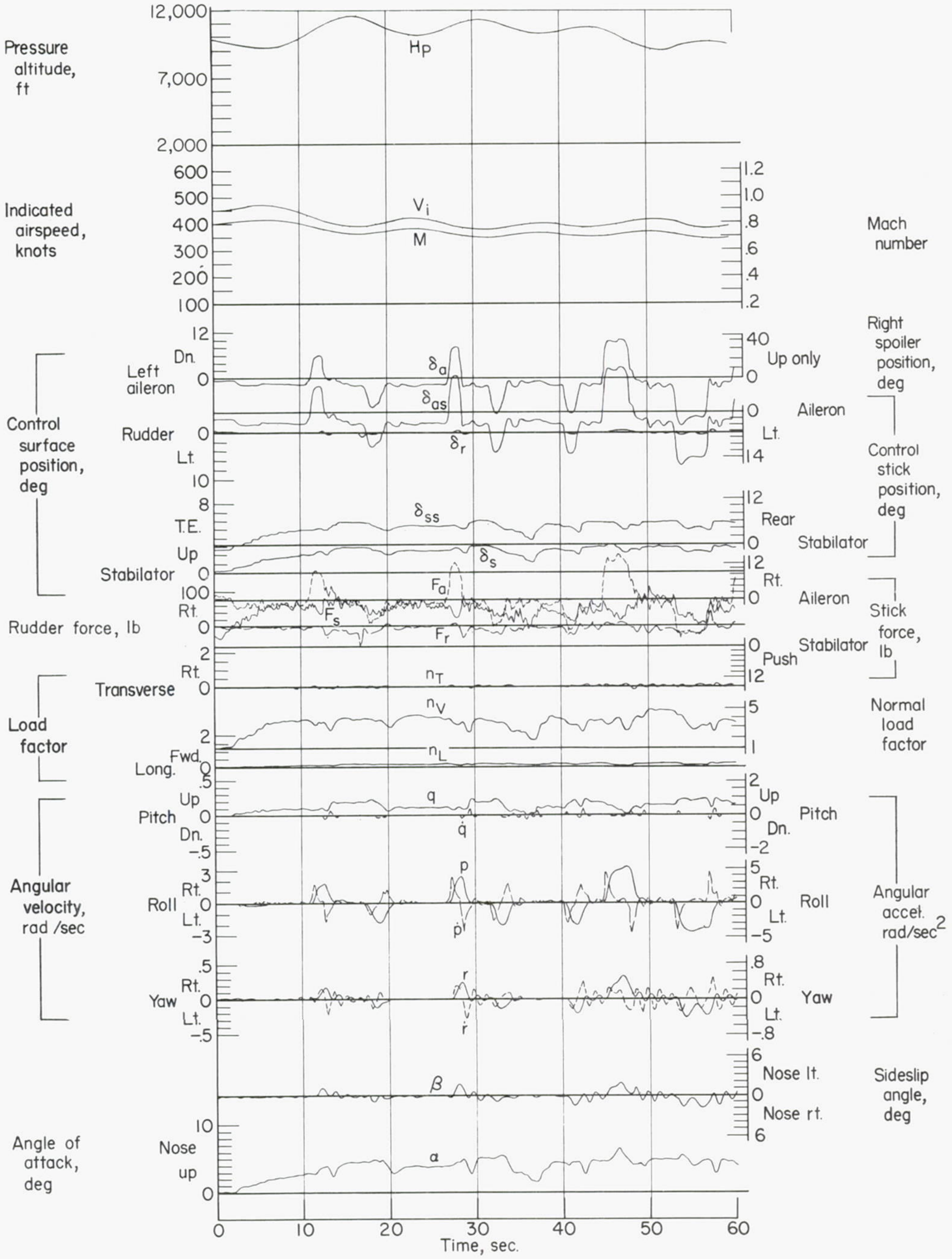

(a)

Figure 16.- Data obtained during barrel rolls. Airplane weight, 17,650 pounds; center of gravity at 22.4 percent $\bar{c}$; flight 20.

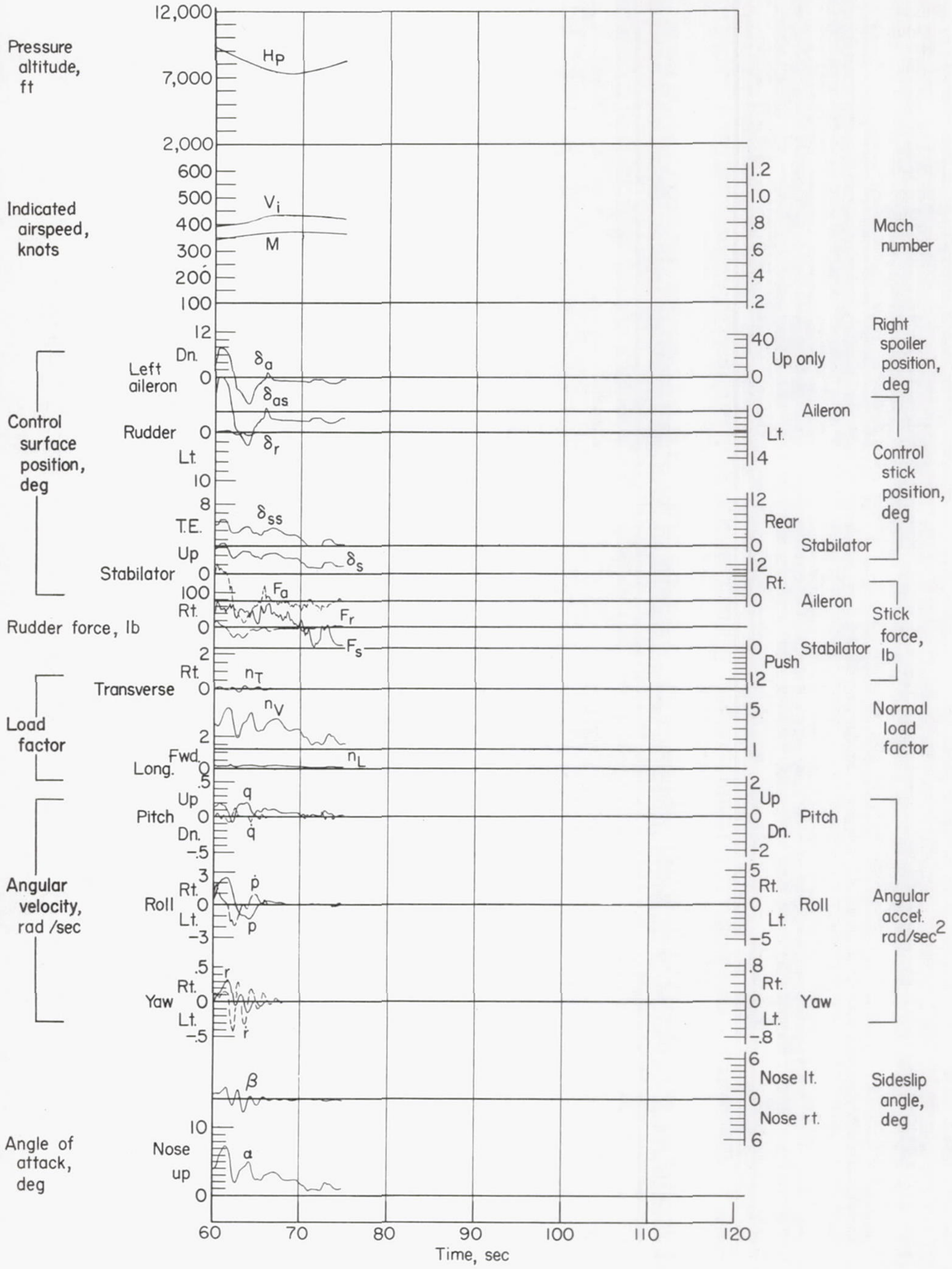

(b)

Figure 16.- Concluded.

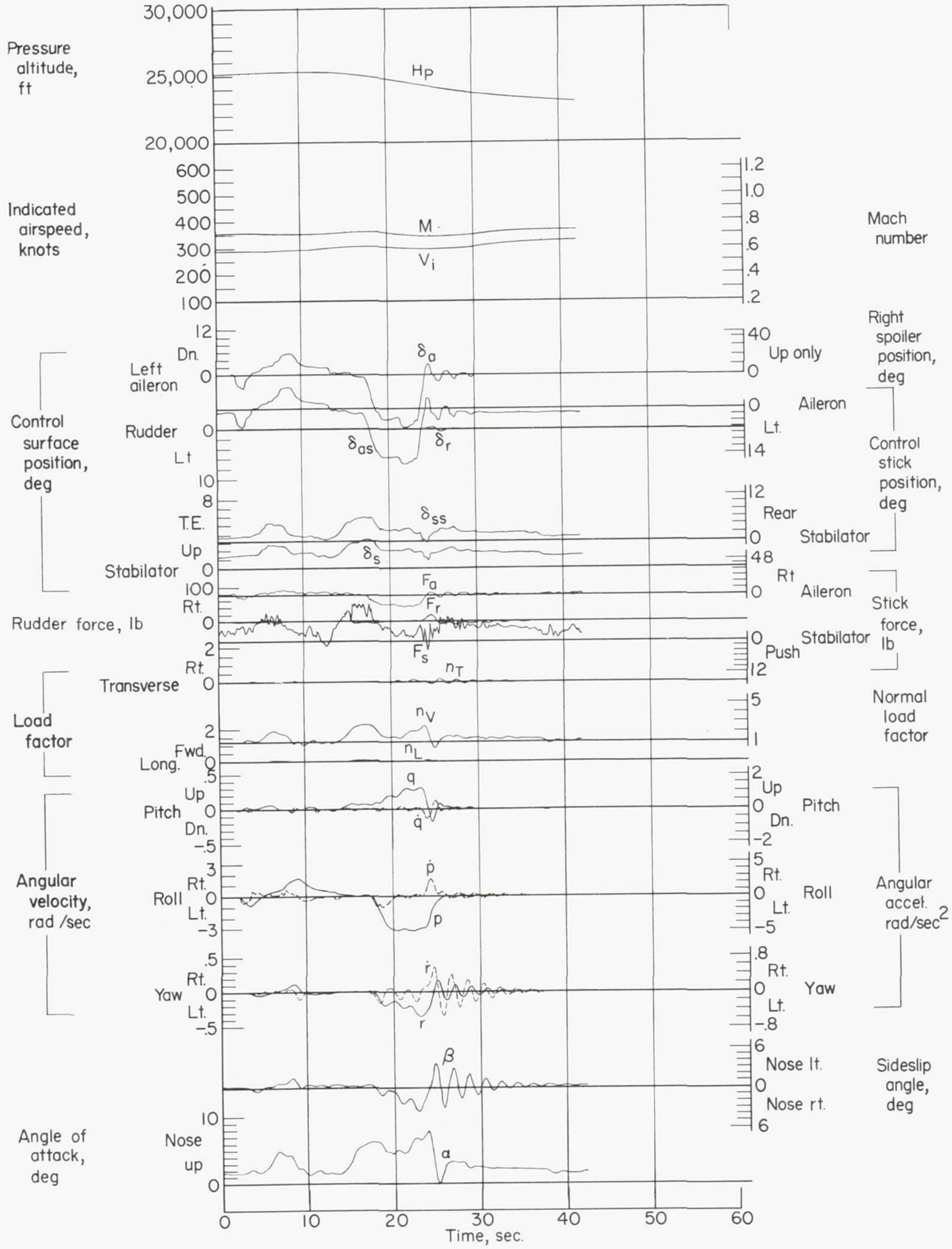

Figure 17.- Data obtained during rolls. Airplane weight, 17,250 pounds; center of gravity at 22.2 percent $\bar{c}$; flight 28.

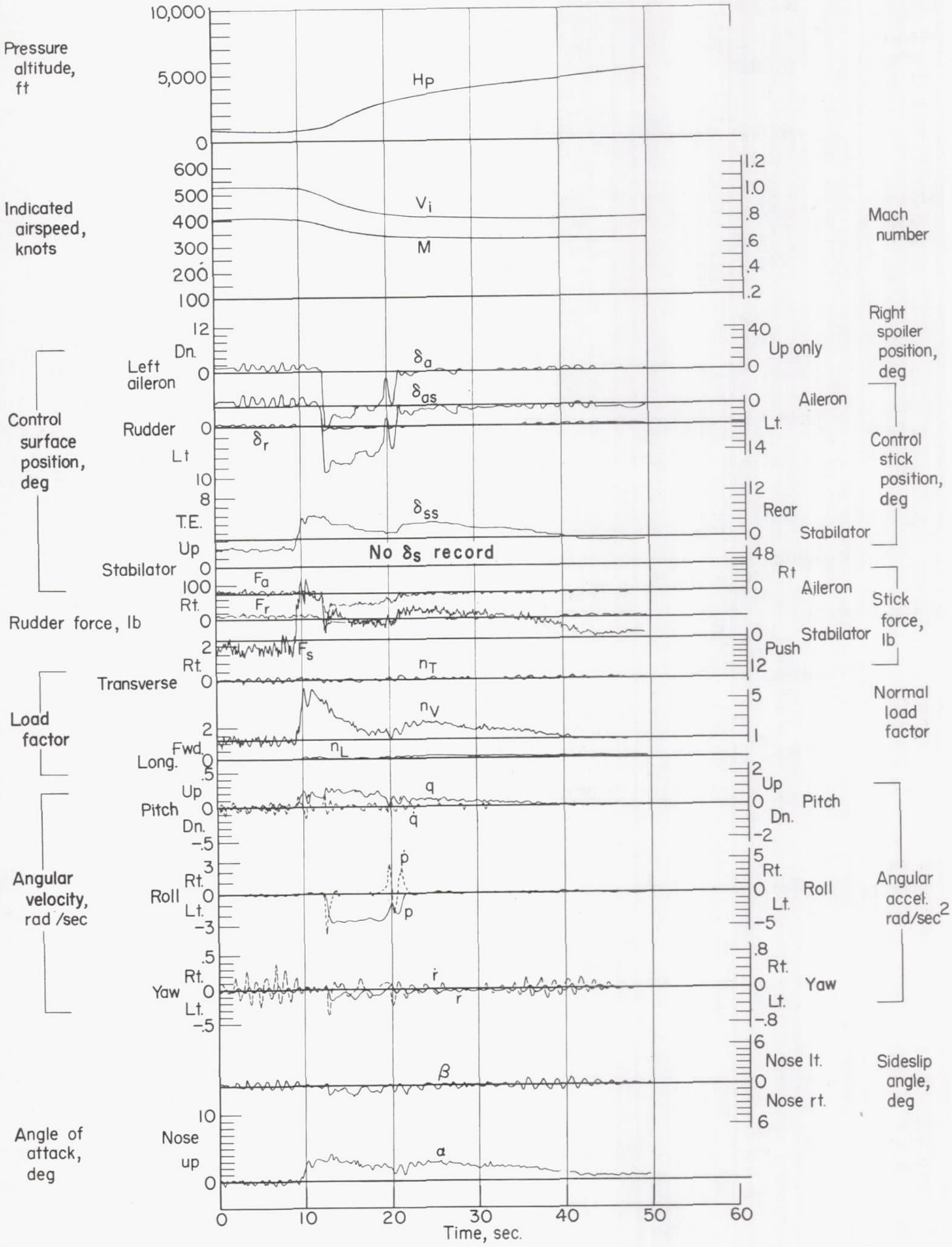

Figure 18.- Data obtained during rolling pullout. Airplane weight, 18,400 pounds; center of gravity at 21.6 percent $\bar{c}$; flight 34.

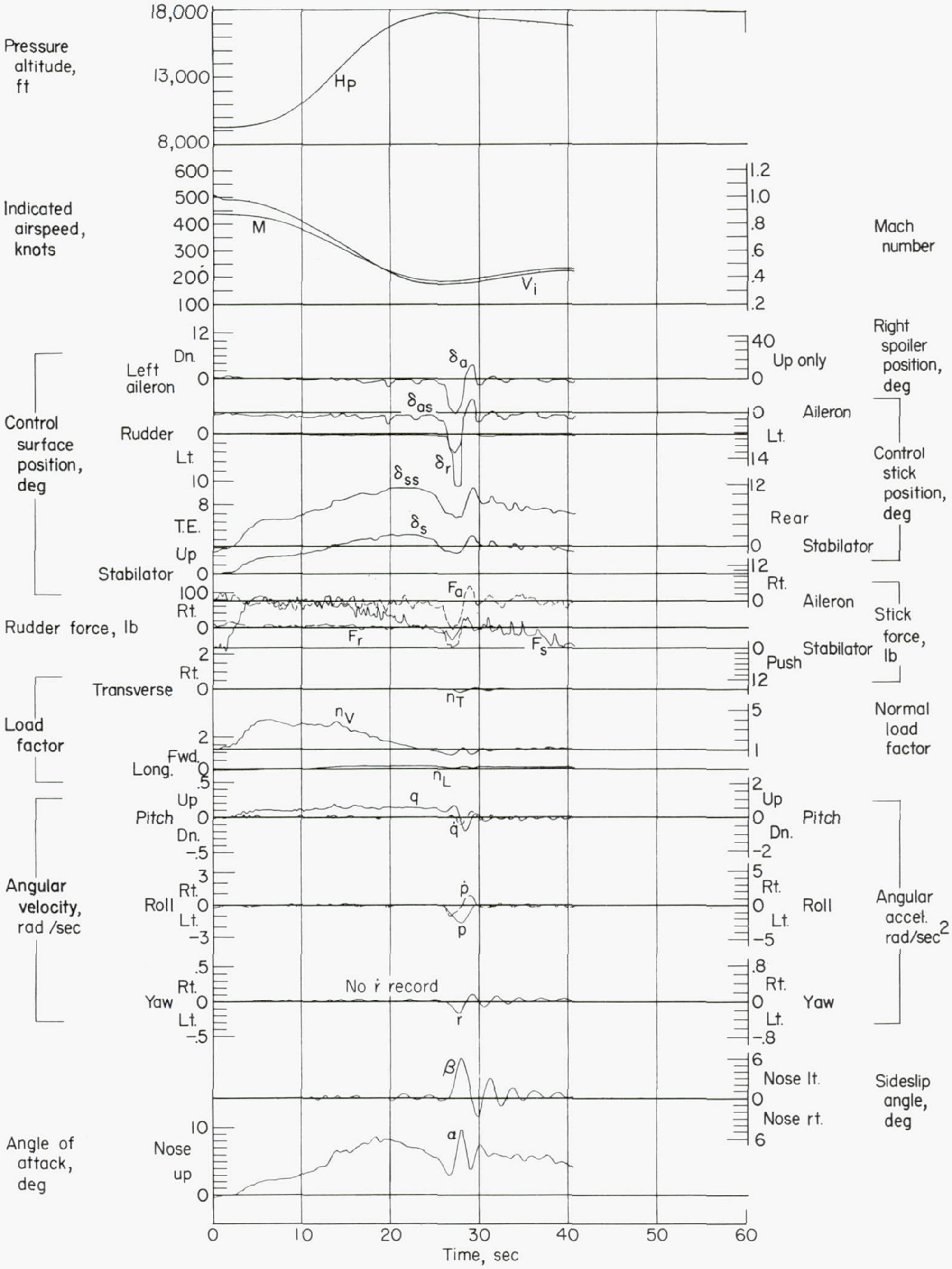

Figure 19.- Data obtained during Immelman. Airplane weight, 16,650 pounds; center of gravity at 22.4 percent $\bar{c}$; flight 2.

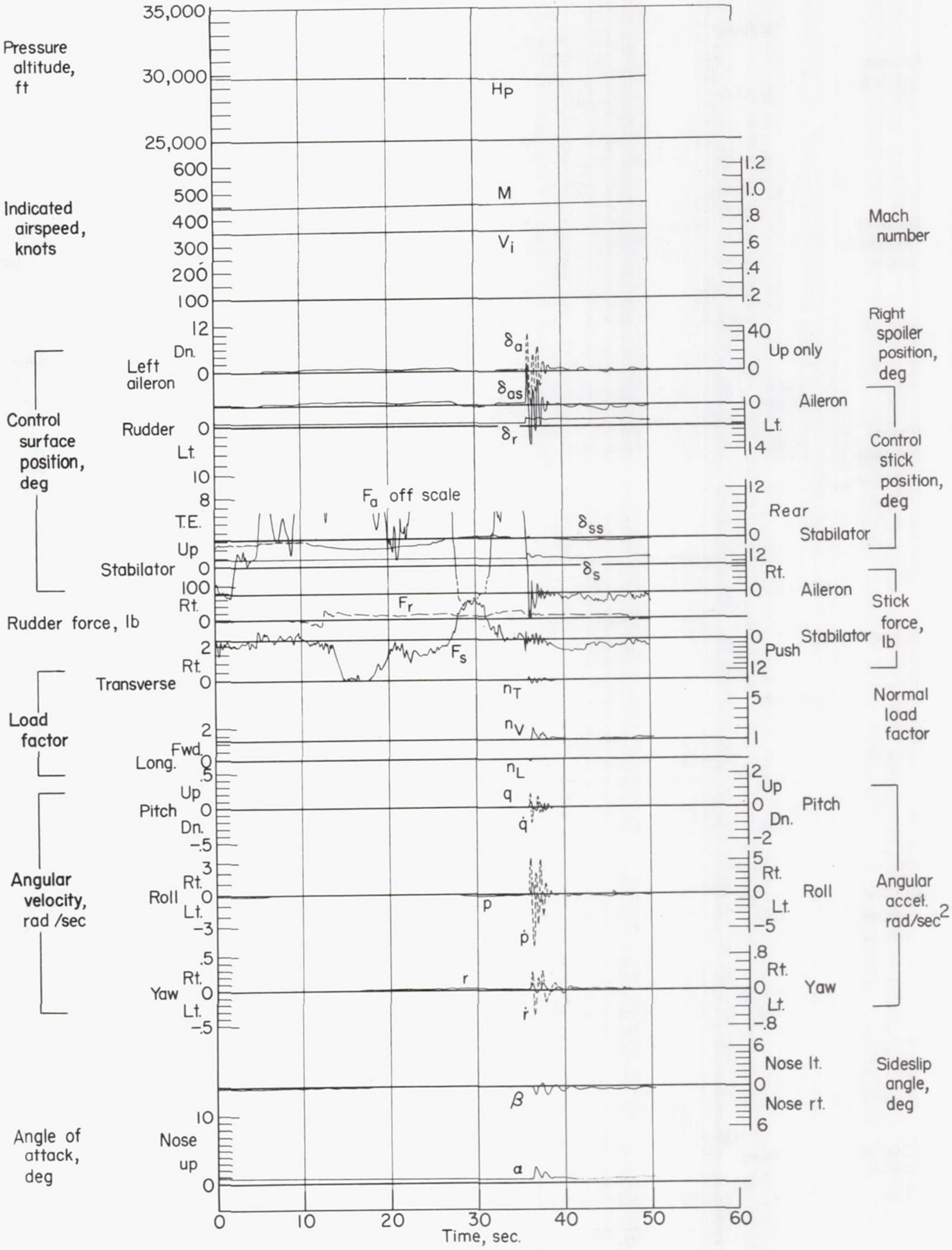

Figure 20.- Data obtained during boost-off flight, boost turned on at time 36 seconds. Airplane weight, 17,000 pounds; center of gravity at 22.0 percent $\bar{c}$; flight 3.

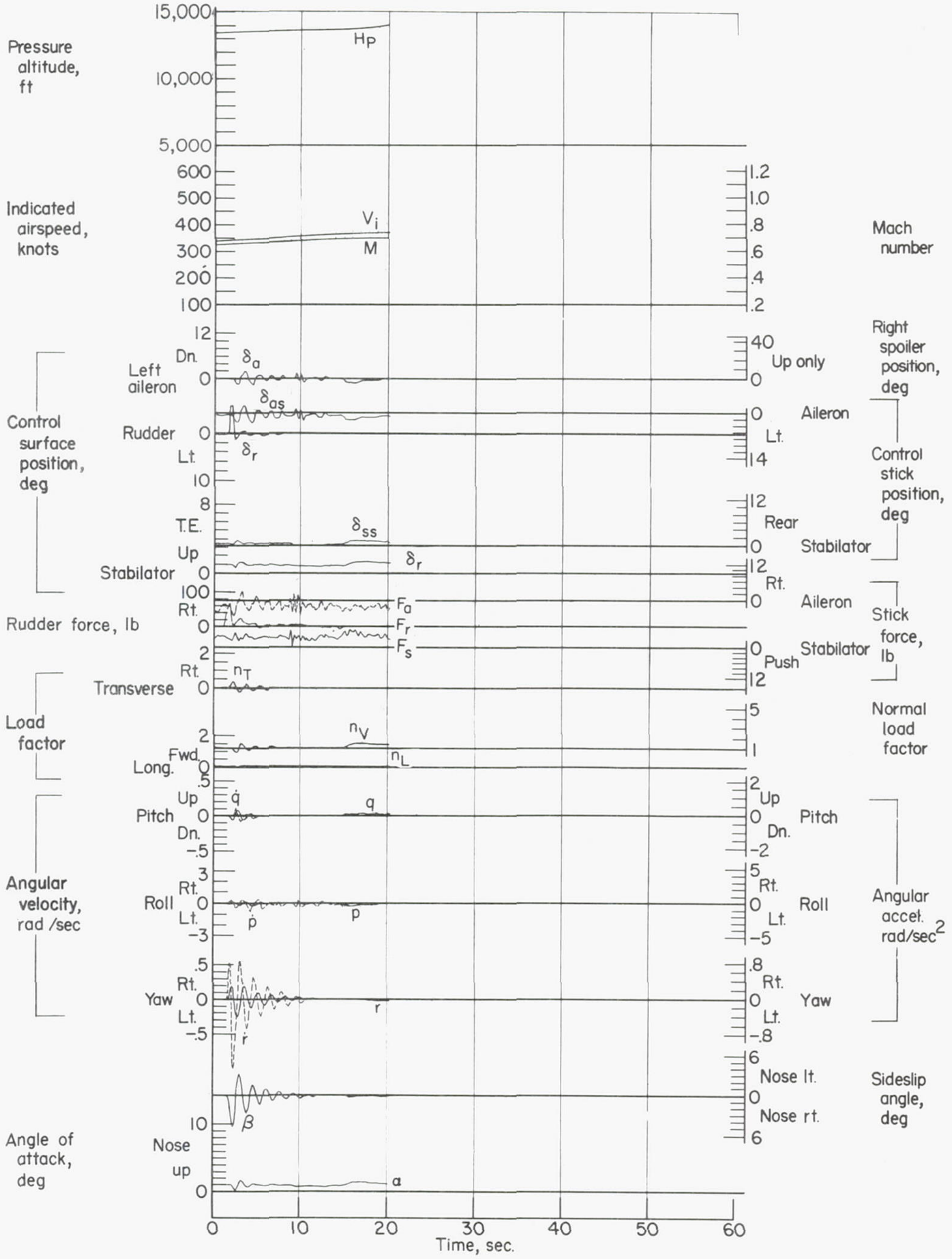

Figure 21.- Data obtained for rudder kick. Airplane weight, 16,400 pounds; center of gravity at 22.0 percent $\bar{c}$; flight 7.

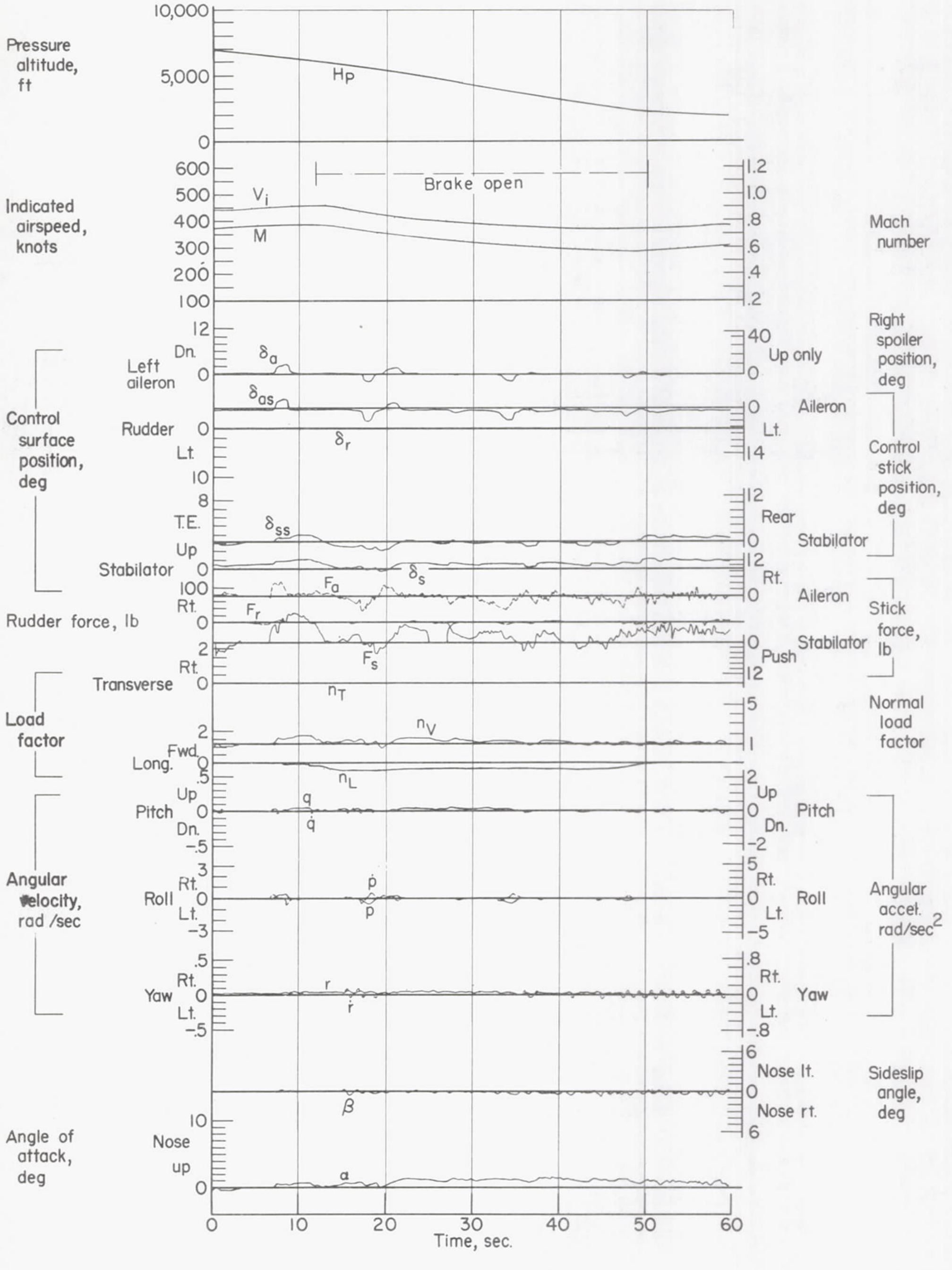

Figure 22.- Data obtained while opening and closing speed brakes. Airplane weight, 16,650 pounds; center of gravity at 21.9 percent $\bar{c}$; flight 13.

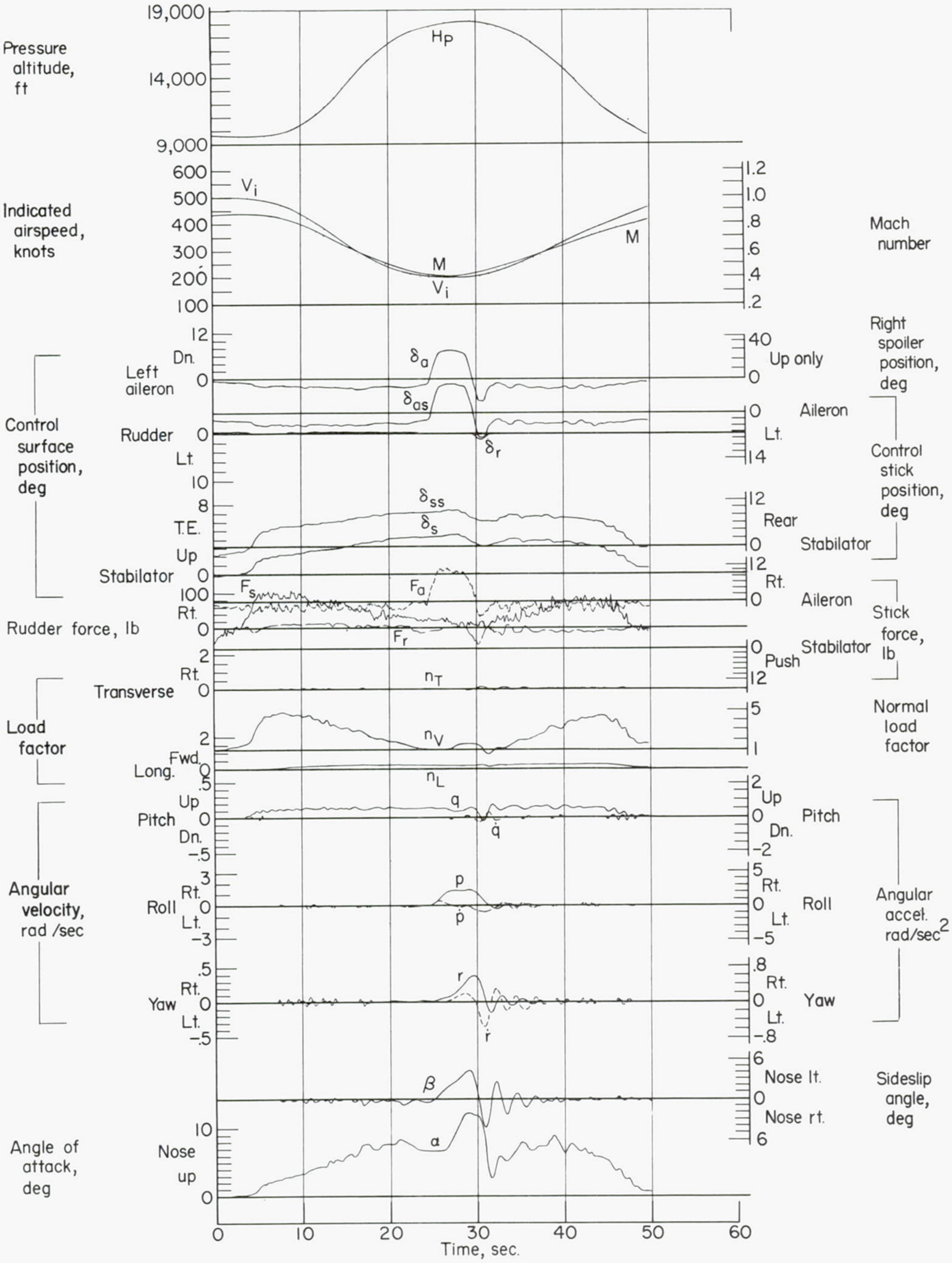

Figure 23.- Data obtained for loop with roll on top. Airplane weight, 17,800 pounds; center of gravity at 22.3 percent $\bar{c}$; flight 20.

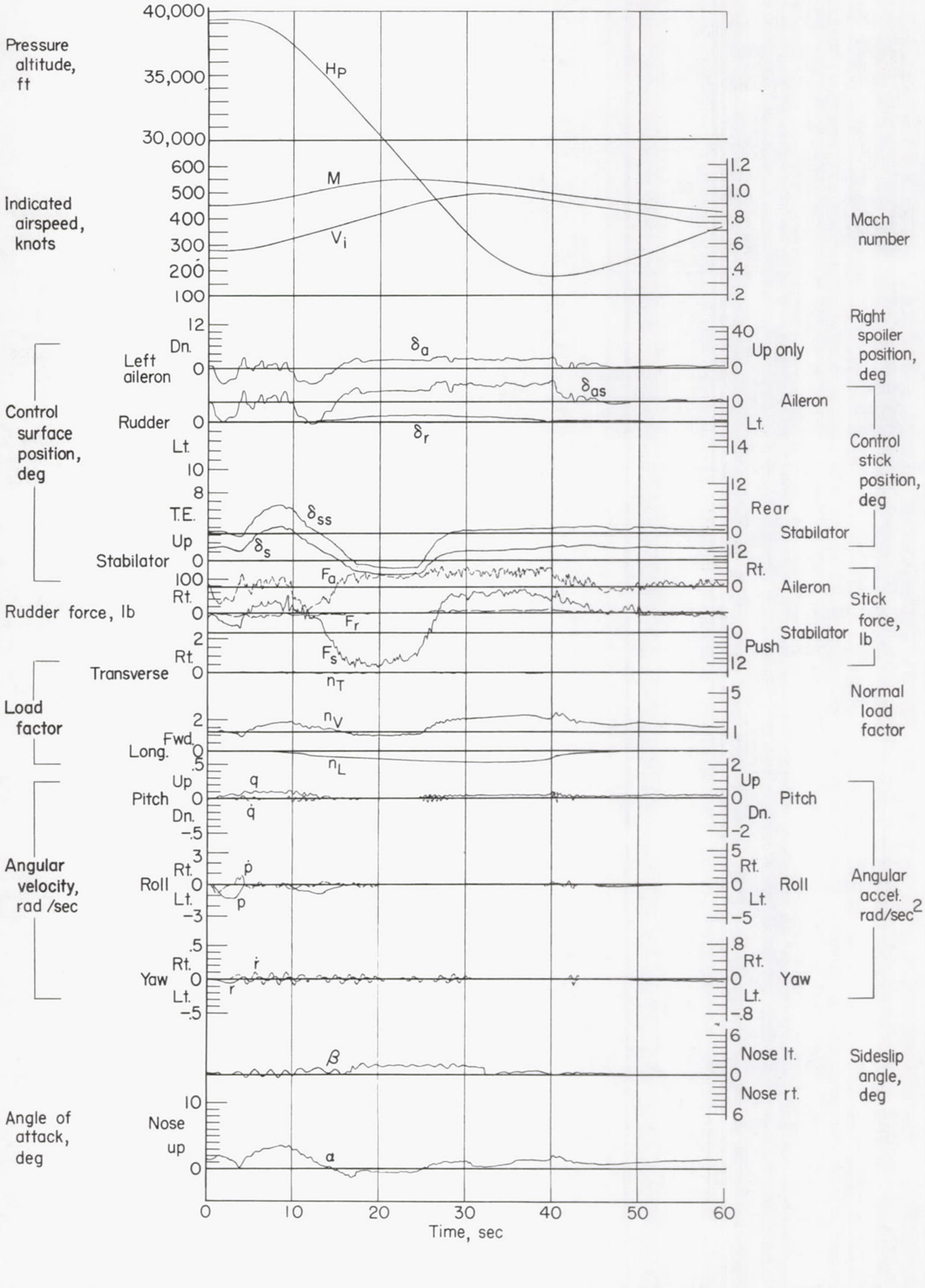

Figure 24.- Data obtained during Mach run. Airplane weight, 17,450 pounds; center of gravity at 21.9 percent $\bar{c}$; flight 3.

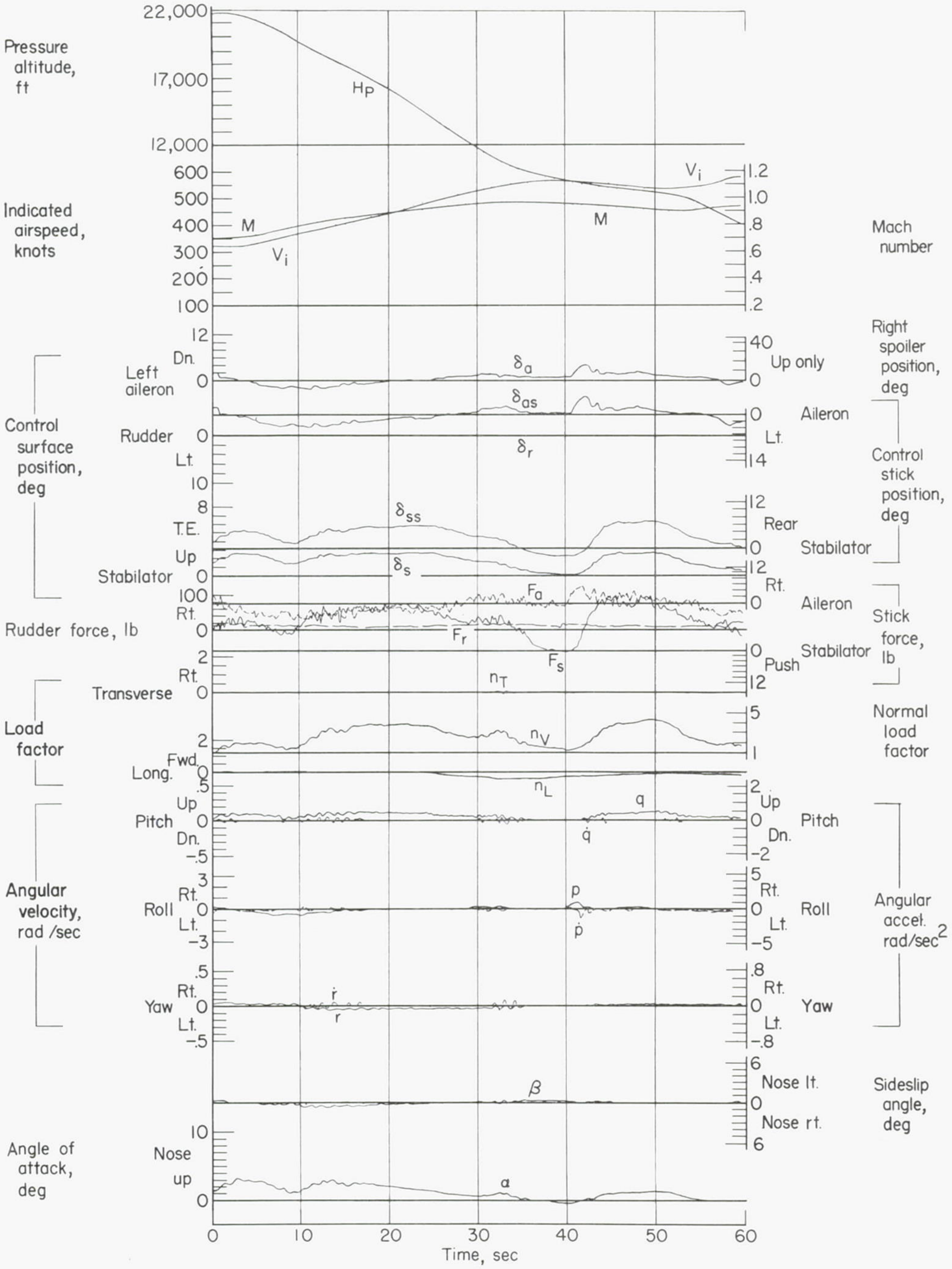

(a)

Figure 25.- Data obtained during high-speed shallow dive and pullout. Airplane weight, 17,400 pounds; center of gravity at 21.7 percent $\bar{c}$; flight 7.

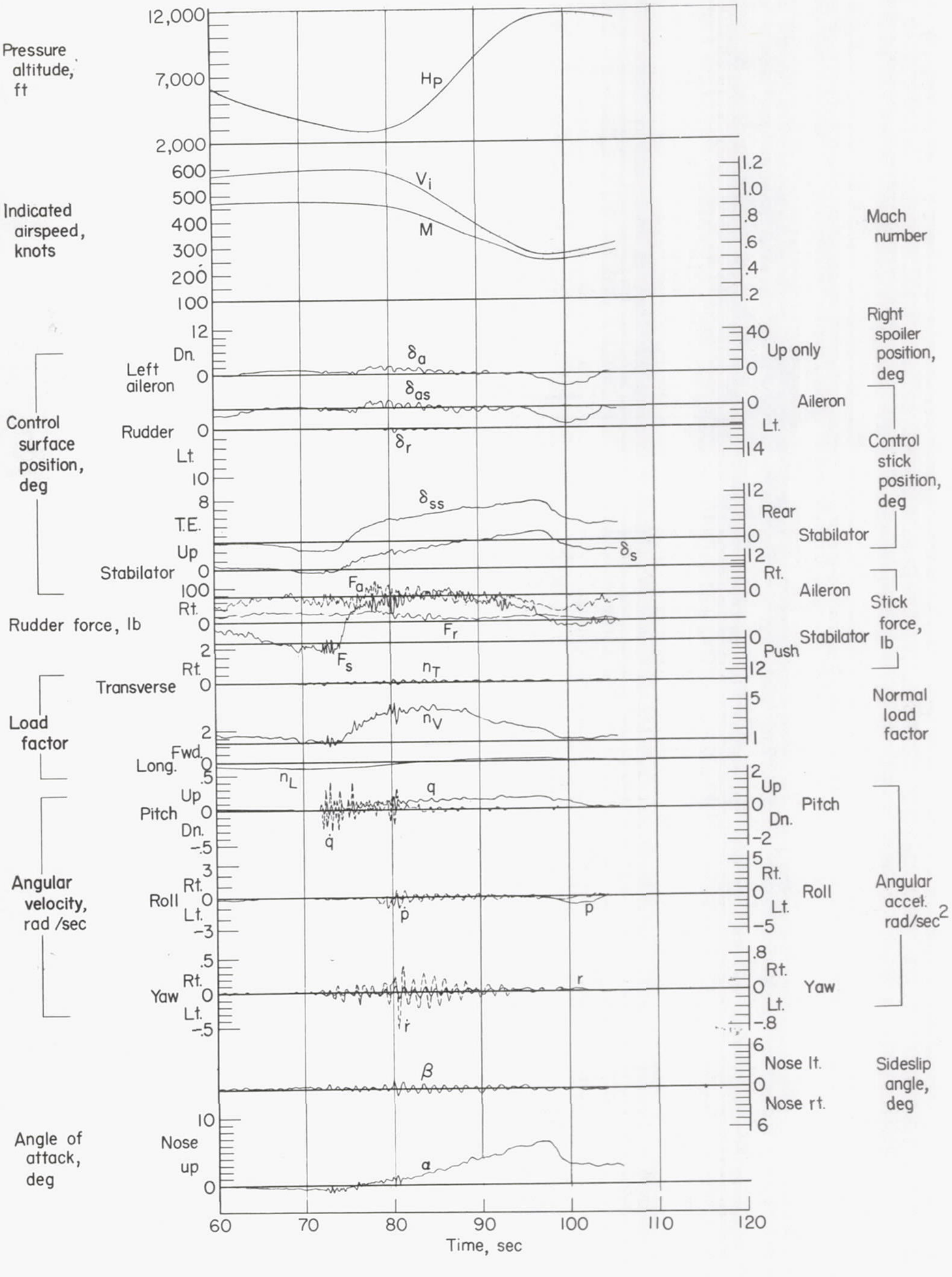

(b)

Figure 25.- Concluded.

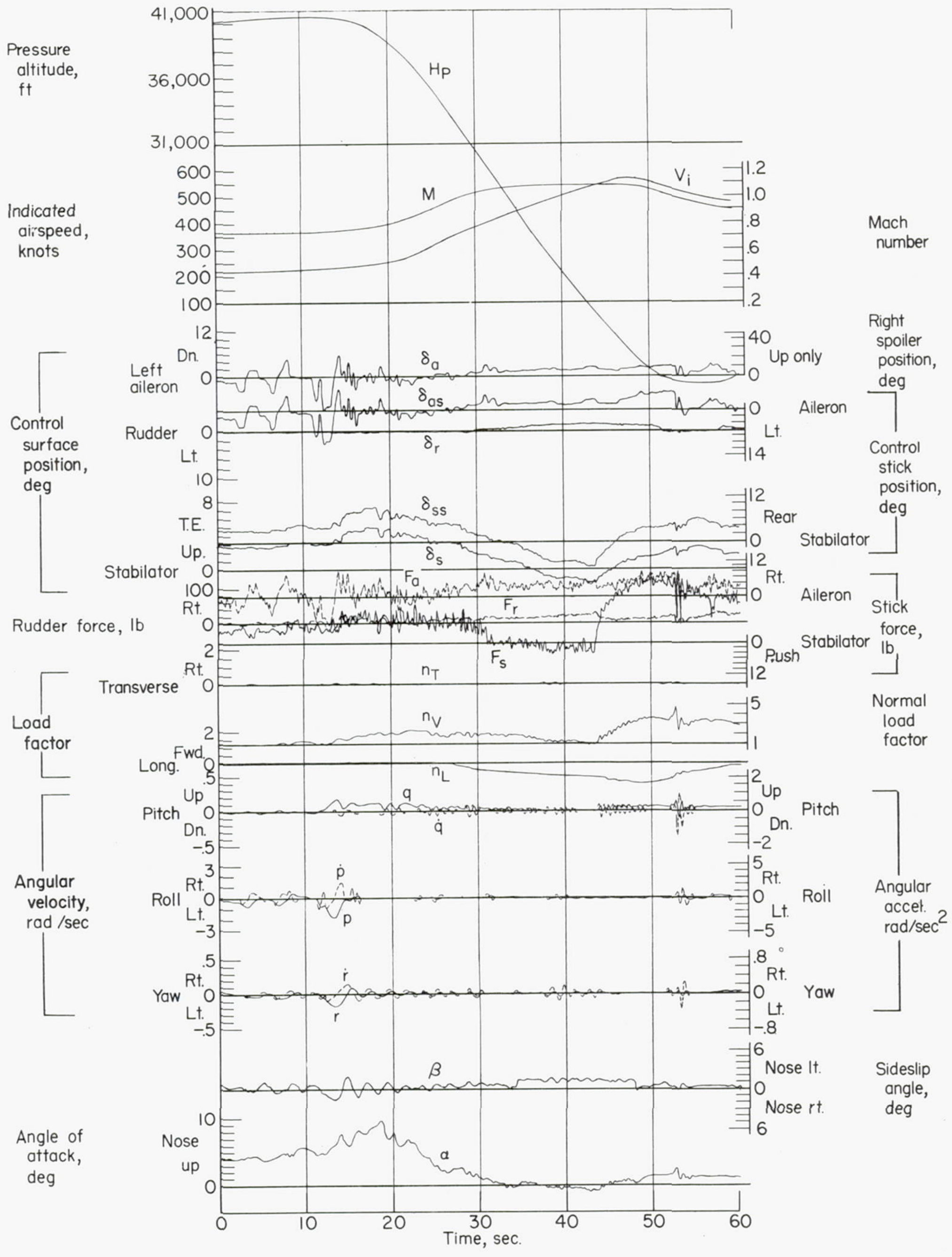

(a)

Figure 26.- Data obtained during split-S into Mach run. Airplane weight, 16,900 pounds; center of gravity at 21.8 percent $\bar{c}$; flight 14.

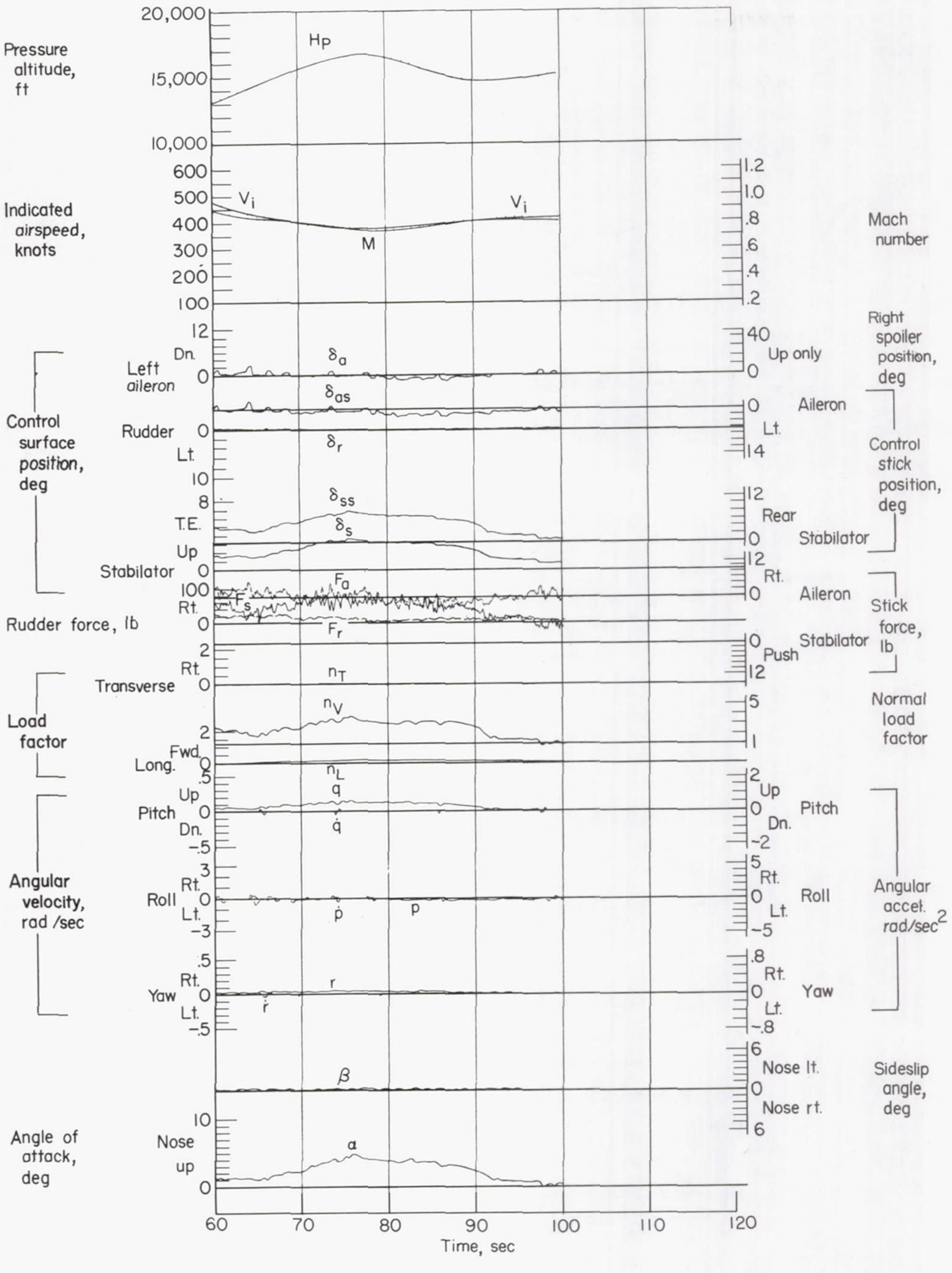

(b)

Figure 26.- Concluded.

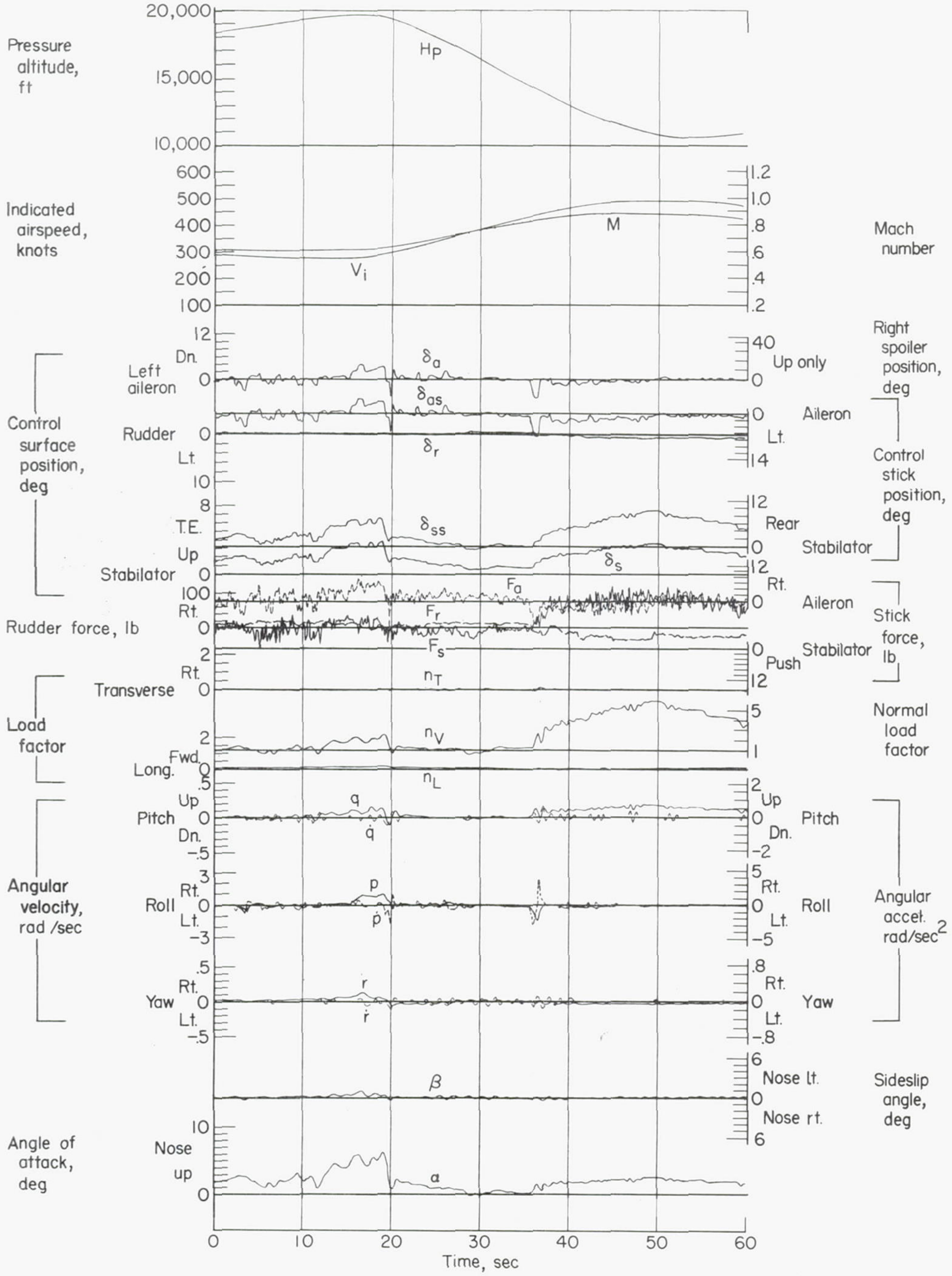

(a)

Figure 27.- Data obtained during dive to high speed and high g pullout. Airplane weight, 16,400 pounds; center of gravity at 22.0 percent $\bar{c}$; flight 14.

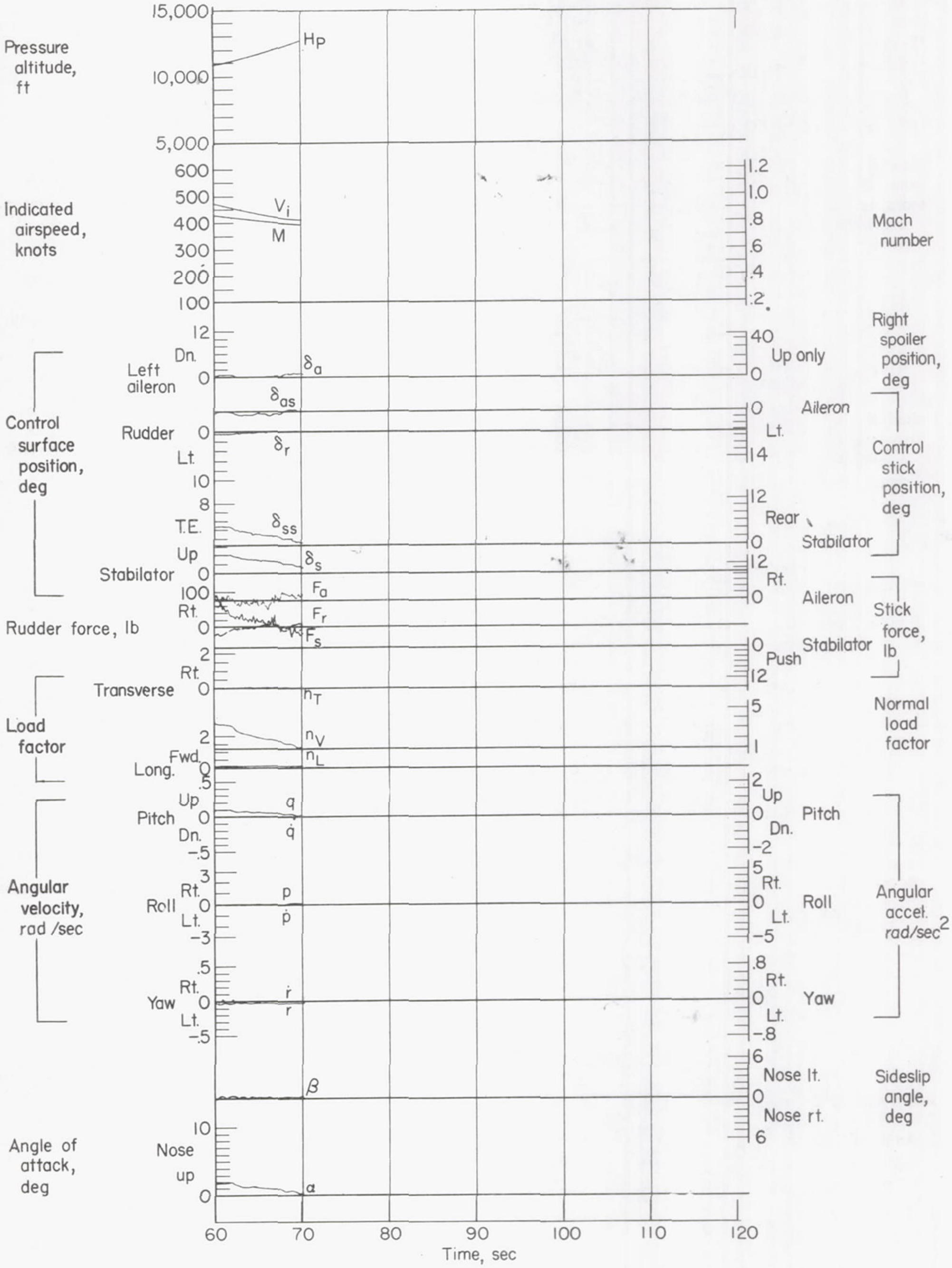

(b)

Figure 27.- Concluded.

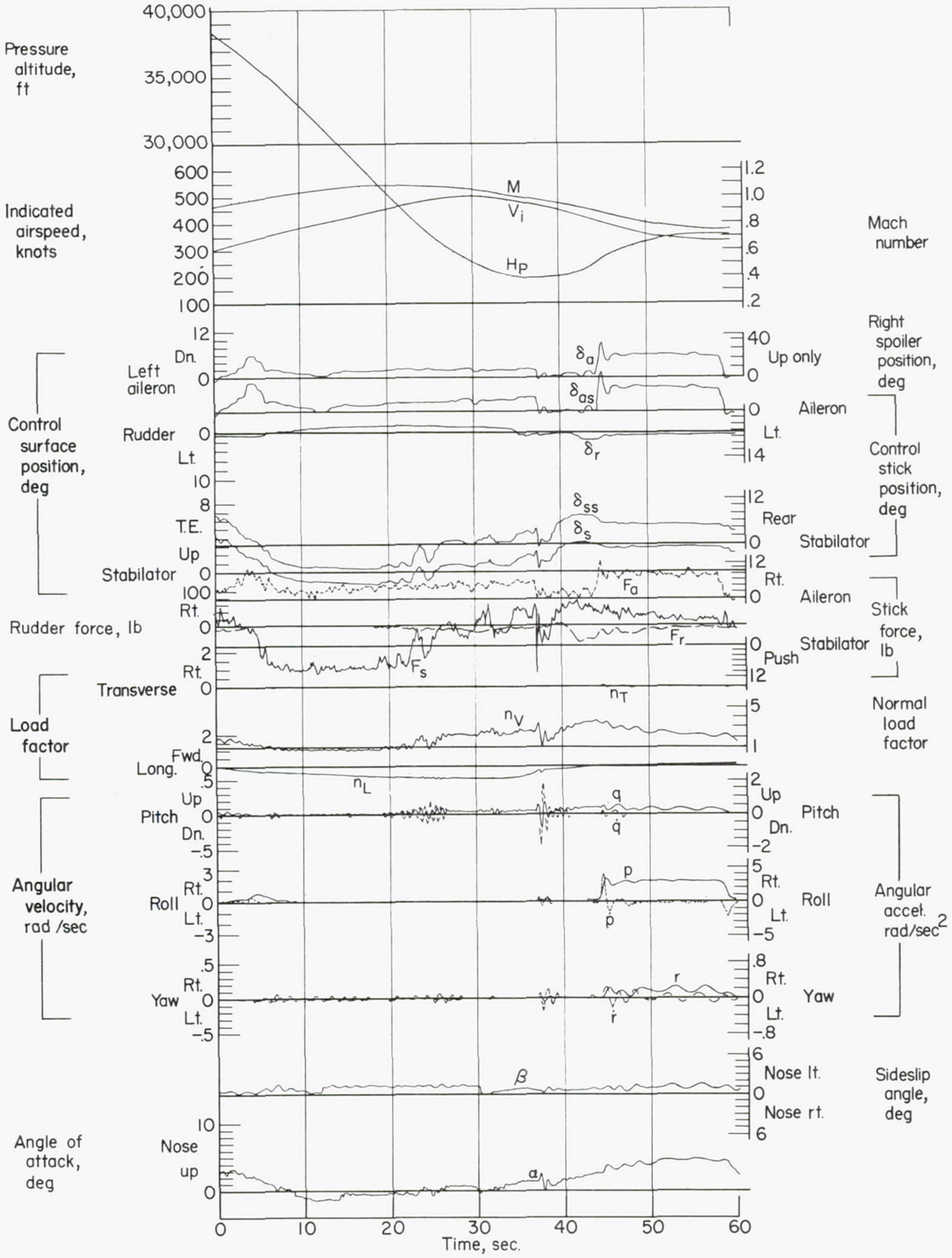

Figure 28.- Data obtained during Mach run followed by six consecutive aileron rolls. Airplane weight, 17,250 pounds; center of gravity at 21.7 percent $\bar{c}$; flight 15.

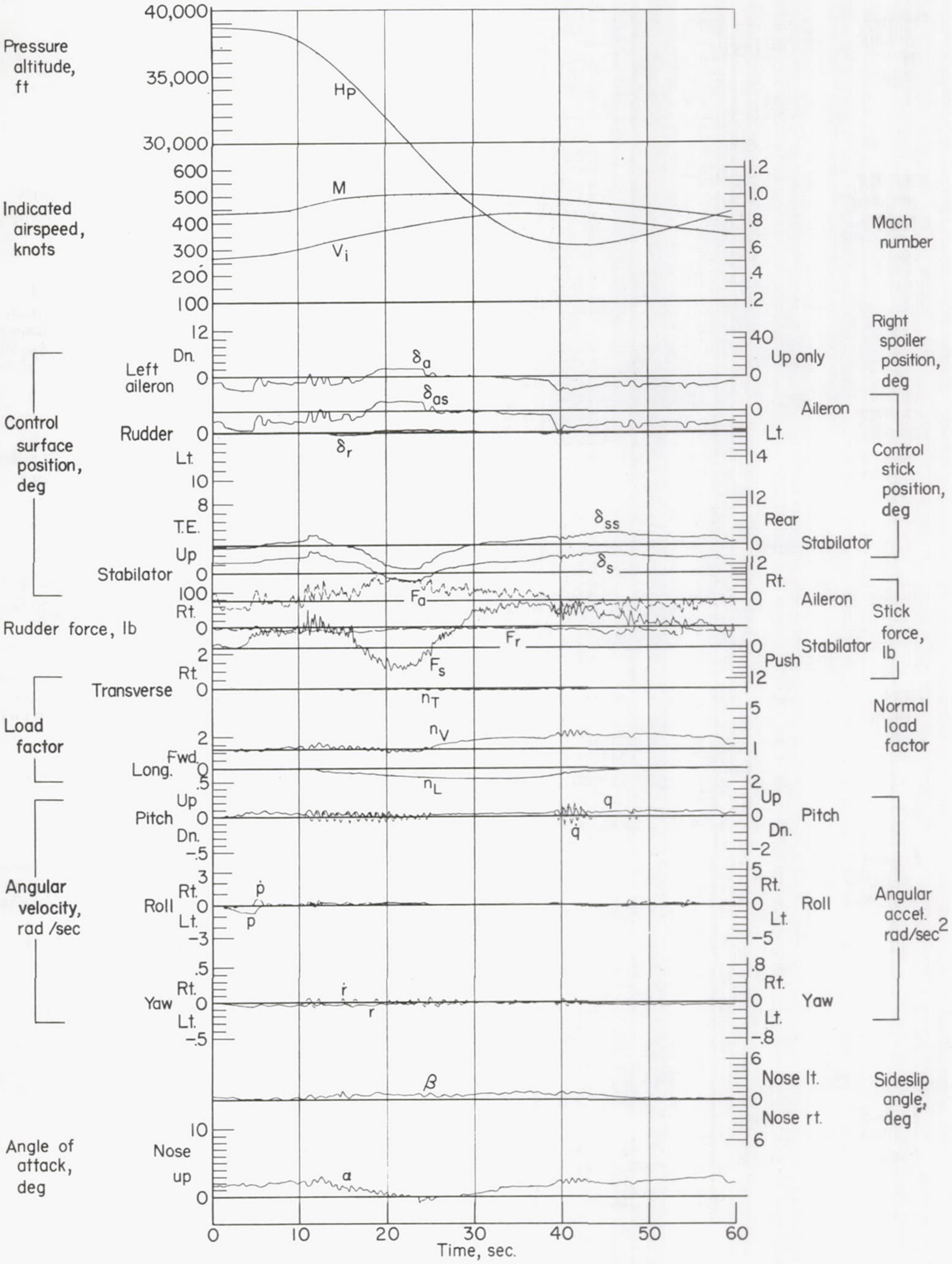

Figure 29.- Data obtained during Mach run. Airplane weight, 18,750 pounds; center of gravity at 20.1 percent $\bar{c}$; flight 19.

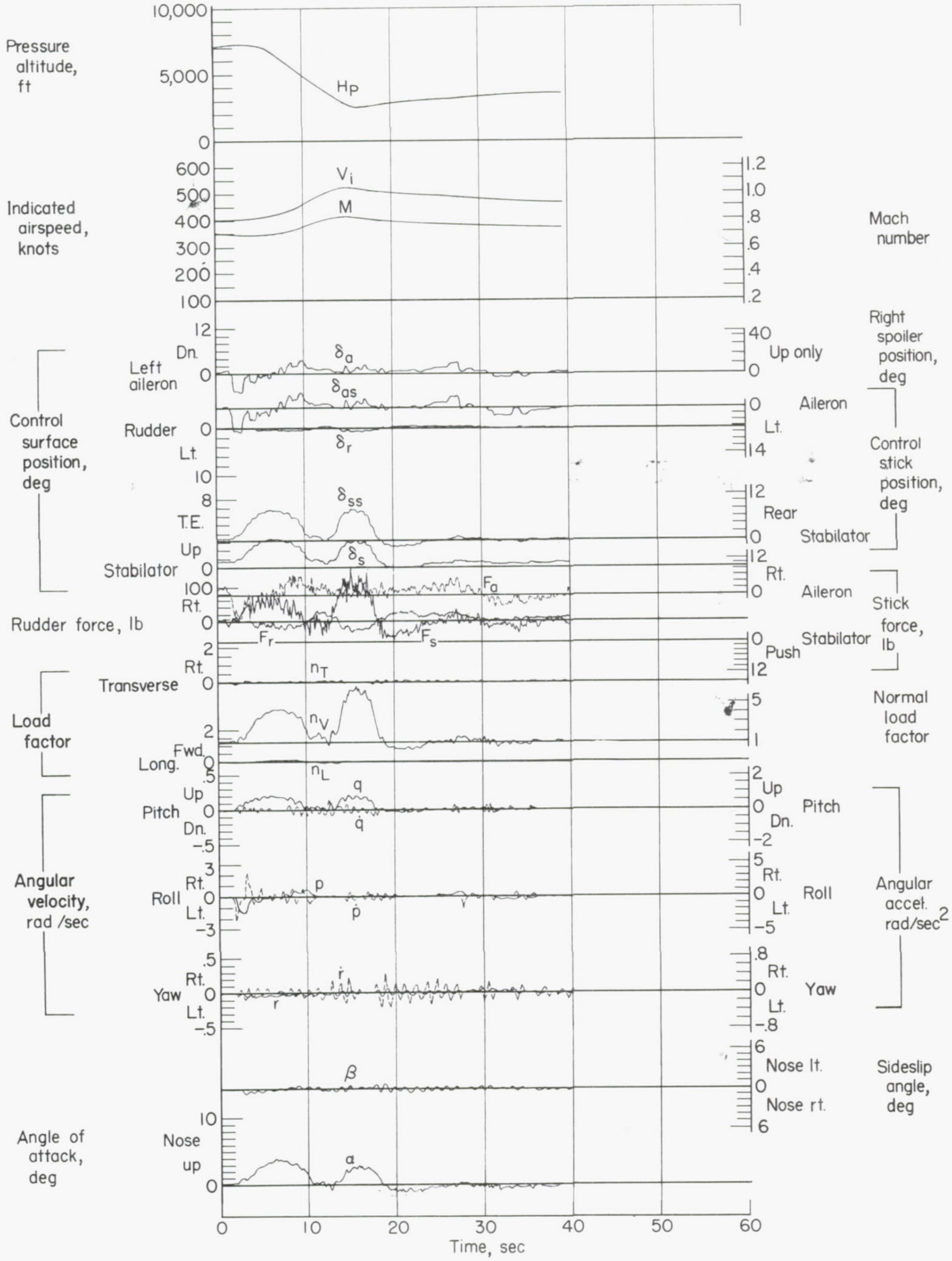

Figure 30.- Data obtained during simulated dive bomb run. Airplane weight, 15,450 pounds; center of gravity at 22.5 percent $\bar{c}$; flight 14.

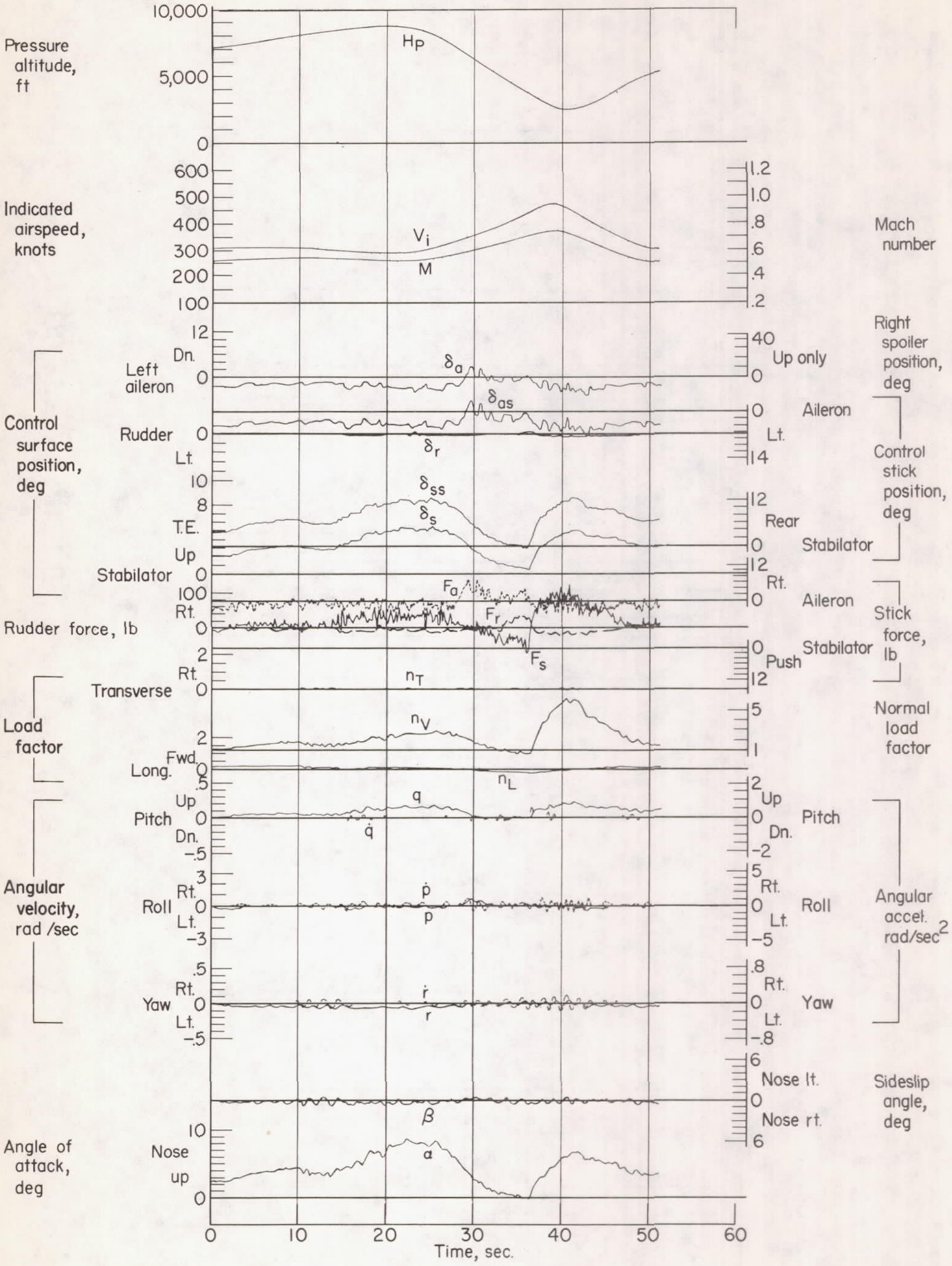

Figure 31.- Data obtained during simulated glide-bomb run. Airplane weight, 19,350 pounds; center of gravity at 19.5 percent $\bar{c}$; flight 16.

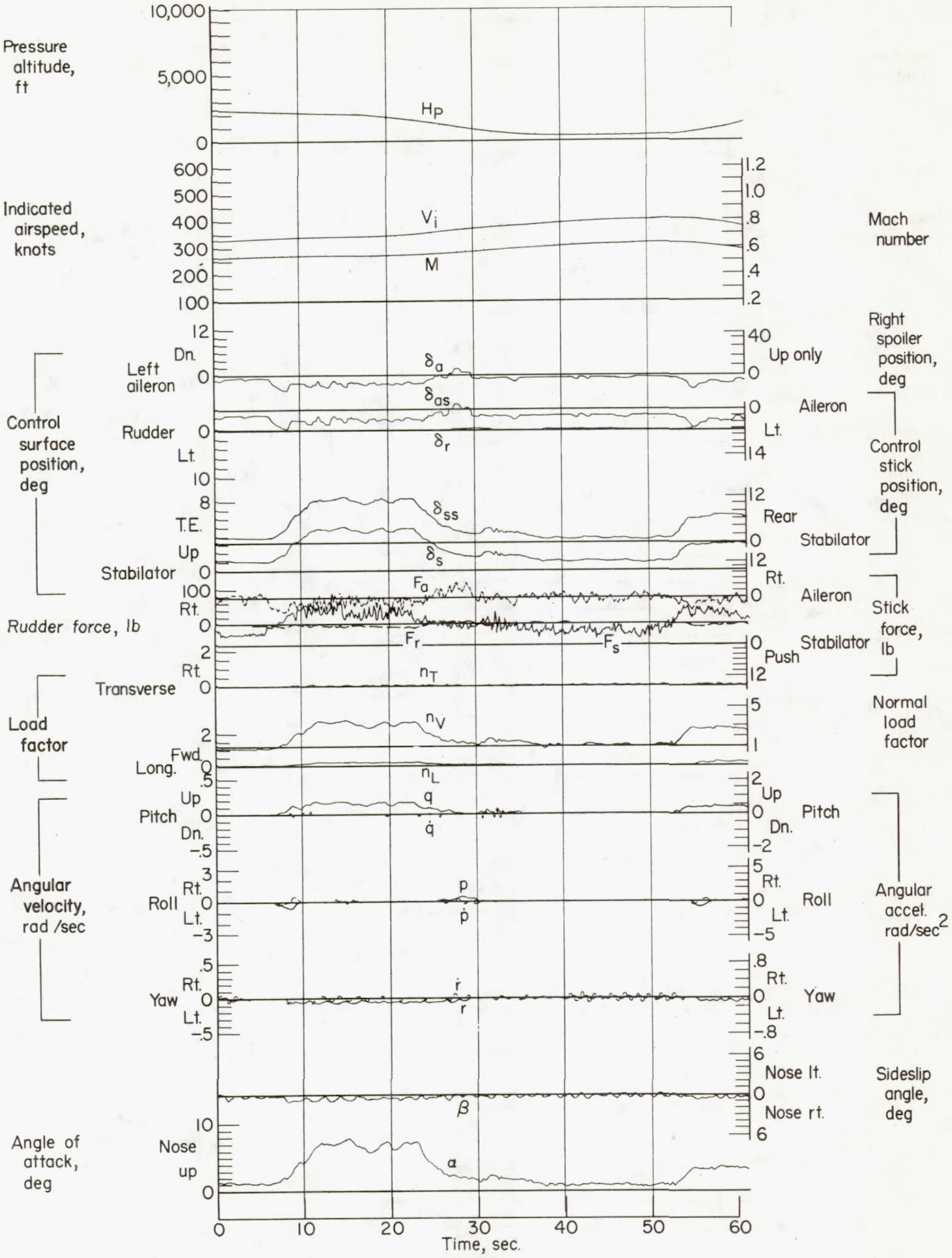

Figure 32.- Data obtained during simulated skip-bomb run. Airplane weight, 18,800 pounds; center of gravity at 19.6 percent $\bar{c}$; flight 16.

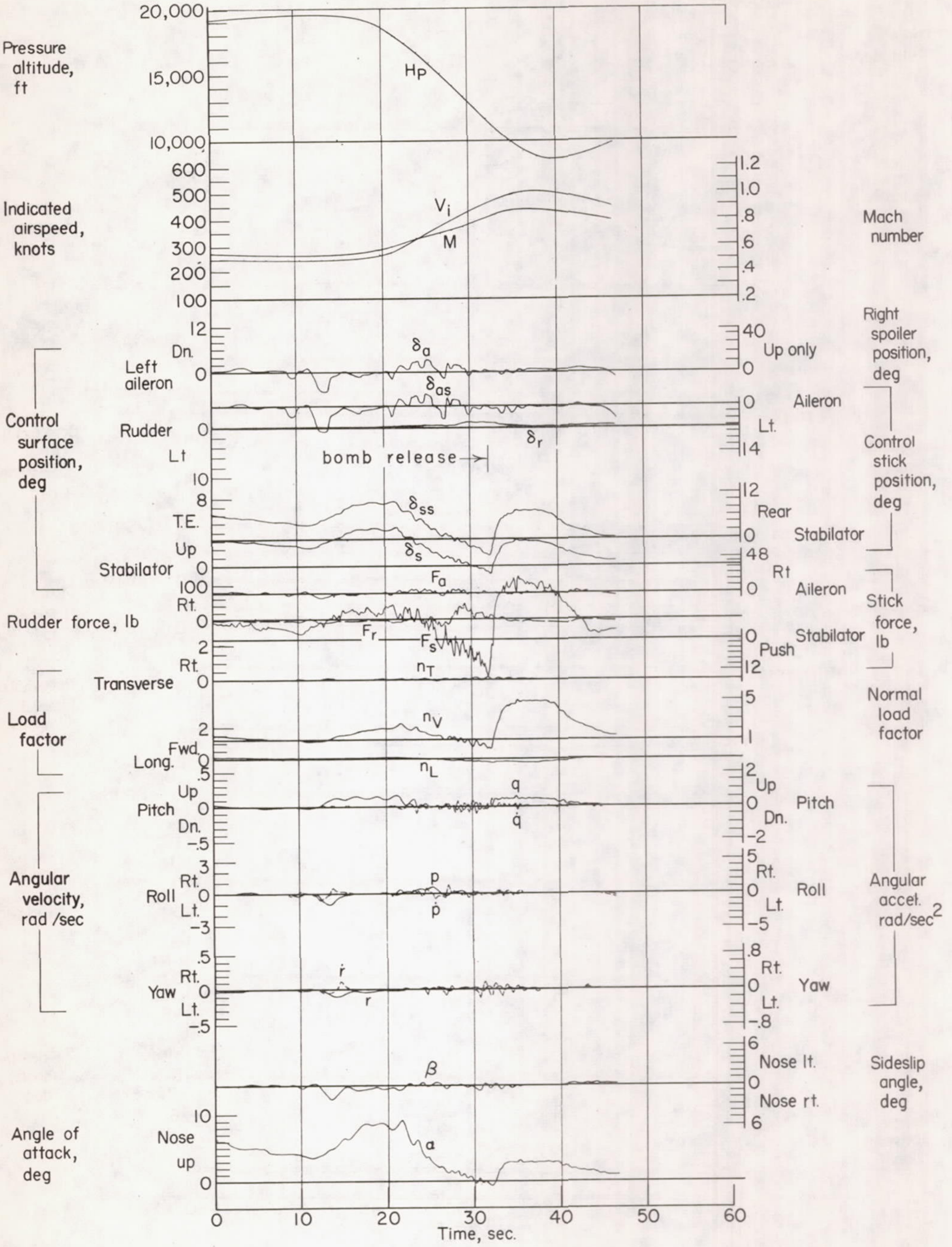

Figure 33.- Data obtained during dive bomb run. Airplane weight, 20,050 pounds; center of gravity at 19.7 percent $\bar{c}$; flight 37.

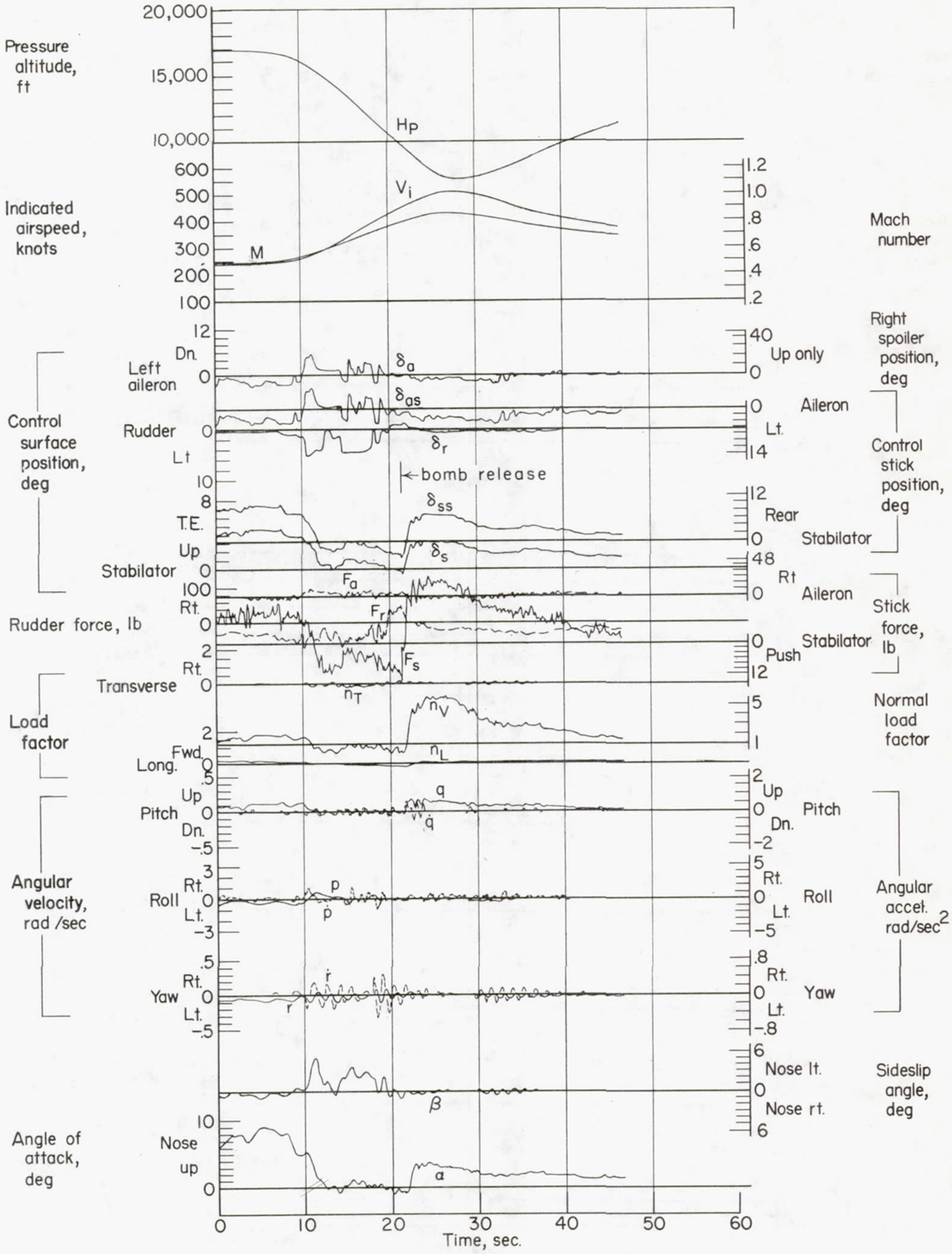

Figure 34.- Data obtained during dive bomb run. Airplane weight, 18,600 pounds; center of gravity at 21.1 percent $\bar{c}$; flight 40.

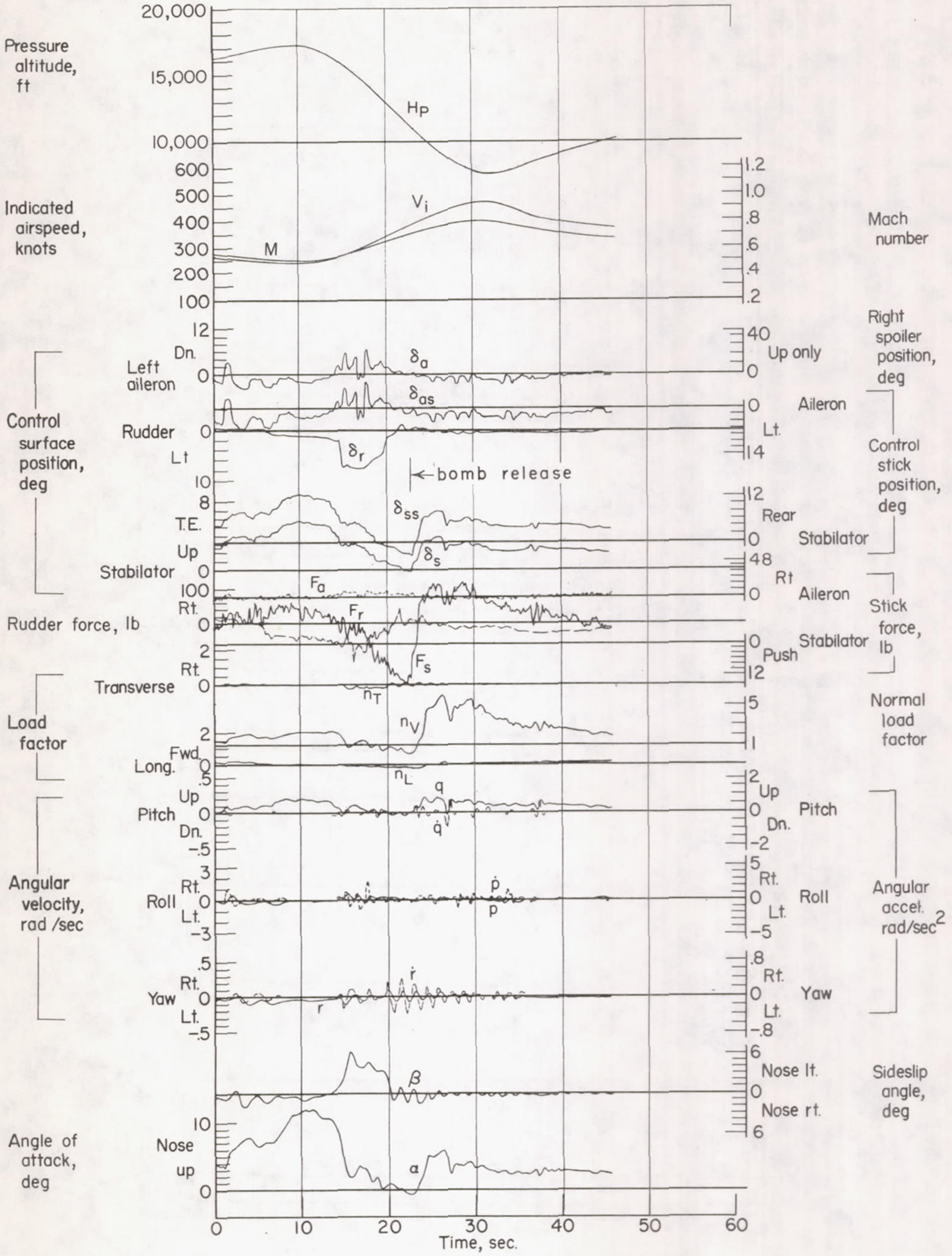

Figure 35.- Data obtained during dive bomb run. Airplane weight, 18,300 pounds; center of gravity at 21.8 percent $\bar{c}$; flight 40.

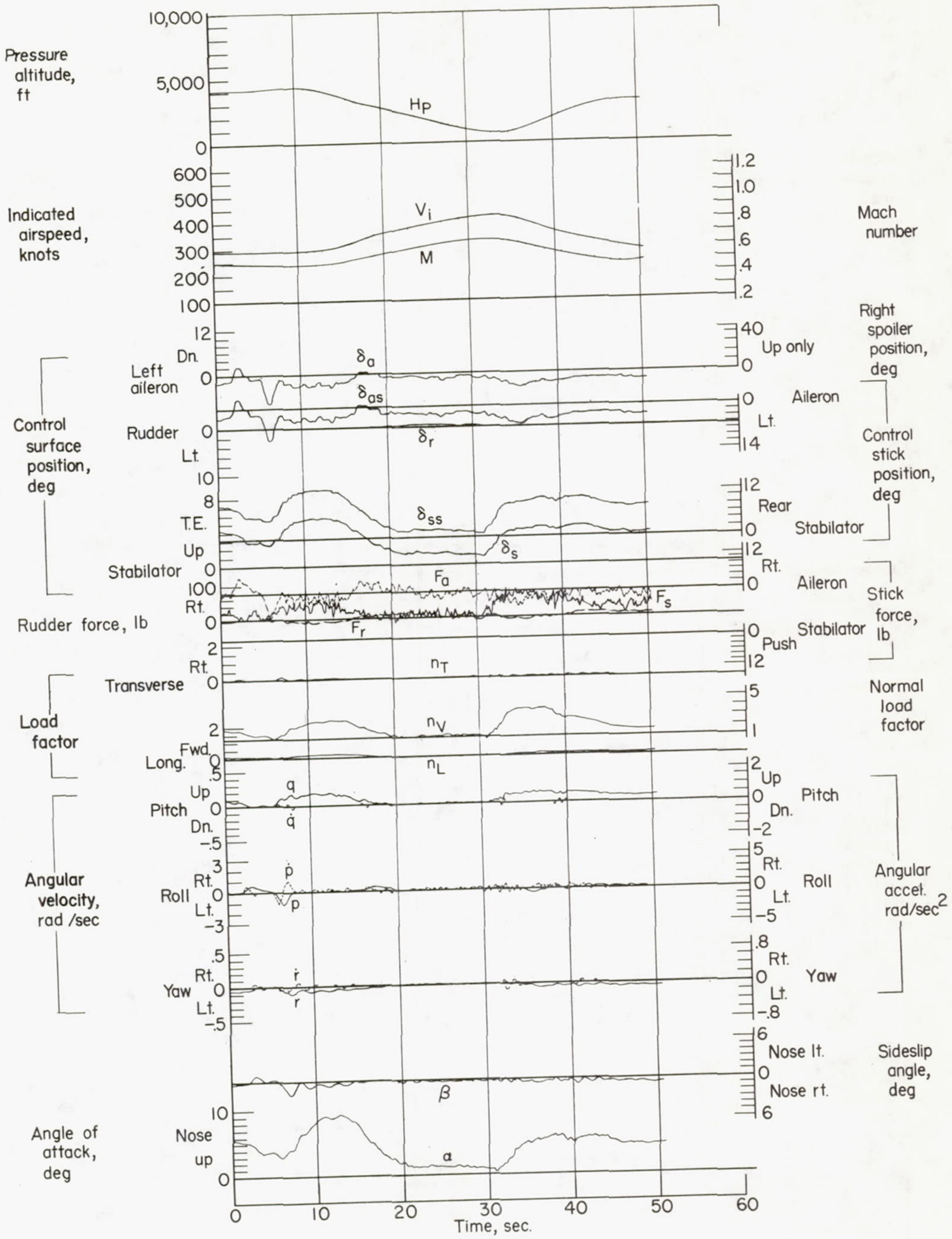

Figure 36.- Data obtained during simulated strafing run. Airplane weight, 19,150 pounds; center of gravity at 19.4 percent $\bar{c}$; flight 16.

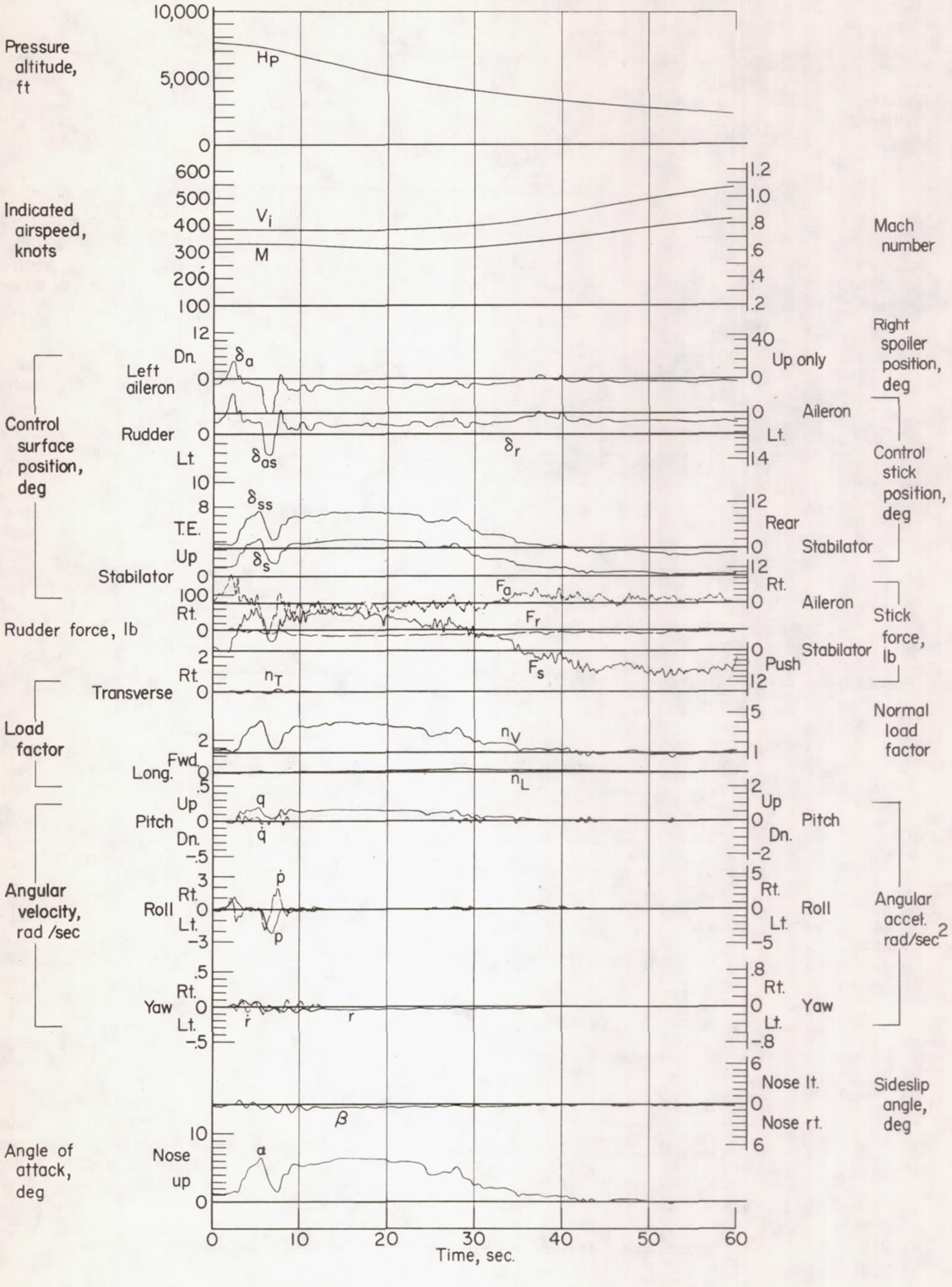

(a)

Figure 37.- Data obtained during turn into simulated strafing run and pullout into Immelman. Airplane weight, 18,450 pounds; center of gravity at 20.9 percent $\bar{c}$; flight 18.

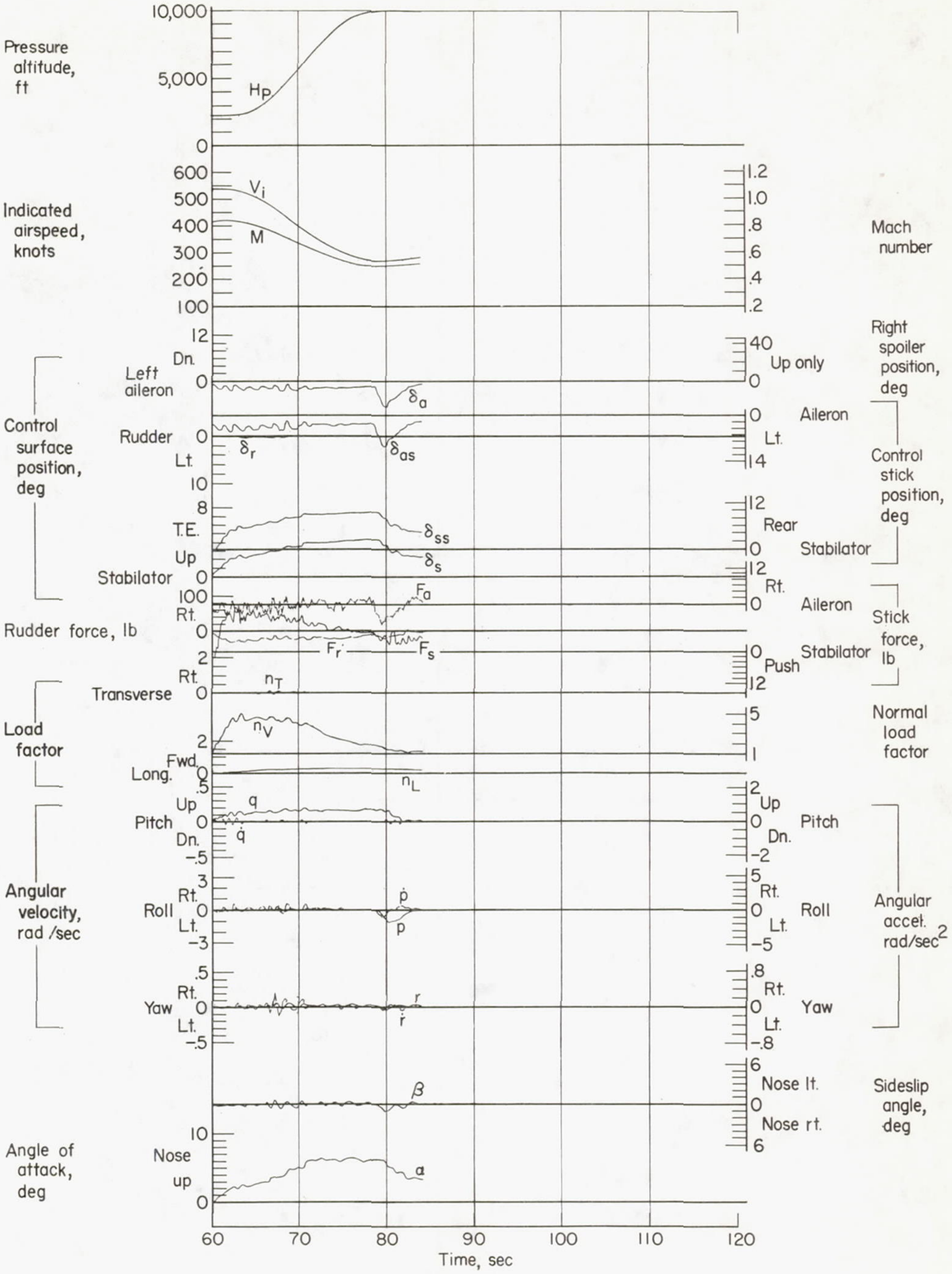

(b)

Figure 37.- Concluded.

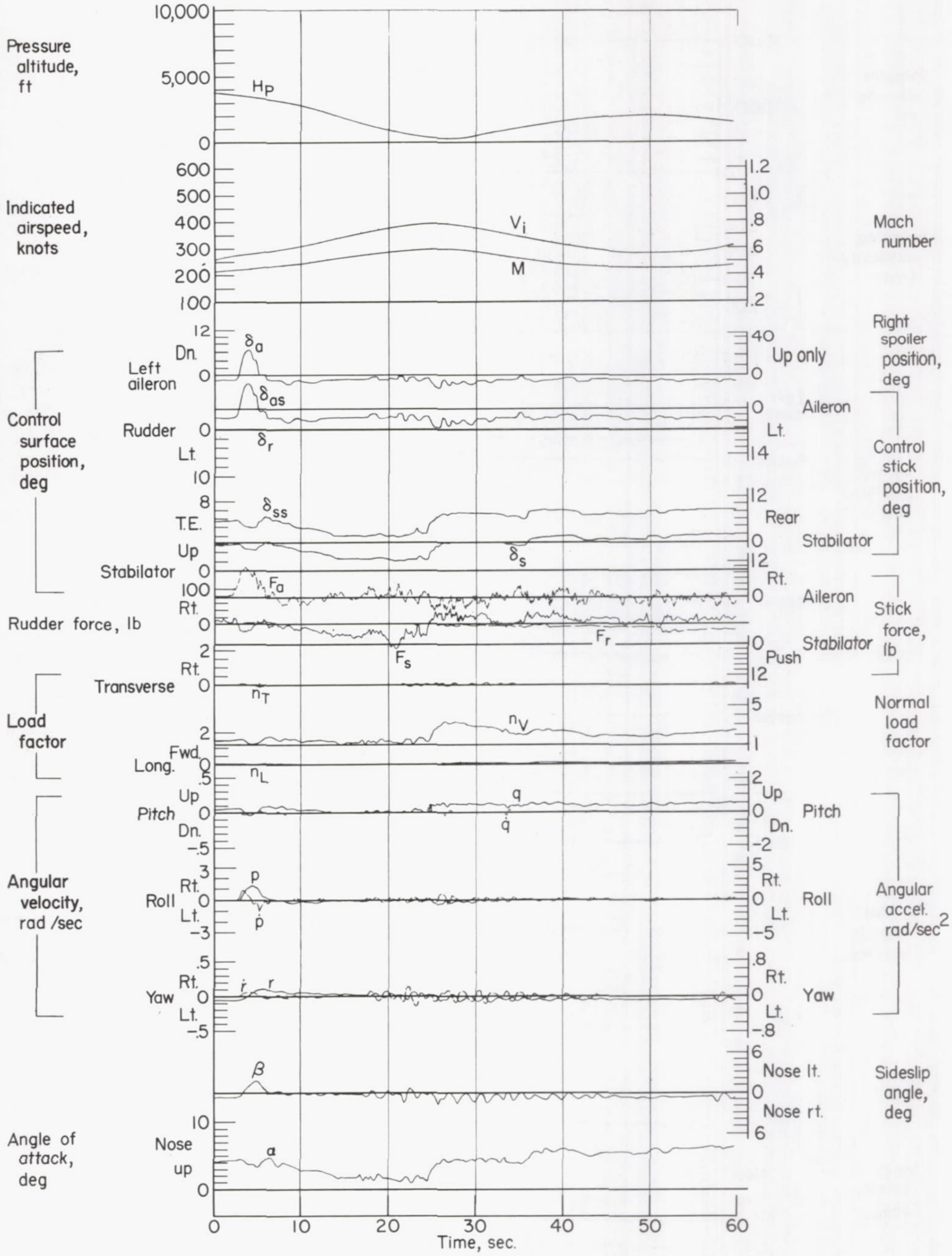

(a)

Figure 38.- Data obtained during three simulated strafing runs. Airplane weight, 17,850 pounds; center of gravity at 22.2 percent $\bar{c}$; flight 18.

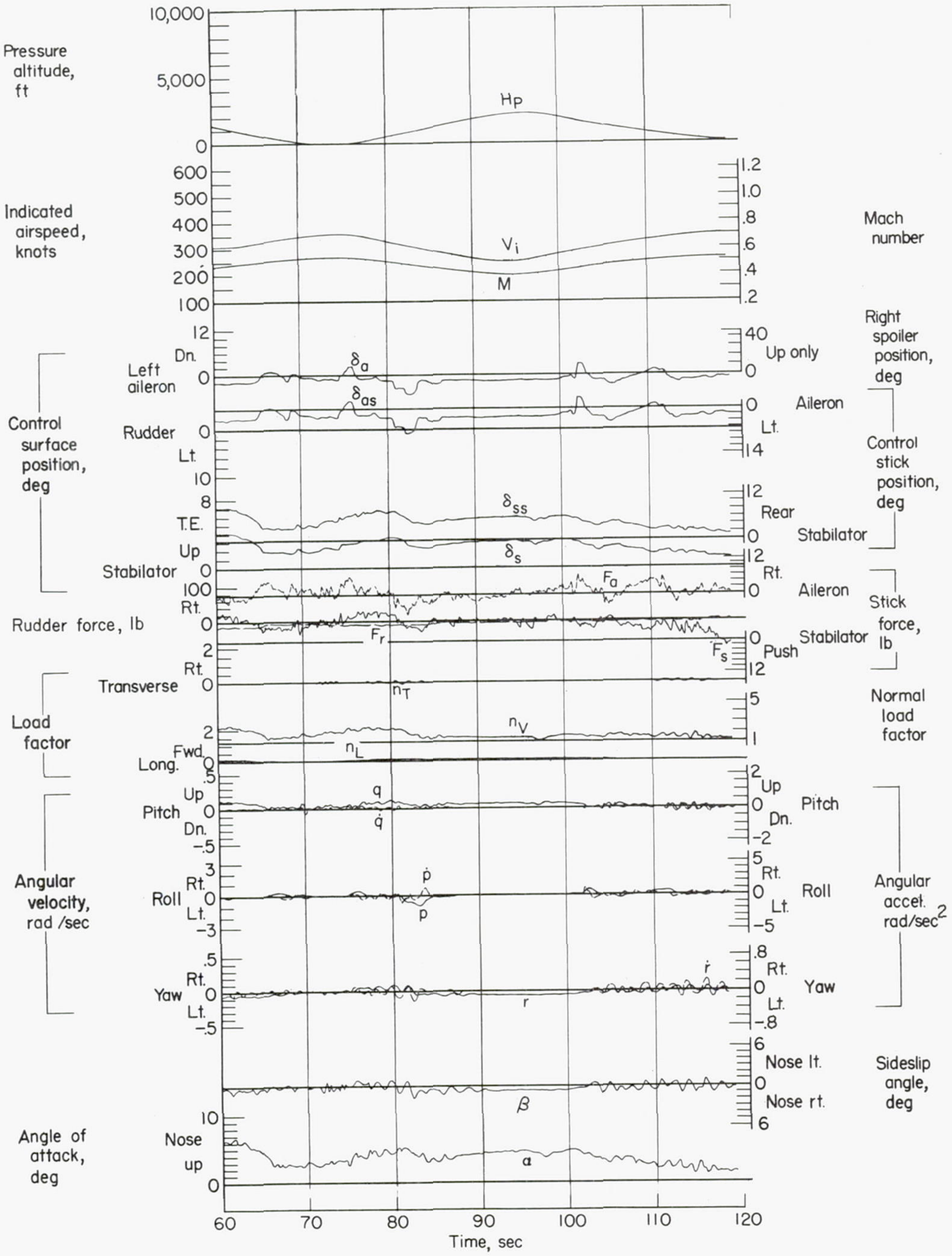

(b)

Figure 38.- Continued.

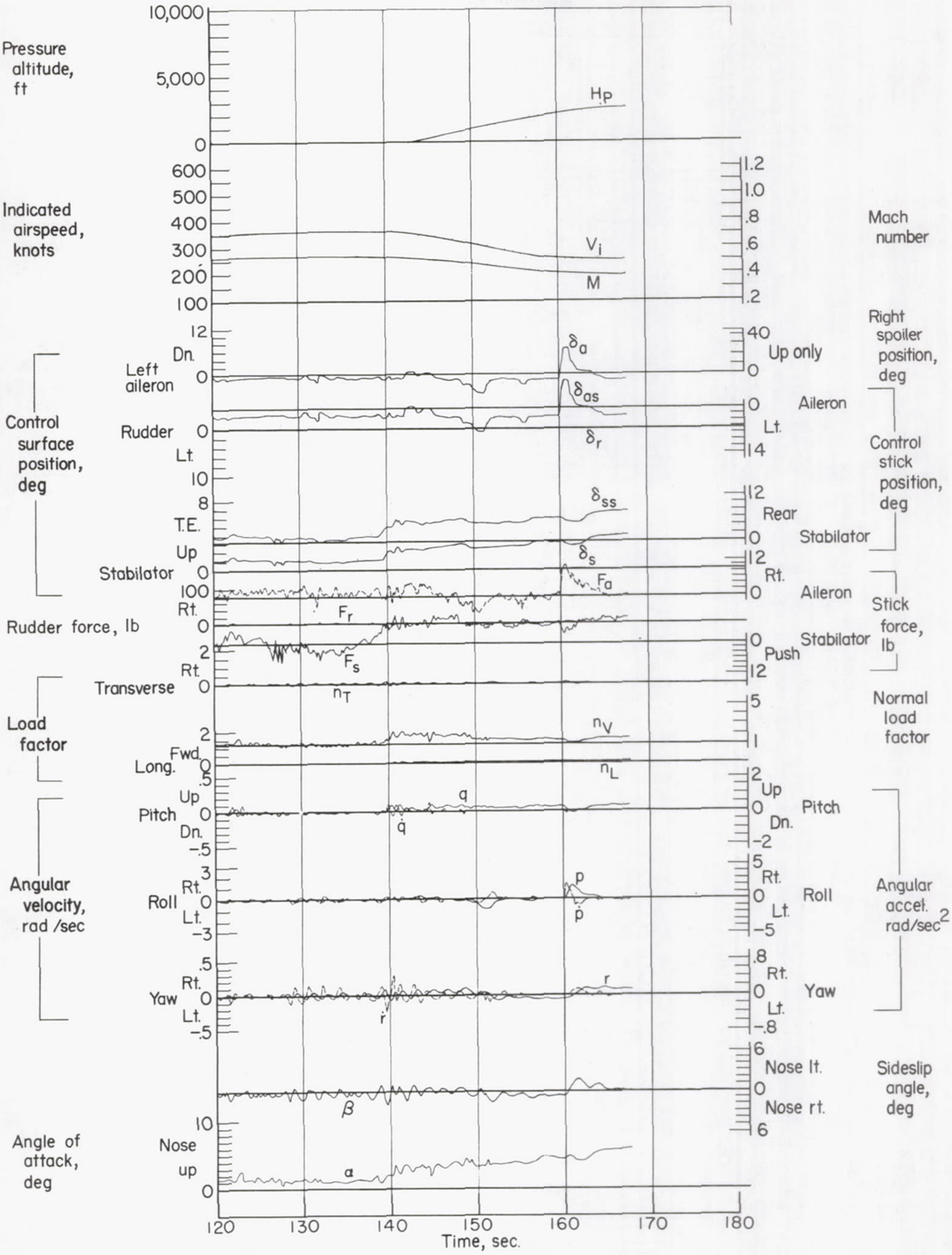

(c)

Figure 38.- Concluded.

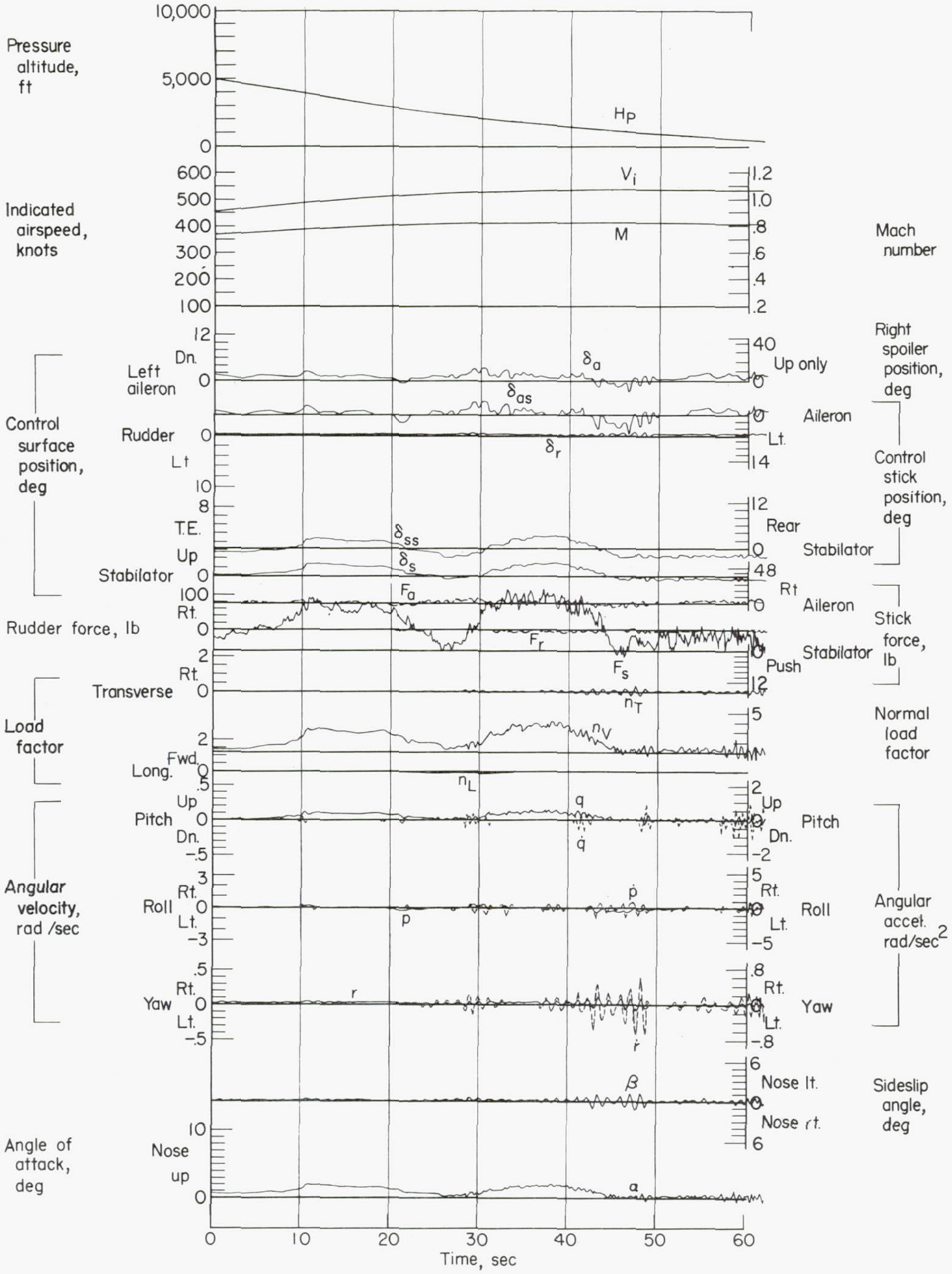

(a)

Figure 39.- Data obtained during over-the-shoulder LABS run. Airplane weight, 19,000 pounds; center of gravity at 20.3 percent $\bar{c}$; flight 29.

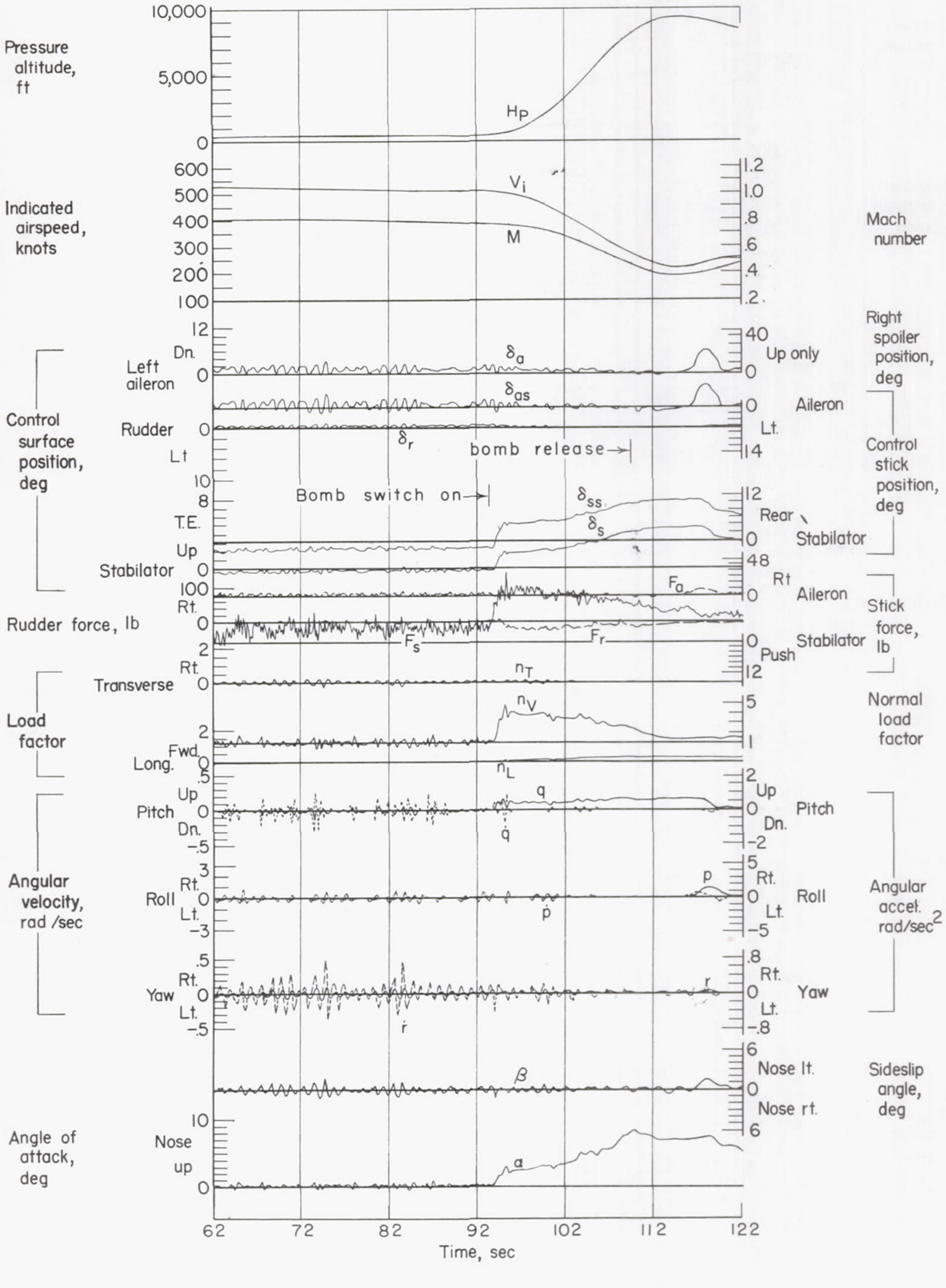

(b)

Figure 39.- Concluded.

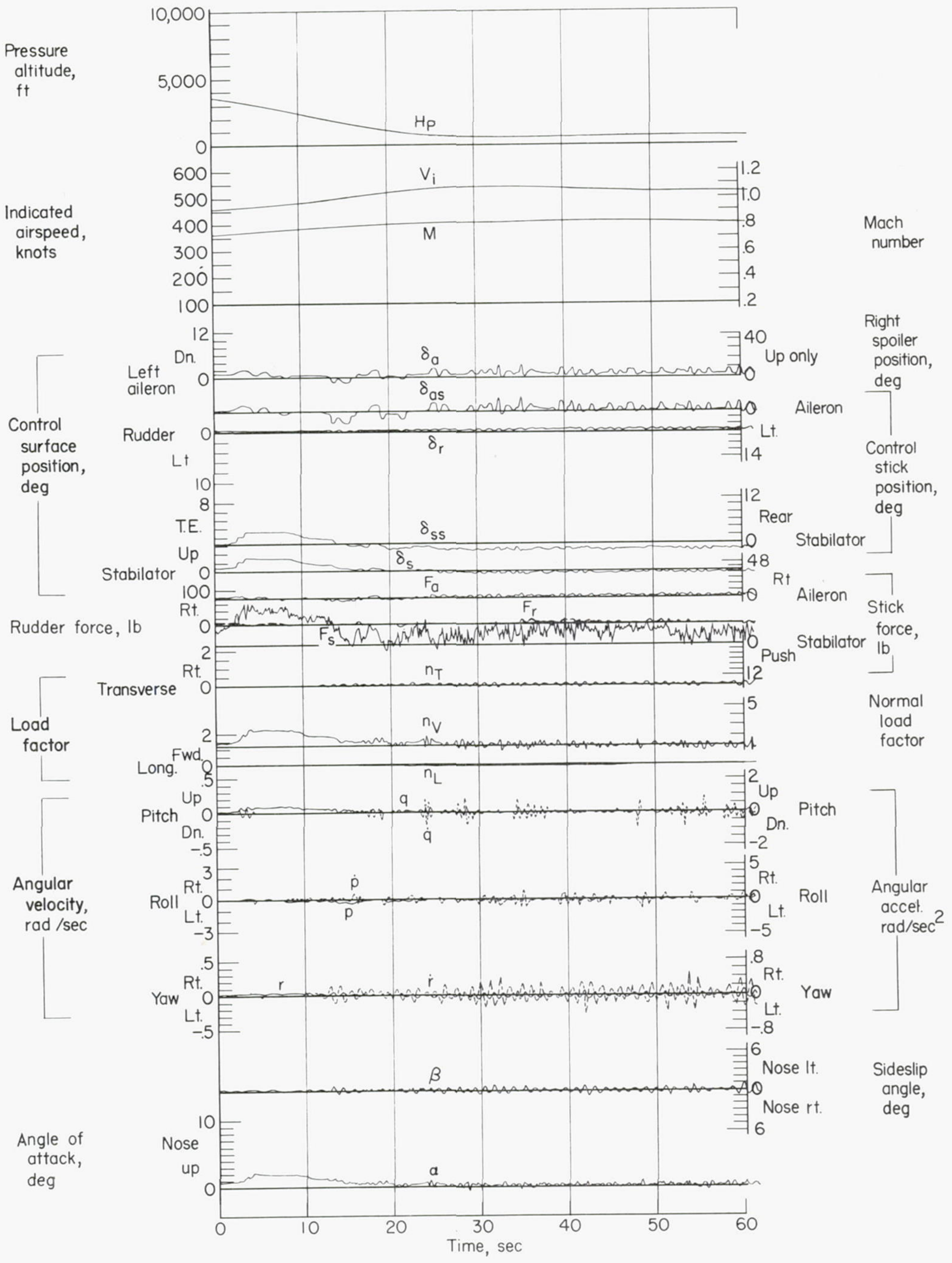

(a)

Figure 40.- Data obtained during over-the-shoulder LABS run. Airplane weight, 20,050 pounds; center of gravity at 19.7 percent $\bar{c}$; flight 29.

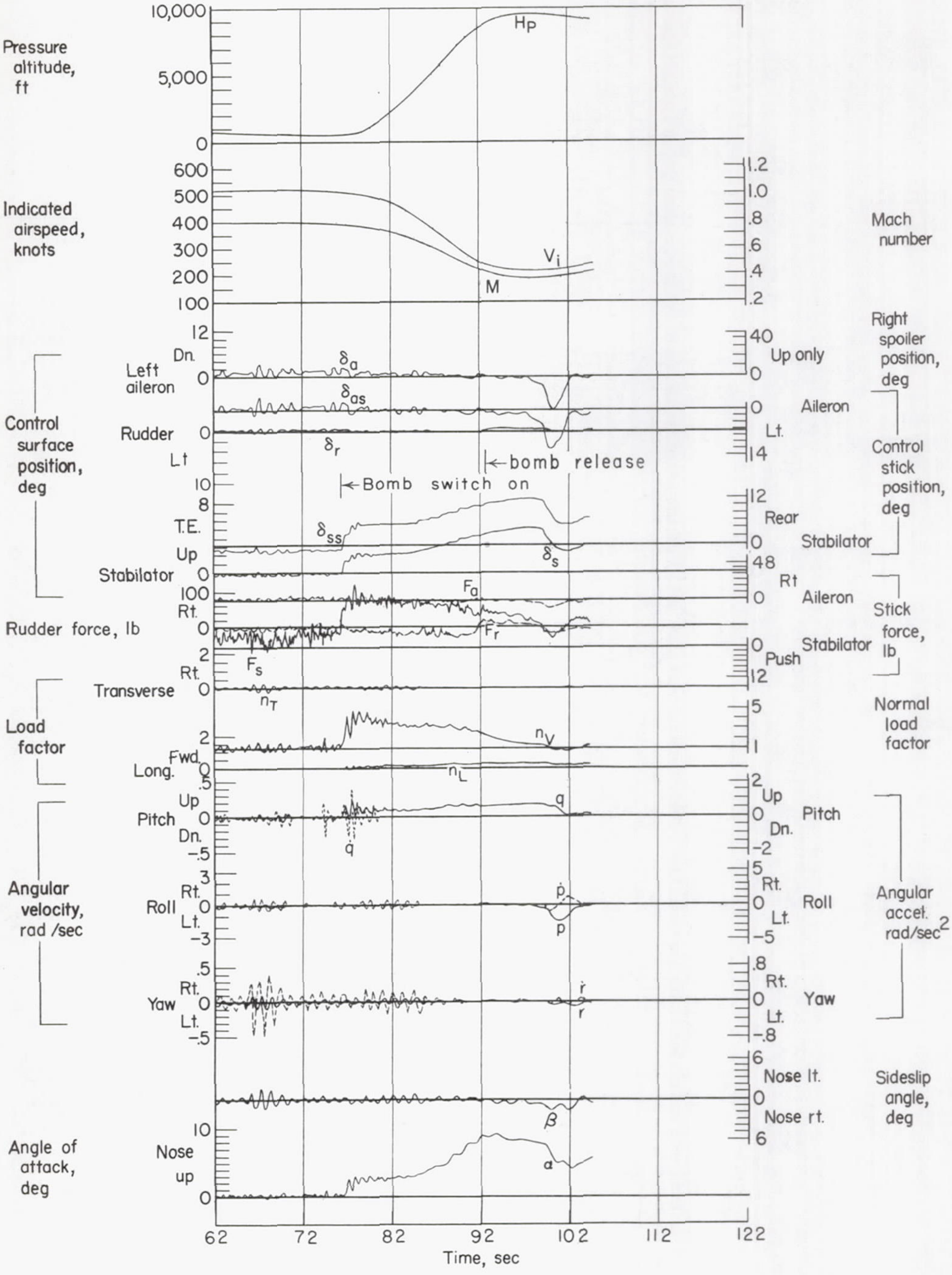

(b)

Figure 40.- Concluded.

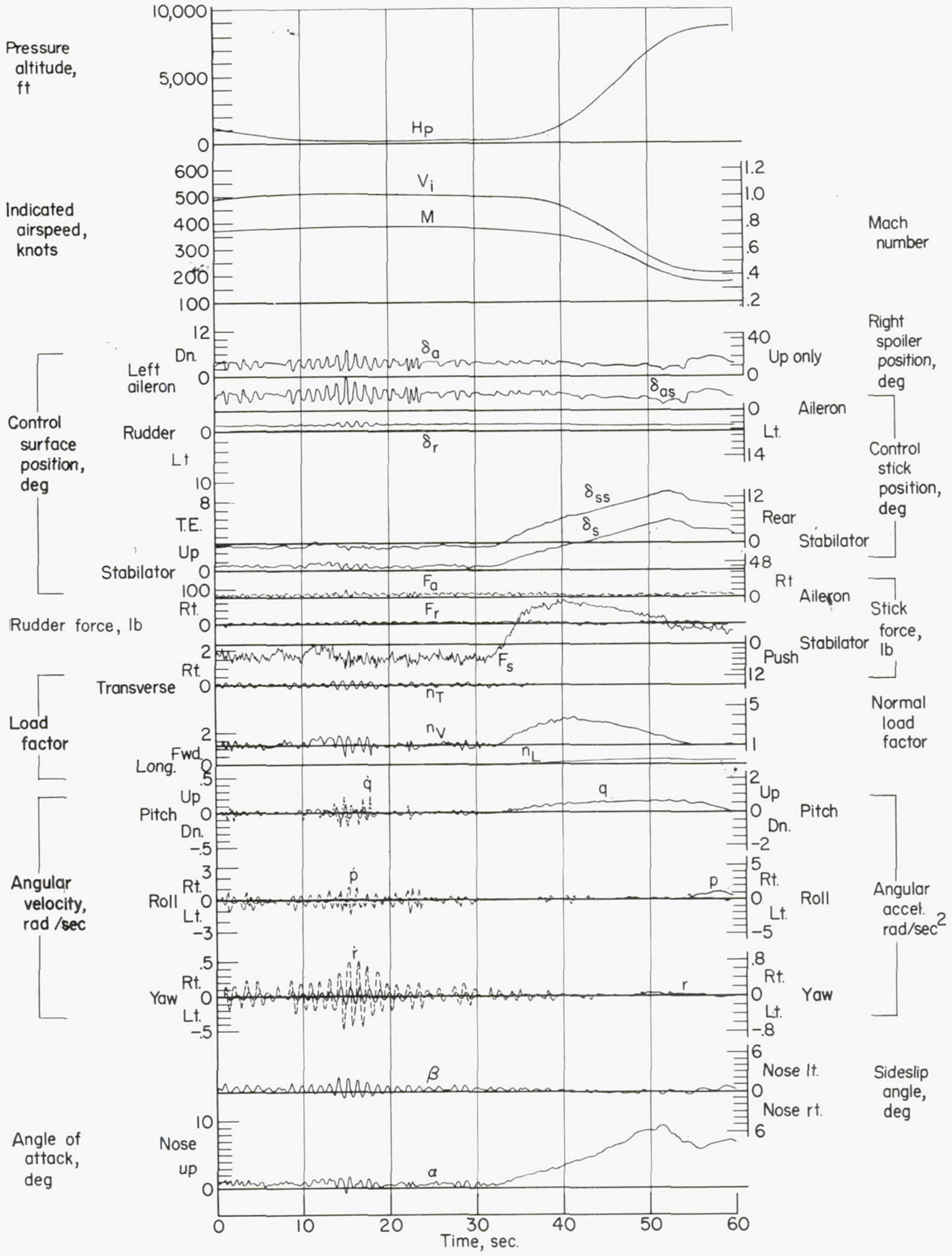

Figure 41.- Data obtained during simulated over-the-shoulder LABS run carrying 1,700-pound practice bomb. Airplane weight, 18,650 pounds; center of gravity at 20.0 percent $\bar{c}$; flight 48.

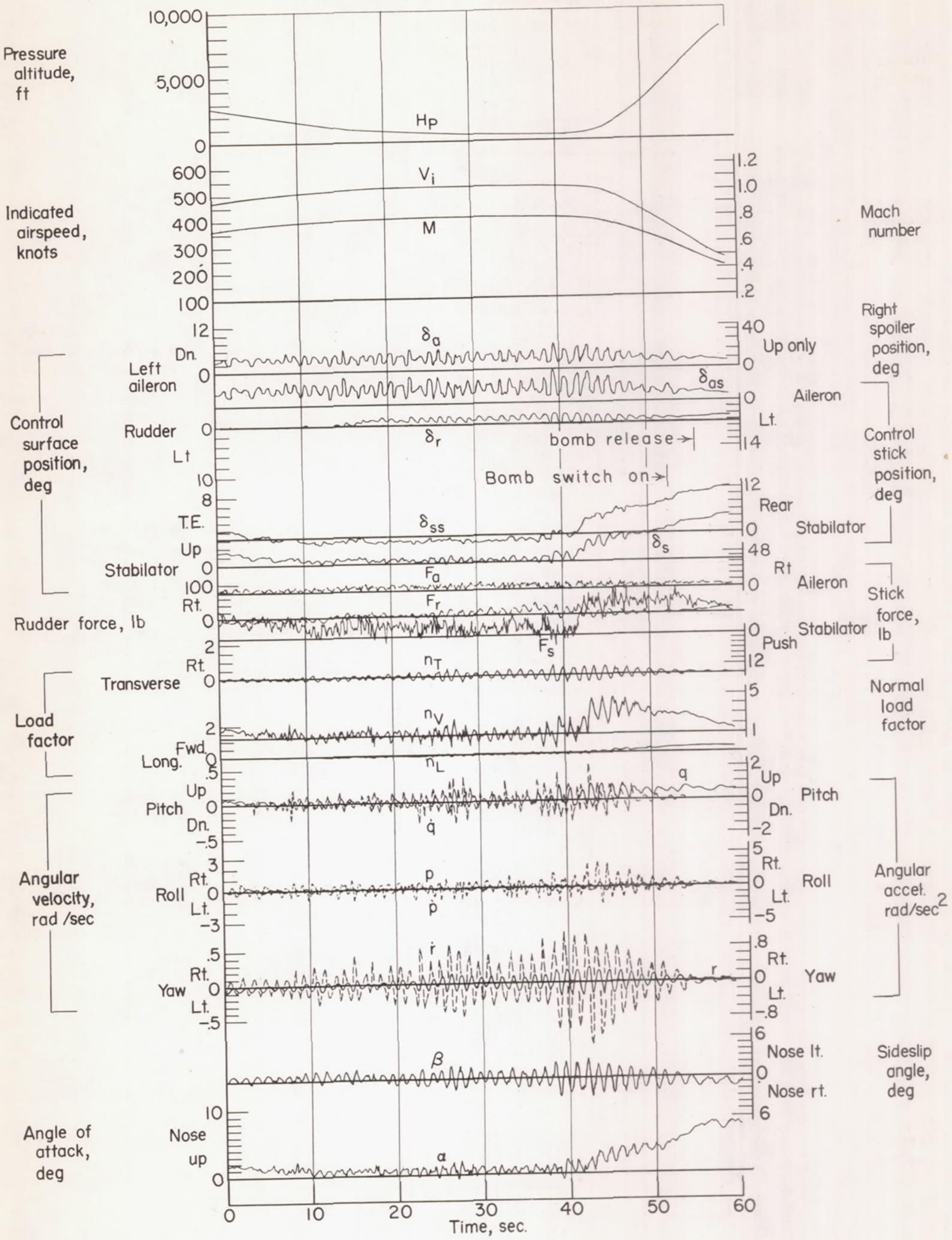

Figure 42.- Data obtained during over-the-shoulder LABS run carrying 1,700-pound practice bomb and dropping 3-pound practice bomb. Airplane weight, 19,750 pounds; center of gravity at 19.5 percent $\bar{c}$; flight 53.

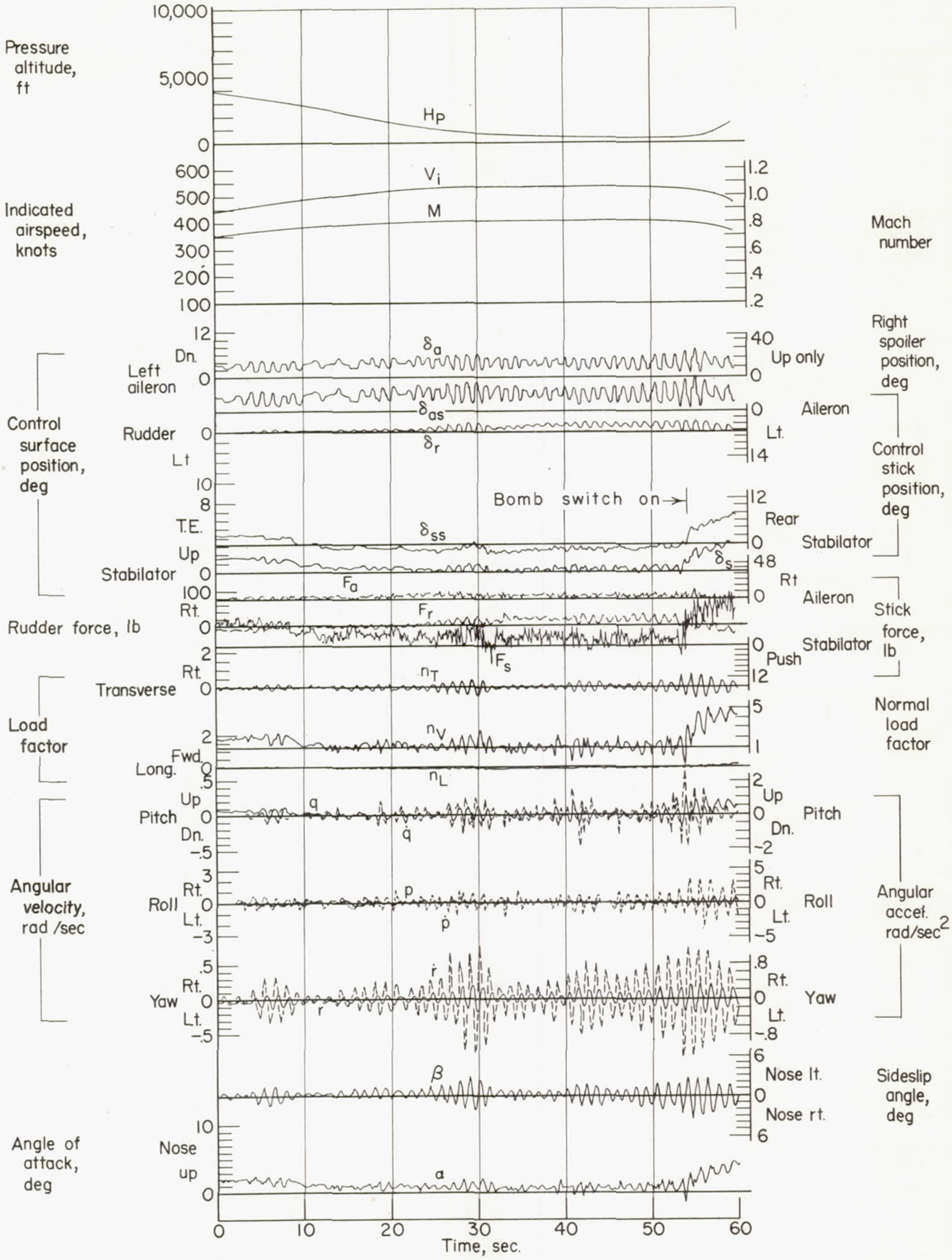

(a)

Figure 43.- Data obtained during over-the-shoulder LABS run dropping a 1,700-pound practice bomb. Airplane weight, before dropping bomb, 19,550 pounds; center of gravity at 19.9 percent $\bar{c}$ with bomb, 20.2 percent $\bar{c}$ after dropping bomb; flight 53.

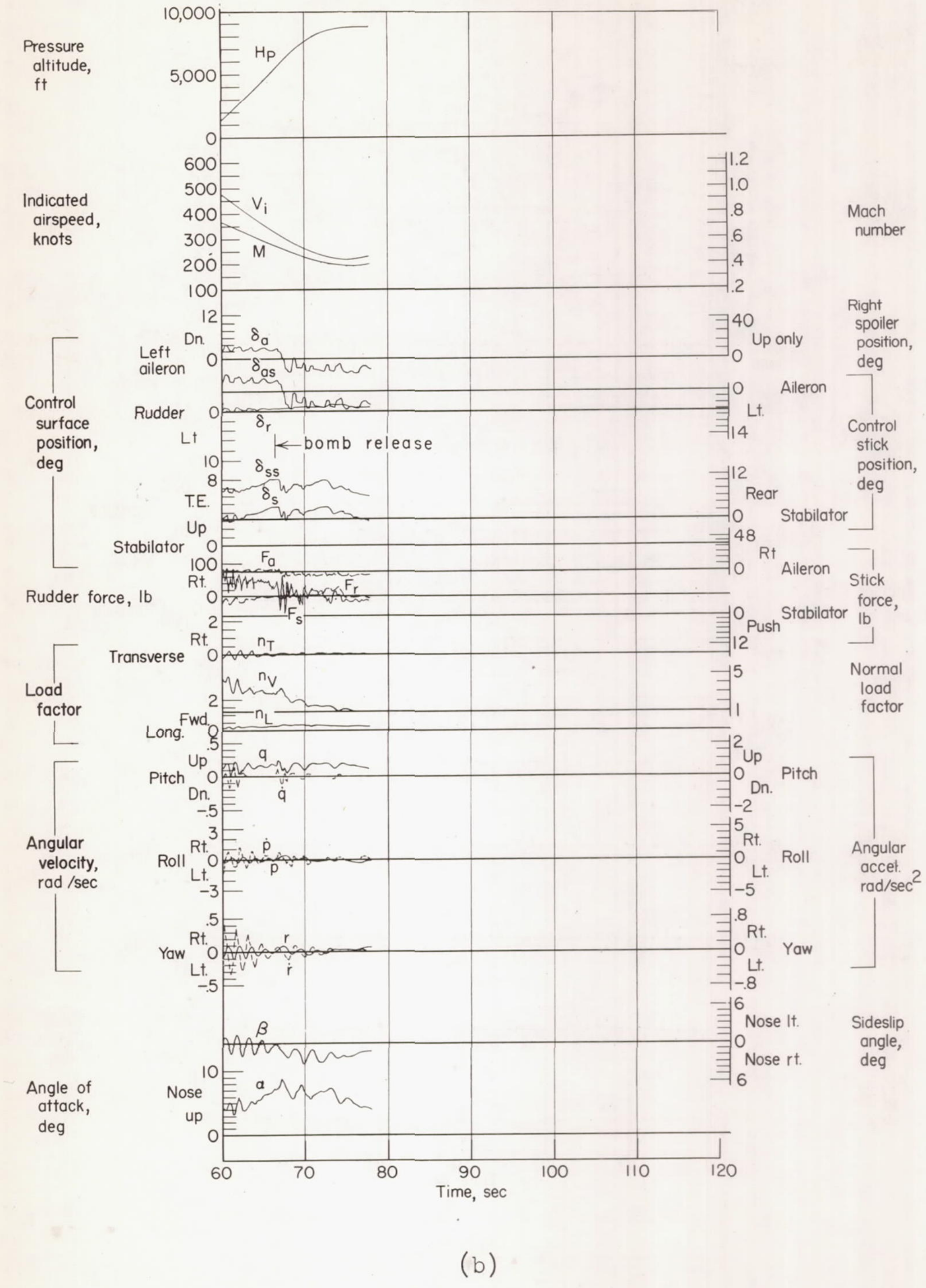

(b)

Figure 43.- Concluded.

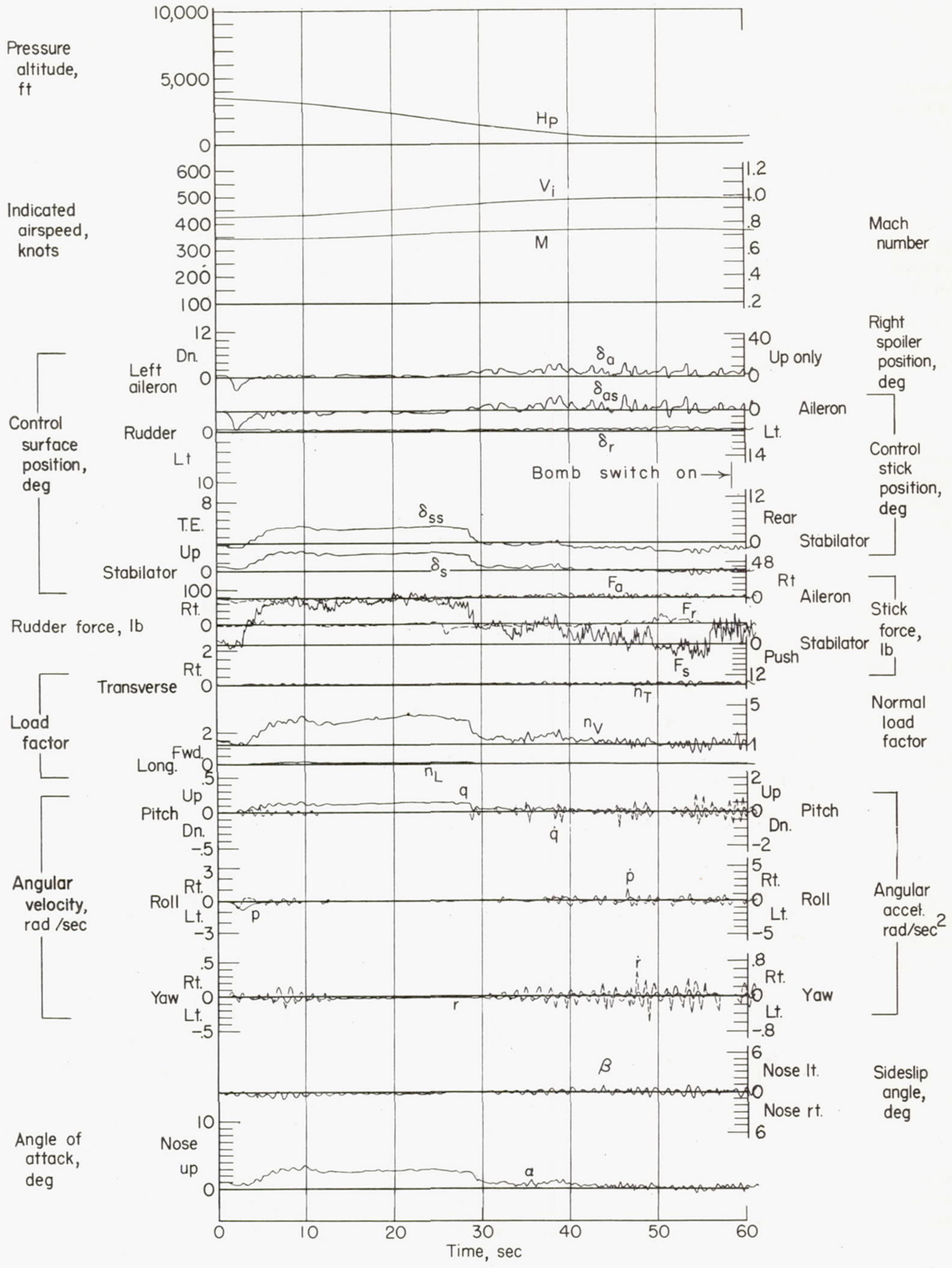

(a)

Figure 44.- Data obtained during initial-point LABS run. Airplane weight, 18,500 pounds; center of gravity at 21.3 percent $\bar{c}$; flight 31.

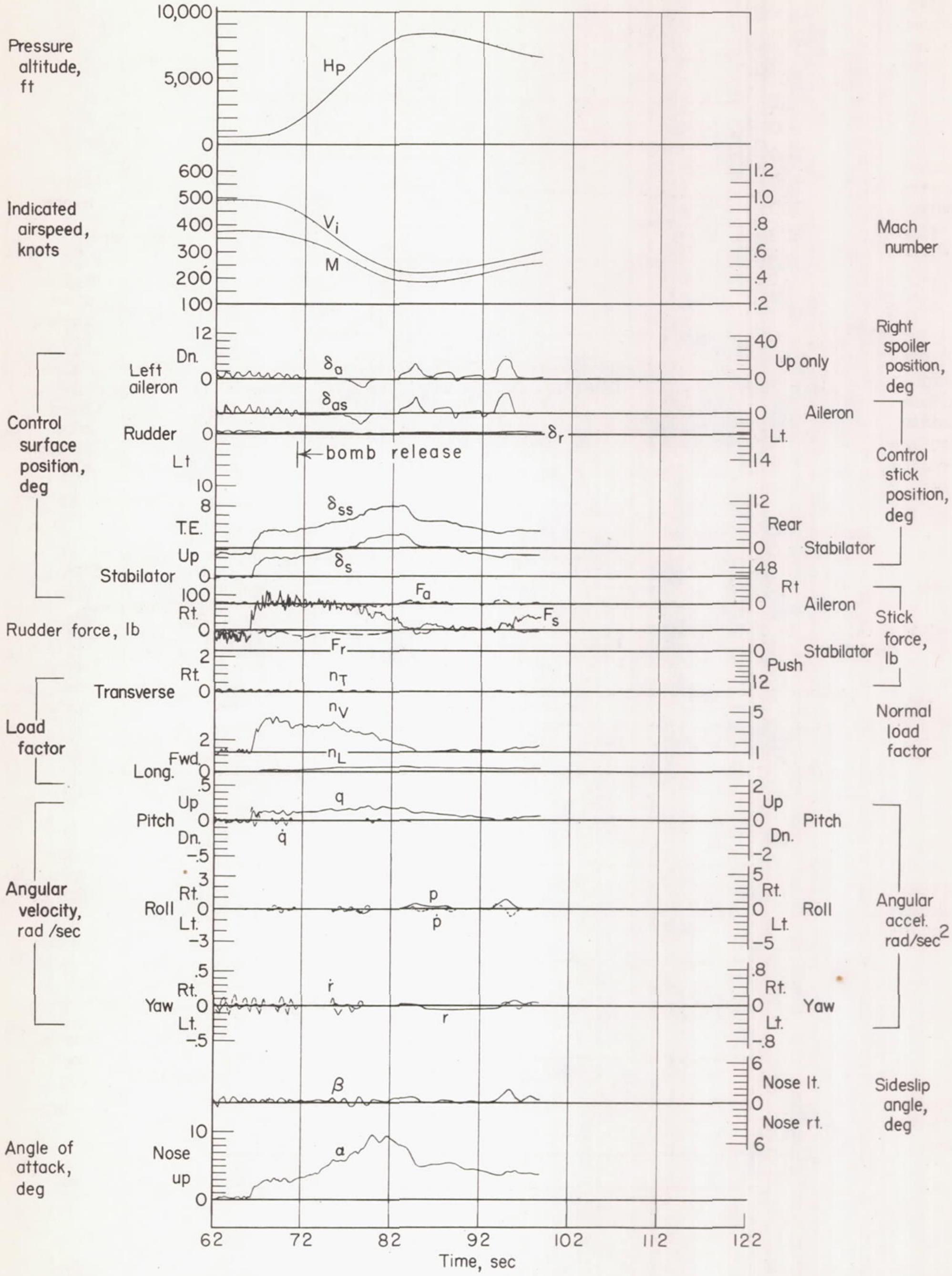

(b)

Figure 44.- Concluded.

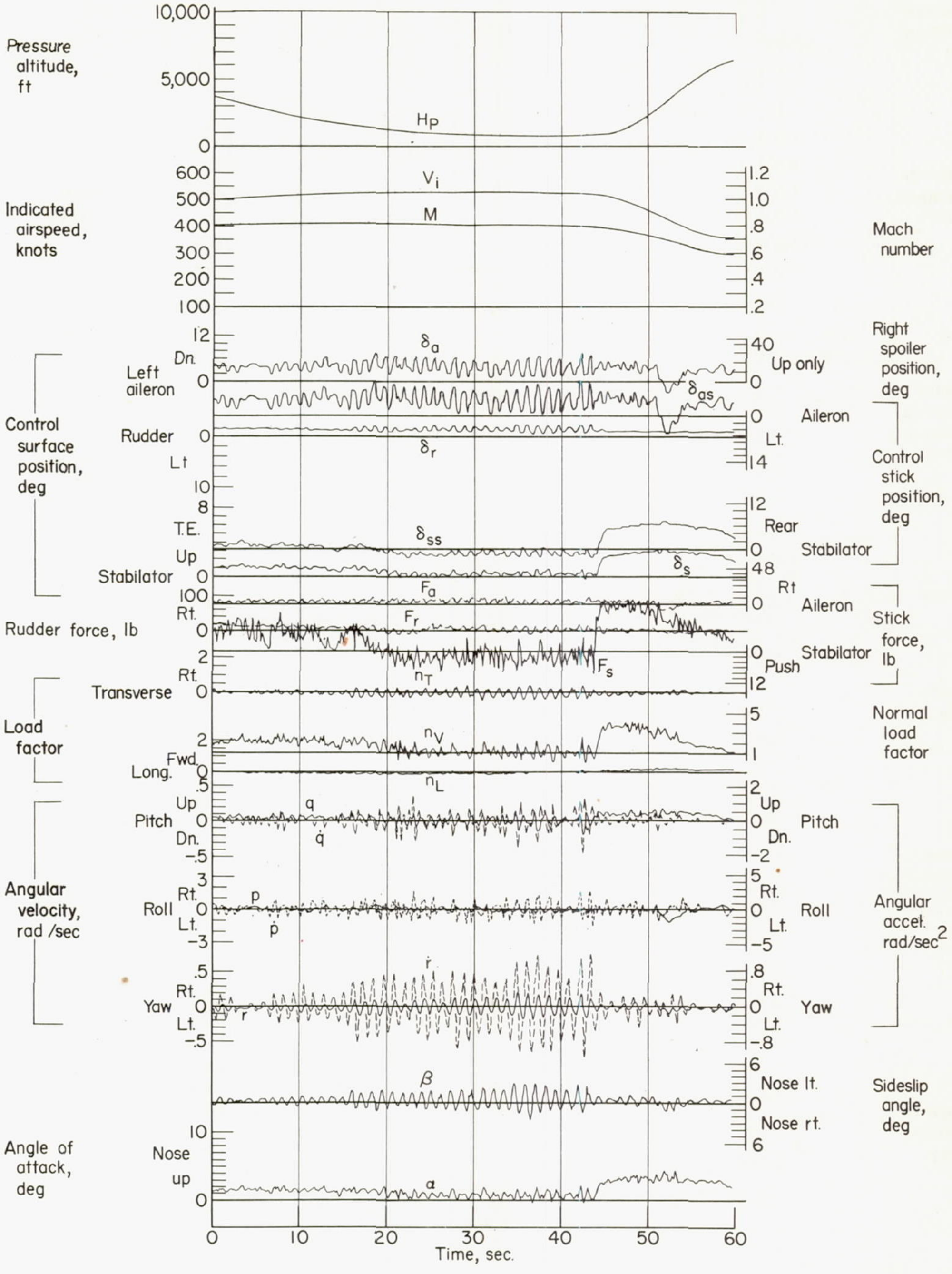

Figure 45.- Data obtained during simulated initial-point LABS run carrying 1,700-pound practice bomb. Airplane weight, 20,450 pounds; center of gravity at 18.2 percent $\bar{c}$; flight 50.

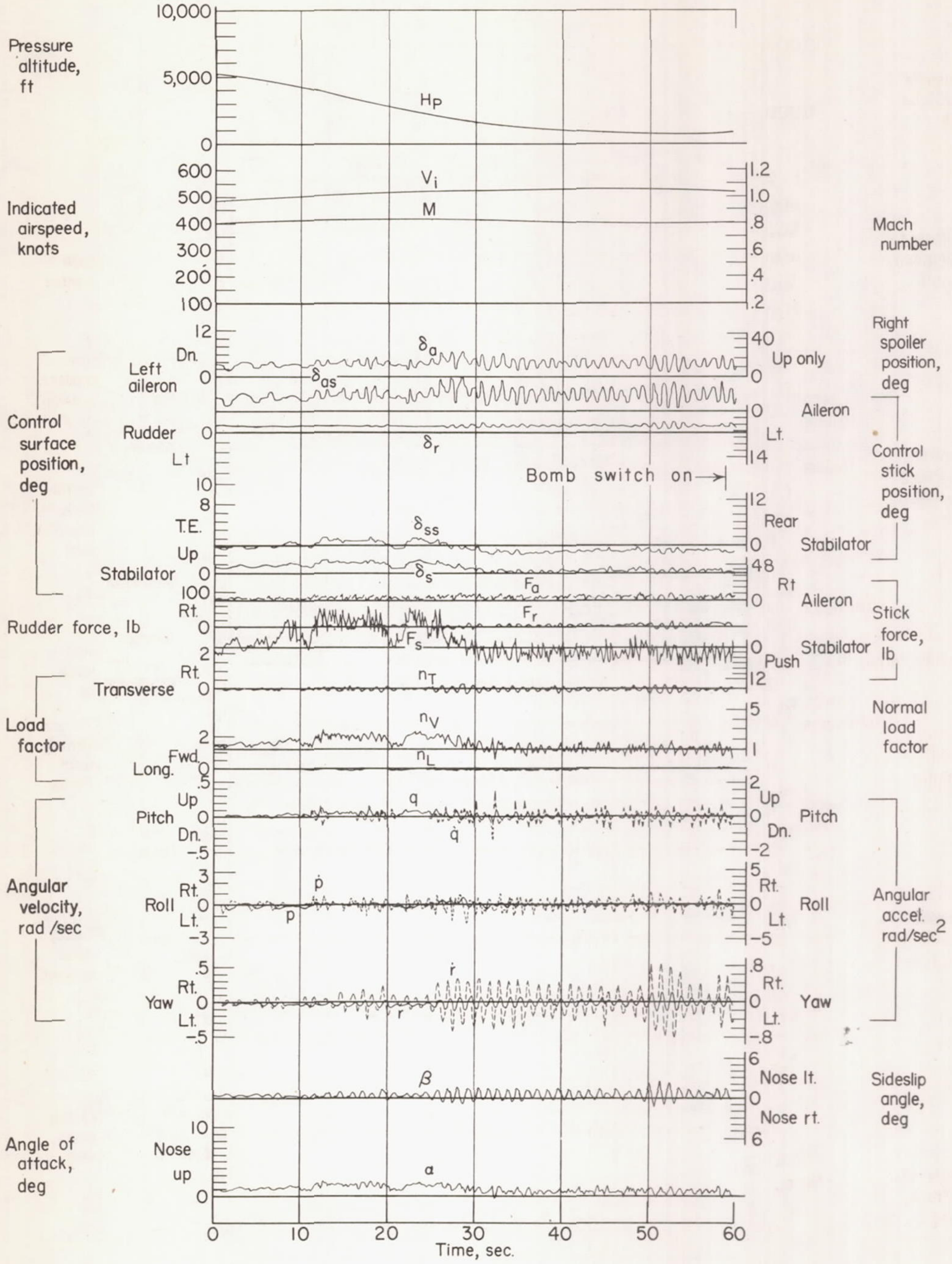

(a)

Figure 46.- Data obtained during initial-point LABS run dropping a 1,700-pound practice bomb. Airplane weight, 20,150 pounds including bomb; center of gravity at 18.7 percent $\bar{c}$ with bomb, 20.1 percent $\bar{c}$ after dropping bomb; flight 50.

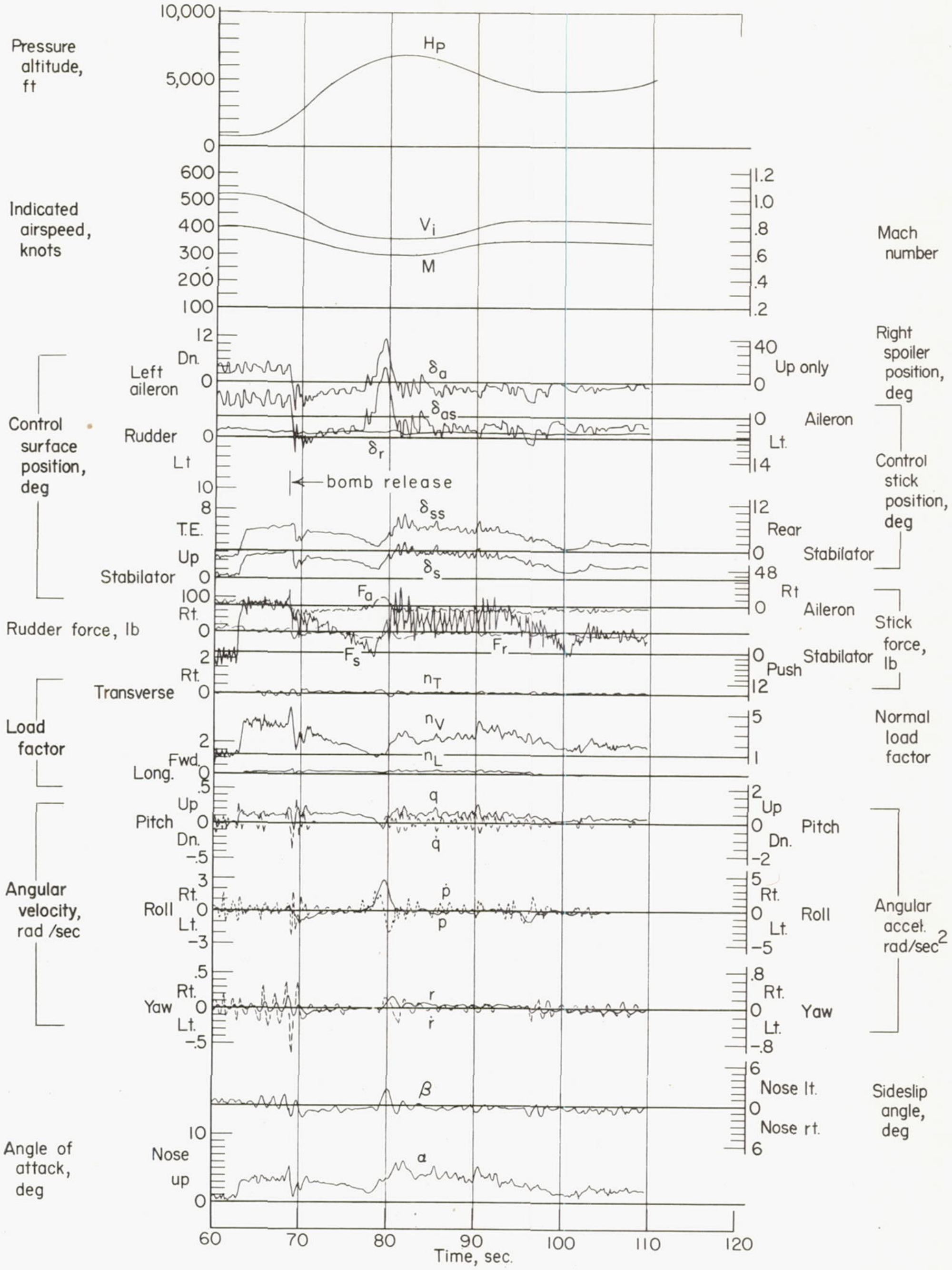

(b)

Figure 46.- Concluded.

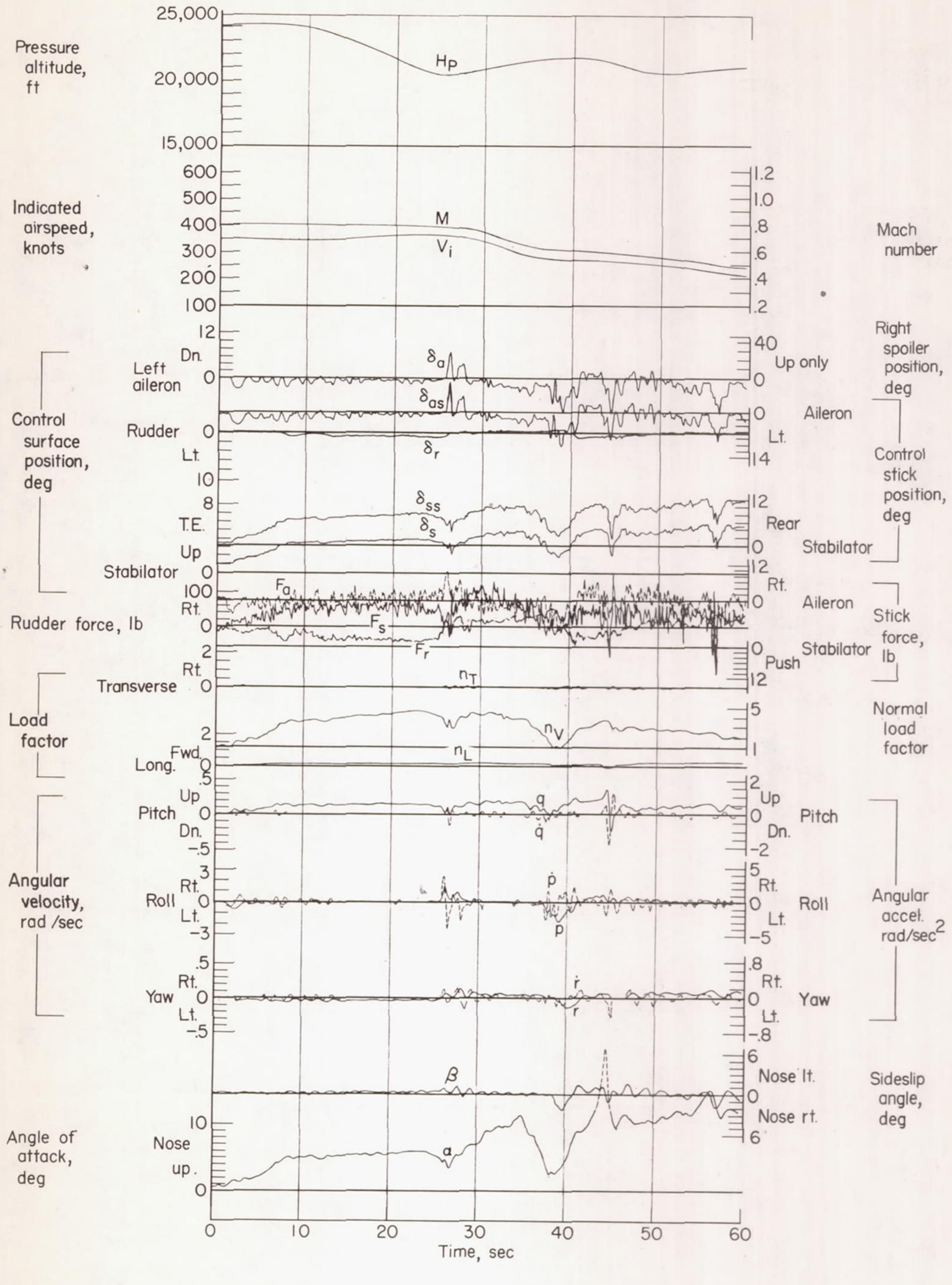

(a)

Figure 47.- Data obtained while rat racing (stall-turns and pitch-up). Airplane weight, 15,950 pounds; center of gravity at 22.1 percent $\bar{c}$; flight 14.

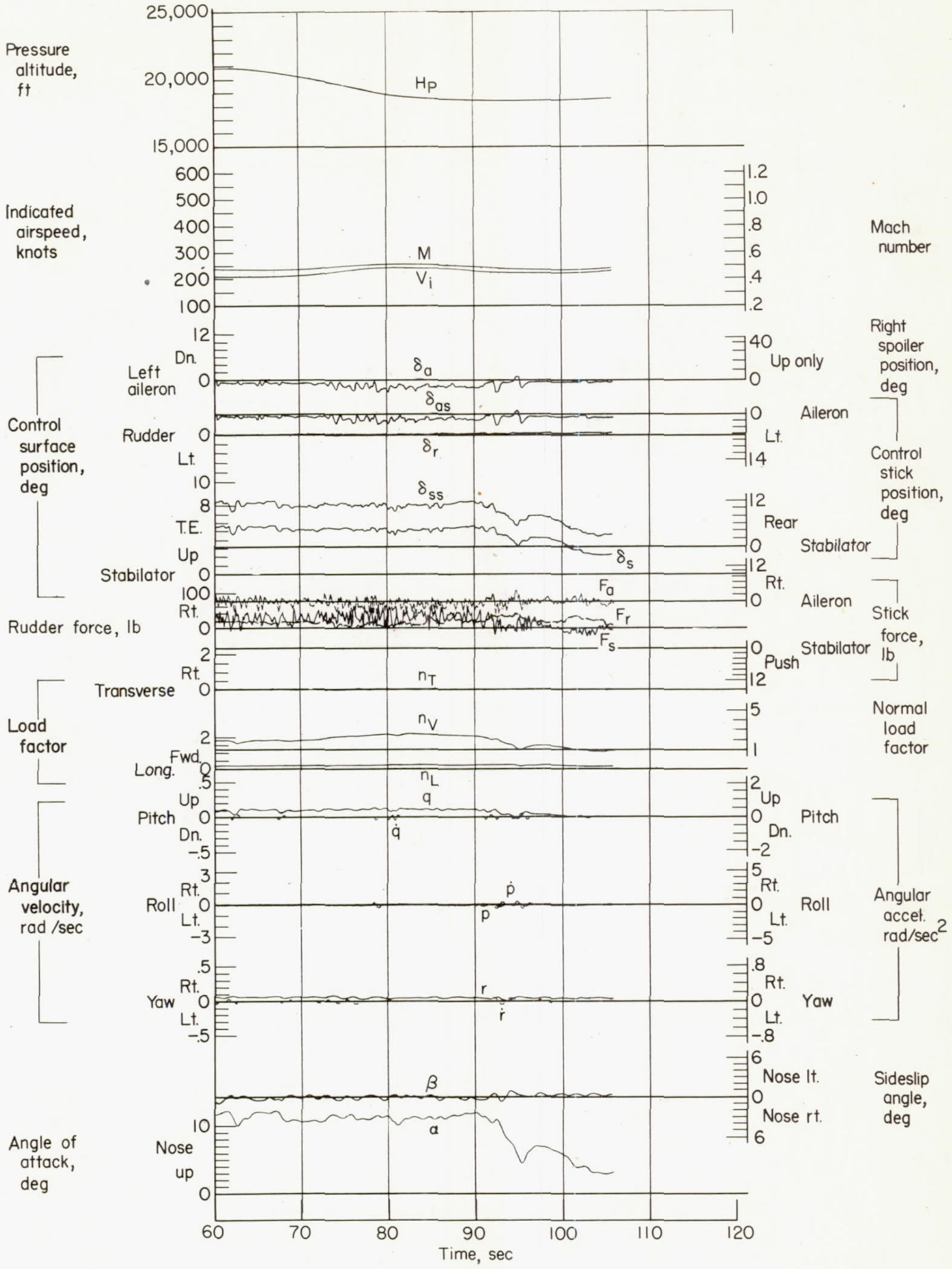

(b)

Figure 47.- Concluded.

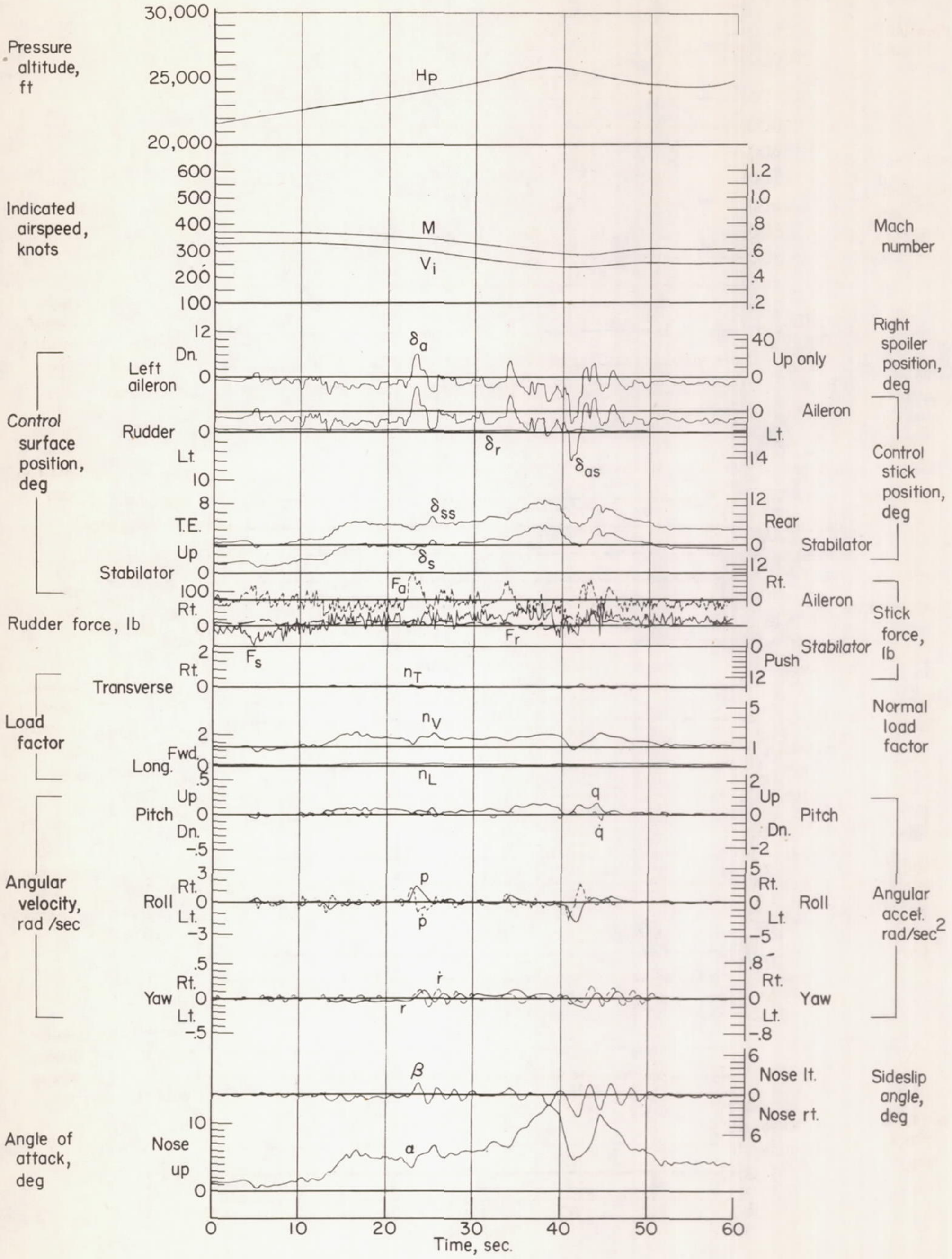

Figure 48.- Data obtained while rat racing. Airplane weight, 18,450 pounds; center of gravity at 20.0 percent $\bar{c}$; flight 16.

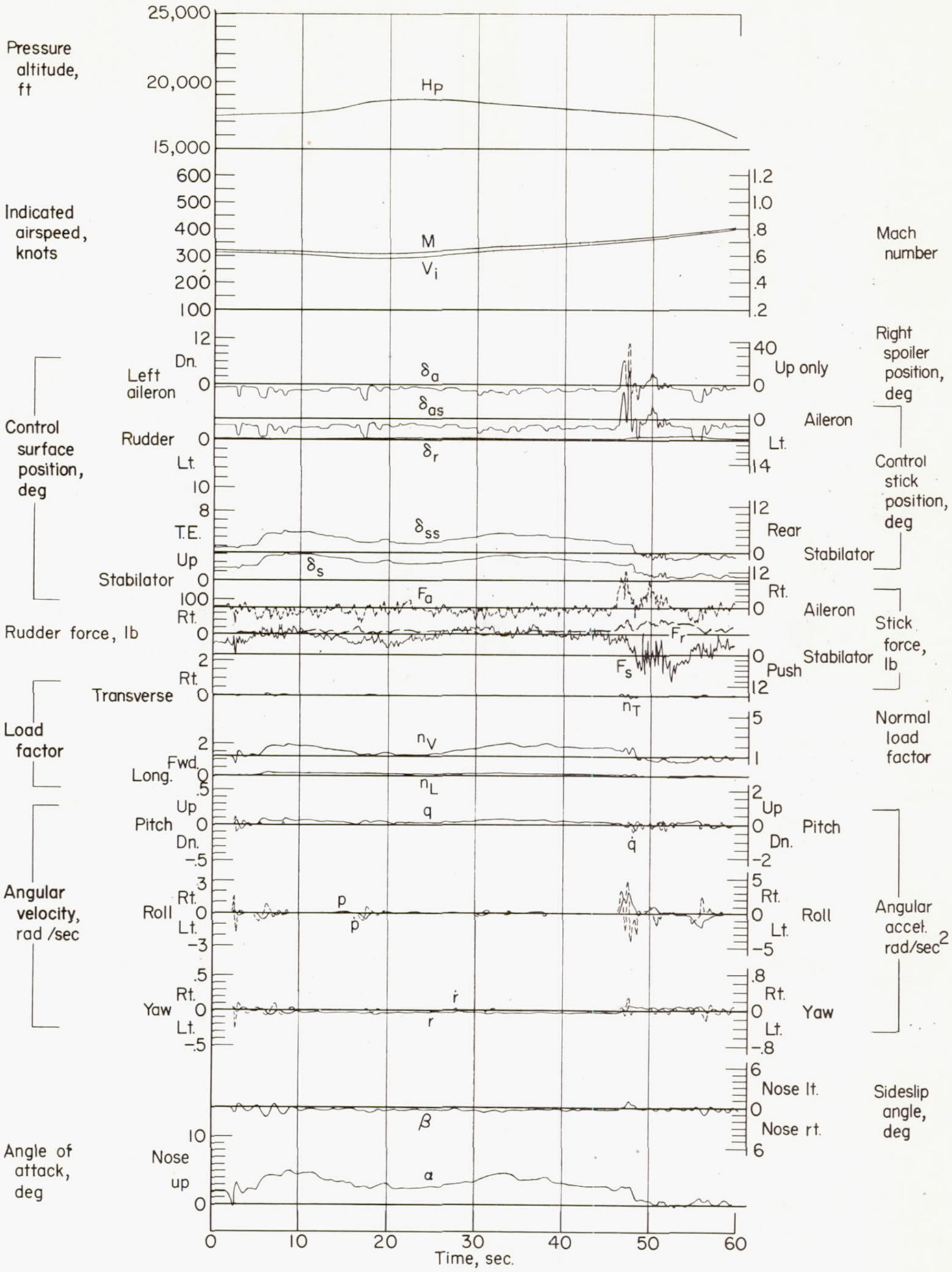

(a)

Figure 49.- Data obtained while rat racing (flew through jet wash at time 2 seconds) with pitch-up. Airplane weight, 17,300 pounds; center of gravity at 22.0 percent $\bar{c}$; flight 16.

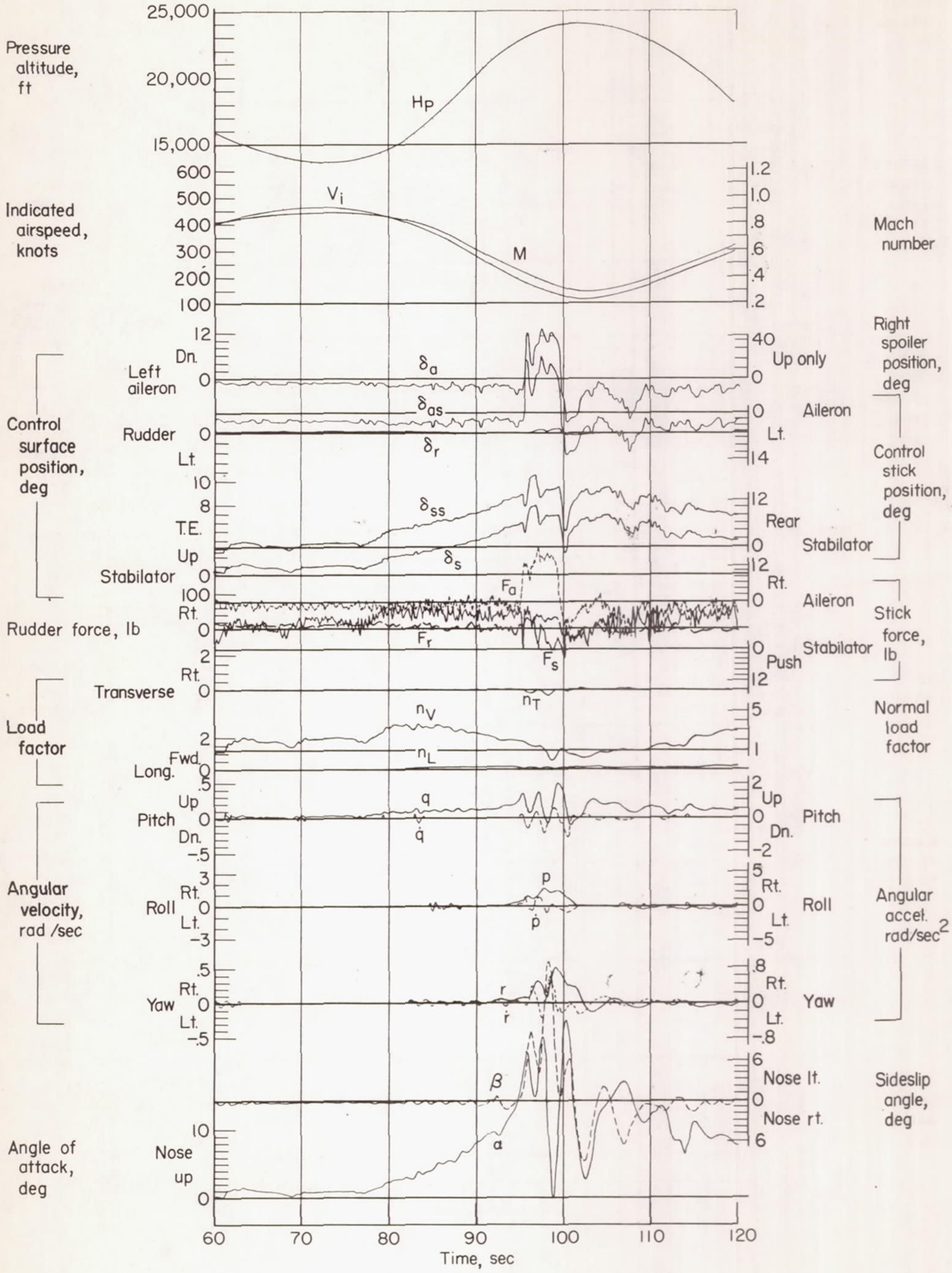

(b)

Figure 49.- Continued.

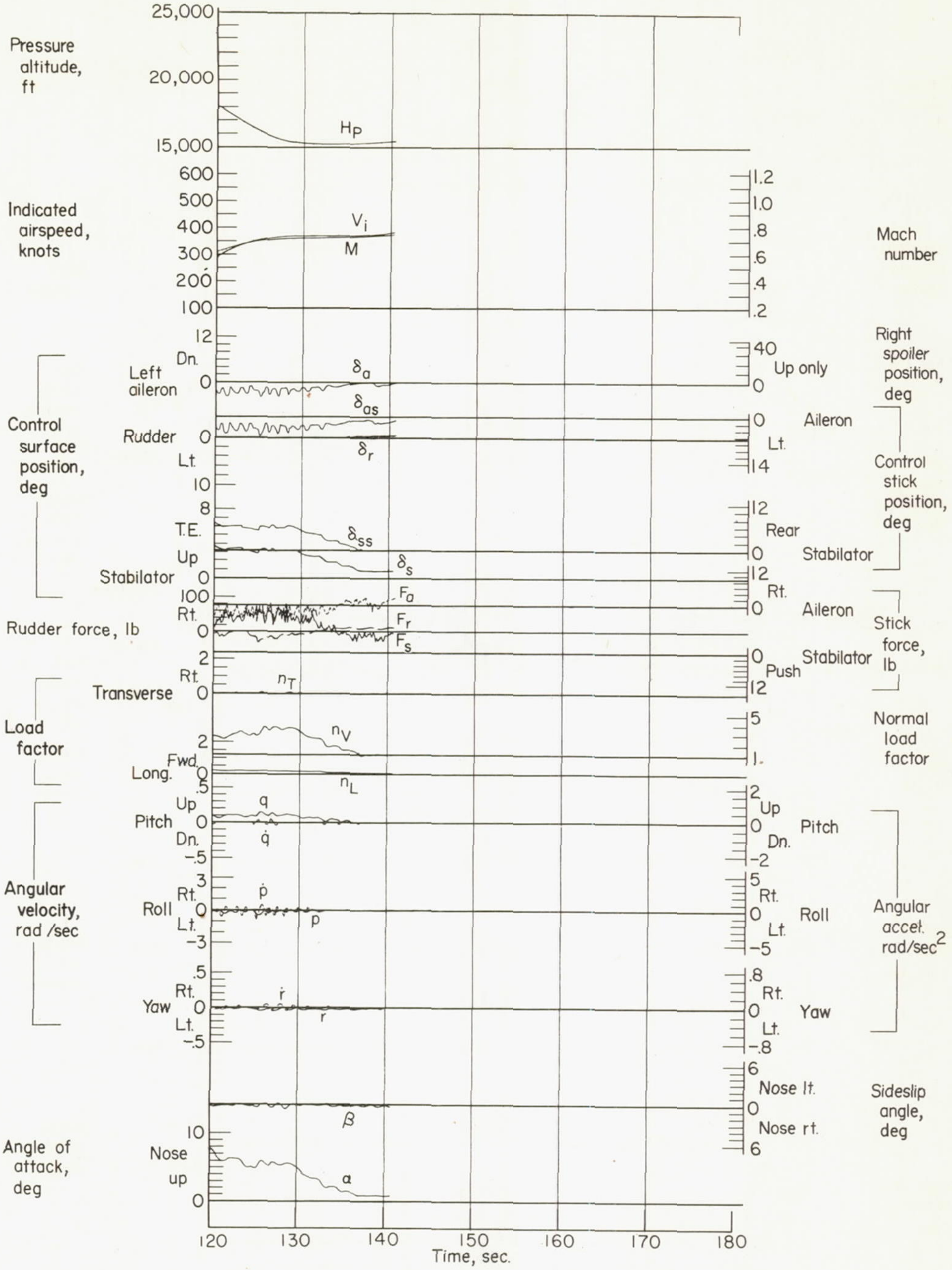

(c)

Figure 49.- Concluded.

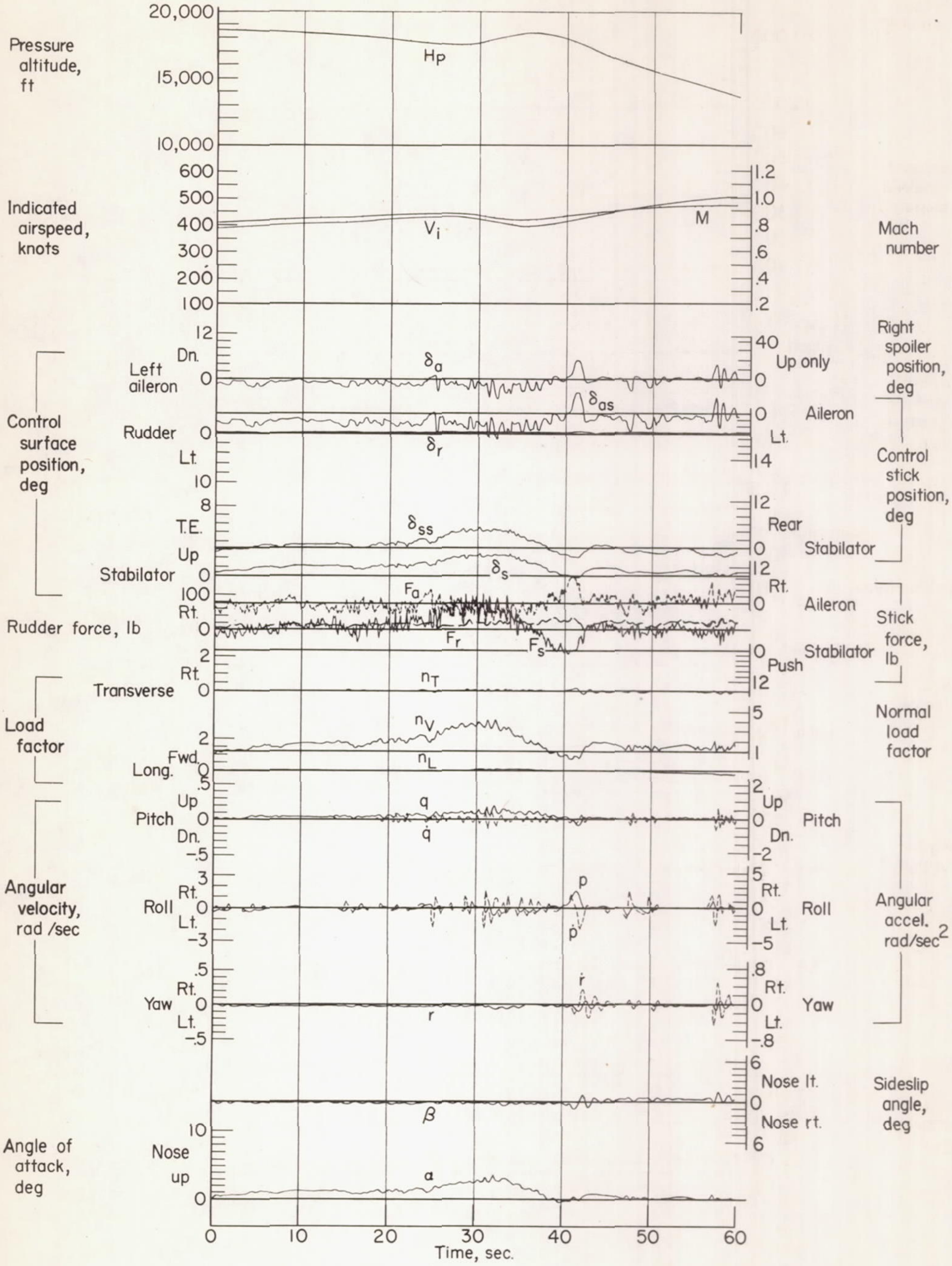

(a)

Figure 50.- Data obtained while rat racing. Airplane weight, 17,050 pounds; center of gravity at 22.1 percent $\bar{c}$; flight 16.

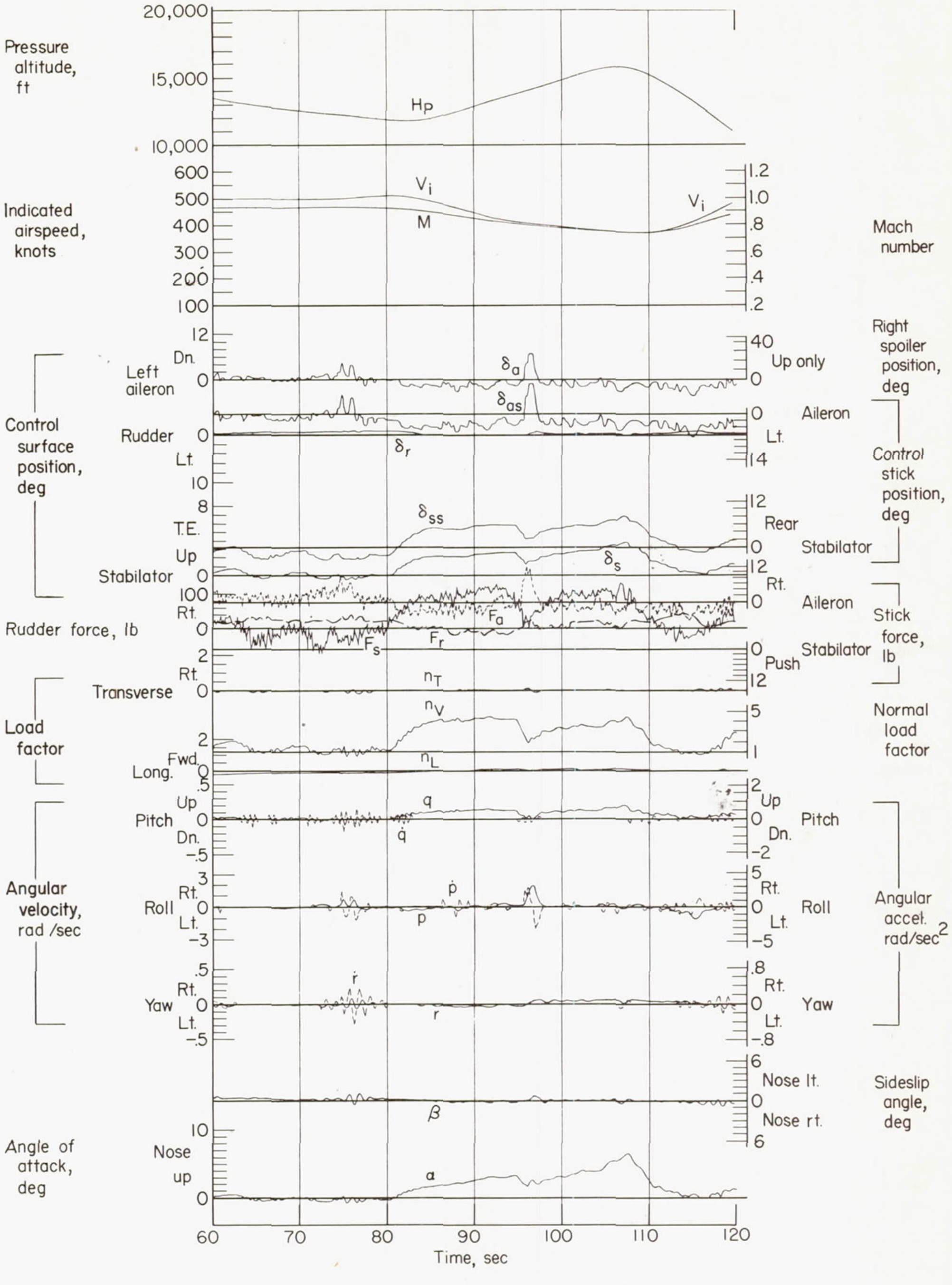

(b)

Figure 50.- Continued.

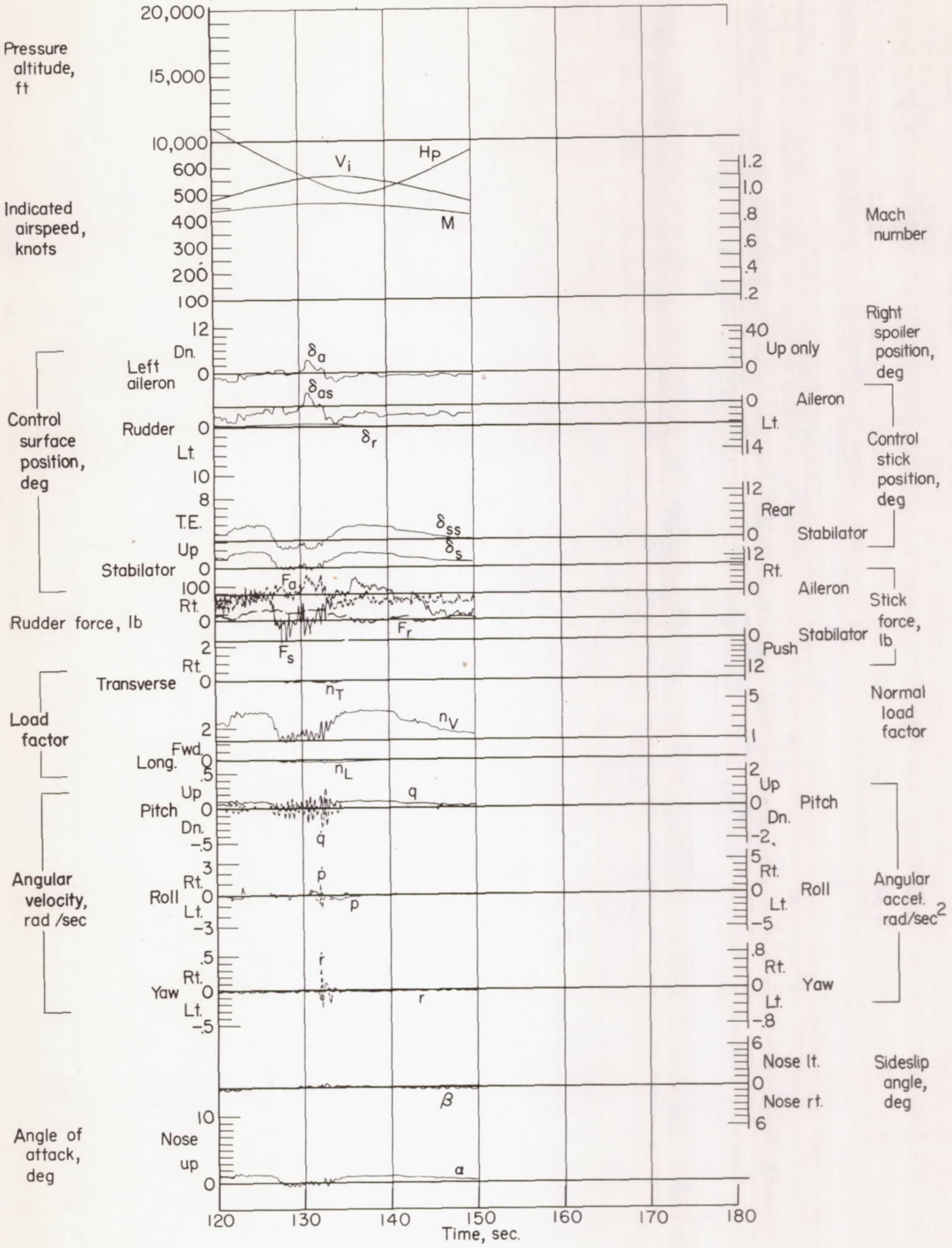

(c)

Figure 50.- Concluded.

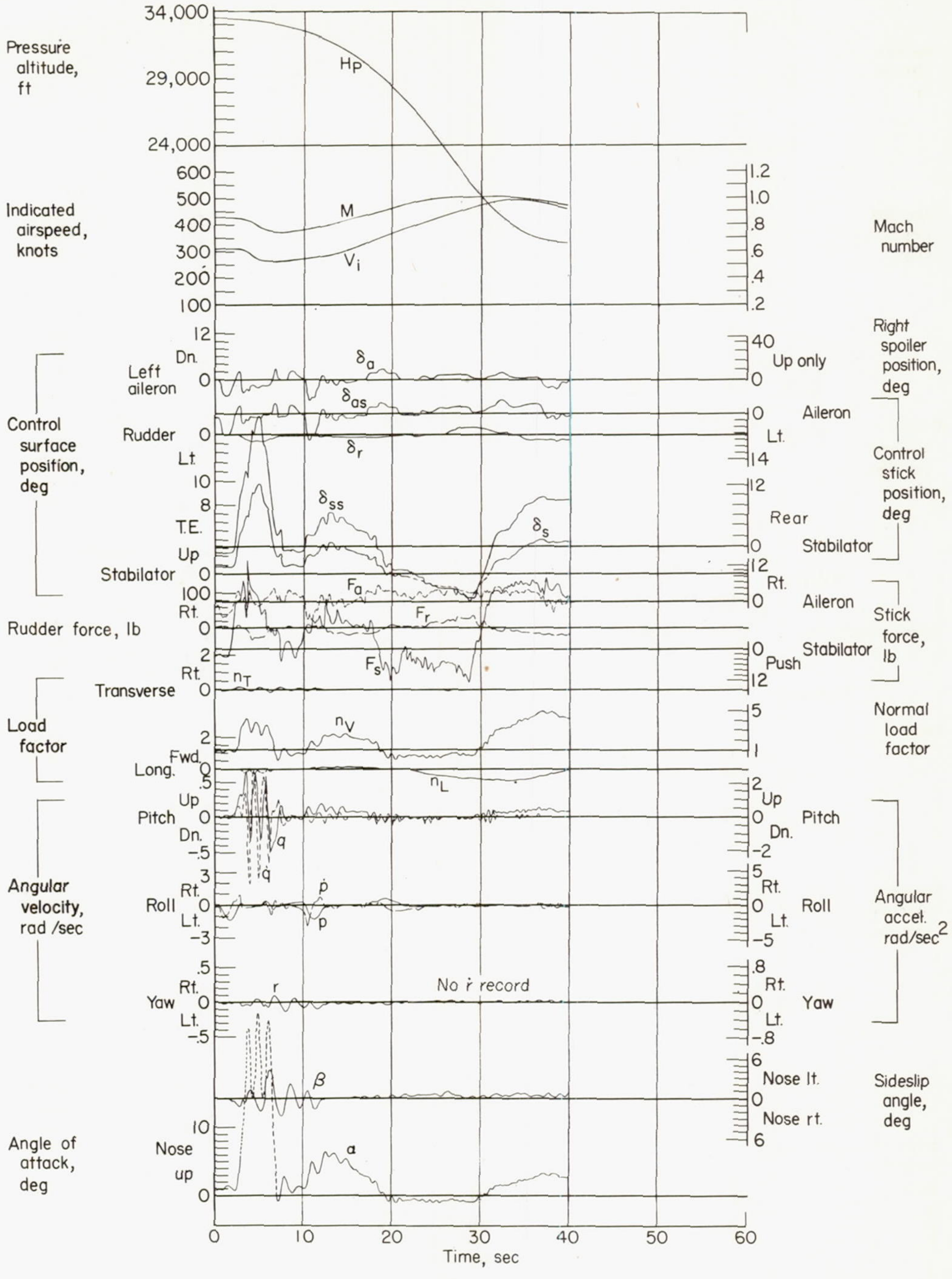

Figure 51.- Data obtained during pitch-up followed by Mach run. Airplane weight, 17,150 pounds; center of gravity at 22.2 percent $\bar{c}$; flight 2.

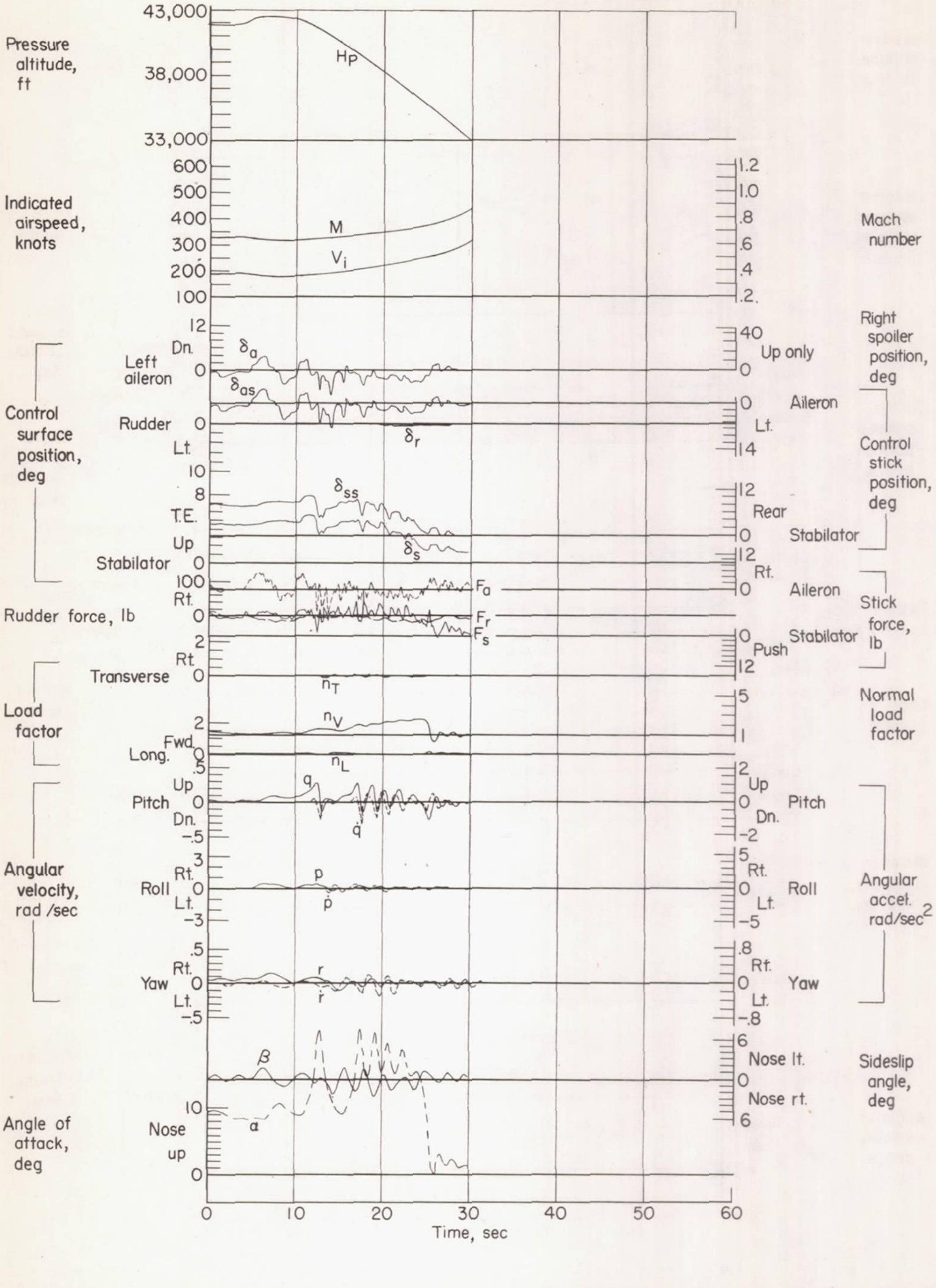

Figure 52.- Data obtained during pitch-up. Airplane weight, 16,900 pounds; center of gravity at 21.8 percent $\bar{c}$; flight 5.

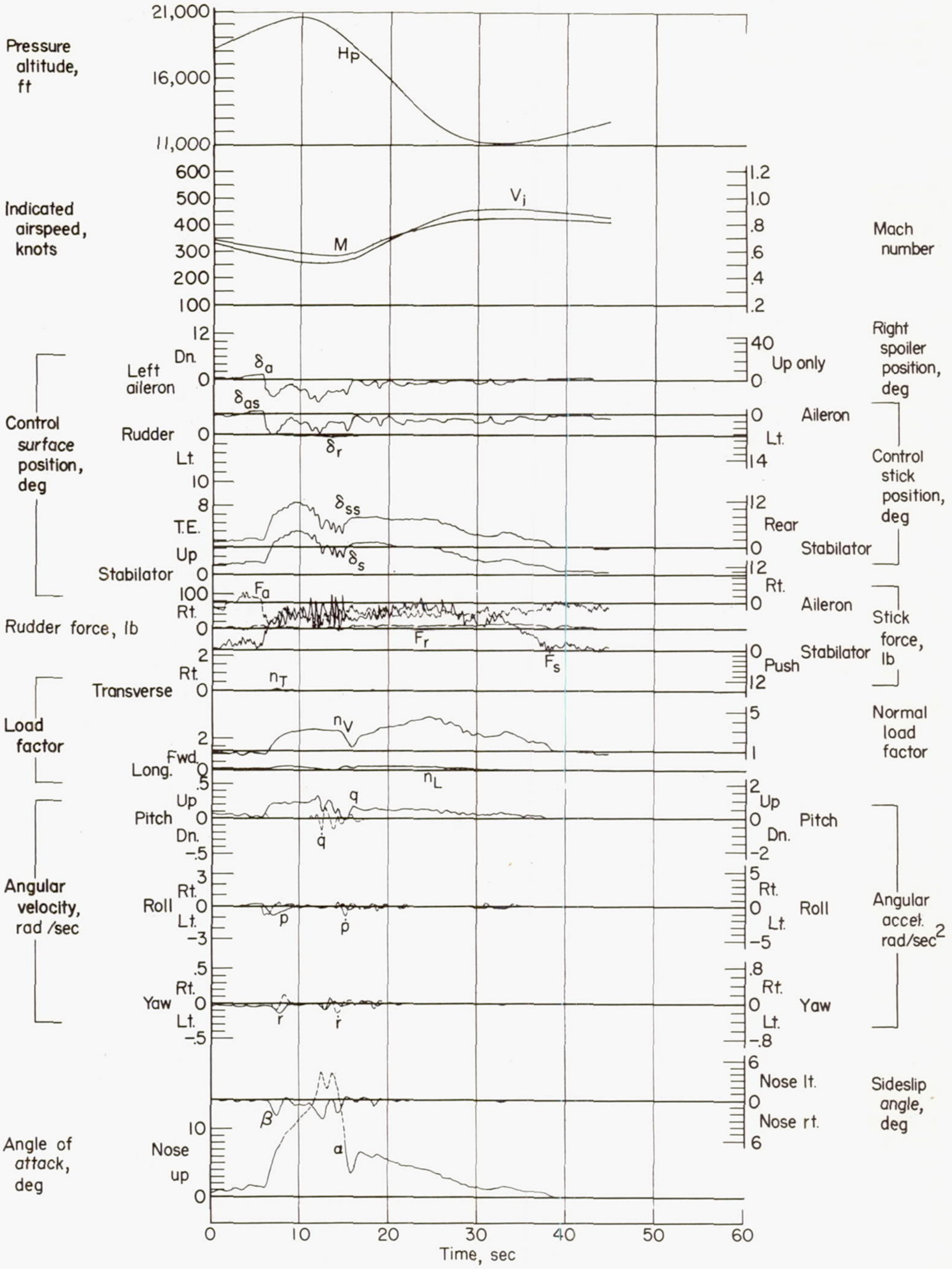

Figure 53.- Data obtained during pitch-up. Airplane weight, 17,550 pounds; center of gravity at 21.5 percent $\bar{c}$; flight 9.

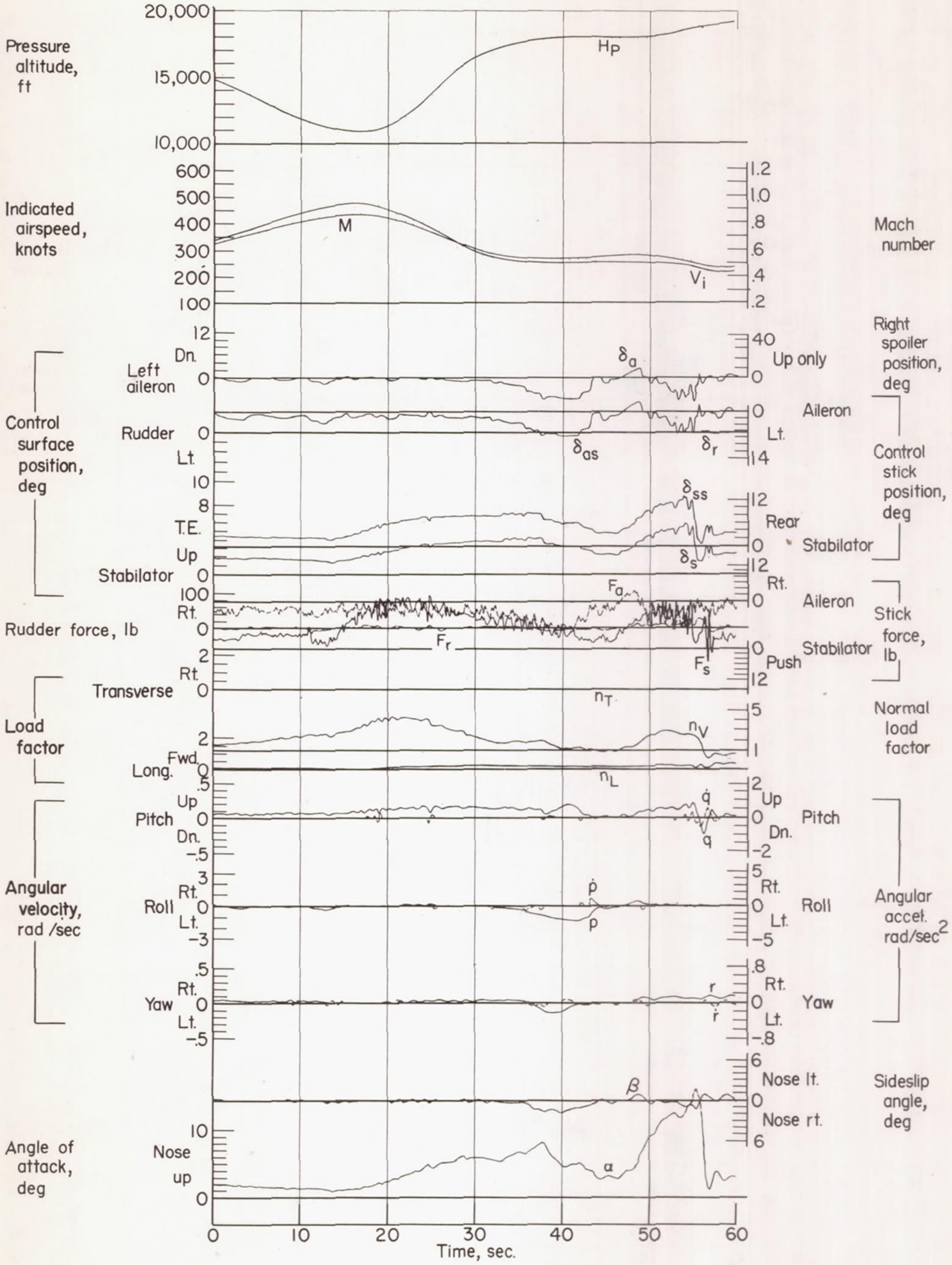

Figure 54.- Data obtained during Immelman followed by pitch-up. Airplane weight, 17,400 pounds; center of gravity at 21.7 percent $\bar{c}$; flight 11.

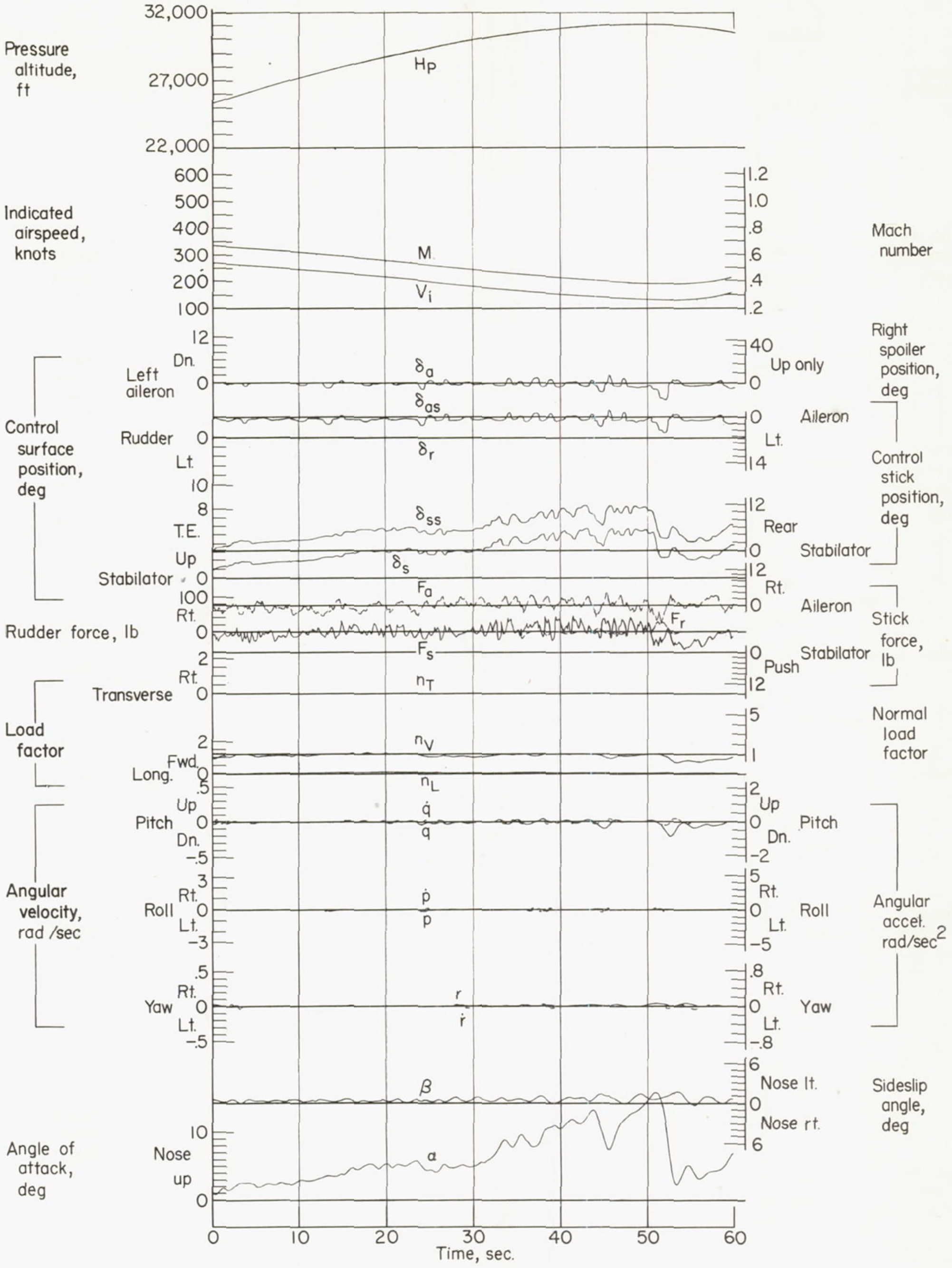

(a)

Figure 55.- Data obtained during stall, a stall turn, and then pitch-up. Airplane weight, 17,000 pounds; center of gravity at 21.8 percent $\bar{c}$; flight 15.

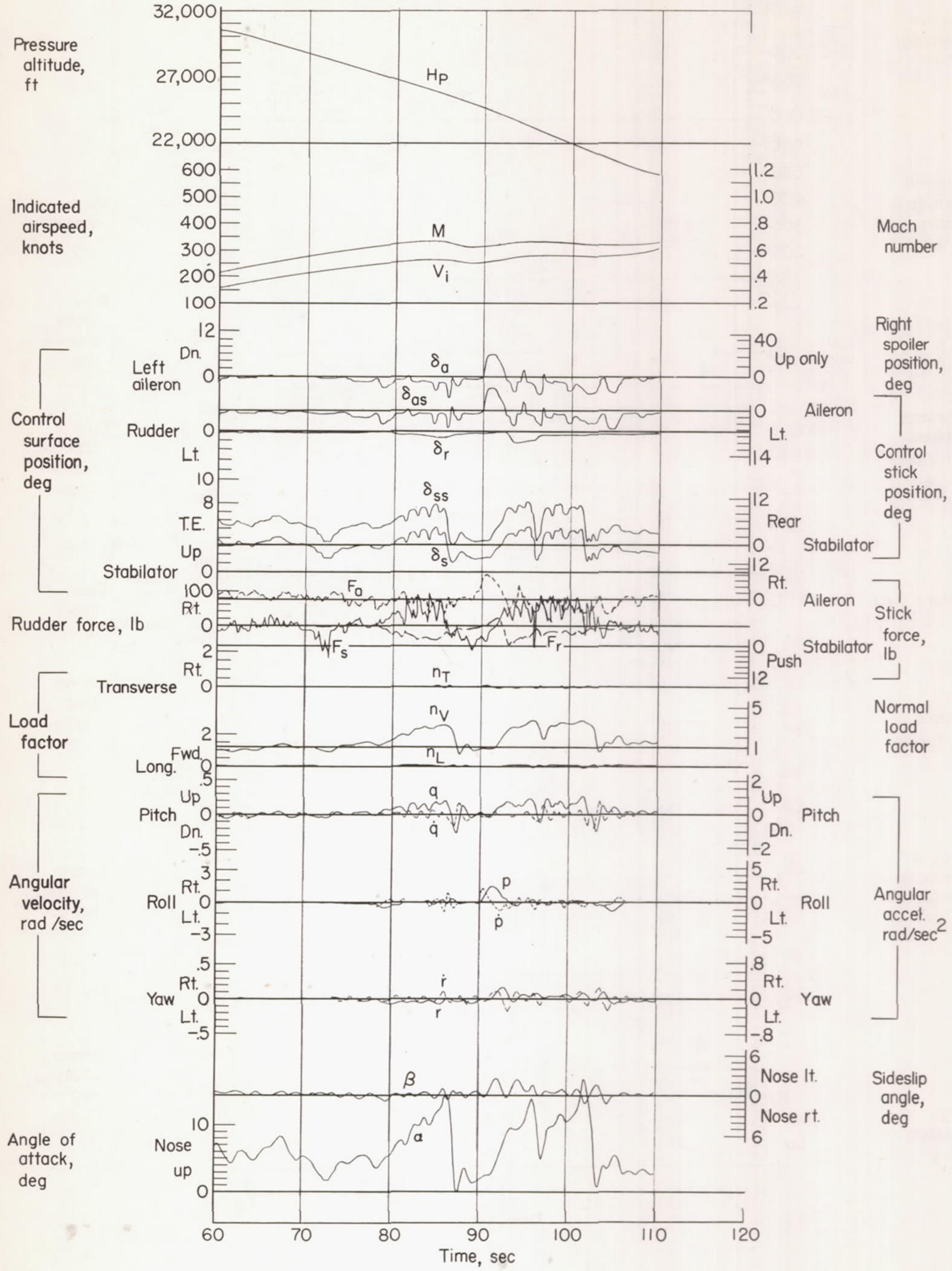

(b)

Figure 55.- Concluded.

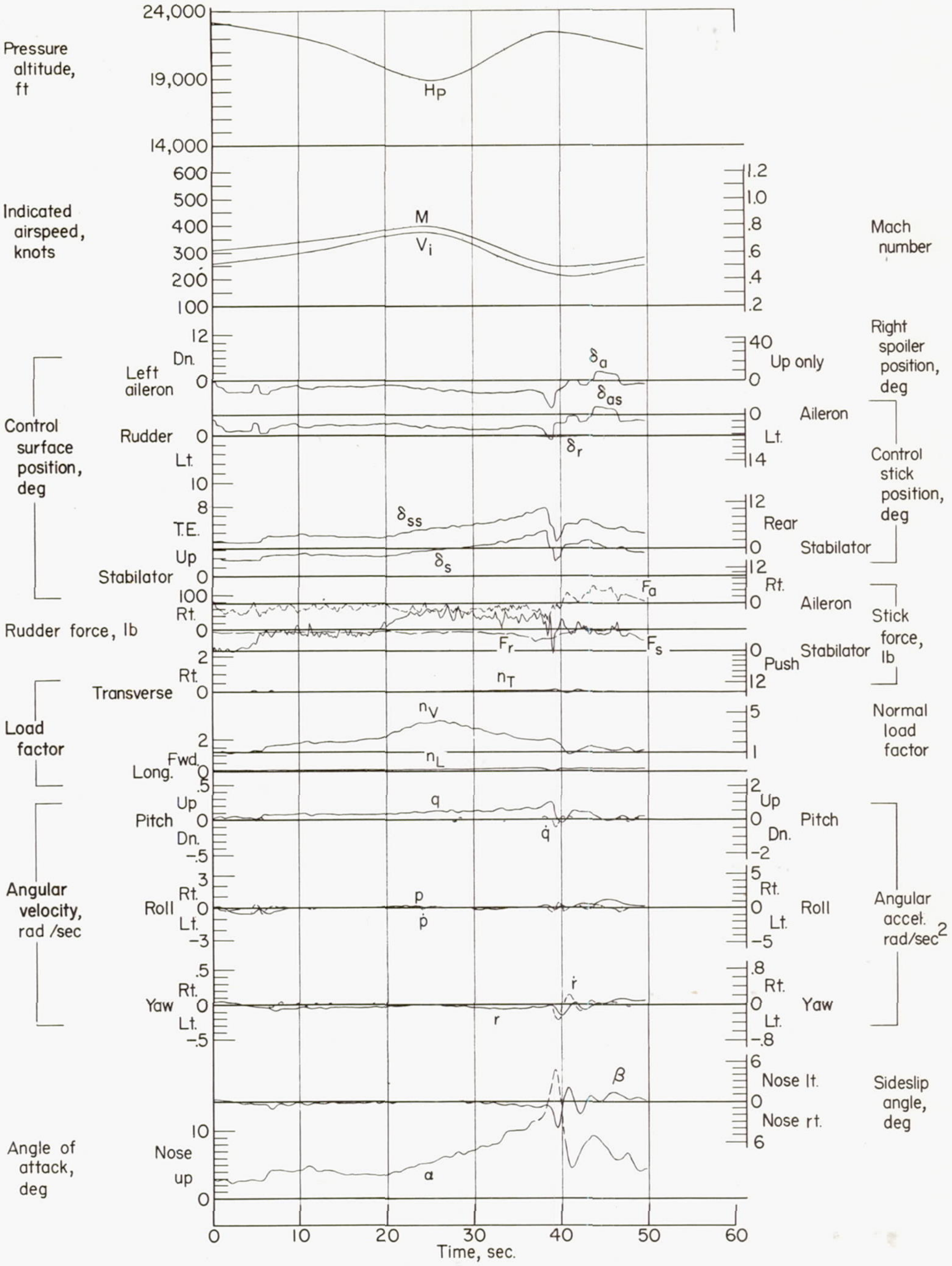

Figure 56.- Data obtained during pitch-up. Airplane weight, 17,100 pounds; center of gravity at 22.5 percent $\bar{c}$; flight 19.

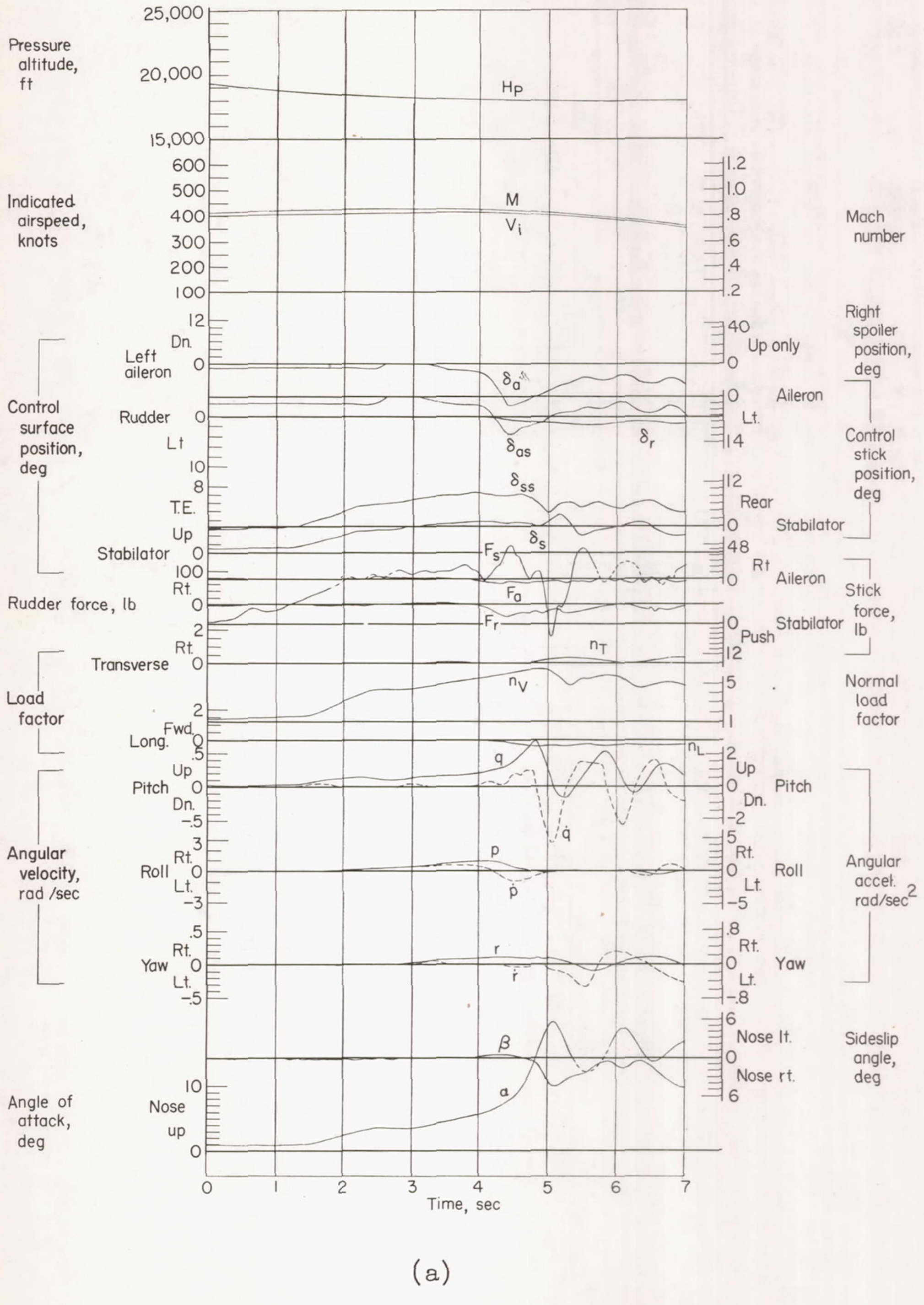

(a)

Figure 57.- Data obtained during pitch-up. Airplane weight, 17,300 pounds; center of gravity at 22.2 percent $\bar{c}$; flight 51.

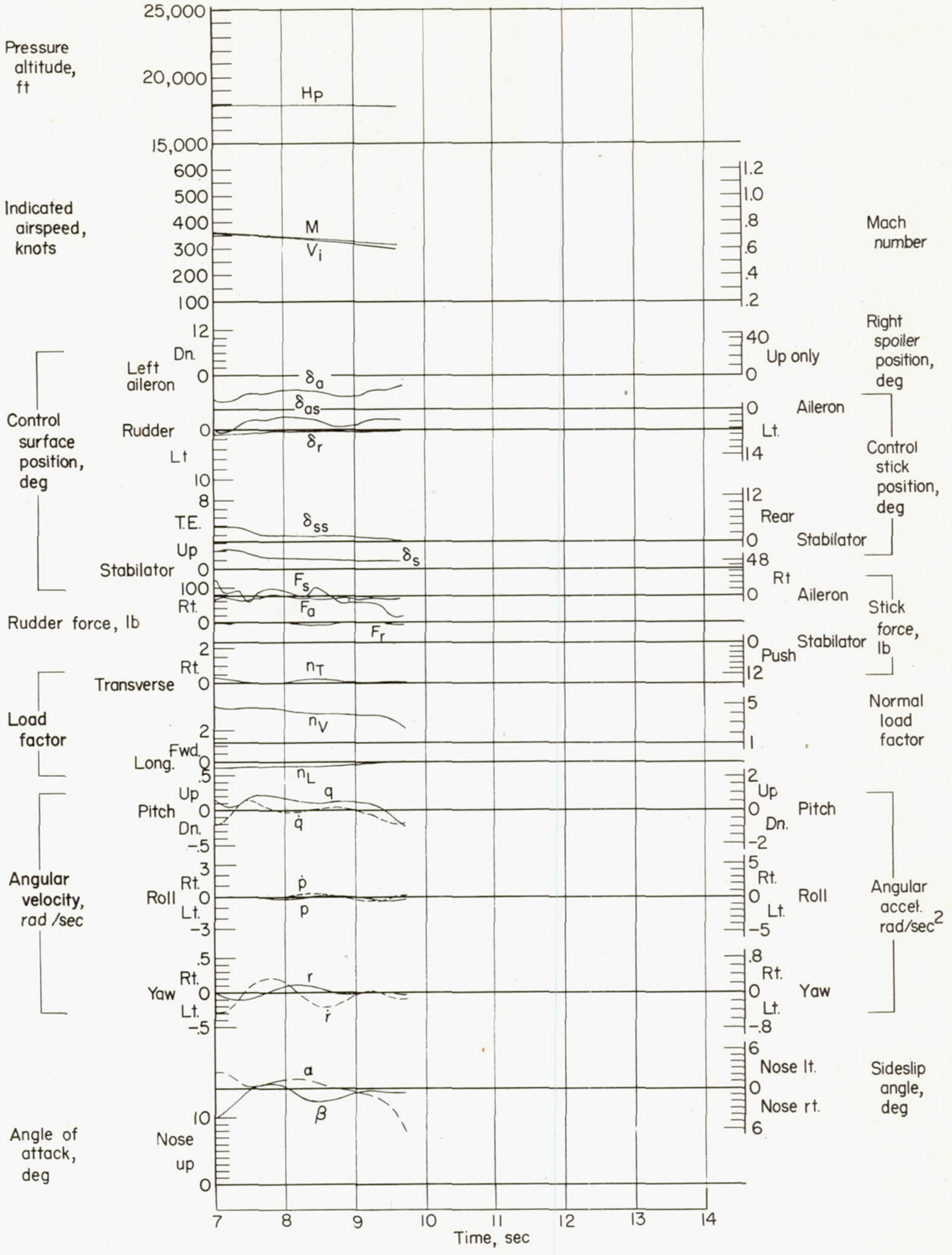

(b)

Figure 57.- Concluded.

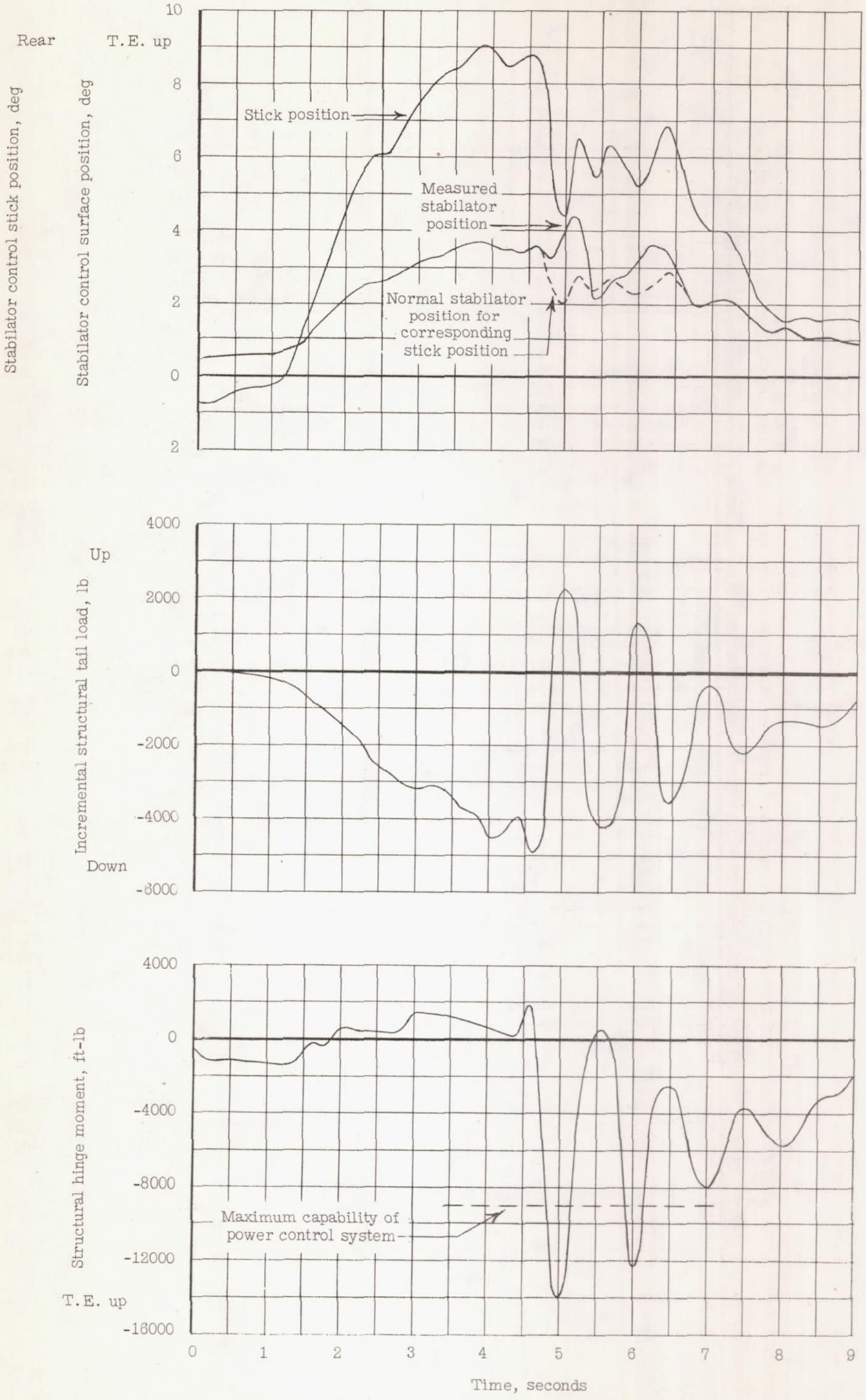

Figure 58.- Calculated horizontal tail loads and hinge moments obtained during the pitch-up of figure 57.

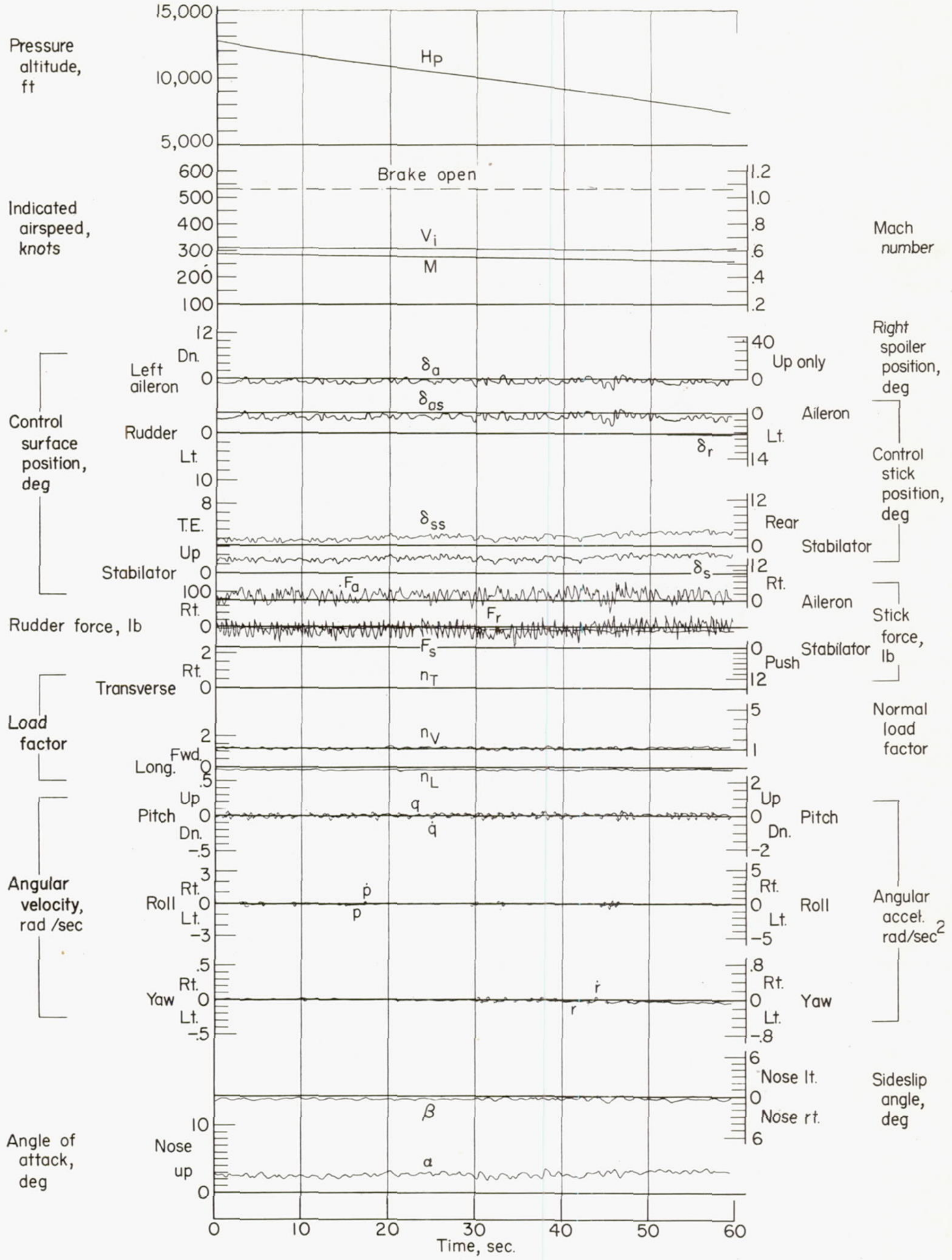

(a)

Figure 59.- Data obtained during ILD (instrument let down) and GCA (ground control approach) in formation. Airplane weight, 18,950 pounds; center of gravity at 19.5 percent $\bar{c}$; flight 17.

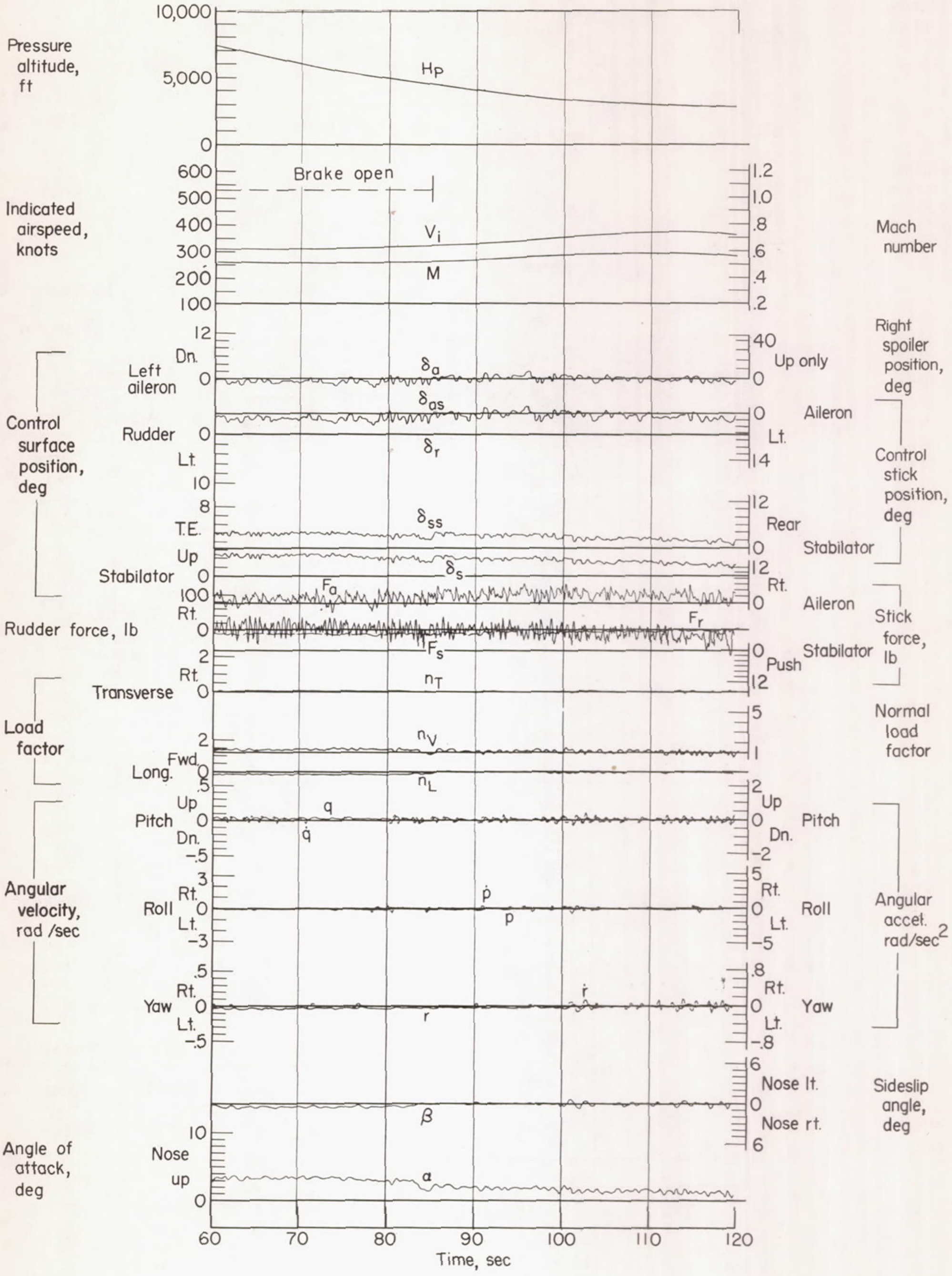

(b)

Figure 59.- Continued.

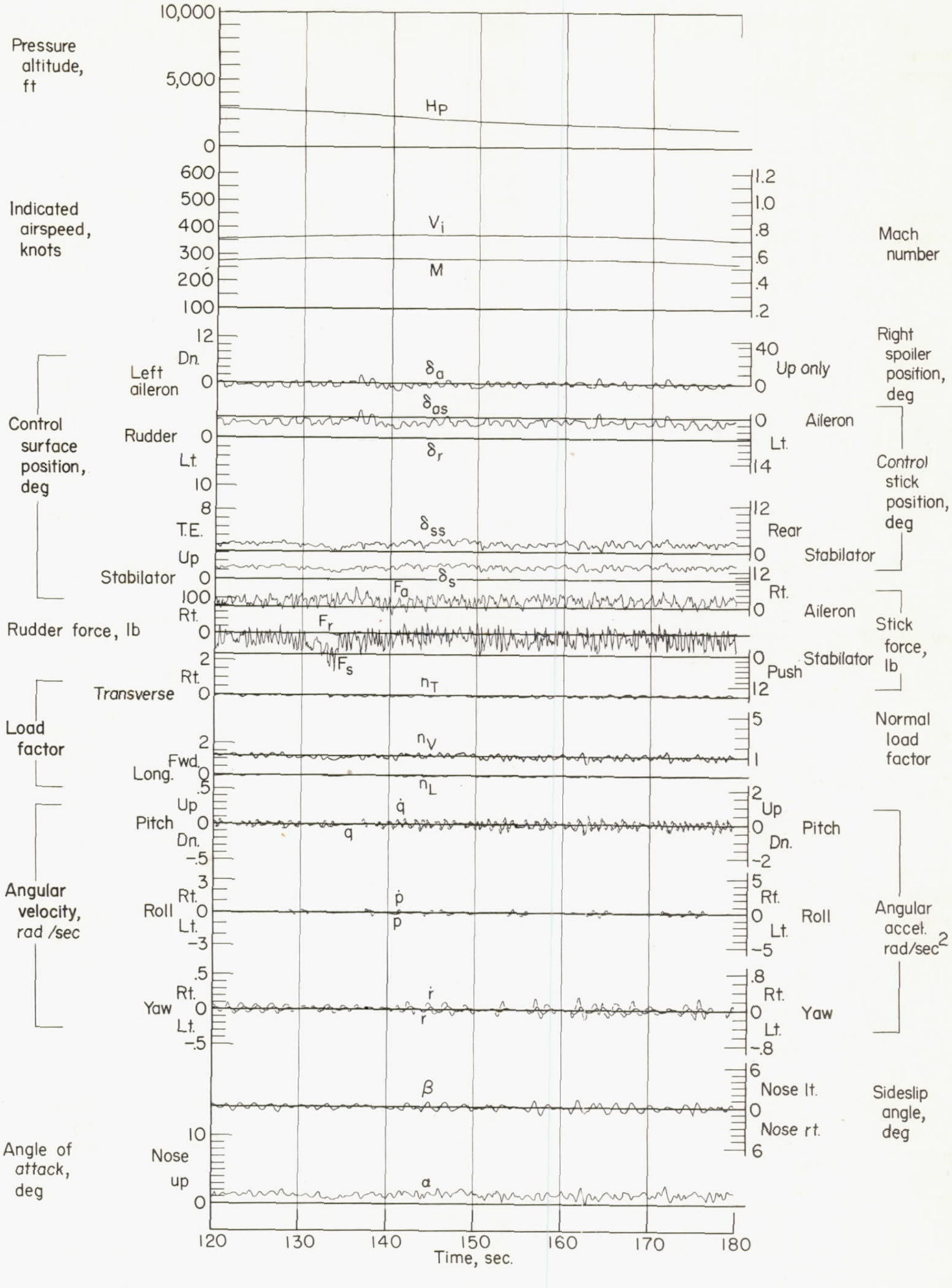

(c)

Figure 59.- Continued.

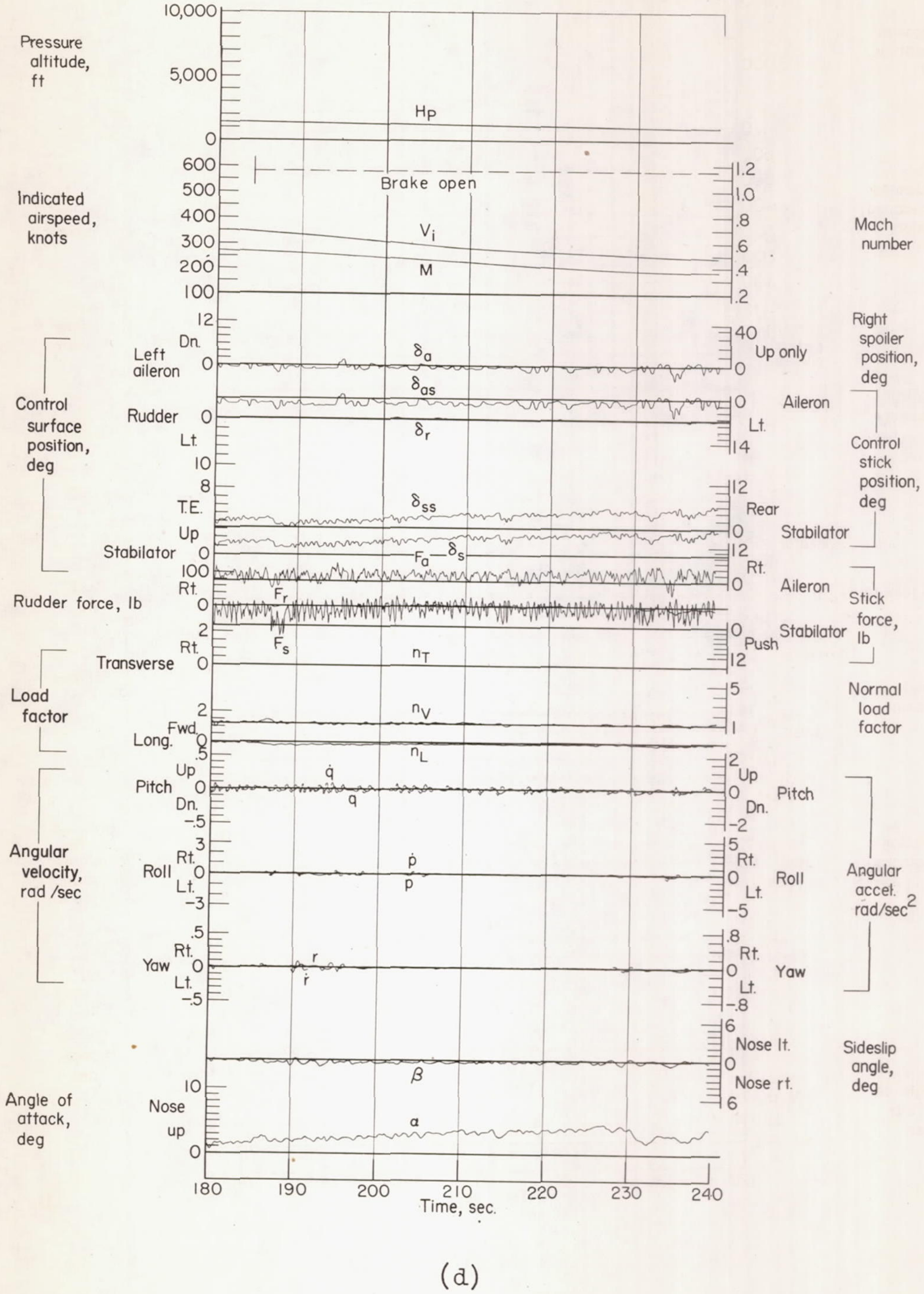

(d)

Figure 59.- Continued.

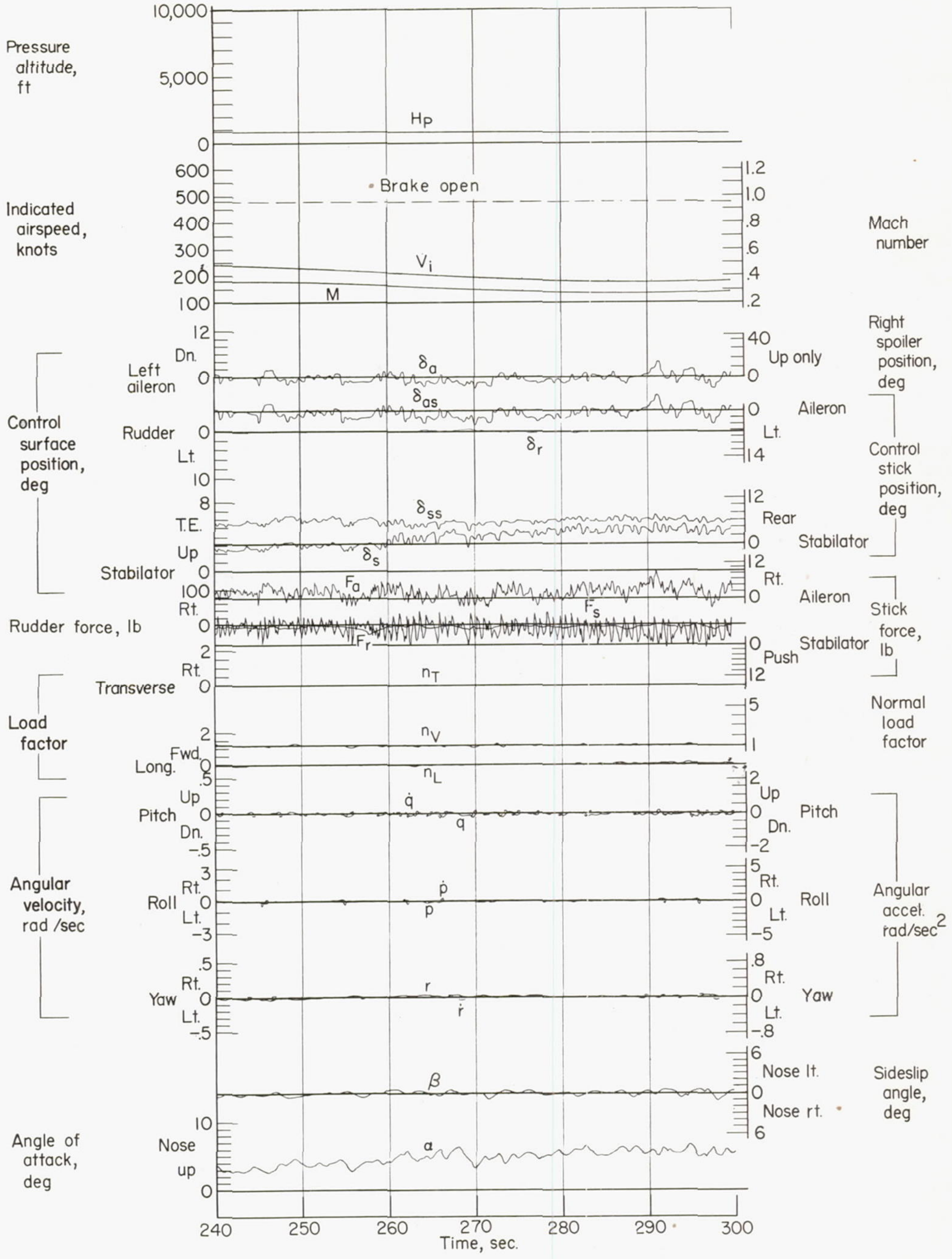

(e)

Figure 59.- Continued.

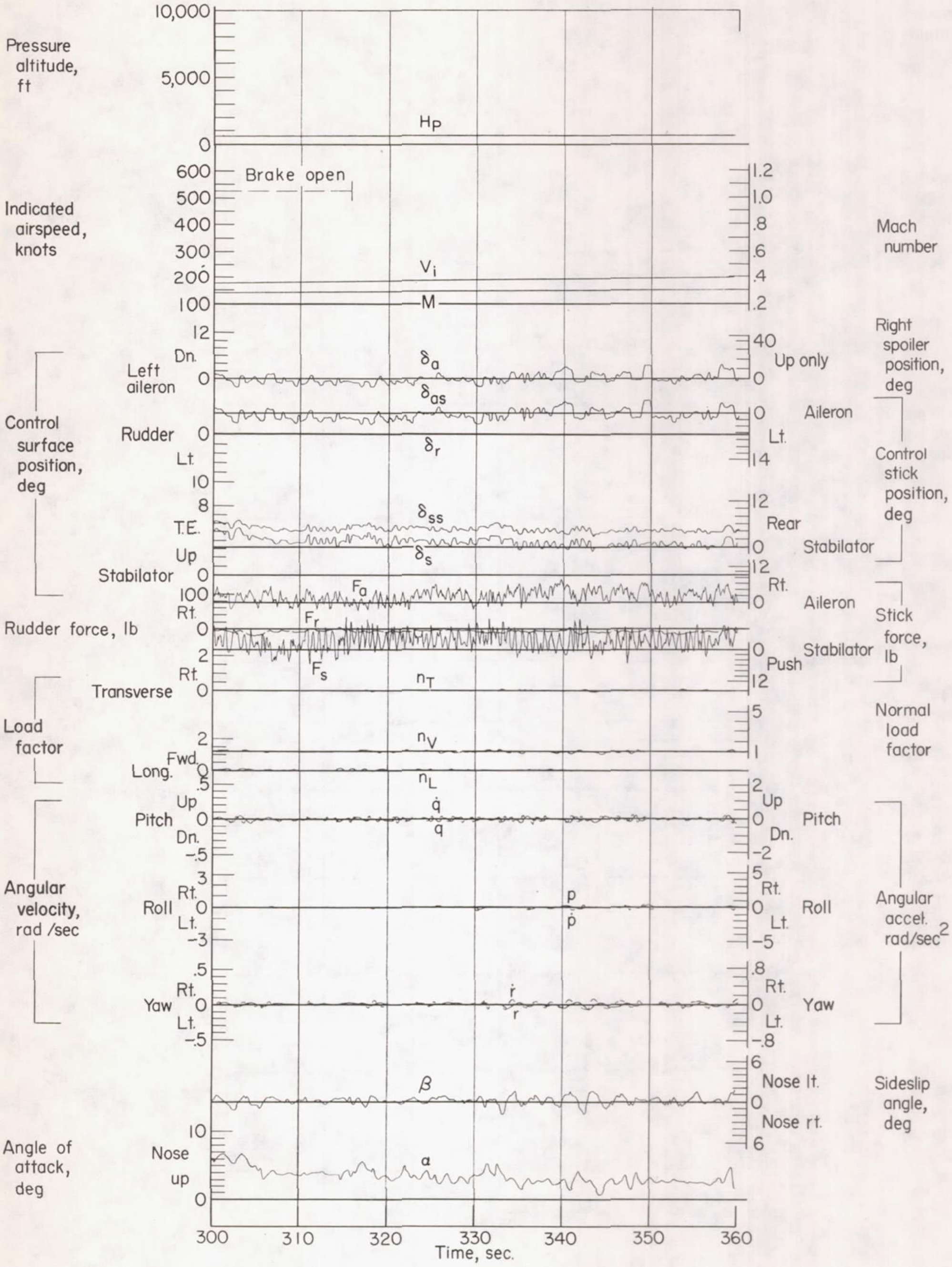

(f)

Figure 59.- Continued.

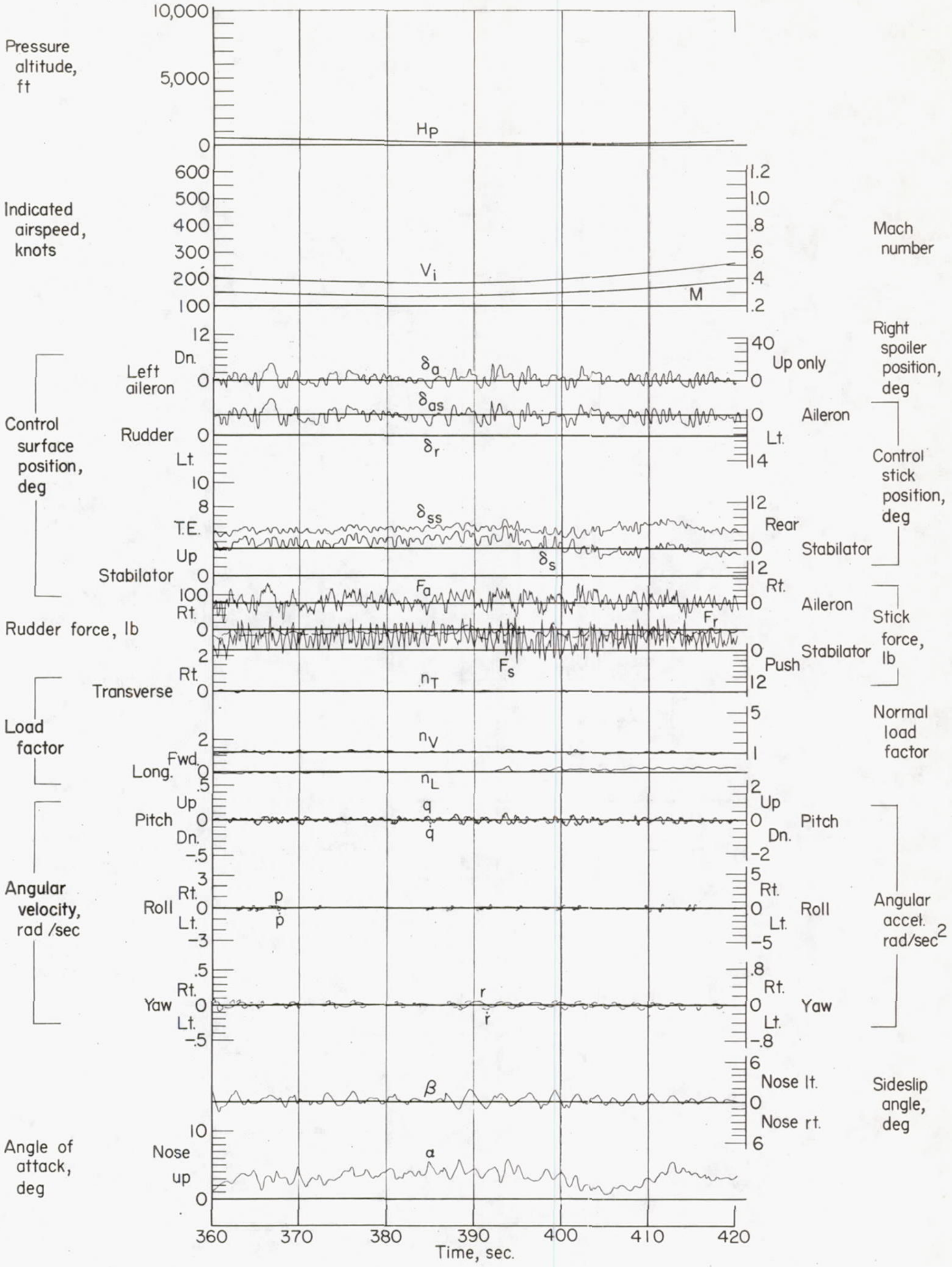

(g)

Figure 59.- Concluded.

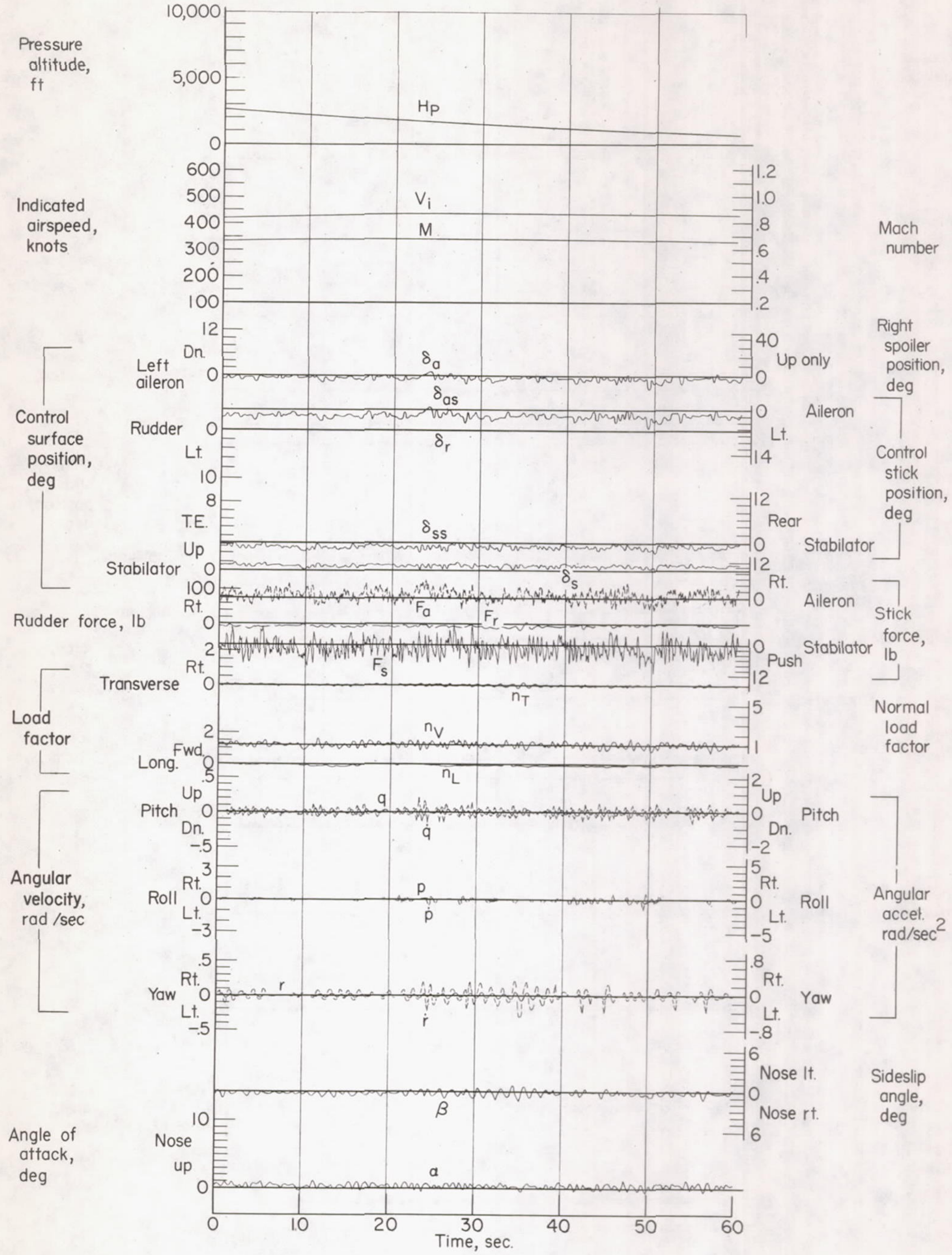

(a)

Figure 60.- Data obtained during formation flying. Airplane weight, 17,450 pounds; center of gravity at 22.5 percent $\bar{c}$; flight 25.

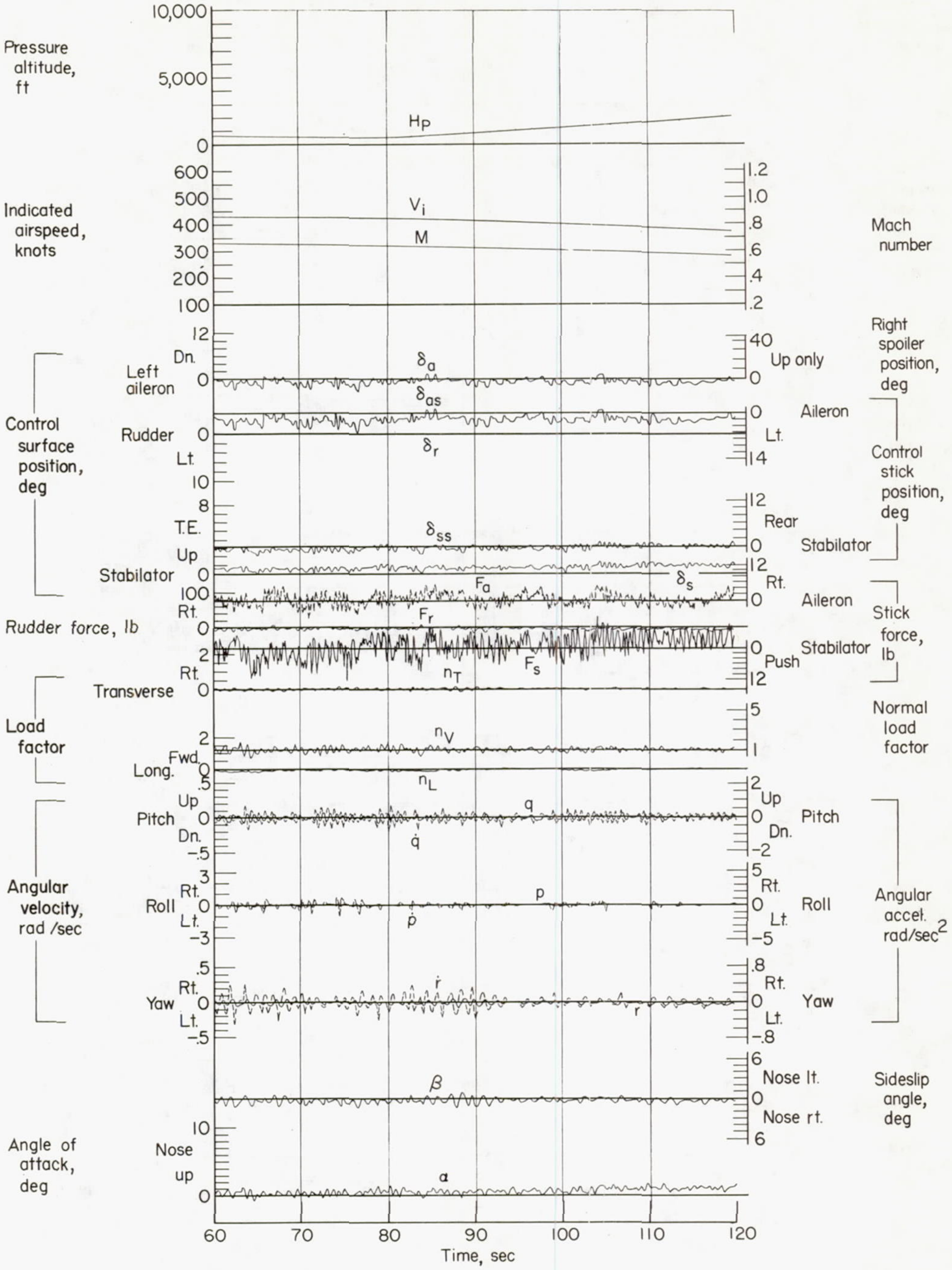

(b)

Figure 60.- Concluded.

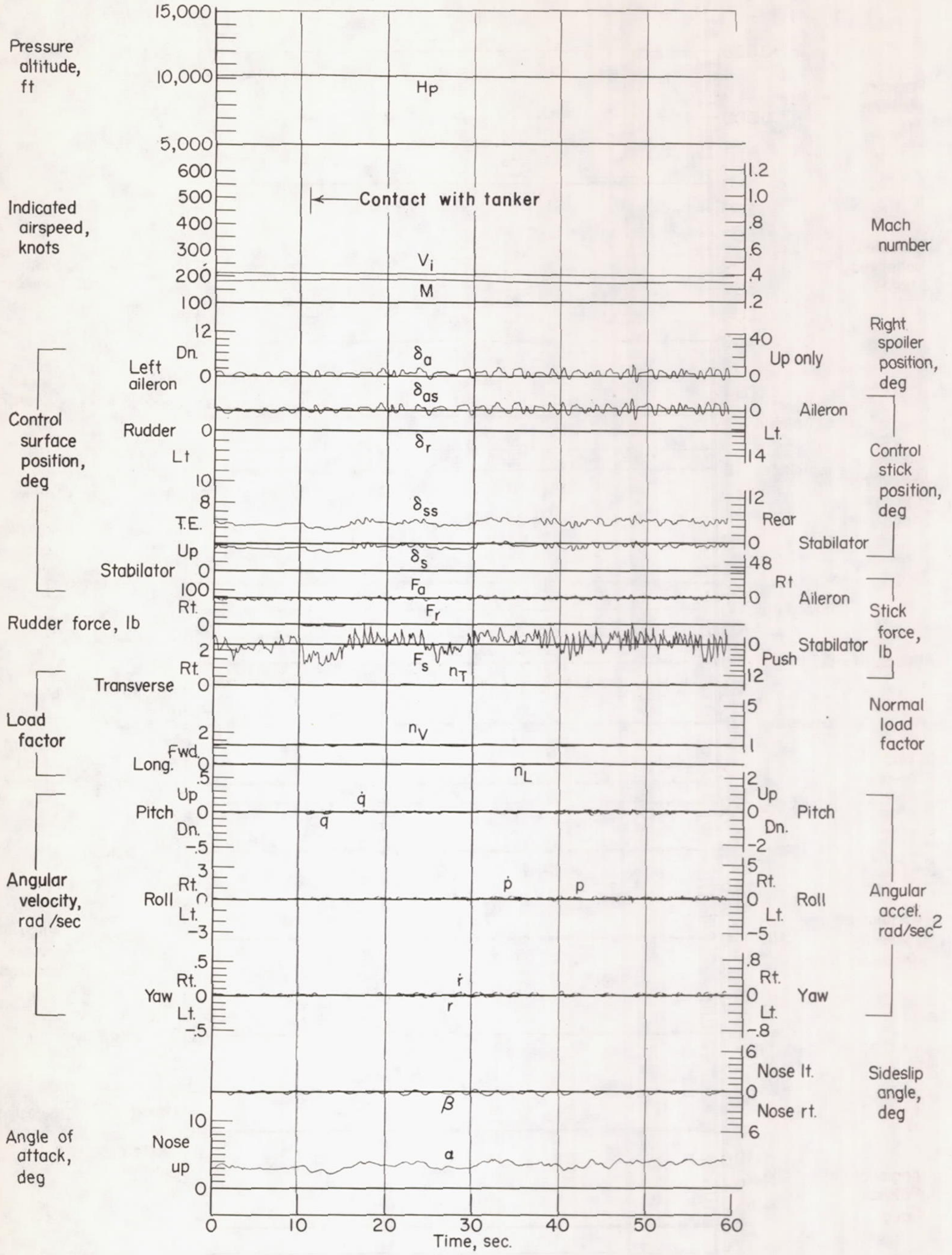

(a)

Figure 61.- Data obtained during in-flight refueling. Airplane weight, 19,900 pounds to 25,450 pounds; center of gravity at 20.0 percent $\bar{c}$ at contact, ranging from 20.0 to 17.7 to 20.6 during refueling; flight 52.

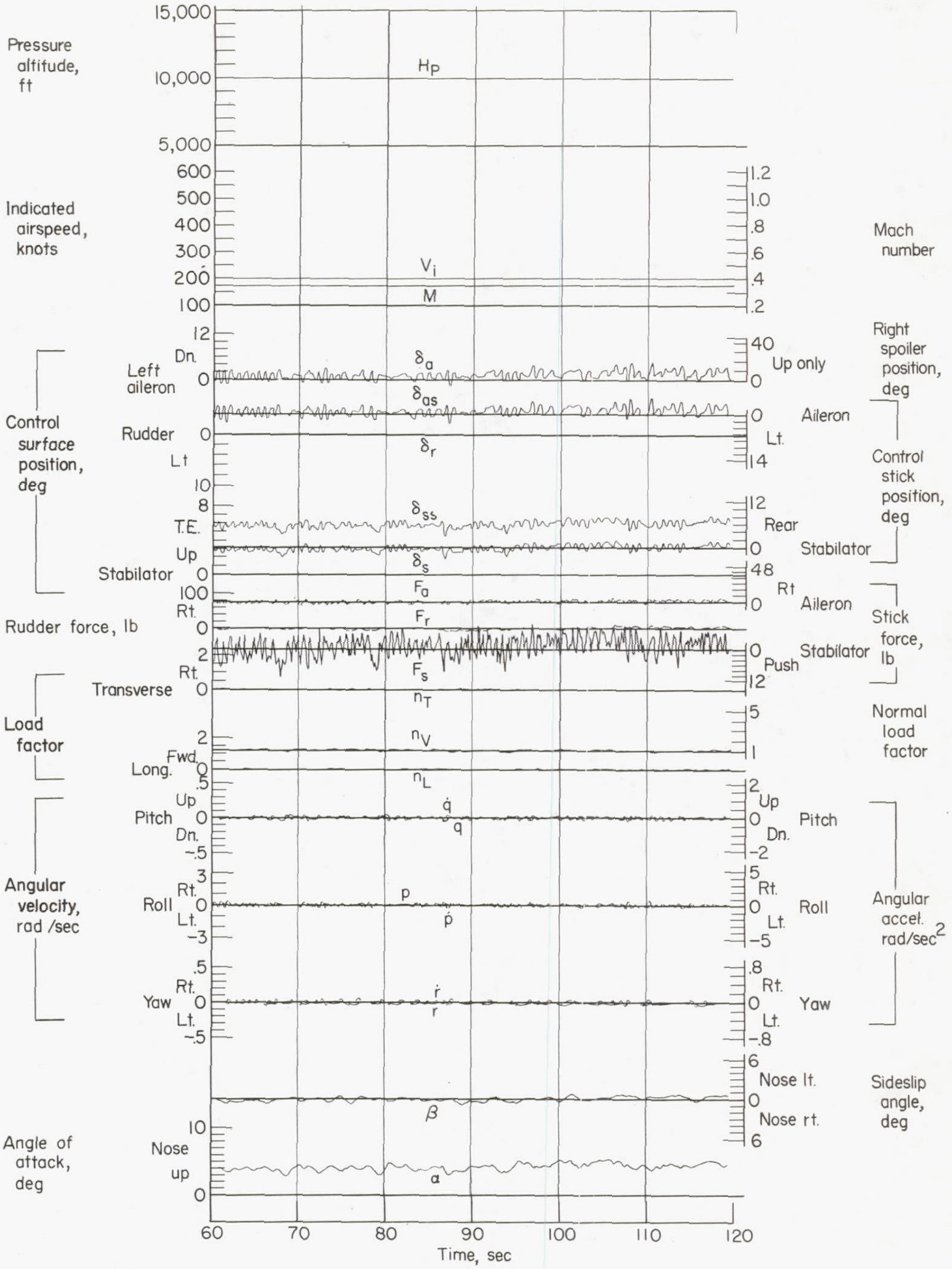

(b)

Figure 61.- Continued.

DECLASSIFIED

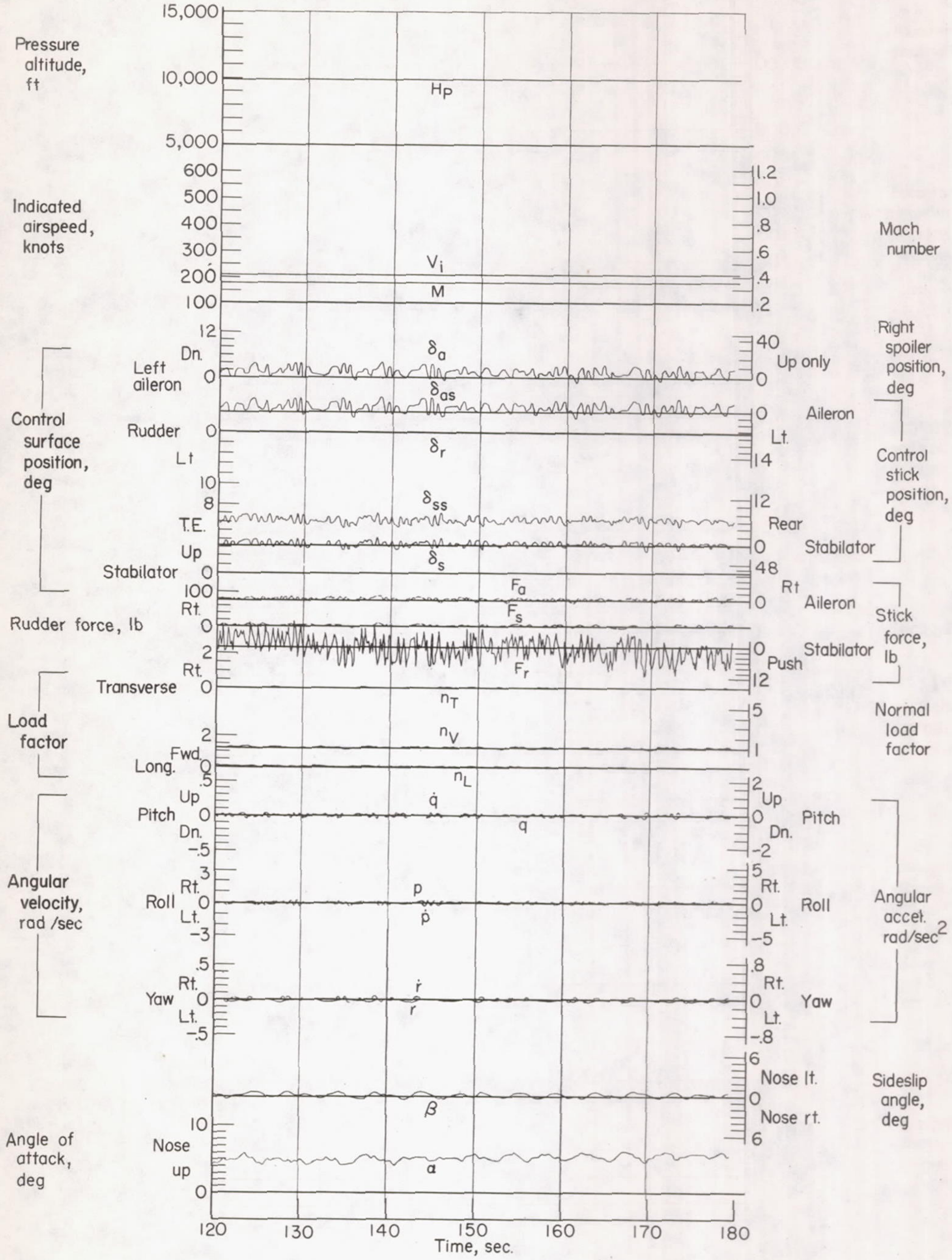

(c)

Figure 61.- Continued.

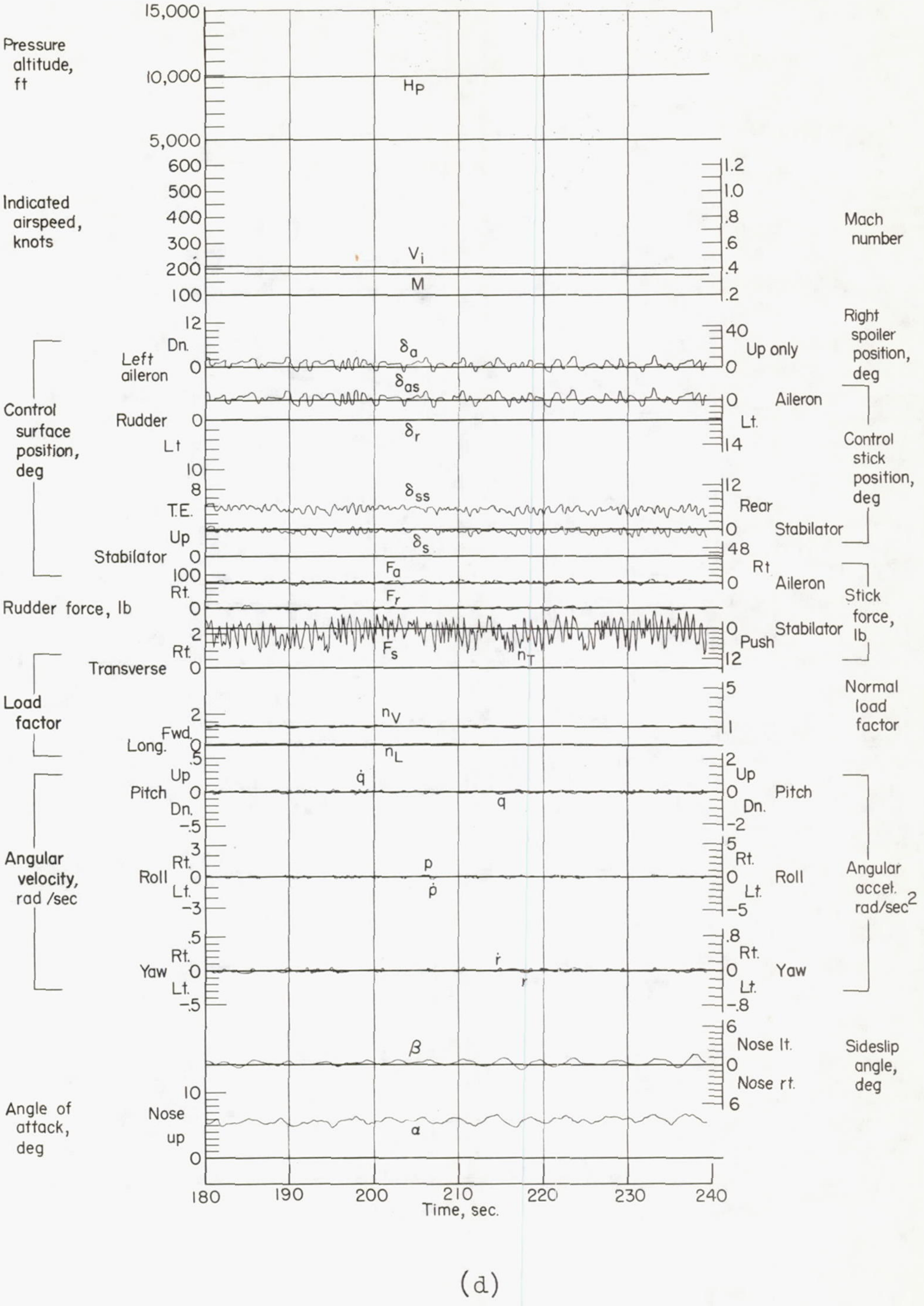

(d)

Figure 61.- Continued.

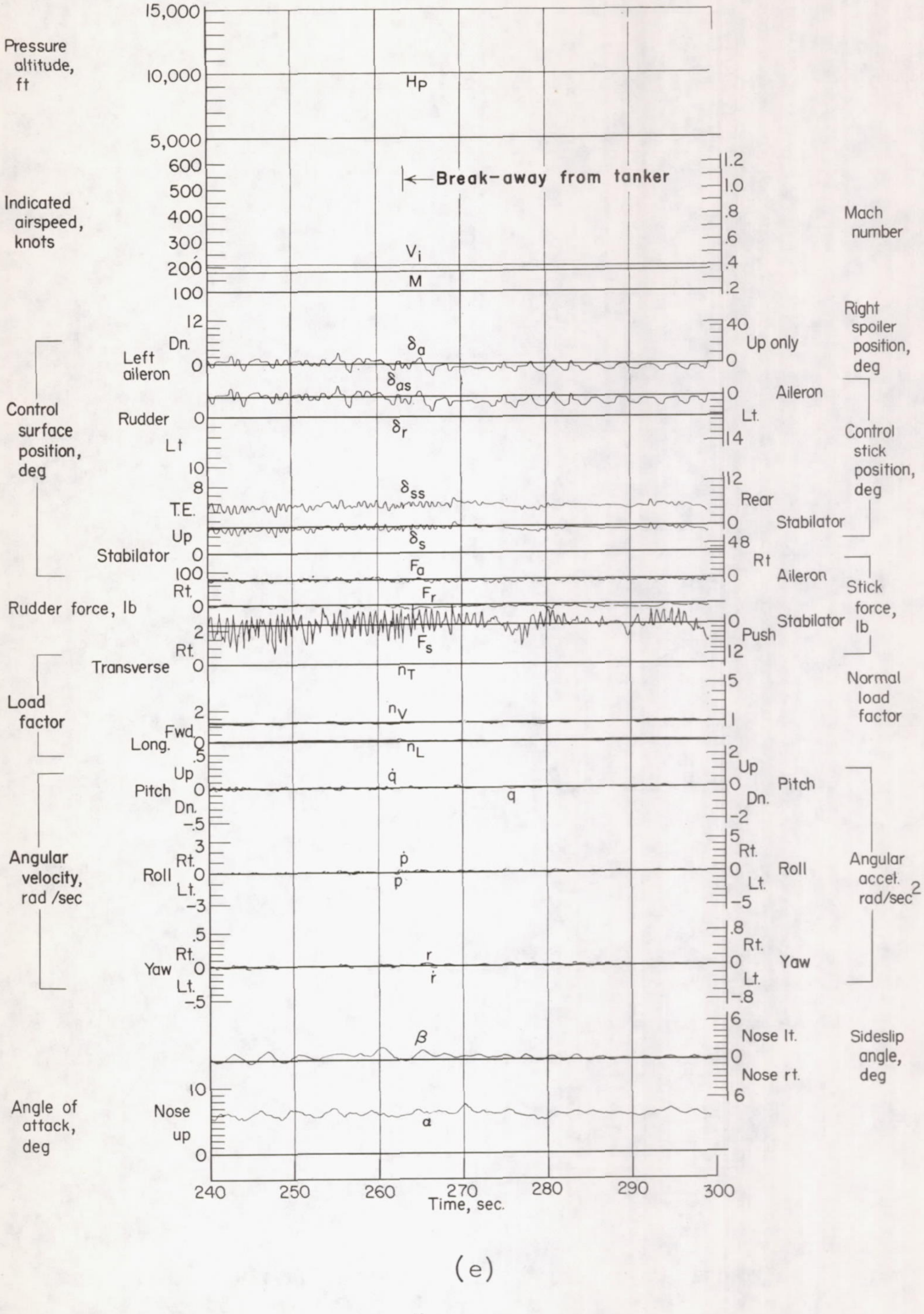

(e)

Figure 61.- Concluded.

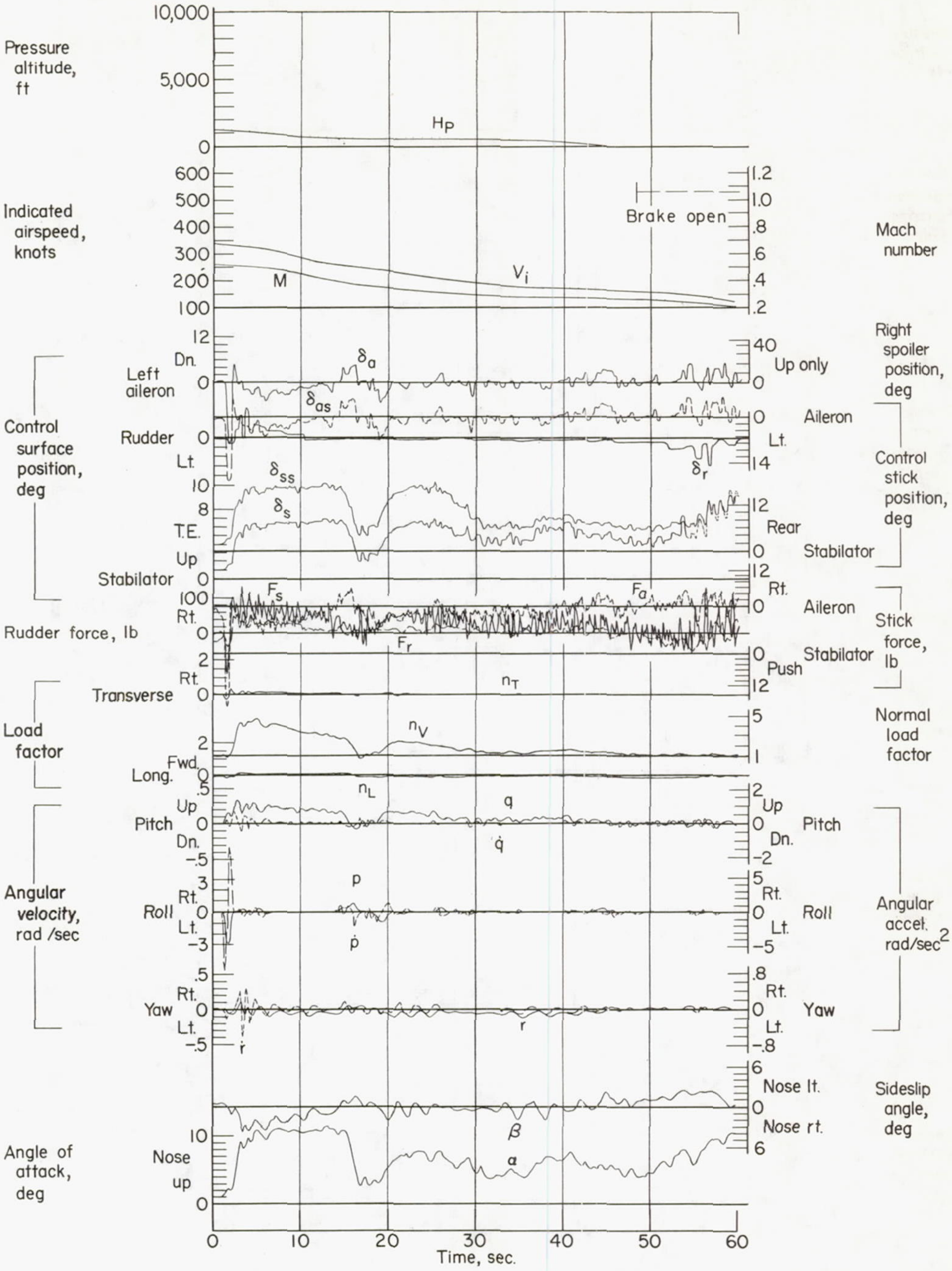

Figure 62.- Data obtained during left turn and landing. Airplane weight, 15,750 pounds; center of gravity at 22.2 percent $\bar{c}$; flight 9.

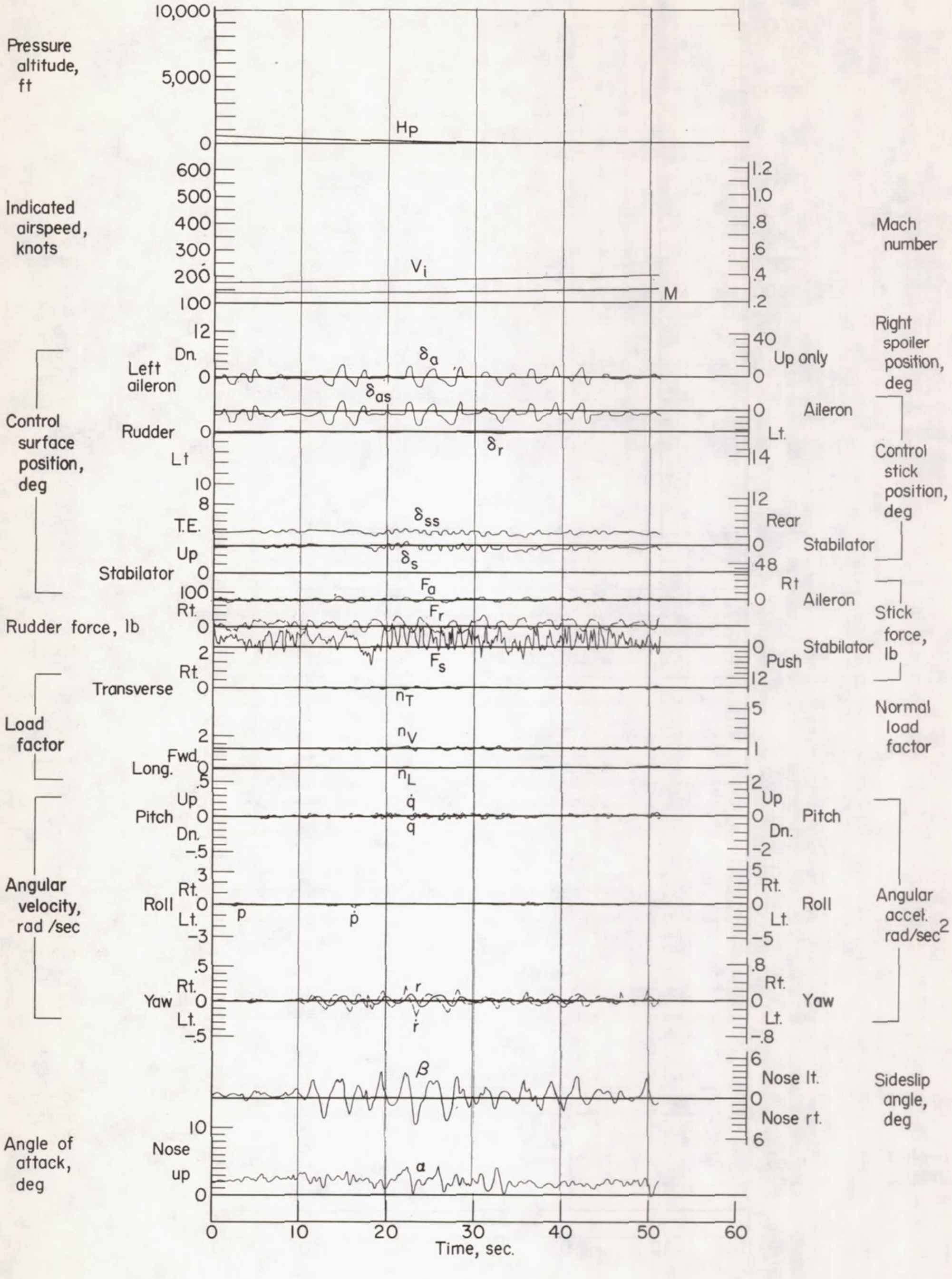

Figure 63.- Data obtained during landing approach, large directional oscillations. Airplane weight, 16,450 pounds; center of gravity at 22.5 percent $\bar{c}$; flight 26.

DECLASSIFIED

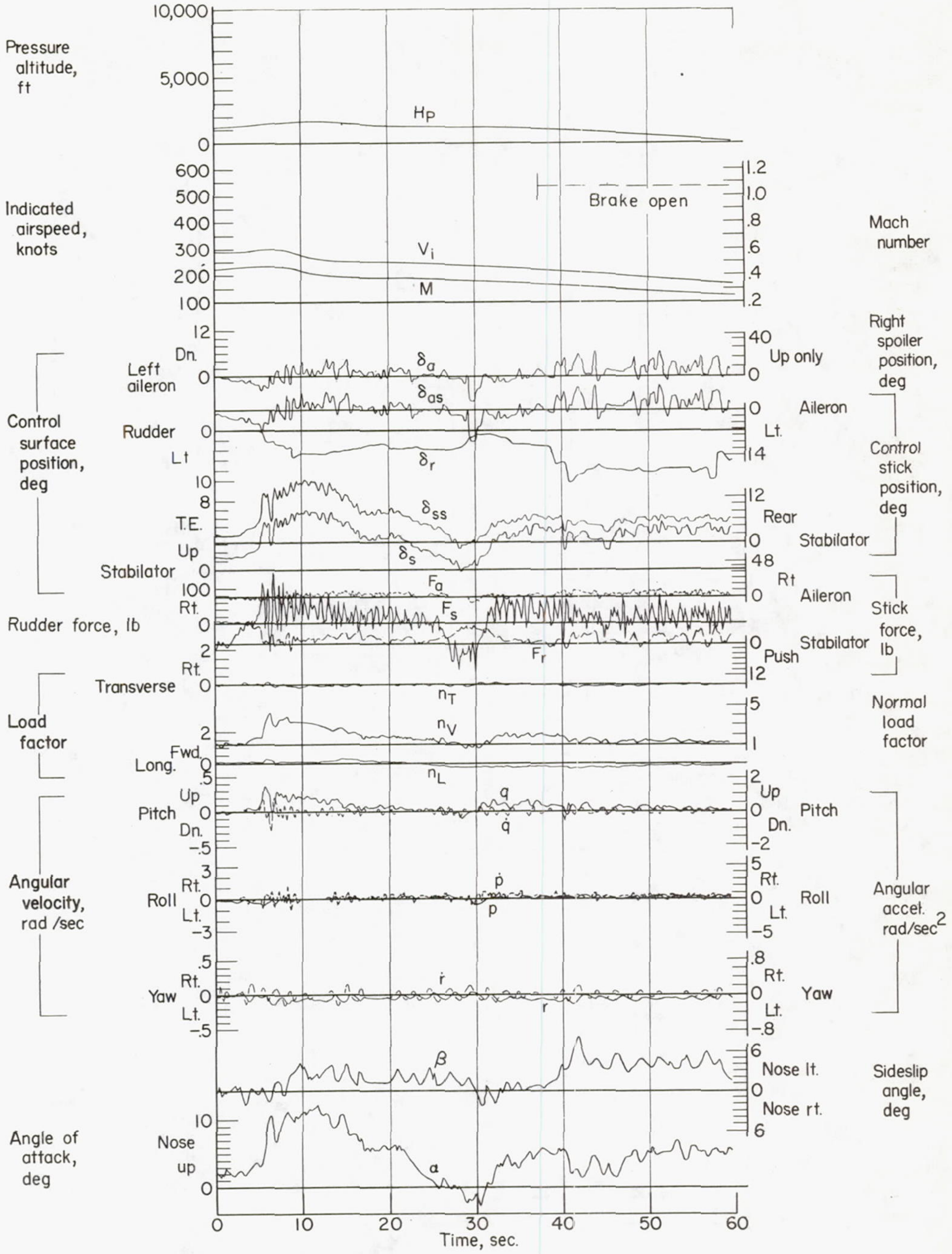

(a)

Figure 64.- Data obtained during landing with large sideslip. Airplane weight, 16,100 pounds; center of gravity at 23.2 percent $\bar{c}$; flight 40.

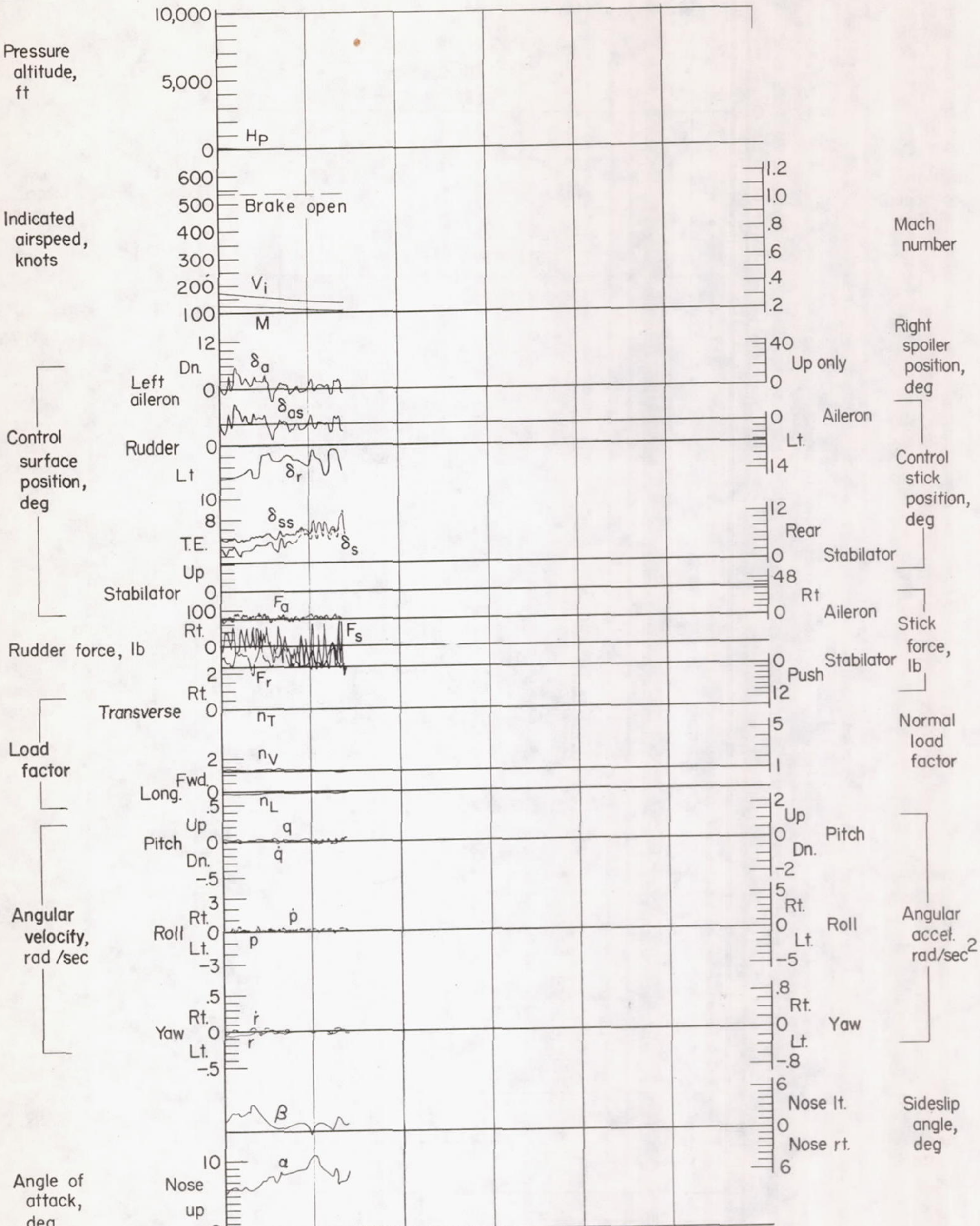

(b)

Figure 64.- Concluded.

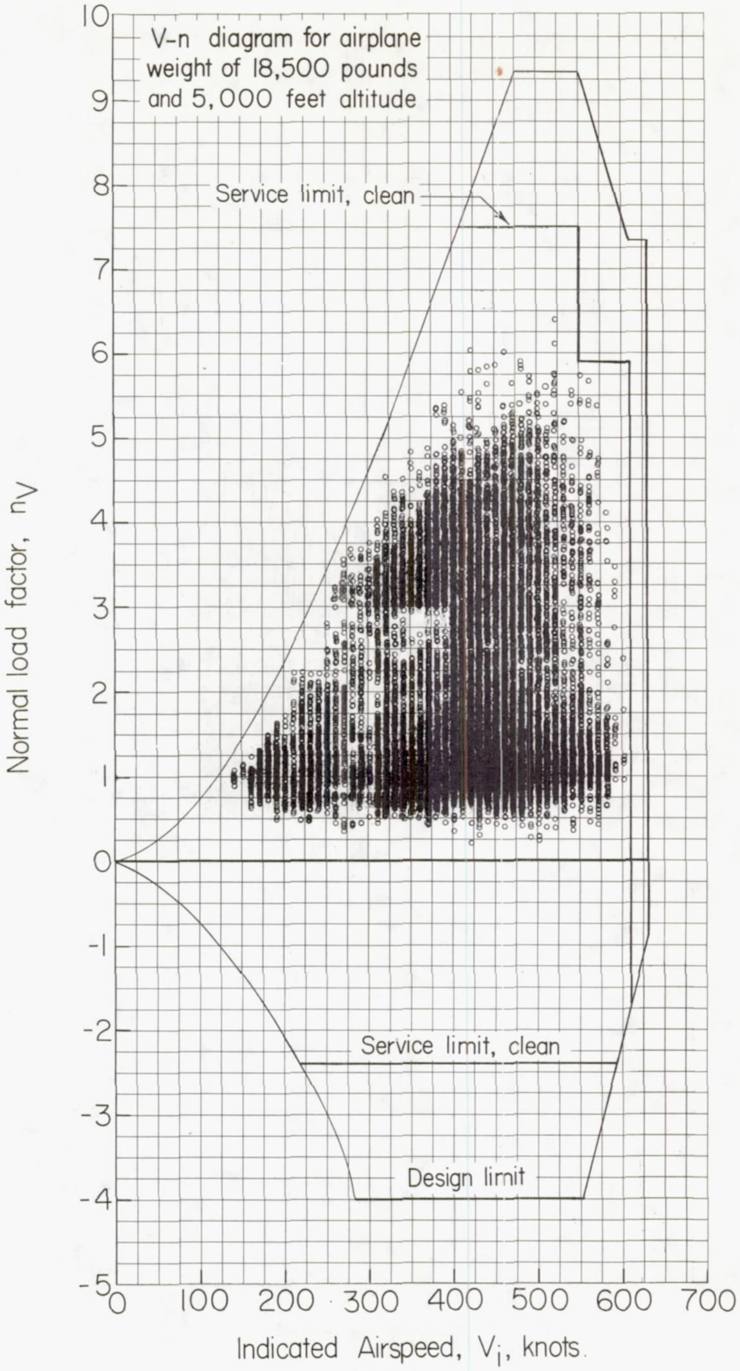

Figure 65.- Comparison of measured normal load factors obtained during general flying with the V-n diagram. Pressure altitude, sea level to 15,000 feet.

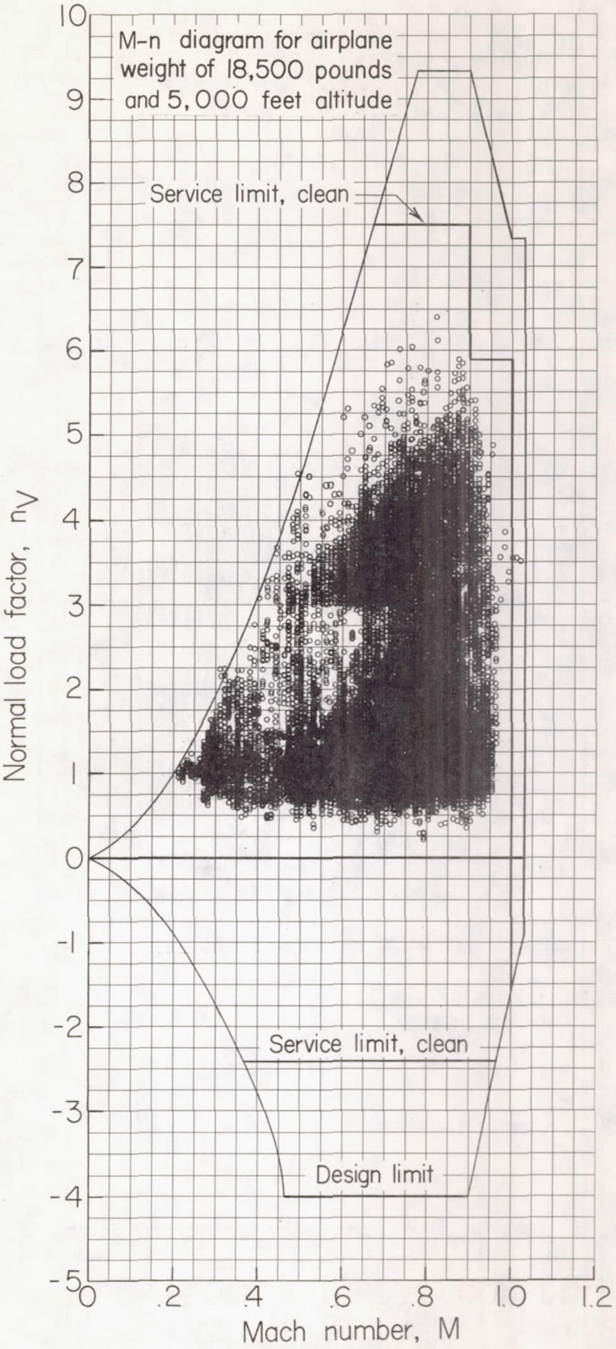

Figure 66.- Comparison of measured normal load factors obtained during general flying with the M-n diagram. Pressure altitude, sea level to 15,000 feet.

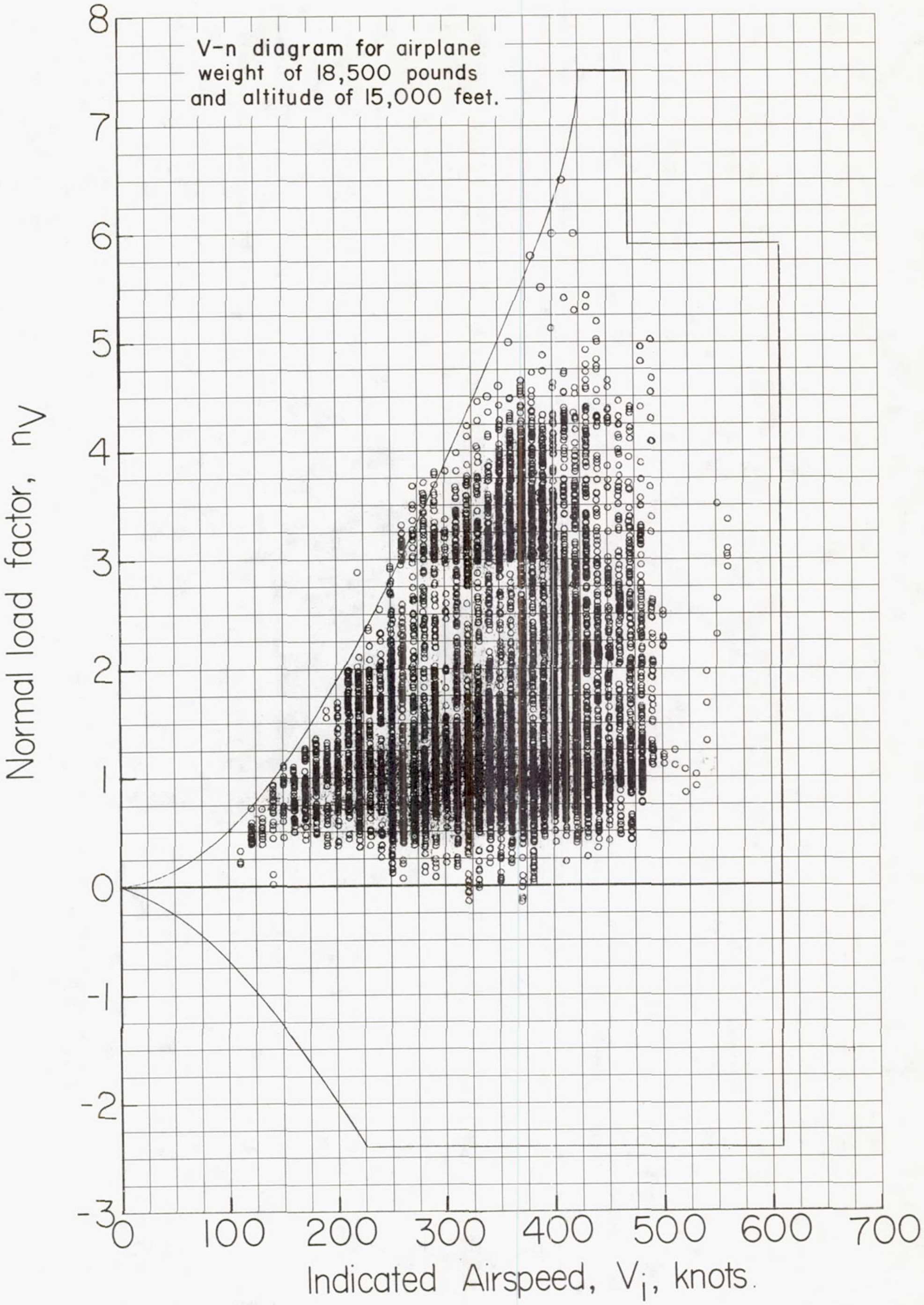

Figure 67.- Comparison of measured normal load factors obtained during general flying with the service V-n diagram. Pressure altitude, 15,000 feet to 30,000 feet.

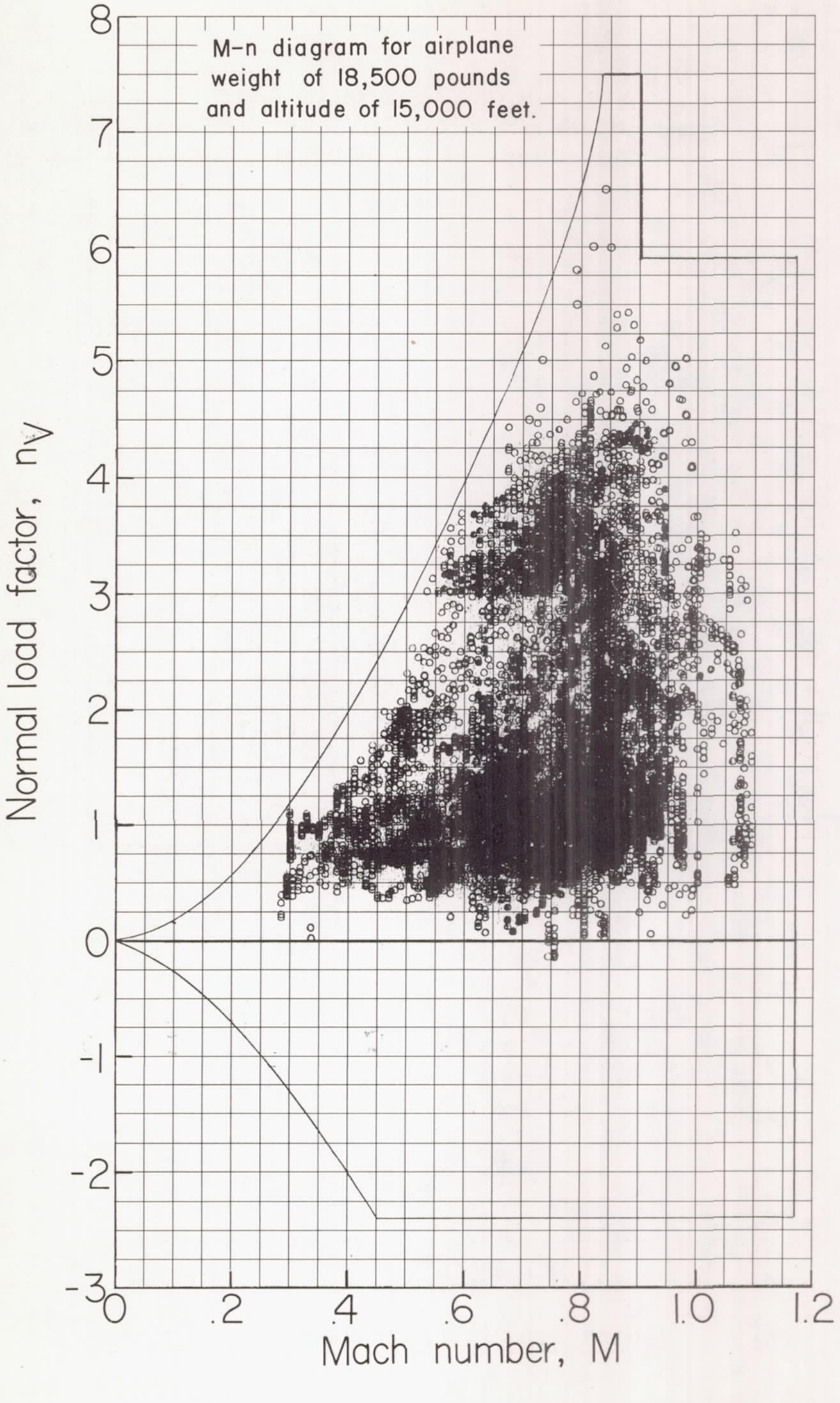

Figure 68.- Comparison of measured normal load factors obtained during general flying with the service M-n diagram. Pressure altitude, 15,000 feet to 30,000 feet.

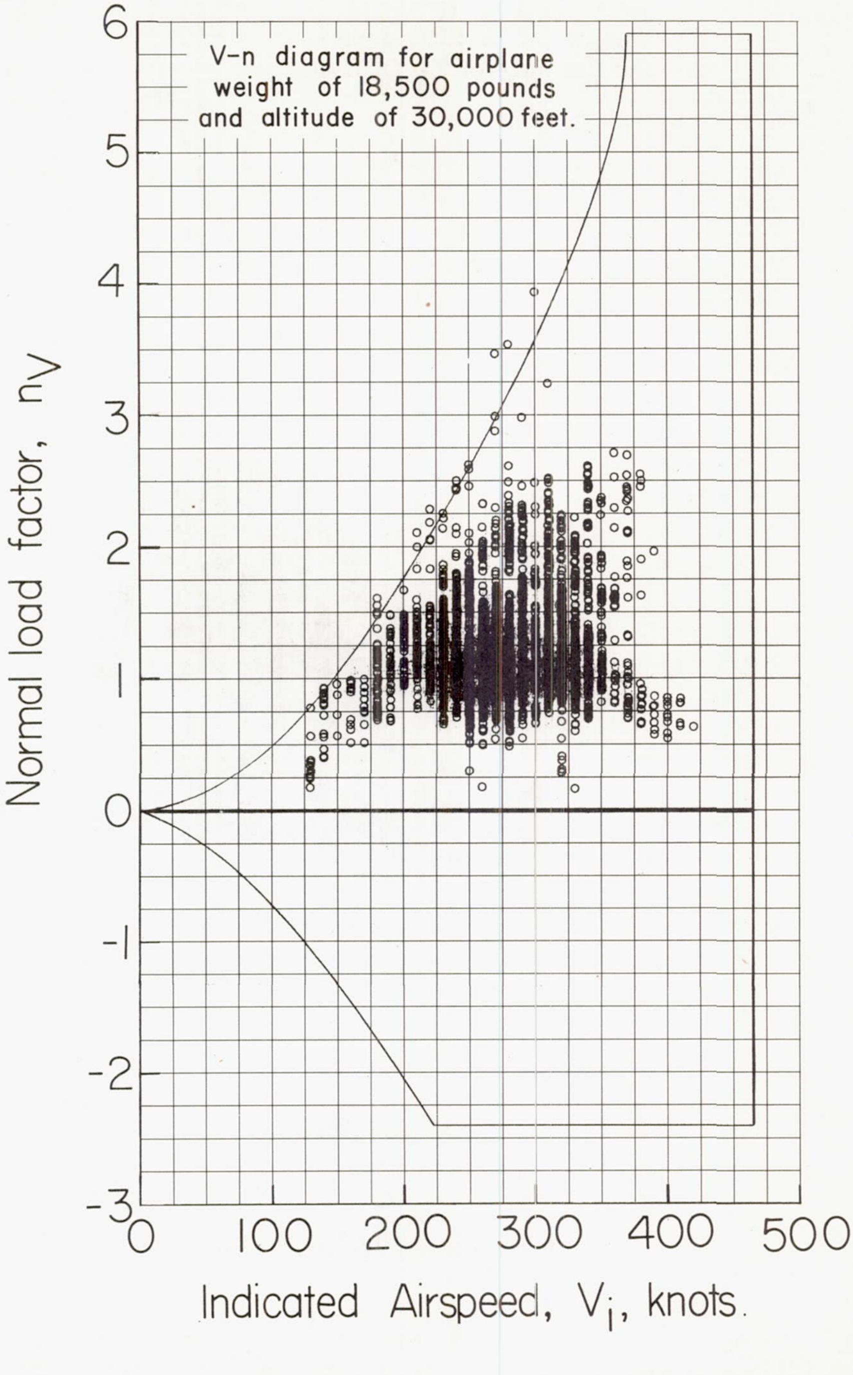

Figure 69.- Comparison of measured normal load factors obtained during general flying with the service V-n diagram. Pressure altitude, 30,000 feet to 42,000 feet.

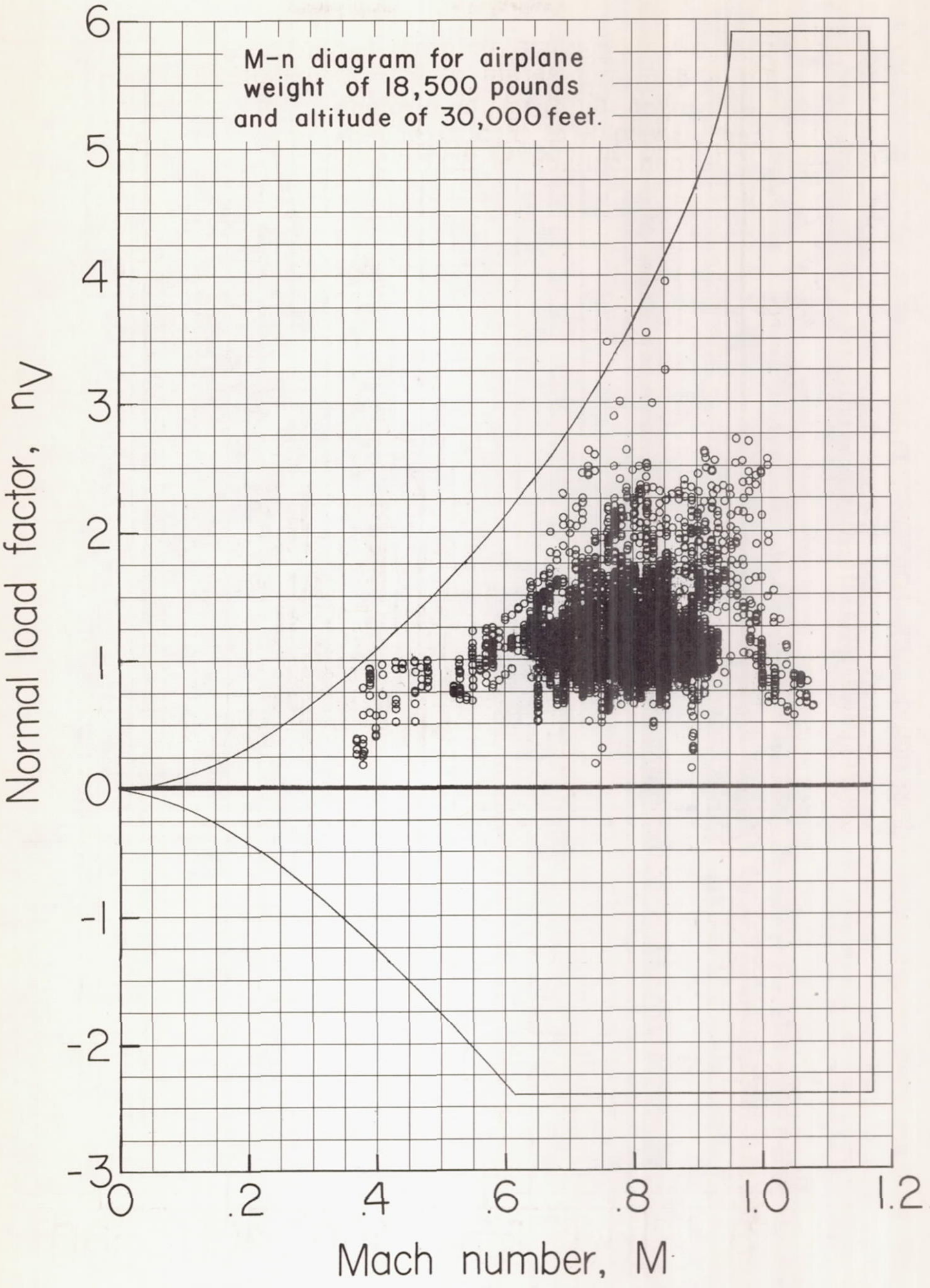

Figure 70.- Comparison of measured normal load factors obtained during general flying with the service M-n diagram. Pressure altitude, 30,000 feet to 42,000 feet.

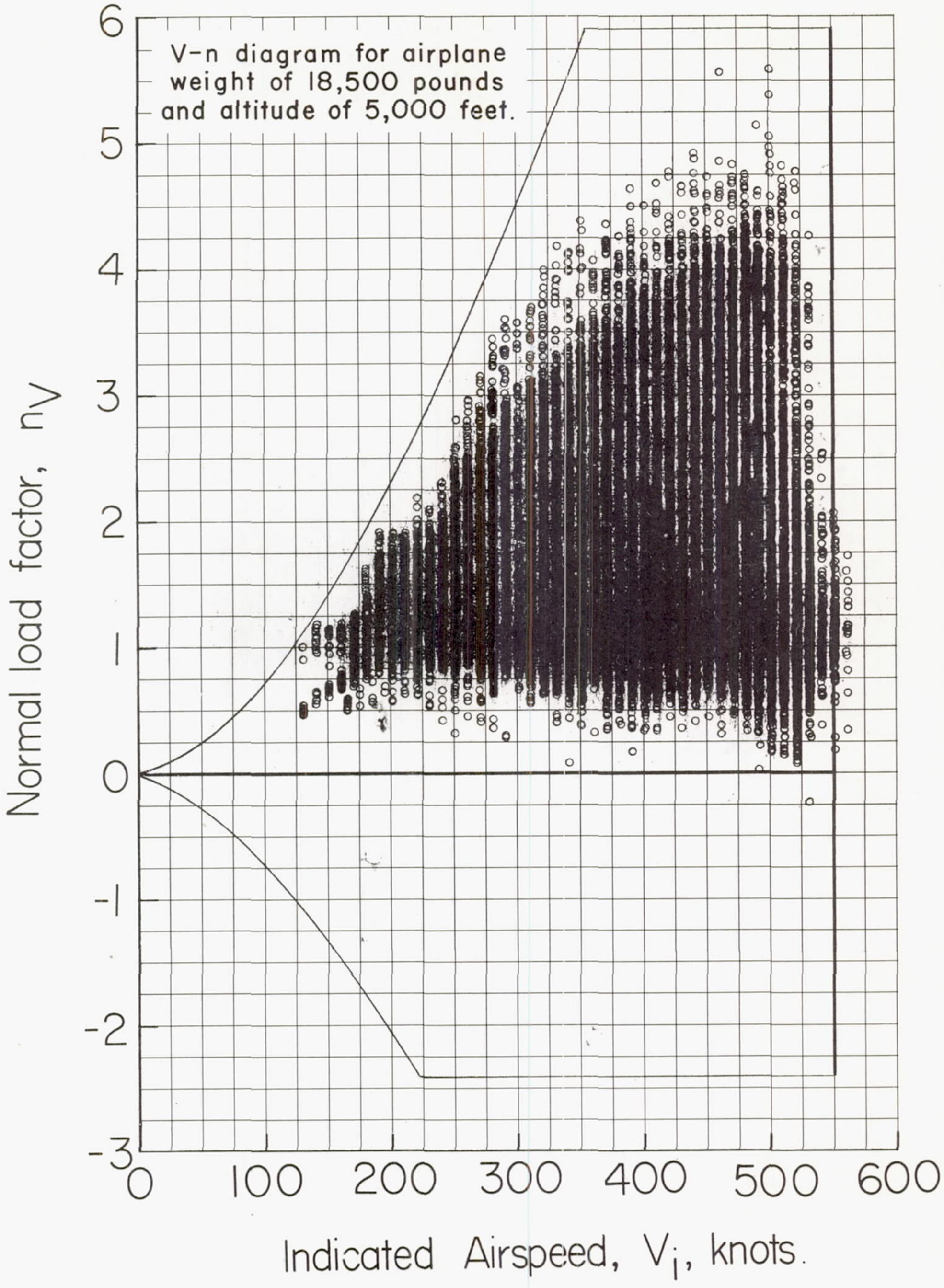

Figure 71.- Comparison of measured normal load factors obtained during LABS missions with the service V-n diagram. Pressure altitude, sea level to 15,000 feet. Airplane configuration, external stores carried.

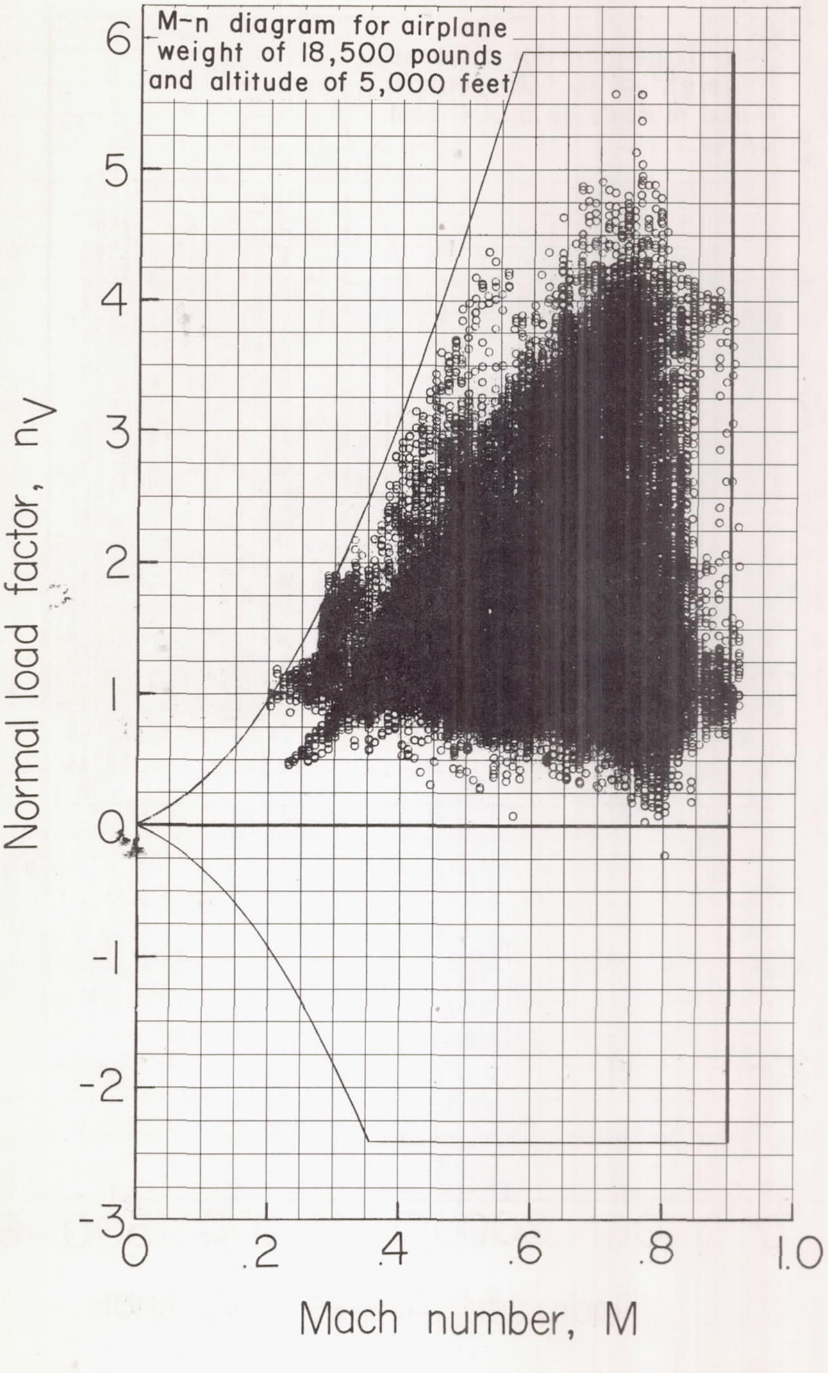

Figure 72.- Comparison of measured normal load factors obtained during LABS missions with the service M-n diagram. Pressure altitude, sea level to 15,000 feet. Airplane configuration, external stores carried.

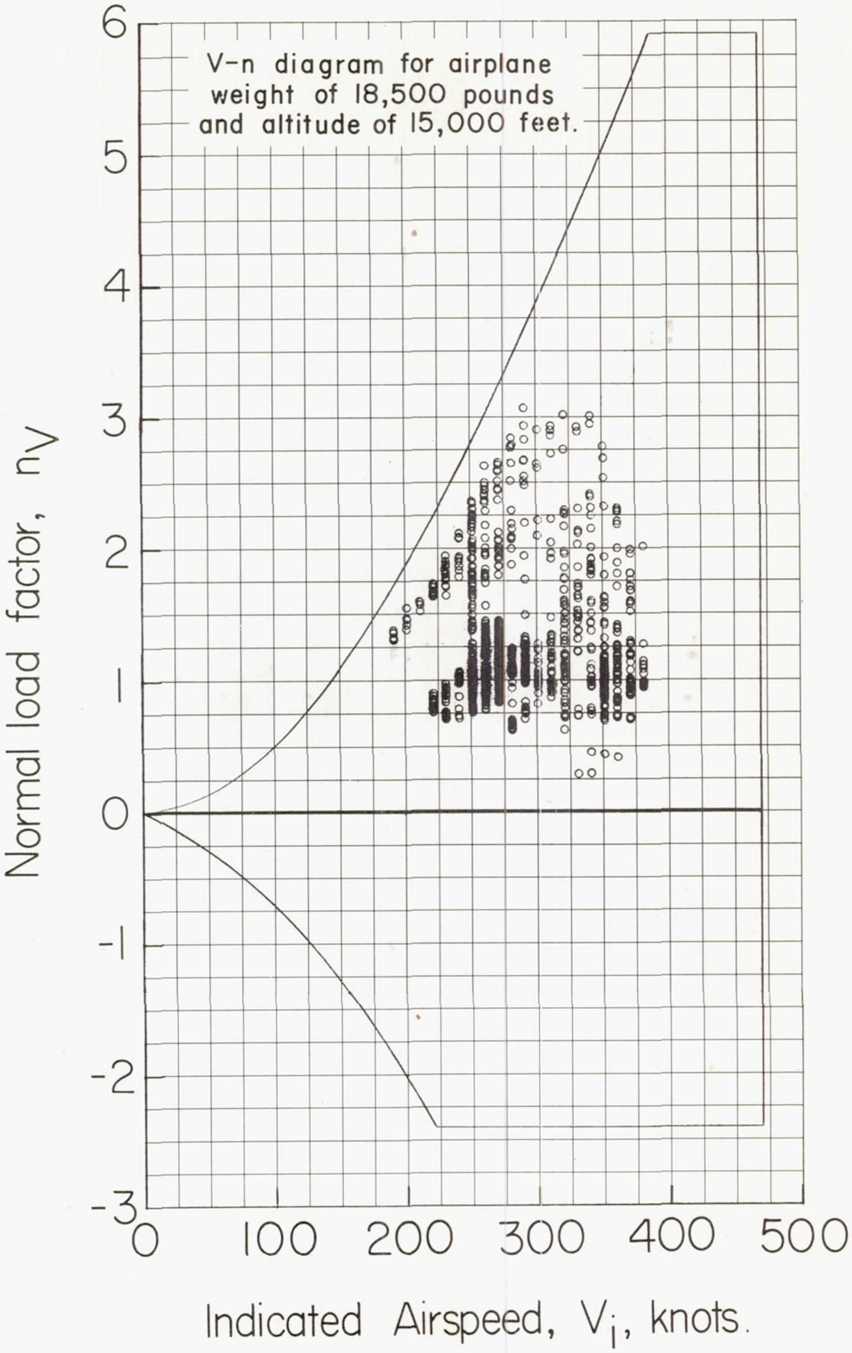

Figure 73.- Comparison of measured normal load factors obtained during LABS missions with the service V-n diagram. Pressure altitude, 15,000 feet to 30,000 feet. Airplane configuration, external stores carried.

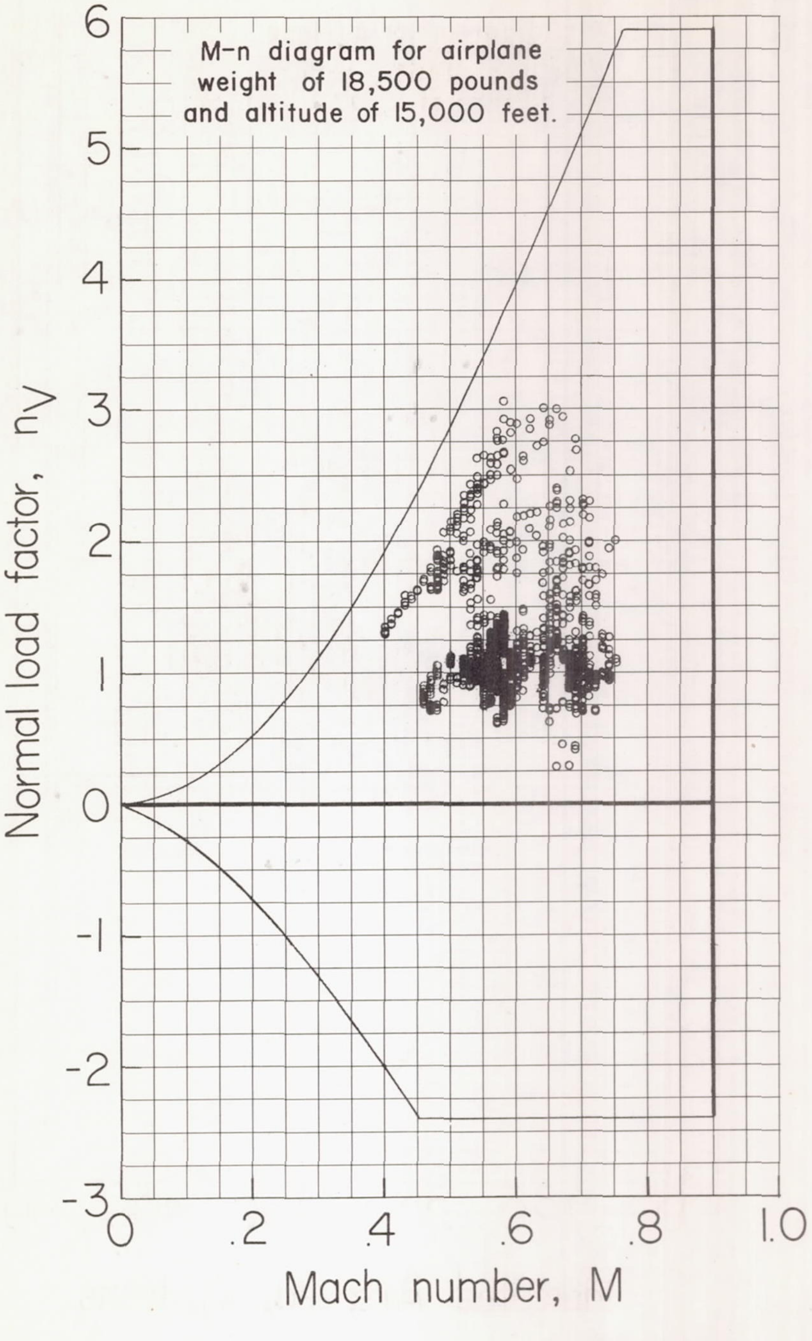

Figure 74.- Comparison of measured normal load factors obtained during LABS missions with the service M-n diagram. Pressure altitude, 15,000 feet to 30,000 feet. Airplane configuration, external stores carried.

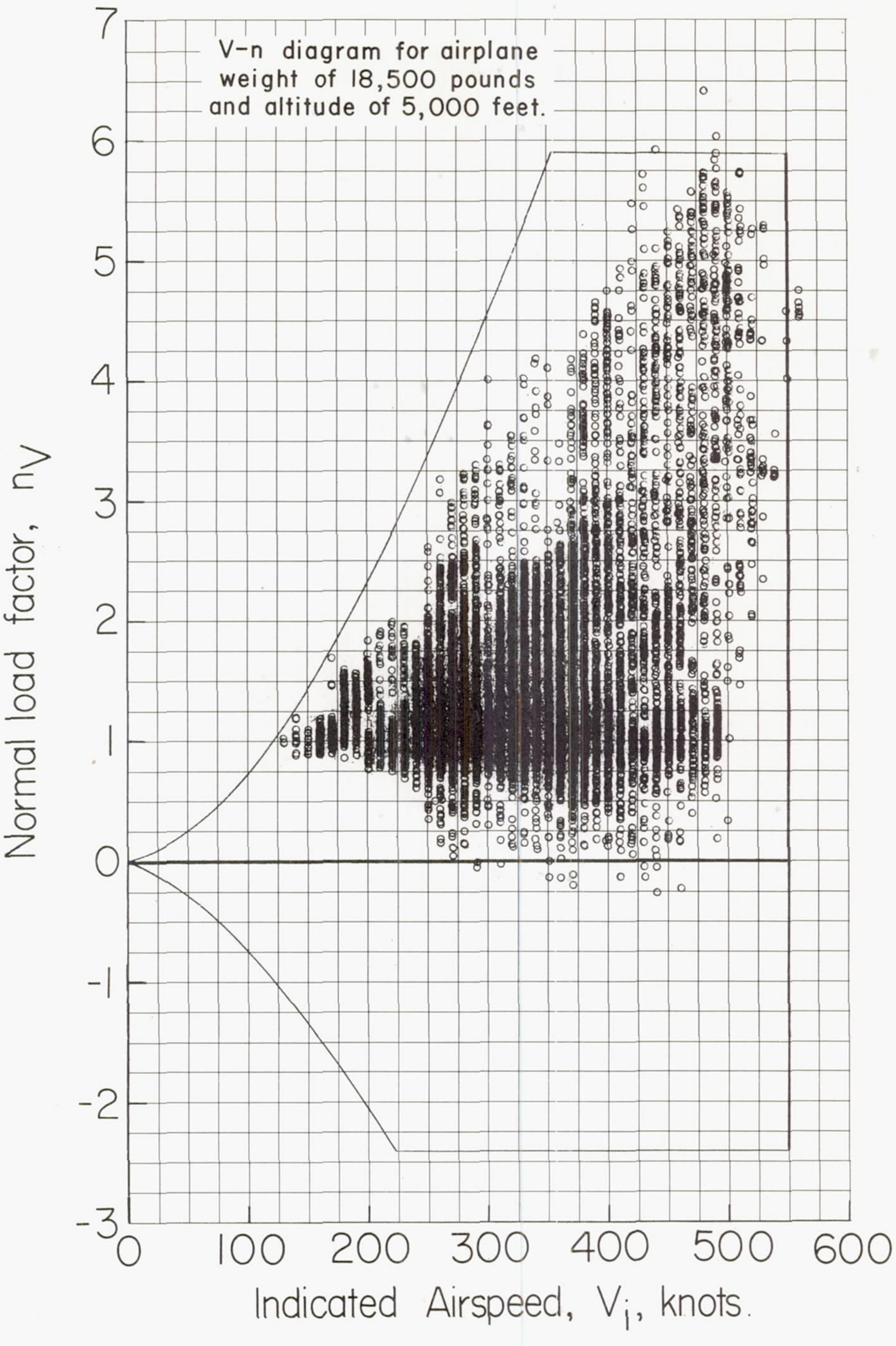

Figure 75.- Comparison of measured normal load factors obtained during dive bombing missions with the service V-n diagram. Pressure altitude, sea level to 15,000 feet. Airplane configuration, external stores carried.

DECLASSIFIED

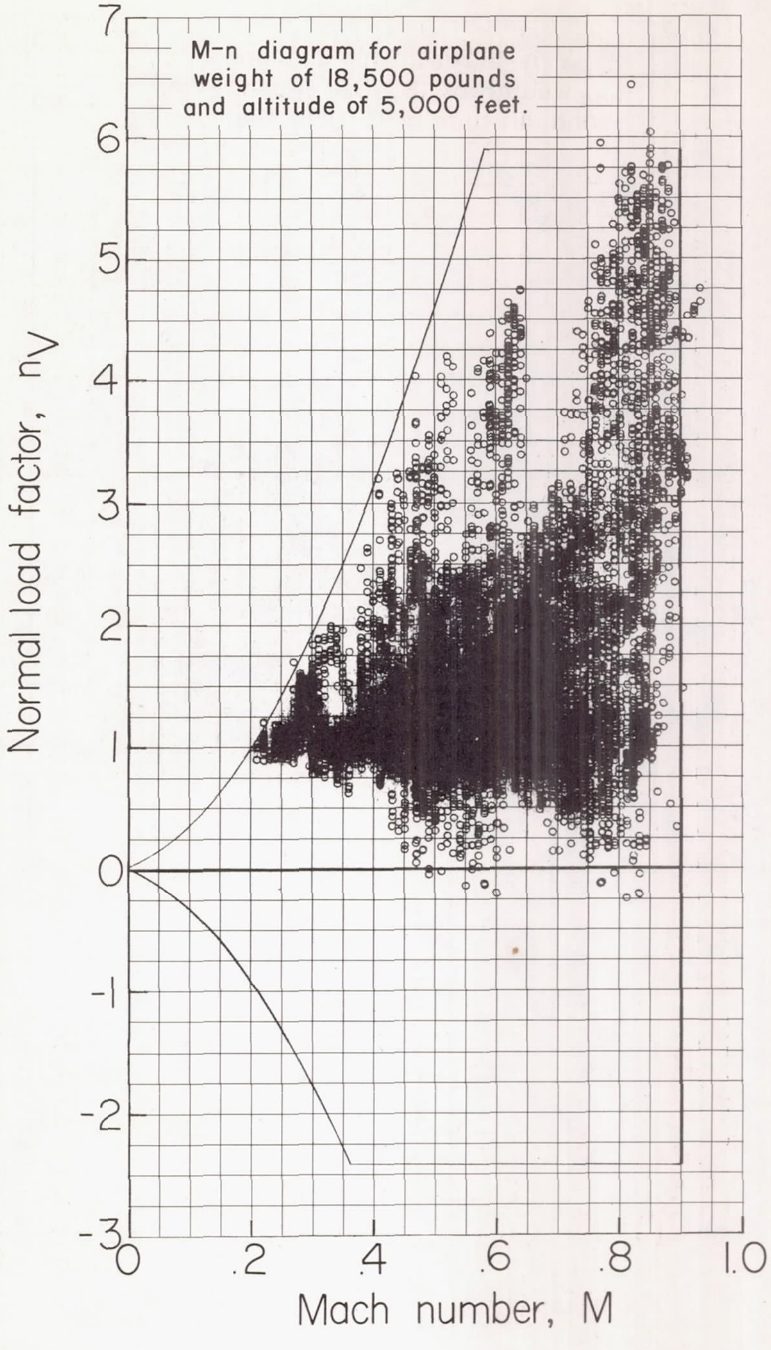

Figure 76.- Comparison of measured normal load factors obtained during dive bombing missions with the service M-n diagram. Pressure altitude, sea level to 15,000 feet. Airplane configuration, external stores carried.

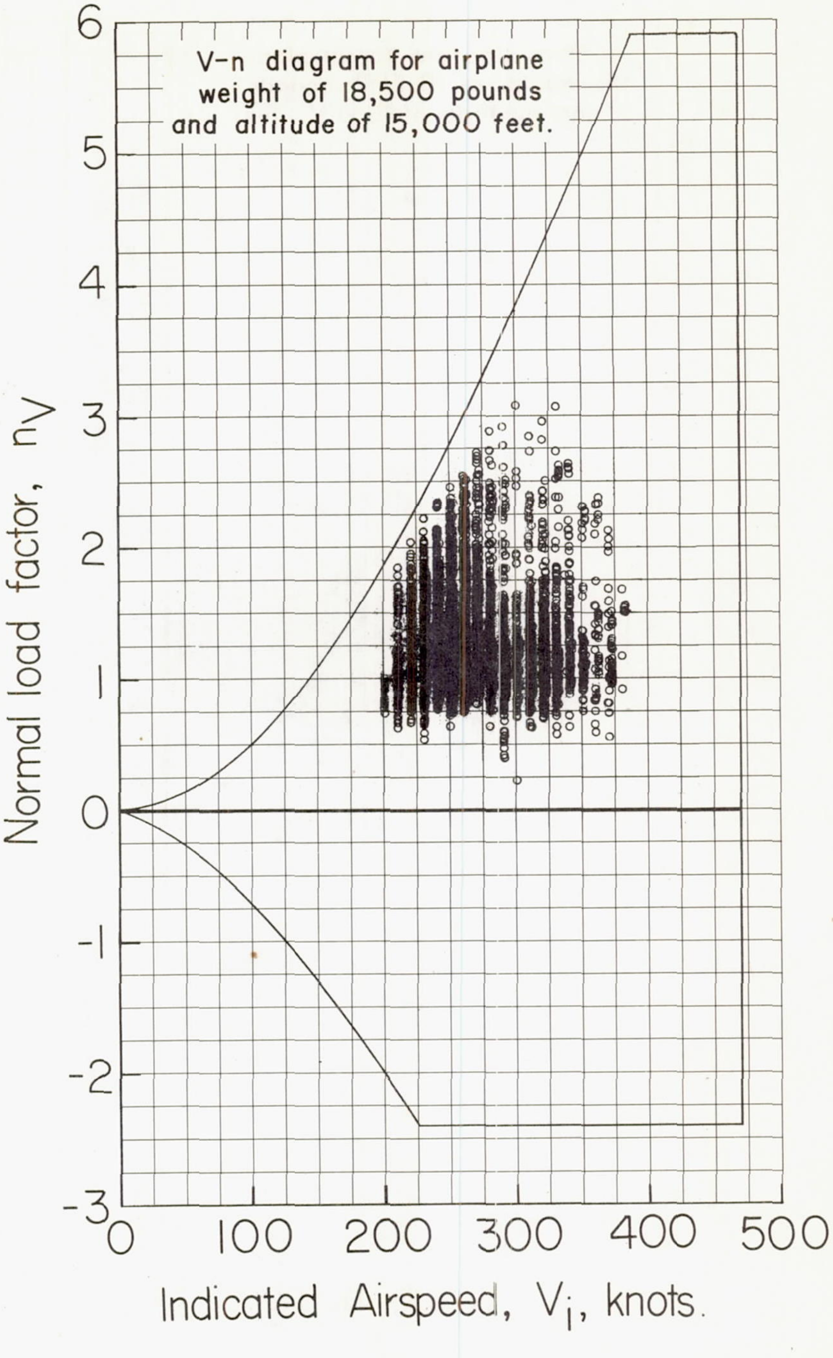

Figure 77.- Comparison of measured normal load factors obtained during dive bombing missions with the service V-n diagram. Pressure altitude, 15,000 feet to 30,000 feet. Airplane configuration, external stores carried.

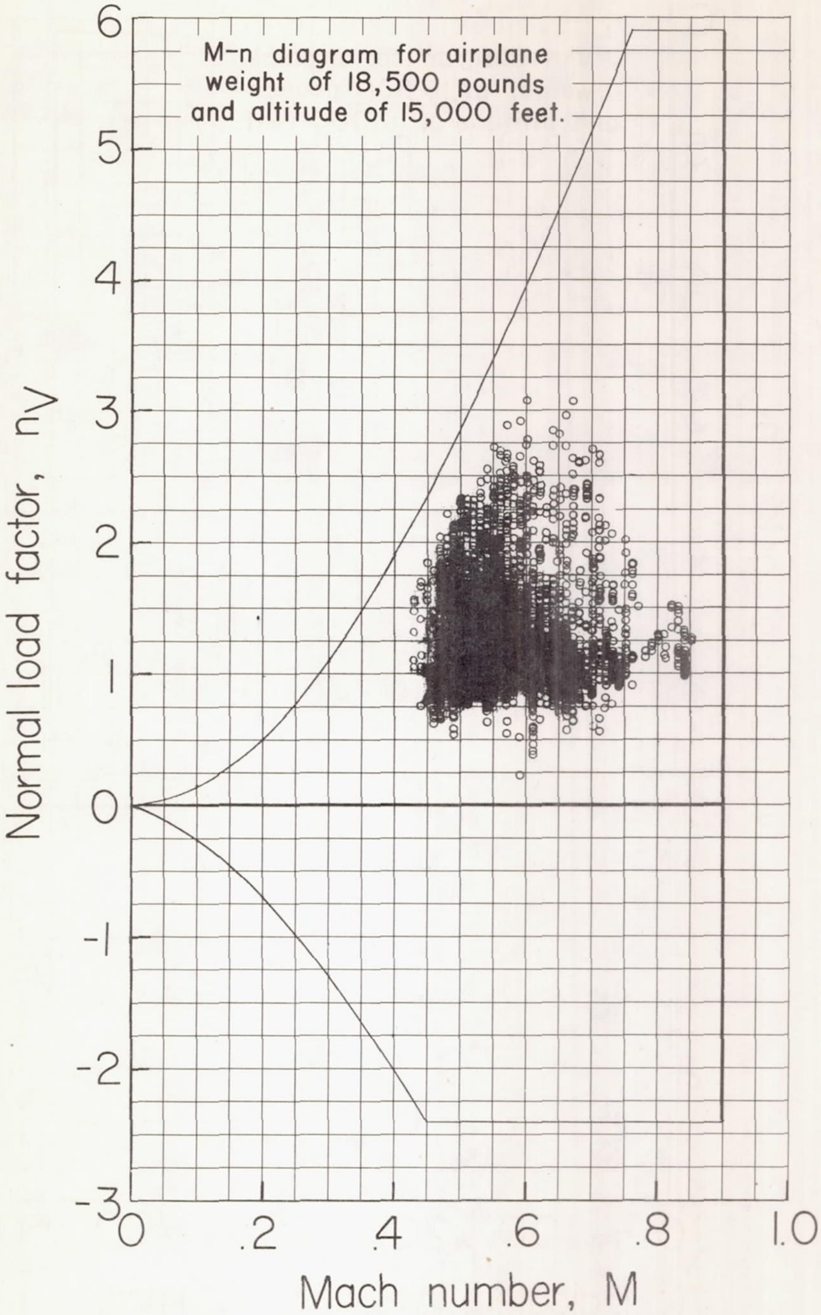

Figure 78.- Comparison of measured normal load factors obtained during dive bombing missions with the service M-n diagram. Pressure altitude, 15,000 feet to 30,000 feet. Airplane configuration, external stores carried.

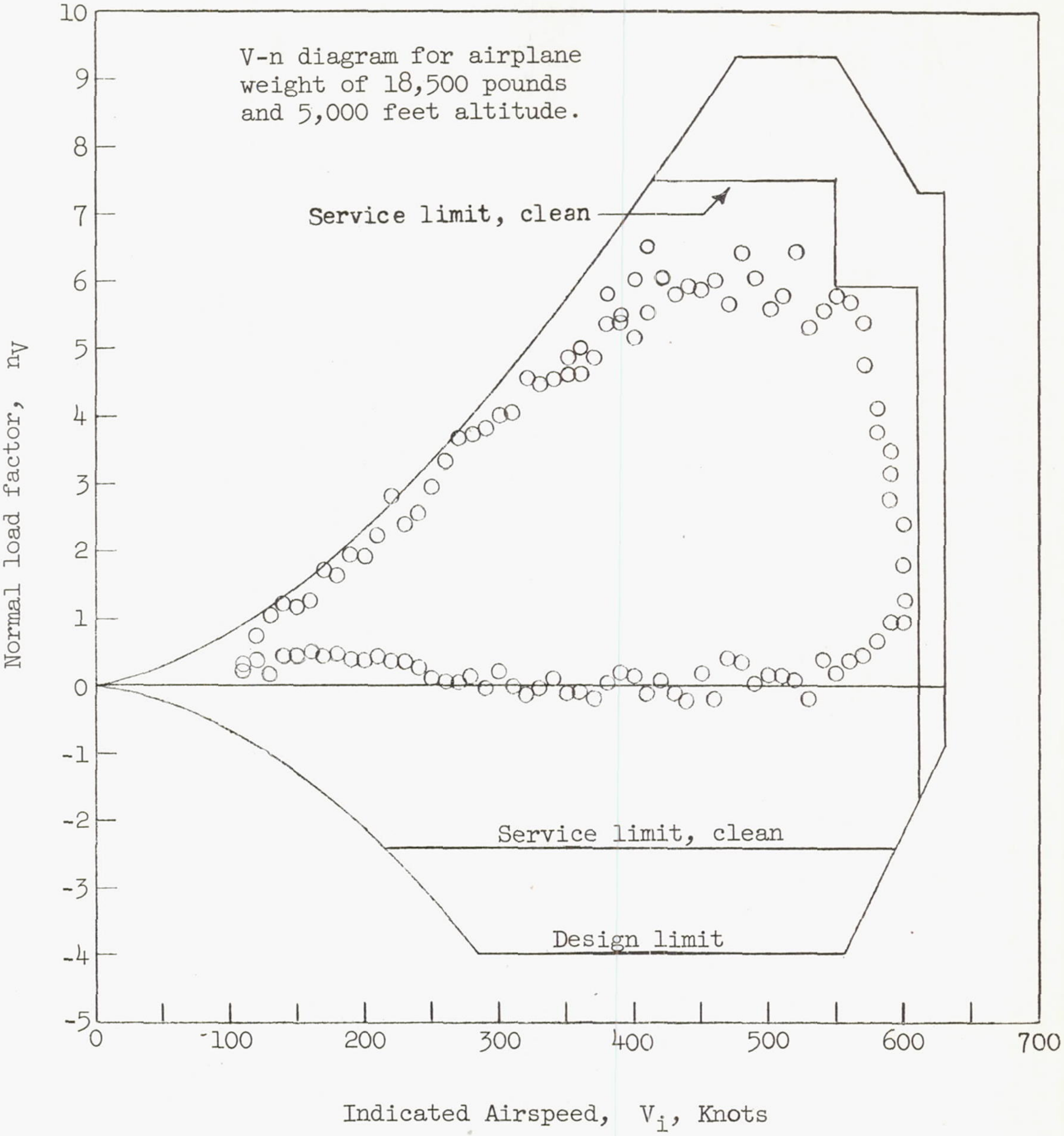

Figure 79.- Comparison of measured normal load factors obtained during general flying and bombing missions with the V-n diagram. Pressure altitude, sea level to 42,000 feet.

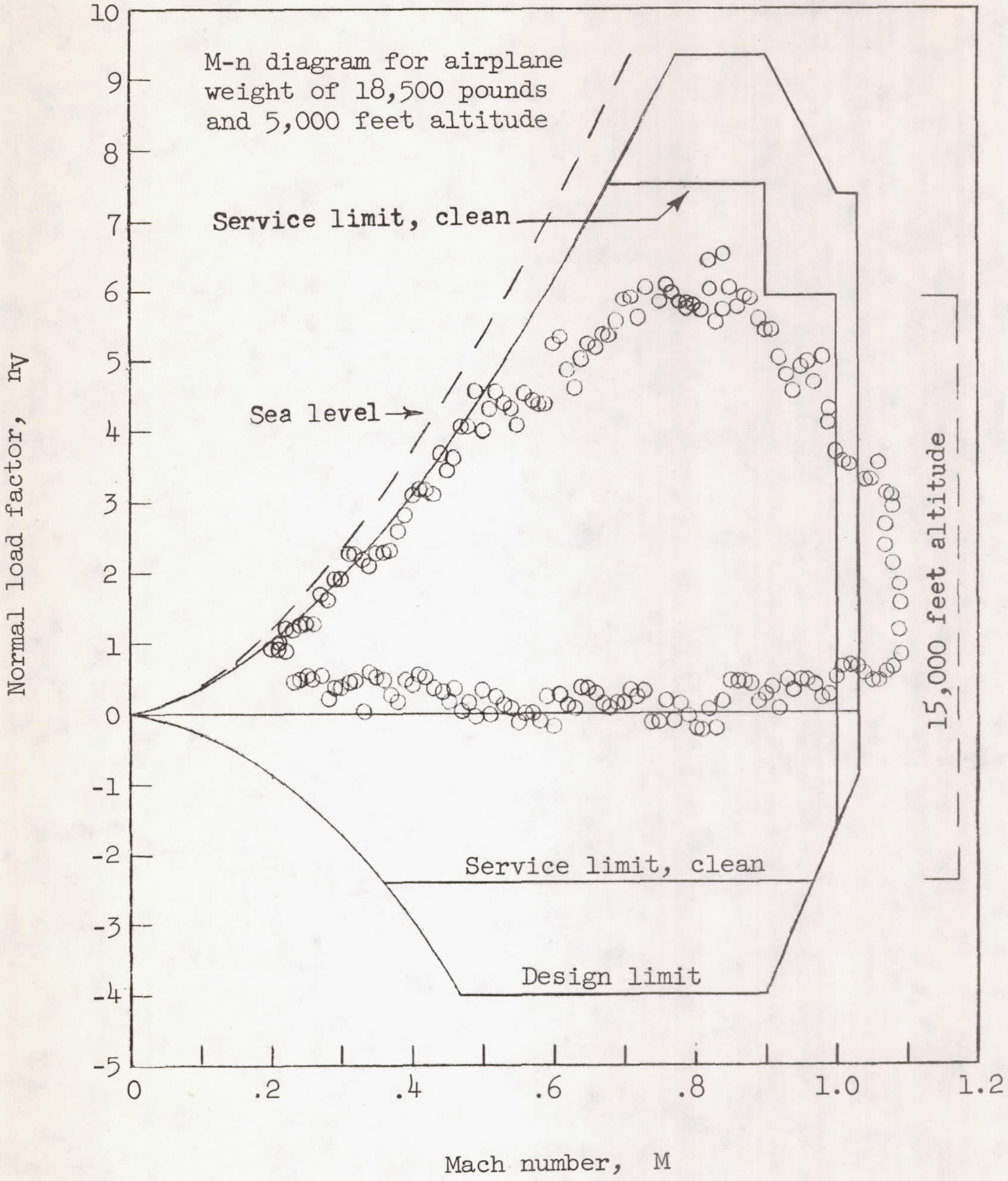

Figure 80.- Comparison of measured normal load factors obtained during general flying and bombing missions with the M-n diagram. Pressure altitude, sea level to 42,000 feet.